Improved treatments for helminth infections, new formulations and drug candidates and screening tools

Inauguraldissertation

zur Erlangung der Würde eines Doktors der Philosophie vorgelegt der
Philosophisch-Naturwissenschaftlichen Fakultät
der Universität Basel
von

Alfredo Valentin Buchter

Basel, 2021

Genehmigt von der Philosophisch-Naturwissenschaftlichen Fakultät auf Antrag von

- Prof. Dr. Jennifer Keiser
- Prof. Dr. Pascal Mäser
- Prof. Dr. Andrew Hemphill

Basel, 15. Dezember 2020

Prof. Dr. Martin Spiess,

Dekan Philosophisch-
Naturwissenschaftliche Fakultät

Table of Contents

Acknowledgements

Dear reader, I am very happy to share this thesis with you. I invite you to go through these pages and enjoy this contribution to the improvement on the treatment of the helminth diseases, that so much harm introduce into developing communities, my own country included.

Over these years, I would like to thank many people who very much supported me and my projects from very different perspectives, and made this phase of my life a very nice and enjoyable time, full of continuous learning and good experiences.

First, I want to thank Jenny, for accepting me with open arms in the group and for always being ready and open for discussion, always finding the moment to attend our needs. I very much appreciate all I learned from you on the research side, finding the reasons and the knowledge gap to develop a certain project and the reason for taking certain decisions. I also thank you for your guidance on how to improve my writing and how to communicate science in a proper way. A distinguishing point that I will take with me, is the learning on how to work efficiently and objectives oriented, keeping the high quality of the work. I very much appreciate your very professional guidance.

I am very thankful to the ESKAS scholarship, not only for selecting my proposal to perform my PhD at Swiss TPH, but also for all the efforts to make the life in Basel a better experience. As contact person from the international office from the University of Basel, I would like to thank Andrea Delpho, for organizing the excursions, meetings with other candidates and for her constant readiness to support us.

To my second supervisor, Pascal Mäser I would like to thank for the great scientific discussions, innovative ideas and for the simplicity to share his enormous knowledge, always with a smile and for accepting the role of supervising me. To Andrew Hemphill I am very thankful for accepting with such a good predisposition the role of external expert and for his time to read and evaluate my thesis and to attend my defense. I am also thankful to Nicolas

Brancucci, for chairing the defense and for his time to support me in the use of the high content imager.

I also would like to thank my collaborators along this project for the constant feedback and positive intention to cooperate and get solid results:

For the OXA project, I would like to thank Gilles Gasser from the PSL University in Paris for always keeping the OXA project working and so professionally integrating such a big number of collaborators from different research fields. I would also like thank Yih Ching for the continuous exchange, results, and contribution during the paper writing. To Francois, Elise, Ursula and Abdallah for their contributions to support the development of this project.

Back in Argentina, I am very thankful to the researchers from the University of Rosario, Celina Lamas and Josefina Priotti for the collaboration on the ABZ and MBZ project. Also from the same university, but not referred to the PhD, I would like to thank Bernardo Basset for his deep and solid friendship despite the short time we shared and for his support on the molecular biology at the beginning of my PhD.

From the wormy group at Swiss TPH I would first like to thank Cécile for all the work and time invested in keeping the labs running, for all I have learned from you, your support in so many experiments and I also apologize for all the times I did not strictly follow the “Cécile’s lab rules”. I would also thank from my heart the “lab crew”, Alex, Anna, Gordana and Noemi at the very beginning, Flavio, Pierre, Stefan, Val and the Civil servants Andi, Luc, Yvan, Julian, who were always ready to help and very much improved the lab experience from a social perspective. The lab experience was excellent, where I only remember good experiences and an excellent teamwork, supporting each other, sharing materials and protocols and for discussing the best ways to fit all our needs, especially for the worm’s availability and the lab’s rotation during the Corona time. I am also very thankful to Jantine, for all the efforts to make R more accessible to me, and to Miriam, for her support with the writing and for the nice conversations. To Dani, I am very thankful for the time and the guidance on the MS and on the writing of the moxidectin

paper. I would also like to emphasize on the people who shared with me their passion for science, Gordana and Anna, for naturally transmitting me optimism, good ideas, energy and for sharing their enormous knowledge with me. Last but not least, I would like to thank the Epi – people, Chandni, Emmanuel, Evelyn, Ladina, Marta, Sophie, Wende for sharing their knowledge in the clinical implementation of our group's research. To all the wormy friends I would like to thank for the nice time, sharing the office and thank you all for making the lunch breaks and private time a social and sharing experience, for the smiles, fun, good times and nice conversations.

To my parents I would like to say thank you, for encouraging my curious mind to follow my dreams and constantly supporting me in my plans and projects, even being so far from home. Thank you so much! To my siblings, I am thankful for always being close, despite the big distances and for the growing together in all aspects of our lives.

I want also like to thank Mariana for always being with me in the good and difficult moments, for the constant support and company, for our personal and joint projects; I love you from the deepest of my heart. To Maite, I would like to thank you for making my last half of the PhD the most intense time in my life, rediscovering myself as a father and for the nicest and most genuine smiles and moments I ever experienced.

With all this said, I gladly invite you to continue reading and wish you a good and fruitful time going through the sections of these research projects.

Summary

Neglected tropical diseases (NTDs) are a group of 20 communicable diseases that account for an enormous disease burden, affecting over a billion people living in 149 countries in all continents. The objective of this thesis was to boost the discovery and improvement of the drugs on helminths, focused on schistosomiasis and soil transmitted helminth (STH) infections, two neglected tropical diseases, for which treatment is available, but there is an urgent need of drug discovery and development.

Four nematodes, the hookworms (*A. duodenale* and *N. americanus*), the whipworm (*T. trichiura)* and the roundworm (*A. lumbricoides*) are normally grouped together as STHs. *S. stercoralis* is also a STH, but I will address this parasite independently, due to the different drugs used to treat this infection. Although four drugs are listed in the WHO list of essential medicines to treat STH infections, the benzimidazoles are the most widely used in the frame of mass drug administration campaigns. Several studies have confirmed their unsatisfactory efficacy, with none of the drugs being 100% effective against all species.

The first objective of my thesis was to evaluate if the increase of the water solubility of the benzimidazoles, albendazole (ABZ) and mebendazole (ABZ) could improve the efficacy of these drugs in the treatment of STH infections. The main limitation of a poorly soluble drug is that only the solubilized molecule can be absorbed by the organism and act on the target. Therefore, the goal of this project was to develop different formulations of ABZ and MBZ with improved solubility and evaluate their potential both *in vitro* and *in vivo* on the model parasite of human hookworm infection, *Heligmosomoides polygyrus*. We tested the effect of four different drug formulations with improved water solubility, compared to the standard pure drug without modification of the formulation. The water solubility of the formulations was improved in all cases, in the range of 1.4 to 81 fold, as was also the dissolution rate, in the range of 4 to 10 fold. Compared to the pure drug, all formulations, with exception of the ABZ - cyclodextrin (CD) formulation, were more efficacious to reduce the worm burden of infected mice. The

highest improvement in efficacy was observed with the mebendazole formulations, where the chitosan microcrystals formulation resulted in a 20-fold reduction of the ED_{50}. With regard to ABZ, the reduction of the ED_{50} was around two fold for all formulations except CD, which even showed a slightly higher ED_{50}.

Strongyloidiasis is caused by infection with the nematode *Strongyloides stercoralis* and transmitted to humans from the soil. Because of differences in the life cycle, diagnostics and treatment, it is rarely included in STH control programs, frequently underdiagnosed, and even called “the neglected among the neglected diseases”. The number of people affected by this disease is suggested to be between 30 and 100 million people. Different to the other STHs, *Strongyloides sp.* parasites can auto-infect the host and features a free-living life cycle. For this infection ivermectin is the gold standard treatment, which is the only drug in use, but counts on several limitations, as are the erratic efficacy and confirmed differential grades of resistance in livestock.

The second objective of my thesis was to evaluate the potential of moxidectin, an antiparasitic drug developed in the 80s’ and widely used in veterinary medicine, as a new treatment for human strongyloidiasis. We evaluated the *in vitro* activity of moxidectin, compared to the standard treatment ivermectin. Additionally, we also investigated its pharmacokinetic – pharmacodynamic profile in *S. ratti* infected rats. *In vitro,* the drug was as effective as ivermectin, killing both L_3 larvae and adult worms and resulting in IC_{50} values in the range of 0.15 to 1.44 µM at the 72h evaluation point. In the treatment of infected rats, the drug was also effective, reaching a 75% reduction of worm burden with a 500 µg/kg dose. The systemic total drug exposure (AUC) observed in rats was independent of the effect. In addition, we discovered limitations in our model, as a shorter half-life compared to other species, and a ceiling effect in the absorption phase, probably due to limited solubility in the digestive tract. Despite these limitations of the rat model, we propose moxidectin as a promising alternative to ivermectin in the treatment of *Strongyloides sp.* and provide additional evidence supporting clinical studies on this drug.

Schistosomiasis is a very well-known water borne parasitic disease, acquired by humans by contact with contaminated water bodies. This disease affects over 270 million people, is caused by five different *Schistosoma* species, but can only be treated with one drug, praziquantel. This drug is massively used worldwide, resulting in an enormous drug pressure, which will ultimately lead to drug resistance. The emergence of resistance risks many years of uninterrupted efforts to control the disease to be lost. On this perspective, new effective drugs, or drug combinations are urgently needed.

The third objective of my thesis was to follow up on the characterization and activity evaluation of three derivatives of oxamniquine, which had showed promising results in the treatment of adult *S. mansoni* and *S. haematobium in vitro.* Our objective, described in chapter four, was to characterize these derivatives in terms of its activity against juvenile *S. mansoni* as well as on *S. haematobium* and *S. japonicum*. We investigated the derivatives profile by means of *in vitro* and *in vivo* experiments, *in silico* predictions, pH and metabolic stability evaluation. Our derivatives were highly active *in vitro* against juvenile *S. mansoni,* adult *S. haematobium* and *S. japonicum,* showing higher activity than oxamniquine (IC_{50} values in the range of 1.3 to 52 µM, compared to > 100 µM for oxamniquine). *In silico* simulations supported the *in vitro* findings. Unfortunately, when testing the derivatives *in vivo,* we observed a pronounced loss of efficacy, which was later explained by the low pH stability and high liver metabolism. These limitations could not be saved by the drug's encapsulation in lipid nanocapsules and we opted for stopping the research process at this phase.

The last objective of this thesis was to validate a recently described method for growing *S. mansoni* worms, in a full *in vitro* setting. Our aim was to set up a simple, fast, reliable and reproducible method for drug screening assays on juvenile worms. We characterized the worms in terms of size, organ development, gender distribution and drug sensitivity and compared them with worms grown *in vivo*. By means of this method, a large number of juvenile *S. mansoni* worms can be grown *in vitro*, which show similar drug sensitivity, gender

distribution, size and morphology as the worms recovered from rodents, supporting the use of this method in drug screening efforts.

Table of abbreviations

ADME	Absorption, distribution, metabolism, excretion
AUR	Auranofin
BW	Body weight
CD	Cyclodextrin
CH	Chitosan
CR	Cure rate
DALYs	Disability adjusted life years
ED_{50}	Effective dose 50%
EPG	Eggs per gram (of stool)
Fc-OXA	Ferrocenyl oxamniquine
FDA	(US) Food and drugs administration
HIV	Human immunodeficiency virus
HTS	High throughput screening
IC_{50}	Inhibitory concentration 50%
LF	Lymphatic filariasis
MBZ	Mebendazole
MDA	Mass drug administration
MFQ	mefloquine
NTD	Neglected tropical diseases
NTS	Newly-transformed schistosomula
OPZ	Omeprazole
OXA	Oxamniquine
P80	Polysorbate 80
PC	Preventive chemotherapy
Ph-OXA	Phenyl oxamniquine
PVA	Polyvinyl alcohol
PZQ	Praziquantel
R.& D	Research and Development
Rc-OXA	Ruthenocenyl oxamniquine
STH	Soil-transmitted helminth(iase)s
WASH	Water, sanitation and hygiene
WHO	World Health Organization

Chapter I

General Introduction

Global burden of helminths

Neglected tropical diseases (NTDs) affect worldwide more than one billion people (WHO, 2020b). They principally affect people living in poverty without adequate sanitation and cost developing economies billions of dollars every year (WHO, 2020b). In 2010, soil transmitted helminthiasis accounted for the highest disease burden of all NTDs, with 5.16 million DALYs, followed by leishmaniasis and schistosomiasis, with 3.31 million DALYs (Hotez *et al.*, 2014). In the last decades, many efforts were oriented to control helminth infections (WHO, 2017, 2020c). As a result, the burden of these diseases decreased, with estimates from 2017 showing almost 2 million DALYs for STH and 1.4 million DALYs for schistosomiasis (Kyu *et al.*, 2018). However, today still 1.5 billion people are infected with one or more STH (WHO, 2020d) and 290 million are infected with *Schistosoma spp.* (WHO, 2020c). Strongyloidiasis, also an intestinal soil transmitted nematode, sometimes referred to as the most neglected of the neglected diseases (Olsen *et al.*, 2009), is not included in the list of NTDs, despite affecting 30 to 100 million people and causing an enormous disease burden and even fatal complications (Schär *et al.*, 2013).

Given the huge impact of these diseases and the alarming number of people affected by them all over the world, this thesis focuses on the different strategies, advances and challenges of drug development against soil transmitted helminths (STHs), strongyloidiasis and schistosomiasis.

Soil transmitted helminths

Epidemiology

STHs are normally approached together owing to: (i) similar geographical endemicity and at-risk groups that are affected; (ii) treatment by the same medicines; (iii) same tools used for diagnosis; and (iv) similar mechanism of impact on human health, which is proportional to the worm burden (WHO, 2017). The causing agents for soil transmitted helminthiasis are the hookworms (*Ancylostoma duodenale, Necator americanus*), the whipworm (*Trichuris trichiura*), and the roundworm (*Ascaris lumbricoides*). *Strongyloides stercoralis* is also a STH,

but due to some differences in its life cycle, epidemiology and drug treatment, will be treated separately in further sections.

These parasites significantly contribute to the vicious cycle of poverty and disease in affected communities due to loss of manpower, impairment of childhood education, and high treatment costs for people already living in destitution (Hotez *et al.*, 2009). Despite all efforts to reduce the burden of soil transmitted helminthiasis, the disease still affects 1.5 billion people in all inhabited continents (WHO, 2020d). On the one hand, prevalence may have declined in some part due to improvements in living conditions and expansion of major deworming efforts; on the other hand, population growth may have increased the number of people infected (Pullan *et al.*, 2014).

Life cycle

All three STH are gonochoric (adult worms have separated genders) nematodes (Despommier, 2017c) and share a direct life cycle, where the human is the definitive host (Figure 1). However, there are slight differences in the infection: while the whipworm and the roundworm infect humans via the fecal-oral route, hookworms infect humans by penetrating the intact skin, normally while people are walking barefoot in regions where open defecation is usual.

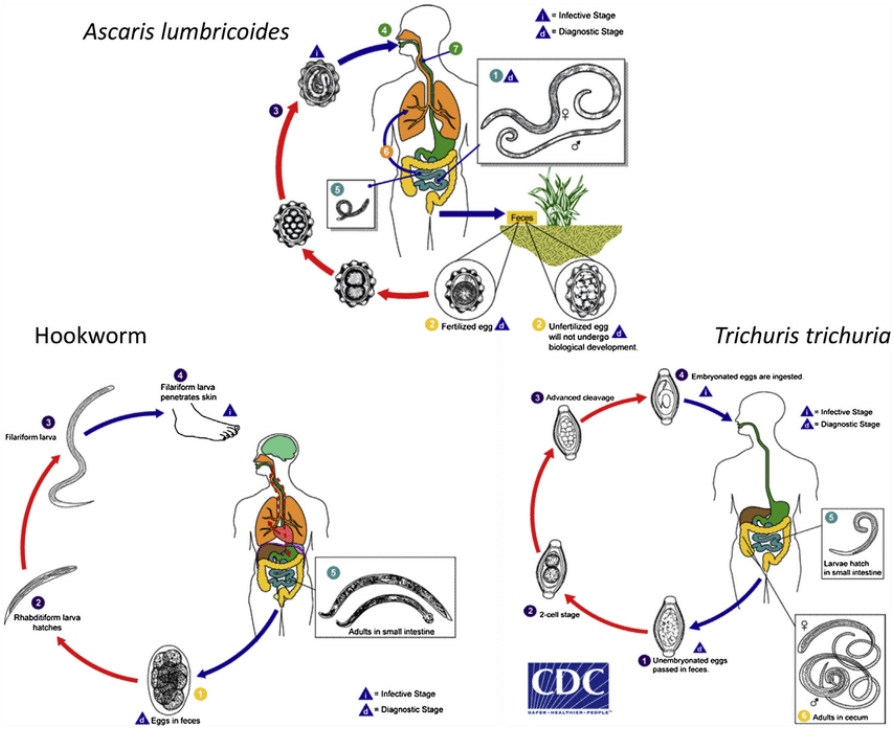

Figure 1: Life cycle of hookworms (*A. duodenale, N americanus*), roundworm (*A. lumbricoides*) and whipworm (*T. trichiura*). From: CDC, 2019.

The number of eggs laid per day and per worm differs between the species, being about 10 – 28'000 in hookworms, 3 - 5'000 in whipworms and up to 200'000 in roundworms. The lifespan inside the host is usually 1 to 2 years (Despommier, 2017c, CDC, 2019). While hookworms feed on blood and adult roundworms on predigested food, less is known on the specific diet requirements of whipworms; however, it is known that they do not feed on blood (Tilney *et al.*, 2005, Despommier, 2017c).

Clinical manifestations and diagnostics

While light infections usually remain asymptomatic, clinical manifestations are proportional to the total number of worms present in the host (Jourdan *et al.*, 2018, WHO, 2020d). STH infections can cause a wide range of consequences, including intestinal manifestations (diarrhea and abdominal pain), malnutrition, general malaise and weakness (WHO, 2020d). In children, infections can lead to growth stunting and deficits in cognitive and intellectual development (Despommier, 2017c, Jourdan *et al.*, 2018). Additionally, if not surgically removed, heavy roundworm infections can result in gut obstruction and biliary complications with deadly consequences (Pullan *et al.*, 2014, WHO, 2020d). A single hookworm can cause

the loss of 0.03 to 0.26 ml blood a day (WHO, 2017), converting hookworm infections into a major cause of anemia globally, particularly in children and pregnant women (Hotez *et al.*, 2004, Brooker *et al.*, 2008).

The number of worms harbored by a person (worm burden) can be calculated directly by counting the worms expelled after treatment, or indirectly, by calculating the number of eggs excreted per gram of stool; the second method being more widely used (WHO, 2017). Despite some limitations such as low sensitivity (Keller *et al.*, 2020) and poor reproducibility (Speich *et al.*, 2010), the Kato-Katz method (KK) (Katz *et al.*, 1972) is widely used as diagnostic tool for quantitative stratification of STH infections (WHO, 2017, Lim *et al.*, 2018). By this method, the intensity of the infection can be categorized as light, moderate and heavy, according to the number of eggs detected per gram of stool (Table 1).

Table 1: Stratification of the intensity of infection according to number or eggs per gram of stool (epg)

Organism	Intensity of infection (epg)		
	Light	Moderate	Heavy
Ascaris lumbricoides (roundworm)	1 - 4,999	5,000 - 49,999	> 50,000
A. duodenale, N. americanus (hookworms)	1 - 999	1,000 - 9,999	> 10,000
T. trichiura (whipworm)	1 - 1,999	2,000 - 3,999	> 4,000

Source: (WHO, 2012)

An alternative to the KK method is the FLOTAC technique, which allows for higher accuracy and sensitivity, which are important for detecting light infections (Speich *et al.*, 2010, Barda *et al.*, 2014). However, this method is more costly and requires qualified staff for analysis and better equipped laboratories (Speich *et al.*, 2010). Similar to FLOTAC, PCR-based methods allow for improved analytical sensitivity (Easton *et al.*, 2016, Barda *et al.*, 2020), but are limited by the need for trained staff, established laboratories and higher costs per test and therefore remain limited to research use (Lim *et al.*, 2018). Recent research compared the KK method to qPCR analysis (Keller *et al.*, 2020). This studyidentified low sensitivity for KK, while for qPCR a highlighted drawback was a limited reproducibility of the results, concluding that further research in the field of diagnostics of STH is still needed (Keller *et al.*, 2020).

Control strategies and treatment

Despite the significant contribution of water, sanitation and hygiene (WASH) implementation strategies in the control of STH (WHO, 2015b), the most cost-effective approach and widely applied strategy is preventive chemotherapy based on mass drug administration (MDA) (Lo *et al.*, 2015, Boisson *et al.*, 2016, Despommier, 2017c, WHO, 2017). In the frame of MDA programs, at-risk populations living in endemic regions are treated with anthelmintic drugs without prior diagnostic of infection (WHO, 2006, 2015a). WHO currently recommends a single administration of 400 mg albendazole (ABZ) or 500 mg mebendazole (MBZ) given once or twice yearly, according to local prevalence (WHO, 2017).

Both benzimidazoles, ABZ and MBZ are the two most widely used drugs for the control of STH (Keiser *et al.*, 2010, WHO, 2015a, Moser *et al.*, 2017). Nonetheless, two additional drugs complement the arsenal of anthelmintic drugs currently included in the WHO model list of essential medicines (WHO, 2019b), namely levamisole and pyrantel (Keiser *et al.*, 2008, Moser *et al.*, 2017). The efficacy of ABZ, MBZ, levamisole and pyrantel against STH has been thoroughly investigated by different systematic reviews (Keiser *et al.*, 2010) and meta-analyses (Keiser *et al.*, 2008, Moser *et al.*, 2017). While all four drugs in the frame of a single dose regimen where highly efficacious against roundworms (CR > 92.6 %), ABZ was the only drug with high cure rates against hookworm infections (CR= 79.5 %) and all drugs had low efficacy against whipworms, with MBZ showing the highest cure rate (CR= 42.1%) (Moser *et al.*, 2017). Additionally, Moser *et al.* highlighted the alarming situation of loss of activity of ABZ against whipworm infections within the past two decades: compared to 1995, by 2015 the egg reduction rates fell from 72.6% to 43.4% while the cure rates fell from 38.6% to 16.4% (Moser *et al.*, 2017).

In parallel to single dose MDA programs, multiple dose schemes have also been studied in the treatment of STH. A recent study demonstrated a 98% cure rate against hookworm infected school-aged children after multiple administration with MBZ (3 days, 100 mg twice a day) compared to a 13% cure rate after single administration with 500 mg (Palmeirim *et al.*, 2018). Despite the existence of evidence showing better outcome by repeated treatment with both

ABZ and MBZ (Bethony *et al.*, 2006), these treatment schemes are more likely to result in a reduced compliance in the frame of preventive chemotherapy programs (Keiser *et al.*, 2008) and single dose regimes remain the first choice for treatment at a population level (WHO, 2020d).

Thiabendazole was the first benzimidazole discovered in 1961 and marked the establishment of a class of low-dose broad-spectrum anthelmintics with a high therapeutic index and selective helminth toxicity (Lacey, 1990). The mechanism of action of the benzimidazoles has been elucidated as a microtubule inhibitor and consists of the interaction with the β-subunit of tubulin, which inhibits the formation of microtubules and leads to the worms' death (Lacey, 1990). One of the limitations which has been highlighted for ABZ and MBZ in the treatment of STH is their erratic bioavailability (Jung *et al.*, 1997), which might contribute to the reported variable efficacy among individuals (Moser *et al.*, 2017). Jung *et al.* investigated this behavior for ABZ and identified the solubility and not necessarily the absorption, as the limiting factor for bioavailability (Jung *et al.*, 1997). With this concept in mind, the first objective of my thesis was to develop formulations of ABZ and MBZ with enhanced water solubility, and evaluate their *in vitro* and *in vivo* activity.

Drug development approach: formulation improvement

To be absorbed in the gastrointestinal tract, an orally administered drug needs to be in the form of a solution at the immediate site of absorption (Savjani *et al.*, 2012). Uncountable drugs fail in the translation from *in vitro* to *in vivo* settings, in many cases due to their chemical properties, which make them poorly soluble in water or resulting in poor permeability (Lipinski *et al.*, 1997). The two main approaches to modulate the solubility of a drug are the reduction of the particle size as well as the enhancement of the wetting properties (Dokoumetzidis *et al.*, 2006). In addition, encapsulation within different matrixes is also an applicable strategy for delivery of low polar drugs (Huynh *et al.*, 2009, Savjani *et al.*, 2012).

ABZ and MBZ are classified as low water soluble and high permeable drugs by the BCS system (Tsume *et al.*, 2014) and many efforts were oriented to improve their water solubility

(Paredes *et al.*, 2018). As described in chapter two, we evaluated the *in vitro* and *in vivo* activity of different formulations with improved wetting properties and enhanced water solubility, aiming to improve the drugs' dissolution in the worms' microenvironment and facilitate the membranes' permeability and worms' uptake. The strategies applied were based on solid dispersion and reduction of particle size (Savjani *et al.*, 2012), for which the following matrixes were used: β-Cyclodextrin inclusion complex, chitosan based microcrystals, polyvinyl alcohol and polysorbate 80-based nanoparticles.

Cyclodextrines (CD) consist of 6, 7 or 8 cyclic-bound glucoses, which expose a hydrophilic exterior and have a lipophilic core (Figure 2). In consequence, CDs result in a very suitable and accessible method for making inclusion complexes for lipophilic drugs with increased total drug's solubility and permeability (Kang *et al.*, 2015). We evaluated the activity of both ABZ and MBZ when complexed in these inclusion complexes.

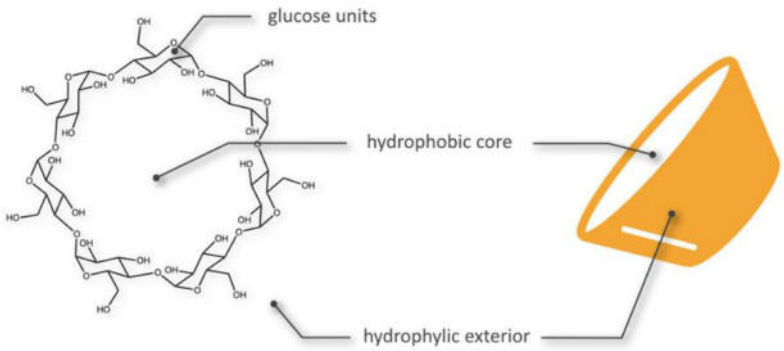

Figure 2: Cyclodextrin structure showing the hydrophobic core and the hydrophilic exterior. From: https://www.okklo.com/technology/cyclodextrins.

Nanoparticles prepared from polyvinyl alcohol and polysorbate 80 take advantage of the double benefit of a small particle size (which allow them to expose a high surface for interaction with the circumventing fluid), and the improvement of the wetting properties (Savjani *et al.*, 2012). Polyvinyl alcohol is a water-soluble synthetic polymer that acts as a stabilizer by forming a protective colloid adsorbed on the drug nanoparticle (Ahmed, 2016). Polysorbate 80 is a non-ionic surfactant, which allows generating micelles around a hydrophobic core, thus increasing the dissolution rate of the drug, masked by the outside hydrophilic core (Savjani et al., 2012).

In consequence, polysorbate 80 creates an amphiphilic interphase between the low polar molecule and the water, favoring its dissolution (Savjani *et al.*, 2012). Finally, the forth excipient evaluated in the frame of the improvement of ABZ and MBZ water solubility was chitosan. Chitosan is a biodegradable and biocompatible cationic polymer frequently used in the development of controlled drug delivery systems, due to its adhesive properties and the ability to enhance the penetration of molecules across mucosal surfaces, providing sustained local drug release (Kang *et al.*, 2015).

Strongyloidiasis

Strongyloides stercoralis has been described for the first time over 100 years ago (Streit, 2008), however, many open questions on its epidemiology, diagnostic tools and treatment options remain today. Consequently, *S. stercoralis* is also referred to as “the most neglected of the neglected tropical diseases” (Olsen *et al.*, 2009). A fascinating feature of this nematode is its ability to ‘shuttle’ between a free-living mode of existence with separated genders and sexual reproduction, and a parthenogenetic life cycle where only adult females manage to parasitize the human host and reproduce asexually (Streit, 2008).

Epidemiology

Knowledge concerning the epidemiologic situation of strongyloidiasis is scarce and estimates about the number of people infected are not much more than an educated guess (Barda *et al.*, 2017). The latest estimates are dated from the 1990’s, when the number of infected people was 30 – 100 million (Genta, 1989, Jorgensen *et al.*, 1996). Today, there is widespread agreement in the scientific community that its prevalence is largely underestimated (Olsen *et al.*, 2009, Bisoffi *et al.*, 2013, Jourdan *et al.*, 2018), with WHO estimates ranging from 30 – 100 million (WHO, 2020e) to 600 million people affected (WHO, 2020d).

Life cycle

S. stercoralis can affect humans, dogs, and other primates (Despommier, 2017a) and its complex life cycle, which includes a direct, an autoinfective and a non-parasitic free-living developmental cycle has been thoroughly investigated (Figure 3)(Olsen *et al.*, 2009).

Only parasitic females are found in the submucosa of the duodenum where they asexually produce dozens of embryonated eggs a day. These hatch in the gut lumen of the host, and are passed out in feces as first stage larvae and develop either into infective third-stage larvae or into free-living adult males and females. Alternatively, larvae may develop to the third stage still within the gastrointestinal tract and penetrate the intestinal mucosa or perianal skin, auto infecting the host. The free-living adults reproduce sexually and the offspring develop into infective third-stage larvae. Third-stage larvae are able to penetrate the skin of the human host, reach the lungs via the blood circulation and enter the respiratory tract, from where they migrate upwards through the trachea to be swallowed and finally reach the small intestine where they mature into adult egg-laying females (Olsen *et al.*, 2009).

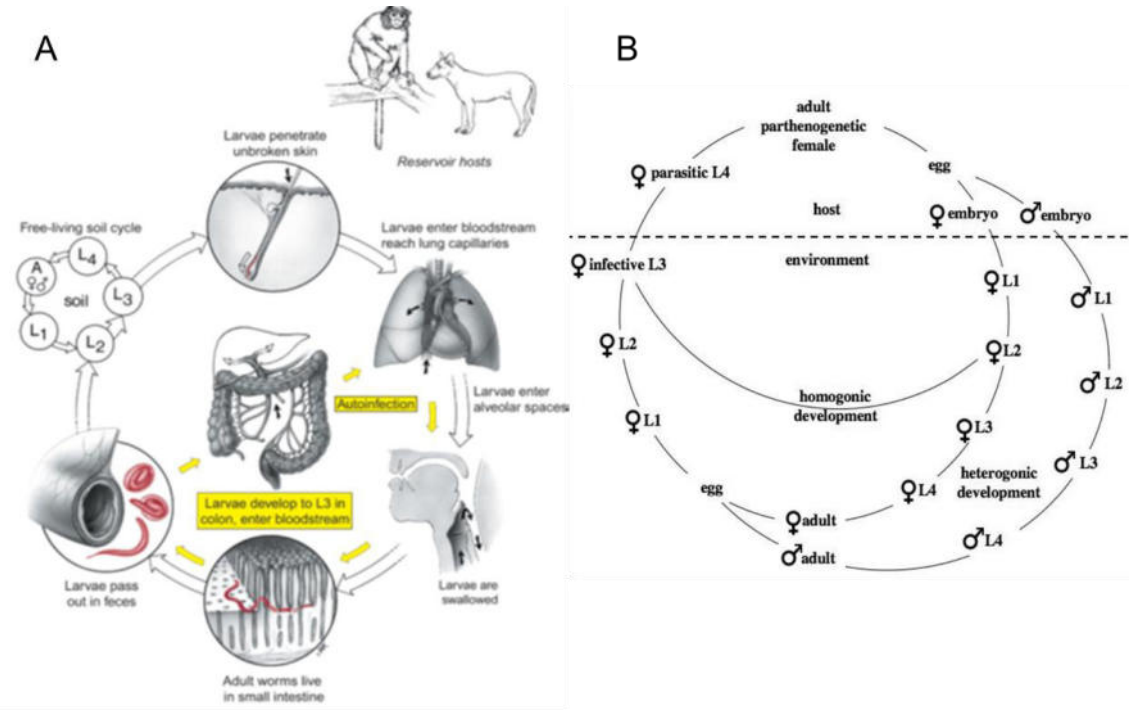

Figure 3: (A) Life cycle of *S. stercoralis* within the host and (B) schematic explanation of the molts happening along the life cycle inside the host and in the environment.

S. stercoralis has the double ability to reproduce asexually within the host and to reproduce sexually as a free-living organism. The infection of the host is percutaneous with the larval stage of the parasite. From: A: Despommier, 2017, B: Streit, 2008

Clinical manifestations and diagnostics

Similar as for STH, light infections are usually asymptomatic, while symptoms and complications are proportional to the worm burden (Olsen *et al.*, 2009). Chronically established infections usually manifest as pruritus, skin eruptions, larva currens (larvae intradermal

migration), diarrhea, abdominal pain, nausea and weight loss (Olsen *et al.*, 2009). Contrary to the classic STH, *S. stercoralis* can reproduce in the host and can lead to severe hyperinfections with larvae disseminating to multiple organs in the body, causing meningitis, pneumonia, septicemia and intestinal obstruction (Despommier, 2017a). These hyperinfections usually lead to fatal consequences in numbers as high as 87% of the cases (Olsen *et al.*, 2009) and can happen within a few days of immunosuppressive therapy (Bisoffi *et al.*, 2013). However, immunosuppression cannot explain 100% of the fatalities, and subclinical malnutrition and reduced control mechanisms in the intestinal mucosa have been hypothesized to contribute to the high fatality rate of hyperinfections (Olsen *et al.*, 2009).

The diagnostic tools used to detect *S. stercoralis* infections differ from the tools used in STH because of the ovo-viviparous life cycle, where the Kato Katz method fails to detect an infection (Steinmann *et al.*, 2007). In consequence, there is no gold standard for detecting *S. stercoralis* infections (Paula *et al.*, 2016). The most widely used technique is the Baermann method, which is based on the photo tactic response of *S. stercoralis* larvae (Yap *et al.*, 2012, Hofmann *et al.*, In press 2020). This method is laborious, time consuming and needs trained technicians to differentiate *S. stercoralis* from hookworm larvae under the microscope (Olsen *et al.*, 2009). Immunological tests, as ELISA, IFAT and Western blot have also been investigated, but were not robust enough (Olsen *et al.*, 2009). In parallel, qPCR methods were evaluated with promising results, but still require further exploration due to unspecific DNA amplification (Olsen *et al.*, 2009, Paula *et al.*, 2016, Barda *et al.*, 2020). In conclusion, the sum of multiple sampling and the application of more than one diagnostic tool seem to provide the most accurate prevalence and infection intensity information (Steinmann *et al.*, 2007). As a result, this approach is costly, laborious and hard to establish, what explains the erratic numbers of global prevalence (Steinmann *et al.*, 2007, Paula *et al.*, 2016).

Control strategies and treatment

No public health strategy for controlling strongyloidiasis exists so far (WHO, 2020e). Importantly, it is an objective from the WHO, to establish an efficient strongyloidiasis control program in school-aged children by 2030 (WHO, 2019a). Additionally, while ABZ and MBZ are

donated for free and distributed through the WHO to National Ministries of Health in endemic countries, this is not the case for strongyloidiasis. As an important step towards control of strongyloidiasis, IVM, the gold standard treatment (Hürlimann *et al.*, 2019) is expected to be available at affordable price by 2021 (WHO, 2020d). In addition, IVM is still not licensed in many endemic countries, allowing *S. stercoralis* infections to disseminate (Mendes *et al.*, 2017, WHO, 2020e).

To treat *S. stercoralis* infections, IVM is administered as a single dose of 200 µg/kg (Hürlimann *et al.*, 2019) while no advantage was observed by dose repeating schedules (Henriquez-Camacho *et al.*, 2016). The parasite is not sensitive to single doses of ABZ or MBZ and therefore not impacted by large-scale preventive treatment campaigns targeting other STH (Bisoffi *et al.*, 2013, WHO, 2020d). Alternative treatment options include ABZ given at 400 mg daily for 3 days (Olsen *et al.*, 2009, Keiser *et al.*, 2010) and thiabendazole administered as two daily doses of 25 mg/kg for two days (Bisoffi *et al.*, 2011, Henriquez-Camacho *et al.*, 2016). Overall, ABZ presents lower cure rates than IVM (Keiser *et al.*, 2010, Mendes *et al.*, 2017), while thiabendazole, despite achieving similar cure rates than IVM (Mendes *et al.*, 2017), resulted in more frequent adverse events (Bisoffi *et al.*, 2011, Henriquez-Camacho *et al.*, 2016).

As a drawback of the treatment with IVM, a recent review showed inconsistent cure rates, reporting values ranging from 55 to 100%, and raising uncertainty in the treatment strategy for strongyloidiasis (Mendes *et al.*, 2017). Additionally, considering the widespread use of IVM against different parasitic infections (*O. volvulus, W. bancrofti*), drug resistance might become a problem (WHO, 2006, 2020a), as was already observed in veterinary medicine (Geurden *et al.*, 2015).

Anticipating resistance development, new treatment alternatives for strongyloidiasis are urgently needed. Moxidectin (MOX) is a drug that has been licensed for use in livestock in 1989 and is used as a broad-spectrum endectocide with activity against a wide range of nematodes, insects and acari (Cobb *et al.*, 2009). In 2018, FDA approved MOX for the

treatment of onchocerciasis (FDA, 2018), supporting its safe use in humans and paving the way for additional human applications. Both MOX and IVM are macrocyclic lactones but belong to different subfamilies: the first is a milbemycin, while the second is an avermectin, which makes them similar in mode of action and broad spectrum activity, but different in terms of pharmacokinetics (PK profile, interaction with export proteins, tissue distribution and half-life), toxicity and resistance profile (Prichard *et al.*, 2012). MOX differs structurally from IVM in having no sugar moiety at the C13 position and an unsaturated side chain at the C25 position (Zulalian *et al.*, 1994). As a result, MOX is more lipophilic, results in a much higher tissue distribution (Zulalian *et al.*, 1994) and therefore has a longer half-life, thus a different PK profile, which modulates the pharmacodynamics (PD) and toxicity profile (Prichard *et al.*, 2012).

Since the development of a new drug takes several years and requires great monetary investment that is not easily available for NTDs, one of the strategies for drug development for NTDs is drug repurposing. Drug repurposing is the application of an already commercialized drug, or a drug in advanced clinical development phases, to be investigated and used for off-label applications (Pasche *et al.*, 2018).

In the frame of my PhD, we applied the drug repurposing strategy to investigate MOX as an alternative treatment for strongyloidiasis, described in detail in chapter three. Given its structural similarity with IVM, MOX has been investigated in the treatment of whipworm infections, with promising results (Barda *et al.*, 2018, Keller *et al.*, 2019). Our aim was to build knowledge on the drug's activity, and investigate the PK-PD profile of MOX in the treatment of *Strongyloides spp.* infections. We evaluated the *in vitro* activity against L3 larvae and adult female *S. ratti* as well as the PK-PD profile of this drug in the treatment of *S. ratti* infected rats, providing important evidence to move the drug further in the drug development pipeline and support clinical research.

Schistosomiasis

Epidemiology

Schistosomiasis is a water borne disease that affects over 229 million people and is distributed in over 78 countries (WHO, 2020c) on all inhabited continents, including Europe (Gryseels *et al.*, 2006, Holtfreter *et al.*, 2014). Five species infect humans, which, according to the location of the adult worms and corresponding morbidity, cause intestinal or urogenital schistosomiasis. Four species cause intestinal schistosomiasis, namely *Schistosoma intercalatum, S. japonicum, S mansoni and S. mekongi,* while one species causes urogenital schistosomiasis: *S. haematobium* (Despommier, 2017b).

In parallel to the world's population increase, cases of schistosomiasis increased as well; until the 1980's, when the number of cases reached a plateau thanks to the wide use of praziquantel (PZQ) (Bergquist, 2017). More recently, many regions made impressive advances in significantly reducing local schistosomiasis prevalence, such as China, Brazil and Egypt, while the disease even disappeared in Japan, Puerto Rico and most Caribbean islands (Bergquist, 2017). Today, over 90% of the cases occur in sub-Saharan Africa (WHO, 2020c), where also most species coexist (Figure 4). They affect primarily children (normally from the age of two) and young adolescents while performing daily activities as bathing or fishing in *Schistosoma spp.* contaminated water bodies (Colley *et al.*, 2014).

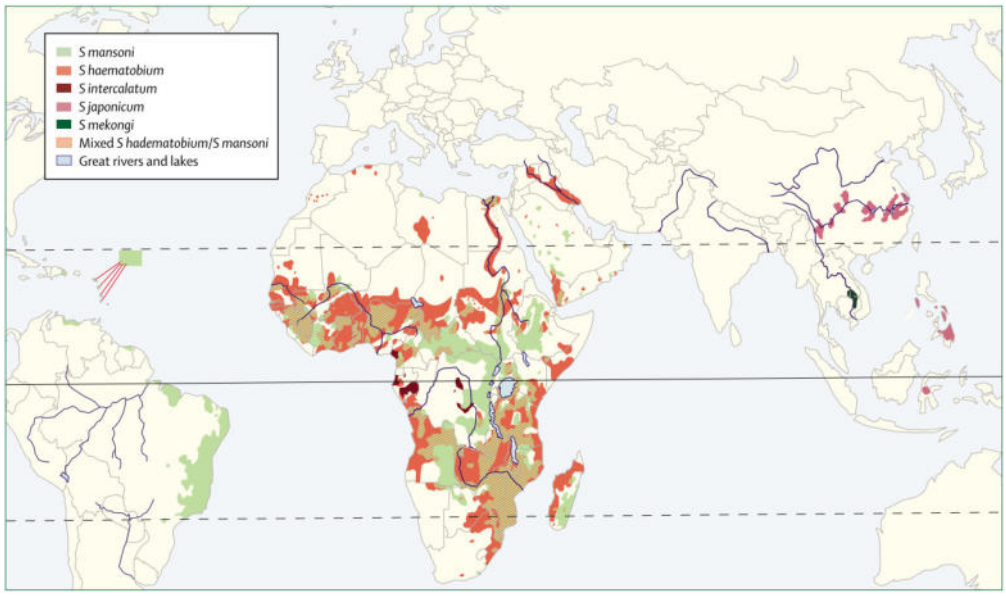

Figure 4: Global distribution of *Schistosoma spp.* according to species.

Only *S. mansoni* is present in the Americas, while *S. mekongi* and *S. japonicum* are present in East Asia. *S. mansoni* and *S. haematobium* account for more than 90% of the cases worldwide, which happen in sub-Saharan Africa. From: Gryseels et al., 2006.

Life cycle

While adult worms of the species causing intestinal schistosomiasis are found in the mesenteric veins and lay eggs that exit the body within the stool, *S. haematobium* adults are found in the perivesicular venules and their eggs exit the body in the urine. Once in contact with water bodies, the eggs of all species hatch and release the miracidia, which then infect freshwater snails. After penetrating the snail, the miracidia multiply asexually into multicellular sporocysts and later develop into thousands of cercarial larvae. Four to six weeks after snail infection and stimulated by daylight, the cercariae leave the snail and swim in the water seeking for a suitable host. Guided by chemotaxis, the cercariae penetrate the skin of humans, migrate in the blood via the lungs to the liver, and transform into young worms or schistosomula. These mature in 4–8 weeks in the portal vein, mate, and, according to the species, migrate to their perivesicular or mesenteric final destination, where the cycle starts again (Gryseels *et al.*, 2006).

Clinical manifestations and diagnostics

In terms of morbidity, it is important to distinguish between urogenital schistosomiasis from intestinal schistosomiasis, and an acute infection from a chronic infection (Despommier,

2017b). While the worms themselves, independent of the species and stage of development, seem not to cause significant morbidity, clinical symptoms arise from the host's immune response against the eggs that cannot leave the body in the stools or urine and remain trapped in the host's circulatory system (Colley *et al.*, 2014, Despommier, 2017b).

The acute phase of the disease, known as Katayama fever, affects people who had no previous contact with the parasite, and appears 4 – 8 weeks after initial exposure, when adult worms pair and begin releasing eggs, which are recognized by the immune system (Despommier, 2017b). Typical symptoms include fever, flu-like symptoms, cough and headache (Despommier, 2017b). If untreated, these symptoms disappear within 2 - 10 weeks, and the infection develops into chronic disease (Despommier, 2017b).

Morbidity during the chronic phase of the disease is caused by the immunopathology resulting from the response against eggs retained either in the liver or in the urinary tract (Despommier, 2017b). Chronic intestinal schistosomiasis is characterized by abdominal pain, diarrhea, and rectal bleeding. Severe cases include extensive fibrosis and subsequent hepatosplenic disease with periportal fibrosis, which can even lead to death (Colley *et al.*, 2014). Different from intestinal schistosomiasis, chronic urogenital schistosomiasis is characterized by hematuria (Colley *et al.*, 2014). If untreated, the poor immunoregulation against the *S. haematobium* eggs leads to chronic fibrosis of the urinary tract, which can facilitate bacterial superinfection as well as result in renal dysfunction with potentially lethal consequences. Additionally, squamous-cell carcinoma of the bladder is also strongly associated with *S. haematobium* infections (Colley *et al.*, 2014).

Two different approaches are normally used for routine diagnosis of intestinal or urogenital schistosomiasis: while the KK method is the gold standard for diagnosis of intestinal schistosomiasis (Gryseels *et al.*, 2006, Yap *et al.*, 2012, WHO, 2020c), the method of choice for urogenital schistosomiasis is urine sedimentation followed by microscopic quantification of eggs (Gryseels *et al.*, 2006, WHO, 2020c). In both cases, the intensity of infection can be estimated from the number of eggs per gram of stool or per 10 ml urine, respectively (Gryseels

et al., 2006). Although these methods are relatively simple and can be applied without major difficulties in the field, they have the limitation of failing to detect light infections and show high inter-day (Kongs *et al.*, 2001) and intra-day variability (Gryseels *et al.*, 2006). As alternative, antibody-based assays proved to detect light infections, but have the limitation of not being able to distinguish between a past and an active infection (Gryseels *et al.*, 2006, WHO, 2020c). Overcoming this limitation, point-of-contact circulating cathodic antigen (POC CCA) and circulating anodic antigen (POC CAA) assays, are able to and detect active infections (de Dood *et al.*, 2018). These assays are based on the detection of circulating schistosomal gut antigens, which are cleared from the kidneys and excreted in urine (de Dood *et al.*, 2018). These sensitive and non-invasive assays are mostly used for mapping and monitoring of endemic areas, but also showed application in non-endemic countries for individual diagnosis of e.g. immigrants (de Dood *et al.*, 2018). As an additional alternative, DNA amplification methods have been evaluated with satisfactory sensitivity as well, but suffered from sampling limitations; given the uneven eggs distribution in the stool samples (Colley *et al.*, 2014).

Control strategies and treatment

The strategy for schistosomiasis control recommended by the WHO includes multiple approaches: (I) large-scale drug treatment of at-risk population groups, (II) access to safe water, improved sanitation, hygiene education (WASH) and (III) snail control (Cioli *et al.*, 2014, Secor, 2014, WHO, 2020c) (Figure 5).

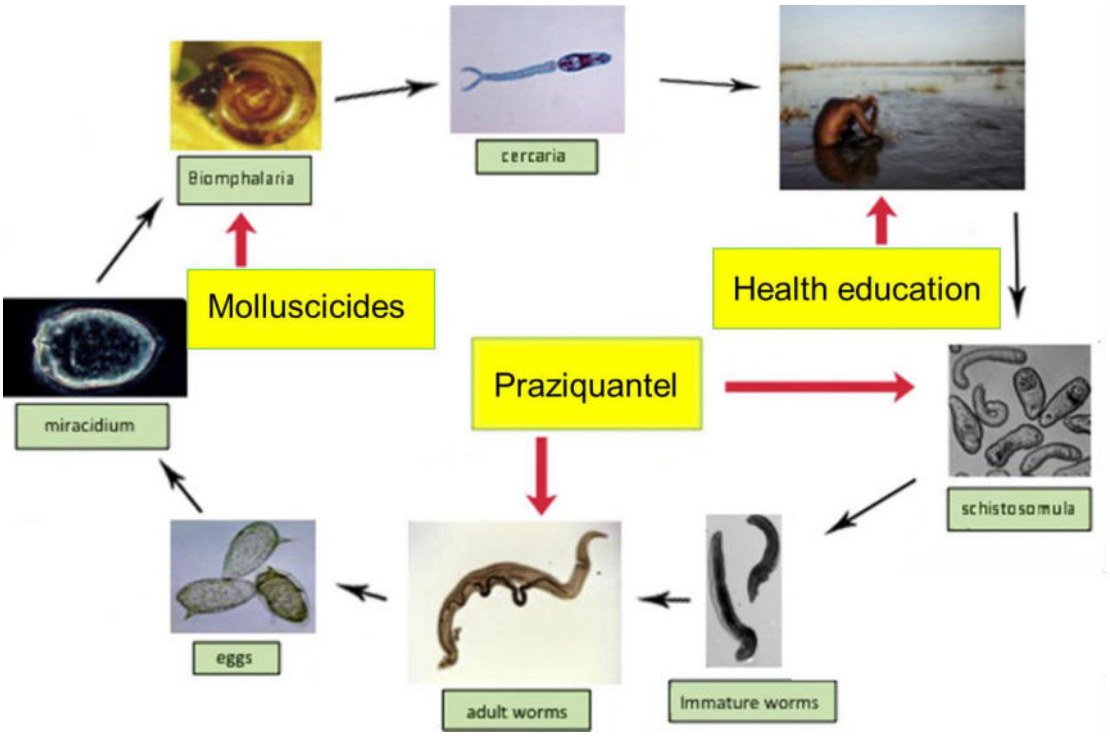

Figure 5: Different approaches used to control *Schistosoma mansoni.*

Integrated control programs are applied in many countries making significant progress. *Schistosoma spp.* control is mostly based on PZQ treatment, while snail control with molluscicides and WASH strategies substantially contribute to the restriction of the transmission cycle. Adapted from Cioli *et al.* 2014.

Many drug candidates were investigated in the last years with more or less success (Lago et al., 2017, Panic et al., 2018). In addition, oxamniquine (OXA), the artemisinins and mefloquine (MFQ), show different degrees of antischistosomal activity but their efficacy is still not satisfactory (Cioli et al., 2014, Colley et al., 2014). As a result, today, the only widely used drug for large-scale administration is PZQ (Colley et al., 2014, WHO, 2020c). Despite having several advantages, such as safety, efficacy against adult stages of all species affecting humans (Lago et al., 2017), low price and ease of distribution, PZQ has several limitations (Cioli et al., 2014). Some of them are its poor activity against juvenile infection stages (Lago et al., 2017), the bitter taste mainly caused by the less active S-isomer (Kovač *et al.*, 2017) and a big tablet size which makes it unattractive to children, for whom pediatric formulations are still under development (Stothard *et al.*, 2013, Consortium, 2020). In addition, the dependence on a single drug for the treatment of millions of people yearly certainly risks the emergence of drug resistance and makes drug development an urgent need (Cioli *et al.*, 2014).

OXA is a safe and highly effective schistosomicidal pro-drug, that is active against adult *S. mansoni* worms and has been the cornerstone of schistosoma control in Brazil for many years (Valentim *et al.*, 2013, Lago *et al.*, 2017), where only *S. mansoni* is present (Gryseels *et al.*, 2006). For activation, OXA needs to be taken up by the worm and sulfonated by a *S. mansoni* specific sulfotransferase (SmSULT), creating an unstable intermediate that alkylates DNA, proteins and macromolecules, thus killing the parasite (Valentim *et al.*, 2013) (Figure 6). Due to point mutations altering the active site of SmSULT, that provided the worms with the ability to survive the treatment, resistance to this drug rapidly spread (Chevalier *et al.*, 2016). In consequence, OXA was withdrawn from the market and replaced by PZQ since 2010 (Valentim *et al.*, 2013).

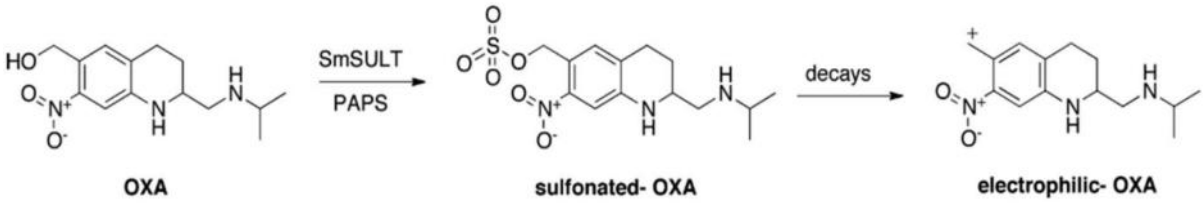

Figure 6: Proposed mechanism of action of OXA.

OXA is a pro-drug that for activation needs the sulfotransferase present in *S. mansoni* and the sulfate-donor, PAPS, to originate a highly reactive molecule (electrophilic OXA). Abbreviations: SmSULT: *S. mansoni* sulfotransferase, PAPS: 3' - phosphoadenosine 5' – phosphosulfate (sulfate donor). From: Hess *et al.,* 2017, adapted from Valentim *et al.,* 2013.

Species-specific sulfotransferases are also present in *S. haematobium* (ShSULT) and *S. japonicum* (SjSULT). ShSULT and SmSULT share over 70% amino acid sequence homology and the active site configurations only differ in three amino acids. Of these three aminoacids, only one significantly affects OXA interaction, and as a result, the pro-drug cannot be activated in *S. haematobium* and OXA is not sufficiently active in this species (Pica-Mattoccia *et al.*, 1997, Valentim *et al.*, 2013).

Alternative molecules under investigation for schistosomiasis are MFQ and the artemisinin derivatives (artemether and artesunate). Complementary to PZQ, the advantage of these drugs is their activity on juvenile stages of parasite development (Liu *et al.*, 2011, El-Beshbishi *et al.*, 2013). However, their efficacy *in vivo* and in clinical trials has not been high enough to be recommended as single therapy (Liu *et al.*, 2011). Considering this situation, it could be

hypothesized that a combination of PZQ and these antimalarials leads to a higher cure rate. However, against chronic *S. haematobium* infections, a study by Keiser et al. showed that the combination of MFQ or MFQ-artesunate with PZQ did not increase the efficacy of PZQ, while the effect on acute infections still needs to be investigated (Keiser *et al.*, 2014). As a result, PZQ still remains the most used drug for *Schistosoma spp.* infections while alternative drugs are urgently needed (Cioli *et al.*, 2014, WHO, 2020c).

Drug development approach: drug derivatization, drug encapsulation

Drug derivatization

By means of the chemical modification of a molecule, important parameters such as polarity, molecular shape, molecular volume, electronic and PK profile or target interaction can be modulated in order to enhance the drug's activity (Chavain *et al.*, 2008). Drug derivatization can be applied to molecules for which the target is known, in order to improve the drug-target interaction, or for the generation of a family of compounds to be investigated in drug screening settings (Patra *et al.*, 2012).

Considering the enzymes structural similarity between Schistosoma species (Pica-Mattoccia *et al.*, 1997) and the great advantage of organometallic derivatization observed in antimalarial drugs (Hess *et al.*, 2015), previous research investigated the potential of organometallic derivatization to enhance OXA's activity (Hess *et al.*, 2017). The third objective of my thesis was to further characterize the activity profile of three promising drug candidates with broad activity spectrum, obtained by organometallic derivatization of OXA. The use of the metal-drug synergism manifests in two beneficial effects resulting from the coordination of an organic drug to a metal ion. The first difference is the enhancement of the biologic activity of the organic drug, possibly due to a longer time of residence of the drug in the organism, allowing it to reach the biological targets more efficiently. The second effect is due to the intrinsic toxicity of the metal moiety itself, which allows for additional redox properties and an improved activity profile with low toxicity (Sánchez-Delgado *et al.*, 2004). Compared to a metallocene administered on its own, while coupled to the organic molecule, the metallocene is less readily available for undesired reactions such as the interaction with enzymes or other damaging reactions, thus

resulting in a localized effect and low systemic toxicity (Sánchez-Delgado *et al.*, 2004, Hess *et al.*, 2017).

Drug encapsulation

Lipid nanocapsules (LNCs) made of Labrafac® (oily phase), Lipoid® S 100 (surfactant) and ethanol can be used to encapsulate hydrophobic molecules and improve their bioavailability (Huynh *et al.*, 2009). LNC provide an inner lipophilic core and protect the molecules loaded from acidic degradation (Huynh *et al.*, 2009). In addition, these LNCs can be covered with polyethylene glycol (PEG), to increase water solubility and extend the parenteral circulation time (Huynh *et al.*, 2009). In the frame of the OXA-derivatives project, once we detected the limitations in the derivatives' solubility and pH stability, we investigated the inclusion of one of the derivatives inside PEGylated - lipid nanocapsules (Figure 7). As described in chapter 4B, we encapsulated the OXA - phenyl derivative in LNC and evaluated its *in vivo* activity.

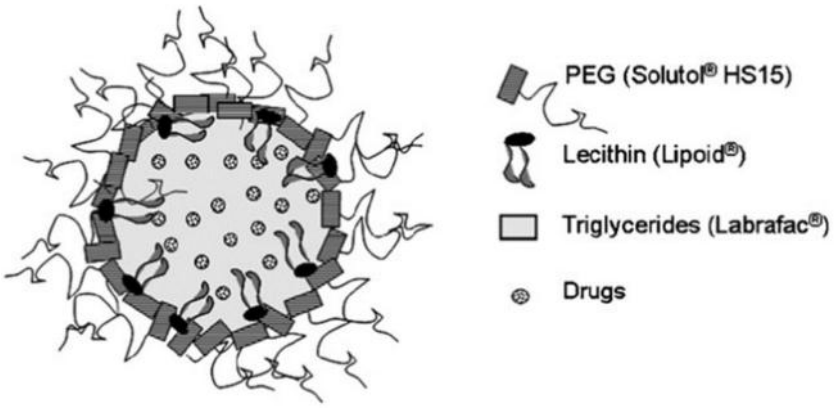

Figure 7: Schematic representation of LNC prepared by the phase-inversion temperature method. From: Huynh *et al.,* 2009.

Animal model for drug research

In contrast to STH and *S. stercoralis*, *Schistosoma spp.* infections can be reproduced in mice (*S. mansoni, S. japonicum)* or hamsters *(S. haematobium).* At Swiss TPH, testing of new drug candidates follows a rational screening cascade (Pasche *et al.*, 2018). Drugs are first tested on larval stages of the parasites that are relatively easily obtained, allowing for large quantities of drugs to be tested. Once a hit has been identified, drug candidates are further tested on adult worms either *in vivo* or *in vitro* (on worms collected from infected mice) (Lombardo *et al.*, 2019). A drawback of this screening cascade is that the activity on juvenile stages of

development is usually missed. The effect of a molecule on juvenile worms is very important to investigate, given the frequently observed differential activity of the drugs against the different stages of development (Kasinathan *et al.*, 2010, Cioli *et al.*, 2014). Drug screening assays on juvenile stages of *S. mansoni* are particularly cumbersome to perform because of the differential maturation time observed between individual worms (Clegg, 1965) and the complex procedure to collect the worms from infected mice (Yolles *et al.*, 1947). In addition, animal welfare regulations promote the reduction of animal use for research purposes (Fenwick *et al.*, 2009). Different strategies have been developed in the last century to grow the worms *in vitro*, but the full life cycle could not be recreated, and reproducibility remains an important drawback (Clegg, 1965, Basch, 1981). Only little advances aiming at recreating the schistosomes life cycle *in vitro* had been done until last year, when Frahm and collaborators described a promising method to fully grow juvenile *S. mansoni in vitro* (Frahm *et al.*, 2019). The fourth objective of my PhD, described in detail in chapter five, was to validate the applicability of this method to drug activity and drug screening assays on juvenile *S. mansoni.* This method allows the growth of high numbers of worms by means of a very simple technique, while saving a high number of mice otherwise needed to grow the worms.

Aim and Objectives

With the overall aim of improving communities' health by developing improved drug treatments, my PhD was focused on four main objectives:

Chapter 2: To improve the efficacy of ABZ and MBZ by enhancing their water solubility and evaluating their *in vivo* and *in vitro* activity against the hookworm model *Heligmosomoides polygyrus.*

Chapter 3: To investigate the PK behavior and the strongycidal potential of MOX in the treatment of rats infected with the *Strongyloides spp.* laboratory model organism *Strongyloides ratti.*

Chapter 4: To fully characterize and evaluate the potential of three organometallic derivatives of OXA as broad-spectrum schistosomicidal drugs.

Chapter 5: To validate the applicability of a full *in vitro* method for growing *S. mansoni* worms as a screening tool on juvenile worms.

References

Ahmed, T. A. 2016. Preparation of finasteride capsules-loaded drug nanoparticles: formulation, optimization, *in vitro*, and pharmacokinetic evaluation. International Journal of Nanomedicine, 11**,** 515-27.

Barda, B., Ame, S. M., Ali, S. M., Albonico, M., Puchkov, M., Huwyler, J.*, et al.* 2018. Efficacy and tolerability of moxidectin alone and in co-administration with albendazole and tribendimidine versus albendazole plus oxantel pamoate against *Trichuris trichiura* infections: a randomised, non-inferiority, single-blind trial. The Lancet Infectious Diseases, 18**,** 864-873.

Barda, B., Cajal, P., Villagran, E., Cimino, R., Juarez, M., Krolewiecki, A.*, et al.* 2014. Mini-FLOTAC, Kato-Katz and McMaster: three methods, one goal; highlights from north Argentina. Parasites & Vectors, 7**,** 271.

Barda, B., Sayasone, S., Phongluxa, K., Xayavong, S., Keoduangsy, K., Odermatt, P.*, et al.* 2017. Efficacy of moxidectin versus ivermectin against *Strongyloides stercoralis* infections: a randomized, controlled noninferiority trial. Clinical Infectious Diseases, 65**,** 276-281.

Barda, B., Schindler, C., Wampfler, R., Ame, S., Ali, S. M. and Keiser, J. 2020. Comparison of real-time PCR and the Kato-Katz method for the diagnosis of soil-transmitted helminthiasis and assessment of cure in a randomized controlled trial. BMC Microbiology, 20**,** 298.

Basch, P. F. 1981. Cultivation of Schistosoma mansoni In vitro. I. Establishment of Cultures from Cercariae and Development until Pairing. The Journal of Parasitology, 67**,** 179-185.

Bergquist, R., Kloos H. and A. Adugna 2017. Schistosomiasis: paleopathological perspectives and historical notes. *In:* Jamieson, B. G. M. (ed.) Schistosoma : biology, pathology and control. Boca Raton: CRC Press Taylor & Francis Group**,** p: 9-34.

Bethony, J., Brooker, S., Albonico, M., Geiger, S. M., Loukas, A., Diemert, D.*, et al.* 2006. Soil-transmitted helminth infections: ascariasis, trichuriasis, and hookworm. The Lancet, 367**,** 1521-1532.

Bisoffi, Z., Buonfrate, D., Angheben, A., Boscolo, M., Anselmi, M., Marocco, S.*, et al.* 2011. Randomized clinical trial on ivermectin versus thiabendazole for the treatment of strongyloidiasis. PLOS Neglected Tropical Diseases, 5**,** e1254.

Bisoffi, Z., Buonfrate, D., Montresor, A., Requena-Méndez, A., Muñoz, J., Krolewiecki, A. J.*, et al.* 2013. *Strongyloides stercoralis*: a plea for action. PLOS Neglected Tropical Diseases, 7**,** e2214.

Boisson, S., Engels, D., Gordon, B. A., Medlicott, K. O., Neira, M. P., Montresor, A.*, et al.* 2016. Water, sanitation and hygiene for accelerating and sustaining progress on neglected tropical diseases: a new Global Strategy 2015–20. International Health, 8**,** i19-i21.

Brooker, S., Hotez, P. J. and Bundy, D. A. P. 2008. Hookworm-related anaemia among pregnant women: a systematic review. PLOS Neglected Tropical Diseases, 2**,** e291.

CDC. 2019. Soil transmitted helminths life cycle [Online]. Available: https://www.cdc.gov/parasites/hookworm/biology.html [Accessed 11.09.2020].

Chavain, N., Vezin, H., Dive, D., Touati, N., Paul, J.-F., Buisine, E.*, et al.* 2008. Investigation of the redox behavior of ferroquine, a new antimalarial. Molecular Pharmaceutics, 5**,** 710-716.

Chevalier, F. D., Le Clec'h, W., Eng, N., Rugel, A. R., Assis, R. R. d., Oliveira, G.*, et al.* 2016. Independent origins of loss-of-function mutations conferring oxamniquine resistance in a brazilian schistosome population. International Journal for Parasitology, 46**,** 417-424.

Cioli, D., Pica-Mattoccia, L., Basso, A. and Guidi, A. 2014. Schistosomiasis control: praziquantel forever? Molecular and Biochemical Parasitology, 195**,** 23-29.

Clegg, J. A. 1965. *In vitro* cultivation of *Schistosoma mansoni*. Experimental Parasitology, 16**,** 133-147.

Cobb, R. and Boeckh, A. 2009. Moxidectin: a review of chemistry, pharmacokinetics and use in horses. Parasites & Vectors, 2**,** S5.

Colley, D. G., Bustinduy, A. L., Secor, W. E. and King, C. H. 2014. Human schistosomiasis. Lancet (London, England), 383**,** 2253-2264.
Consortium, P. P. 2020. Pediatric praziquantel formulation [Online]. Available: https://www.pediatricpraziquantelconsortium.org/node/36 [Accessed 23.09.2020].
de Dood, C. J., Hoekstra, P. T., Mngara, J., Kalluvya, S. E., van Dam, G. J., Downs, J. A.*, et al.* 2018. Refining diagnosis of *Schistosoma haematobium* infections: antigen and antibody detection in urine. Frontiers in immunology, 9**,** 1-9.
Despommier, D., Griffin, D, Gwadz, R, Hotez, P, Knirsch, C. 2017a. Chapter 20: *Strongyloides stercoralis*. Parasitic Diseases Sixth Edition. 6th ed. New York, US: Parasites Without Borders**,** p: 241 - 252.
Despommier, D., Griffin, D, Gwadz, R, Hotez, P, Knirsch, C. 2017b. Chapter 33: The Schistosomes. Parasitic Diseases Sixth Edition. 6 ed. New York, US: Parasites Without Borders**,** p: 391 - 418.
Despommier, D., Griffin, D, Gwadz, R, Hotez, P, Knirsch, C. 2017c. Parasitic Diseases Sixth Edition, New York, US, Parasites Without Borders.
Dokoumetzidis, A. and Macheras, P. 2006. A century of dissolution research: from Noyes and Whitney to the biopharmaceutics classification system. International Journal of Pharmaceutics, 321**,** 1-11.
Easton, A. V., Oliveira, R. G., O'Connell, E. M., Kepha, S., Mwandawiro, C. S., Njenga, S. M.*, et al.* 2016. Multi-parallel qPCR provides increased sensitivity and diagnostic breadth for gastrointestinal parasites of humans: field-based inferences on the impact of mass deworming. Parasites & Vectors, 9**,** 38.
El-Beshbishi, S. N., Taman, A., El-Malky, M., Azab, M. S., El-Hawary, A. K. and El-Tantawy, D. A. 2013. *In vivo* effect of single oral dose of artemether against early juvenile stages of *Schistosoma mansoni* egyptian strain. Experimental Parasitology, 135**,** 240-245.
FDA. 2018. Drug approval and databases: moxidectin [Online]. Available: https://www.fda.gov/drugs/drug-approvals-and-databases/drug-trials-snapshots-moxidectin [Accessed 08.14.2020 2020].
Fenwick, N., Griffin, G. and Gauthier, C. 2009. The welfare of animals used in science: how the "Three Rs" ethic guides improvements. The Canadian veterinary journal, 50**,** 523-530.
Frahm, S., Anisuzzaman, A., Prodjinotho, U. F., Vejzagić, N., Verschoor, A. and Costa, C. P. d. 2019. A novel cell-free method to culture *Schistosoma mansoni* from cercariae to juvenile worm stages for *in vitro* drug testing. PLOS Neglected Tropical Diseases, 13**,** e0006590.
Genta, R. M. 1989. Global prevalence of strongyloidiasis: critical review with epidemiologic insights into the prevention of disseminated disease. Reviews of Infectious Diseases, 11**,** 755-67.
Geurden, T., Chartier, C., Fanke, J., di Regalbono, A. F., Traversa, D., von Samson-Himmelstjerna, G.*, et al.* 2015. Anthelmintic resistance to ivermectin and moxidectin in gastrointestinal nematodes of cattle in Europe. International Journal for Parasitology: Drugs and Drug Resistance, 5**,** 163-171.
Gryseels, B., Polman, K., Clerinx, J. and Kestens, L. 2006. Human schistosomiasis. The Lancet, 368**,** 1106-1118.
Henriquez-Camacho, C., Gotuzzo, E., Echevarria, J., White, A. C., Jr., Terashima, A., Samalvides, F.*, et al.* 2016. Ivermectin versus albendazole or thiabendazole for *Strongyloides stercoralis* infection. Cochrane Database Syst Rev**,** Cd007745.
Hess, J., Keiser, J. and Gasser, G. 2015. Toward organometallic antischistosomal drug candidates. Future Medicinal Chemistry, 7**,** 821-830.
Hess, J., Panic, G., Patra, M., Mastrobuoni, L., Spingler, B., Roy, S.*, et al.* 2017. Ferrocenyl, ruthenocenyl, and benzyl oxamniquine derivatives with cross-species activity against *Schistosoma mansoni* and *Schistosoma haematobium*. ACS infectious diseases, 3**,** 645-652.
Hofmann, D., Sayasone, S., Sengngam, K., Chongvilay, B., Hattendorf, J. and Keiser, J. In press 2020. Efficacy and safety of ascending dosages of moxidectin against

Strongyloides stercoralis infections in adults: a randomized, blinded, placebo-controlled, dose-ranging, phase 2a trial. Accepted: The Lancet Infectious Diseases.
Holtfreter, M. C., Moné, H., Müller-Stöver, I., Mouahid, G. and Richter, J. 2014. *Schistosoma haematobium* infections acquired in Corsica, France, August 2013. Euro Surveillance, 19**,** 20821.
Hotez, P. J., Alvarado, M., Basáñez, M.-G., Bolliger, I., Bourne, R., Boussinesq, M.*, et al.* 2014. The global urden of disease study 2010: interpretation and implications for the neglected tropical diseases. PLOS Neglected Tropical Diseases, 8**,** e2865.
Hotez, P. J., Brooker, S., Bethony, J. M., Bottazzi, M. E., Loukas, A. and Xiao, S. 2004. Hookworm Infection. The New England Journal of Medicine, 351**,** 799-807.
Hotez, P. J., Fenwick, A., Savioli, L. and Molyneux, D. H. 2009. Rescuing the bottom billion through control of neglected tropical diseases. The Lancet, 373**,** 1570-1575.
Hürlimann, E. and Keiser, J. 2019. A single dose of ivermectin is sufficient for strongyloidiasis. Lancet Infectious Diseases, 19**,** 1150-1151.
Huynh, N. T., Passirani, C., Saulnier, P. and Benoit, J. P. 2009. Lipid nanocapsules: a new platform for nanomedicine. International Journal of Pharmaceutics, 379**,** 201-9.
Jorgensen, T., Montresor, A. and Savioli, L. 1996. Effectively controlling strongyloidiasis. Parasitology Today, 12**,** 164.
Jourdan, P. M., Lamberton, P. H. L., Fenwick, A. and Addiss, D. G. 2018. Soil-transmitted helminth infections. Lancet, 391**,** 252-265.
Jung, H., Medina, L., García, L., Fuentes, I. and Moreno-Esparza, R. 1997. Biopharmaceutics: absorption studies of albendazole and some physicochemical properties of the drug and its metabolite albendazole sulphoxide. Journal of Pharmacy and Pharmacology, 50**,** 43-48.
Kang, B.-S., Lee, S.-E., Ng, C. L., Kim, J.-K. and Park, J.-S. 2015. Exploring the preparation of albendazole-loaded chitosan-tripolyphosphate nanoparticles. Materials, 8**,** 486-498.
Kasinathan, R. S., Morgan, W. M. and Greenberg, R. M. 2010. *Schistosoma mansoni* express higher levels of multidrug resistance-associated protein 1 (SmMRP1) in juvenile worms and in response to praziquantel. Molecular and Biochemical Parasitology, 173**,** 25-31.
Katz, N., Chaves, A. and Pellegrino, J. 1972. A simple device for quantitative stool thick-smear technique in *Schistosomiasis mansoni*. Revista do Instituto de Medicina Tropical de Sao Paulo, 14**,** 397-400.
Keiser, J., Silué, K. D., Adiossan, L. K., N'Guessan, N. A., Monsan, N. C., Utzinger, J.*, et al.* 2014. Praziquantel, mefloquine-praziquantel, and mefloquine-artesunate-praziquantel against *Schistosoma haematobium*: a randomized, exploratory, open-label trial. PLOS neglected tropical diseases, 8**,** e2975-e2975.
Keiser, J. and Utzinger, J. 2008. Efficacy of current drugs against soil-transmitted helminth infections: systematic review and meta-analysis. JAMA, 299**,** 1937-1948.
Keiser, J. and Utzinger, J. 2010. Chapter 8 - The drugs we have and the drugs we need against major helminth infections. *In:* Zhou, X.-N., Bergquist, R., Olveda, R. & Utzinger, J. (eds.) Advances in Parasitology. Academic Press**,** p: 197-230.
Keller, L., Palmeirim, M. S., Ame, S. M., Ali, S. M., Puchkov, M., Huwyler, J.*, et al.* 2019. Efficacy and safety of ascending dosages of moxidectin and moxidectin-albendazole against *Trichuris trichiura* in adolescents: a randomized controlled trial. Clinical Infectious Diseases.
Keller, L., Patel, C., Welsche, S., Schindler, T., Hürlimann, E. and Keiser, J. 2020. Performance of the Kato-Katz method and real time polymerase chain reaction for the diagnosis of soil-transmitted helminthiasis in the framework of a randomised controlled trial: treatment efficacy and day-to-day variation. Parasites & Vectors, 13**,** 517.
Kongs, A., Marks, G., Verlé, P. and Van der Stuyft, P. 2001. The unreliability of the Kato-Katz technique limits its usefulness for evaluating *S. mansoni* infections. Tropical Medicine and International Health, 6**,** 163-169.
Kovač, J., Vargas, M. and Keiser, J. 2017. *In vitro* and *in vivo* activity of R- and S- praziquantel enantiomers and the main human metabolite trans-4-hydroxy-praziquantel against *Schistosoma haematobium*. Parasites & Vectors, 10.

Kyu, H. H., Abate, D., Abate, K. H., Abay, S. M., Abbafati, C., Abbasi, N., *et al.* 2018. Global, regional, and national disability-adjusted life-years (DALYs) for 359 diseases and injuries and healthy life expectancy (HALE) for 195 countries and territories, 1990–2017: a systematic analysis for the Global Burden of Disease Study 2017. The Lancet, 392**,** 1859-1922.

Lacey, E. 1990. Mode of action of benzimidazoles. Parasitology Today, 6**,** 112-115.

Lago, E. M., Xavier, R. P., Teixeira, T. R., Silva, L. M., da Silva Filho, A. A. and de Moraes, J. 2017. Antischistosomal agents: state of art and perspectives. Future Medicinal Chemistry, 10**,** 89-120.

Lim, M. D., Brooker, S. J., Belizario, V. Y., Jr., Gay-Andrieu, F., Gilleard, J., Levecke, B., *et al.* 2018. Diagnostic tools for soil-transmitted helminths control and elimination programs: a pathway for diagnostic product development. PLOS neglected tropical diseases, 12**,** e0006213-e0006213.

Lipinski, C. A., Lombardo, F., Dominy, B. W. and Feeney, P. J. 1997. Experimental and computational approaches to estimate solubility and permeability in drug discovery and development settings. Advanced Drug Delivery Reviews, 23**,** 3-25.

Liu, R., Dong, H.-F., Guo, Y., Zhao, Q.-P. and Jiang, M.-S. 2011. Efficacy of praziquantel and artemisinin derivatives for the treatment and prevention of human schistosomiasis: a systematic review and meta-analysis. Parasites & Vectors, 4**,** 201.

Lo, N. C., Bogoch, II, Blackburn, B. G., Raso, G., N'Goran, E. K., Coulibaly, J. T., *et al.* 2015. Comparison of community-wide, integrated mass drug administration strategies for schistosomiasis and soil-transmitted helminthiasis: a cost-effectiveness modelling study. Lancet Global Health, 3**,** e629-38.

Lombardo, F. C., Pasche, V., Panic, G., Endriss, Y. and Keiser, J. 2019. Life cycle maintenance and drug-sensitivity assays for early drug discovery in *Schistosoma mansoni*. Nature Protocols**,** 1.

Mendes, T., Minori, K., Ueta, M., Miguel, D. C. and Allegretti, S. M. 2017. Strongyloidiasis current status with emphasis in diagnosis and drug research. Journal of Parasitology Research, 2017**,** 5056314.

Moser, W., Schindler, C. and Keiser, J. 2017. Efficacy of recommended drugs against soil transmitted helminths: systematic review and network meta-analysis. BMJ**,** j4307.

Olsen, A., van Lieshout, L., Marti, H., Polderman, T., Polman, K., Steinmann, P., *et al.* 2009. Strongyloidiasis – the most neglected of the neglected tropical diseases? Transactions of The Royal Society of Tropical Medicine and Hygiene, 103**,** 967-972.

Palmeirim, M. S., Ame, S. M., Ali, S. M., Hattendorf, J. and Keiser, J. 2018. Efficacy and safety of a single dose versus a multiple dose regimen of mebendazole against hookworm infections in children: a randomised, double-blind trial. E Clinical Medicine, 1**,** 7-13.

Panic, G. and Keiser, J. 2018. Acting beyond 2020: better characterization of praziquantel and promising antischistosomal leads. Current Opinion in Pharmacology, 42**,** 27-33.

Paredes, A. J., Bruni, S. S., Allemandi, D., Lanusse, C. and Palma, S. D. 2018. Albendazole nanocrystals with improved pharmacokinetic performance in mice. Therapeutic Delivery, 9**,** 89-97.

Pasche, V., Laleu, B. and Keiser, J. 2018. Screening a repurposing library, the Medicines for Malaria Venture Stasis Box, against *Schistosoma mansoni*. Parasites & Vectors, 11**,** 298.

Patra, M., Ingram, K., Pierroz, V., Ferrari, S., Spingler, B., Keiser, J., *et al.* 2012. Ferrocenyl derivatives of the anthelmintic praziquantel: design, synthesis, and biological evaluation. Journal of Medicinal Chemistry, 55**,** 8790-8798.

Paula, F. M. d., Malta, F. M., Corral, M. A., Marques, P. D., Gottardi, M., Meisel, D. M. C. L., *et al.* 2016. Diagnosis of *Strongyloides stercoralis* infection in immunocompromised patients by serological and molecular methods. Revista do Instituto de Medicina Tropical de Sao Paulo, 58**,** 63-63.

Pica-Mattoccia, L., Novi, A. and Cioli, D. 1997. Enzymatic basis for the lack of oxamniquine activity in *Schistosoma haematobium* infections. Parasitology Research, 83**,** 687-689.

Prichard, R., Ménez, C. and Lespine, A. 2012. Moxidectin and the avermectins: consanguinity but not identity. International journal for parasitology: Drugs and drug resistance, 2**,** 134-153.
Pullan, R. L., Smith, J. L., Jasrasaria, R. and Brooker, S. J. 2014. Global numbers of infection and disease burden of soil transmitted helminth infections in 2010. Parasites & Vectors, 7**,** 37.
Sánchez-Delgado, R. A. and Anzellotti, A. 2004. Metal complexes as chemotherapeutic agents against tropical diseases: trypanosomiasis, malaria and leishmaniasis. Mini Reviews in Medicinal Chemistry, 4**,** 23-30.
Savjani, K. T., Gajjar, A. K. and Savjani, J. K. 2012. Drug solubility: importance and enhancement techniques. ISRN Pharmaceutics, 2012.
Schär, F., Trostdorf, U., Giardina, F., Khieu, V., Muth, S., Marti, H.*, et al.* 2013. *Strongyloides stercoralis*: global distribution and risk factors. PLOS Neglected Tropical Diseases, 7**,** e2288-e2288.
Secor, E. W. 2014. Water-based interventions for schistosomiasis control. Pathogens and Global Health, 108**,** 246-254.
Speich, B., Knopp, S., Mohammed, K. A., Khamis, I. S., Rinaldi, L., Cringoli, G.*, et al.* 2010. Comparative cost assessment of the Kato-Katz and FLOTAC techniques for soil-transmitted helminth diagnosis in epidemiological surveys. Parasites & Vectors, 3**,** 71.
Steinmann, P., Zhou, X.-N., Du, Z.-W., Jiang, J.-Y., Wang, L.-B., Wang, X.-Z.*, et al.* 2007. Occurrence of *Strongyloides stercoralis* in Yunnan province, China, and comparison of diagnostic methods. PLOS Neglected Tropical Diseases, 1**,** e75-e75.
Stothard, J. R., Sousa-Figueiredo, J. C., Betson, M., Bustinduy, A. and Reinhard-Rupp, J. 2013. Schistosomiasis in african infants and preschool children: let them now be treated! Trends in Parasitology, 29**,** 197-205.
Streit, A. 2008. Reproduction in *Strongyloides* (Nematoda): a life between sex and parthenogenesis. Parasitology, 135**,** 285-294.
Tilney, L. G., Connelly, P. S., Guild, G. M., Vranich, K. A. and Artis, D. 2005. Adaptation of a nematode parasite to living within the mammalian epithelium. Journal of Experimental Zoology, 303A**,** 927-945.
Tsume, Y., Mudie, D. M., Langguth, P., Amidon, G. E. and Amidon, G. L. 2014. The biopharmaceutics classification system: subclasses for *in vivo* predictive dissolution (IPD) methodology and IVIVC. European Journal of Pharmaceutical Sciences: Official Journal of the European Federation for Pharmaceutical Sciences, 57**,** 152-163.
Valentim, C. L. L., Cioli, D., Chevalier, F. D., Cao, X., Taylor, A. B., Holloway, S. P.*, et al.* 2013. Genetic and molecular basis of drug resistance and species-specific drug action in schistosome parasites. Science (New York, N.Y.), 342**,** 1385-1389.
WHO 2006. Preventive chemotherapy in human helminthiasis: coordinated use of anthelminthic drugs in control interventions - A manual for health professionals and programme managers. .
WHO 2012. Soil transmitted helminthiasis: eliminating soil transmitted helminthiasis as a public health problem in children. *In:* Montresor, D. A. (ed.).
WHO 2015a. Investing to overcome the global impact of neglected tropical diseases. Third WHO report on neglected tropical diseases. Geneva, Switzerland.
WHO 2015b. Water sanitation and hygiene for accelerating and sustaining progress on neglected tropical diseases: a global strategy 2015-2020.
WHO 2017. Guideline: preventive chemotherapy to control soil-transmitted helminth infections in at-risk population groups

Guideline: preventive chemotherapy to control soil-transmitted helminth infections in at-risk population groups. Geneva: WHO.
WHO 2019a. 2030 targets for soil-transmitted helminthiases control programmes. Licence: CC BY-NC-SA 3.0 IGO. ed.: Geneva: WHO.
WHO. 2019b. World Health Organization - Model list of essential medicines - 21st list [Online]. Available: https://apps.who.int/iris/bitstream/handle/10665/325771/WHO-MVP-EMP-IAU-2019.06-eng.pdf?ua=1 [Accessed 11.09.2020].

WHO. 2020a. African programme for onchocerciasis control (APOC) [Online]. Available: https://www.who.int/apoc/cdti/ivermectin/en/ [Accessed 21.08 2020].
WHO. 2020b. Neglected tropical diseases [Online]. Available: https://www.who.int/neglected_diseases/diseases/en/ [Accessed 04.09 2020].
WHO. 2020c. Schistosomiasis [Online]. Available: https://www.who.int/news-room/fact-sheets/detail/schistosomiasis [Accessed 04.11 2020].
WHO. 2020d. Soil-transmitted helminth infections [Online]. Available: https://www.who.int/news-room/fact-sheets/detail/soil-transmitted-helminth-infections [Accessed 04.11.2020].
WHO. 2020e. Strongyloidiasis [Online]. Available: https://www.who.int/intestinal_worms/epidemiology/strongyloidiasis/en/ [Accessed 04.11 2020].
Yap, P., Fürst, T., Müller, I., Kriemler, S., Utzinger, J. and Steinmann, P. 2012. Determining soil-transmitted helminth infection status and physical fitness of school-aged children. Journal of visualized experiments : JoVE**,** e3966-e3966.
Yolles, T. K., Moore, D. V., DeGiusti, D. L., Ripsom, C. A. and Meleney, H. E. 1947. A technique for the perfusion of laboratory animals for the recovery of schistosomes. The Journal of Parasitology, 33**,** 419-426.
Zulalian, J., Stout, S. J., daCunha, A. R., Garces, T. and Miller, P. 1994. Absorption, tissue distribution, metabolism, and excretion of moxidectin in cattle. Journal of Agricultural and Food Chemistry, 42**,** 381-387.

Chapter II

Preparation, physicochemical characterization and *in vitro* and *in vivo* activity against *Heligmosomoides polygyrus* of novel oral formulations of albendazole and mebendazole

Journal of Pharmaceutical Sciences 109 (2020) 1819-1826

Contents lists available at ScienceDirect

Journal of Pharmaceutical Sciences

journal homepage: www.jpharmsci.org

Global Health

Preparation, Physicochemical Characterization and *In Vitro* and *In Vivo* Activity Against *Heligmosomoides polygyrus* of Novel Oral Formulations of Albendazole and Mebendazole

Valentin Buchter [1, 2], Josefina Priotti [3], Darío Leonardi [3, 4], María C. Lamas [3, 4], Jennifer Keiser [1, 2, *]

[1] *Swiss Tropical and Public Health Institute, Socinstrasse 57, P.O. Box CH-4002, Basel, Switzerland*
[2] *University of Basel, Petersplatz 1, P.O. Box CH-4001, Basel, Switzerland*
[3] *IQUIR-CONICET, Suipacha 570, S2002LRK, Rosario, Argentina*
[4] *Departamento de Farmacia, Facultad de Ciencias Bioquímicas y Farmacéuticas, Universidad Nacional de Rosario, Suipacha 570, S2002LRK, Rosario, Argentina*

ARTICLE INFO

Article history:
Received 2 August 2019
Revised 19 December 2019
Accepted 7 February 2020
Available online 15 February 2020

Keywords:
albendazole
mebendazole
chitosan microcrystals
cyclodextrin complexes
polysorbate 80
polyvinyl alcohol

ABSTRACT

Albendazole (ABZ) and mebendazole (MBZ) are the 2 most commonly used drugs in the treatment of soil-transmitted helminth infections in humans, but their performance is hampered by low solubility and physicochemical properties. We developed different formulations (β-cyclodextrin inclusion complexes, chitosan-based microcrystals (CH), and polyvinyl alcohol and polysorbate 80–based nanoparticles [P80]) of ABZ and MBZ with an improved *in vitro* solubility profile and tested their activities *in vitro* and *in vivo* against the hookworm *Heligmosomoides polygyrus*. We found that all formulations tested showed a faster and higher dissolution level and were more active than the standard drugs. When compared to ABZ, ABZ-P80 revealed the highest improvement in terms of solubility increase (4-fold increase) and *in vivo* activity (an ED_{50} of 7.0 mg/kg for ABZ and of 4.1 mg/kg for ABZ-P80). Although the activity of MBZ was in all cases lower than ABZ, the improved formulations of MBZ performed better than standard MBZ, where MBZ-CH showed a significantly higher *in vivo* activity (ED_{50} of 8.02 mg/kg vs. an ED_{50} of 203 mg/kg for MBZ). In this work, we identified MBZ-CH and ABZ-P80 formulations as lead formulations hence further studies should be conducted.

Introduction

Soil-transmitted helminth (STH) infections are human parasitic diseases caused by the infection with at least one of the following nematodes: roundworms (*Ascaris lumbricoides*), hookworms (*Ancylostoma duodenale, Necator americanus*), or whipworms (*Trichuris trichiura*). These parasites affect one of 4 habitants worldwide—1.5 billion people or 24% of the world population—living in tropical and subtropical settings where sanitation is poor.[1] To control STH infections, 4 drugs are currently on the WHO model list of essential medicines, namely albendazole (ABZ), mebendazole (MBZ), levamisole, and pyrantel pamoate,[2,3] the former 2 are the most widely used in preventive chemotherapy programs. Different systematic reviews and meta-analyses performed in the last years comparing the efficacy of these anthelmintics used in a single-dose regimen agree that both drugs reach acceptable cure rates for *A. lumbricoides*, whereas only ABZ shows moderate cure rates against hookworm infections (72%[4]) and none of the drugs perform well against *T. trichiura* infections.[4-6]

ABZ has a solubility of 1 μg/mL,[7] and MBZ shows polymorphism with different solubility in water, 9.8, 71.3, and 35.4 μg/mL for polymorphs A, B, and C, respectively.[8] According to the United States Pharmacopeia (USP), both active pharmaceutical ingredients (APIs) are practically insoluble in water and are categorized as class II in the Biopharmaceutical Classification System[9]; therefore, they present high permeability and low water solubility. Because of these properties, a big limitation of these drugs is the resulting erratic

Abbreviations used: ABZ, albendazole; MBZ, mebendazole; STH, soil-transmitted helminth; P80, polysorbate 80-based nanoparticles; CH, chitosan-based microcrystals; PVA, polyvinyl alcohol nanoparticles; IC_{50}, half-maximal inhibitory concentration; ED_{50}, effective 50% dose; DR, dissolution rate.

This article contains supplementary material available from the authors by request or via the Internet at https://doi.org/10.1016/j.xphs.2020.02.002.

* *Correspondence to:* Jennifer Keiser (Telephone: +41612848218).
E-mail address: jennifer.keiser@swisstph.ch (J. Keiser).

https://doi.org/10.1016/j.xphs.2020.02.002
0022-3549/

bioavailability,[6,10] which might contribute to the variable efficacy observed among individuals. Jung et al.[10] identified the solubility and not the absorption mechanism (supposed to be passive) as the limiting factor for bioavailability; thus, *in vivo* dissolution is a critical determinant for absorption, bioavailability, and subsequent bioequivalence determinations.[11]

All commercialized forms of ABZ and MBZ in Europe include solubility-enhancing excipients and matrixes (e.g., sodium lauryl sulfate).[12,13] Nonetheless, in the last decades, significant amount of work has been carried out to refine the solubility and dissolution rate (DR), improving the physicochemical properties of ABZ and MBZ including particle size reduction, solid dispersion, inclusion complex formation with cyclodextrins (CDs), nanosuspensions using polymers and surfactants,[14-16] and salt formation.[13] The smaller the particle size, the larger the surface area and the faster the DR of drug particles.[17] The drug DR is a direct proportion of its effective surface area and could be increased mainly in 2 ways: decreasing the particle size of the drug and optimizing the wettability, a parameter directly related to the contact angle.[18,19]

The main objective of this study was to prepare novel formulations of ABZ and MBZ: nanoparticles, microcrystals, and CD inclusion complexes aiming to increase their solubility and DR, based on the increase of total exposure surface as well as on optimizing the wetting characteristics, to enhance the anthelmintic effect. We quantitatively compared the *in vitro* dissolution profiles and *in vivo*/*in vitro* activity of these formulations of ABZ and MBZ using the mouse hookworm *Heligmosomoides polygyrus* as a model of helminth infection to identify the best formulation, which could proceed into further preclinical studies.

Experimental Section

Chemicals

ABZ, albendazole sulfoxide (ABZSO), and MBZ used as reference APIs were purchased from Sigma-Aldrich (Buchs, Switzerland). ABZ, MBZ, maltodextrin (MD), and polysorbate 80 (P80) for the improved formulations were purchased from Parafarm (Buenos Aires, Argentina). Polyvinyl alcohol ((PVA), 87%-89%, mol. wt. 13,000-23,000) and chitosan ((CH), mol. wt. 310-375 kDa, >75% deacetylated) were obtained from Sigma-Aldrich.

Preparation of the Improved Formulations of ABZ and MBZ

The content of API in each of the formulations and the proportion of excipients used in each of the formulations are summarized in Table 1.

Preparation of Microcrystals

Microcrystals of ABZ and MBZ were obtained by controlled precipitation (bottom-up technique).[16,20,21] A 0.1% w/v CH solution was prepared in 1% v/v acetic acid. ABZ was dissolved in acetic acid and MBZ in formic acid, followed by addition of absolute ethanol at a ratio organic acid/alcohol 1/1.5 to get a final drug concentration of 40 mg/mL. These solutions were added to the CH solution, under stirring at 1000 rpm. After 10 min, the suspensions obtained were dried using a Mini Büchi Spray Dryer B-290 (inlet temperature 135°C, pump efficiency 12%, and aspirator 100%).

Preparation of the Nanoparticles from the Nanosuspensions

Nanoparticles were produced by controlled precipitation and stabilization. The procedure was carried out with a hydrophilic polymer (PVA) and a nonionic surfactant (P80).

To obtain PVA nanosuspensions, ABZ and MBZ were dissolved in acetic and formic acid, respectively (50 mg/mL) and then 1 mL of the solutions was precipitated into 10 mL of PVA solution (0.5% w/v) and MD under stirring at 1000 rpm.

ABZ-P80 nanoparticles were prepared by adding 1 mL of the ABZ solution in acetic acid (100 mg/mL) to 5 mL of P80 solution (0.5% v/v) and MD, under stirring at 300 rpm. Nanosuspensions were immediately dried using a Mini Büchi Spray Dryer B-290 (inlet temperature 130°C, pump efficiency 15%, and aspirator 100%). The ratios of ABZ or MBZ to MD in all formulations were 1:1 (weight ratio) (Table 1).

Preparation of Inclusion Complexes with Citrate-β-Cyclodextrin

Inclusion complexes with citrate-β-CD (C-β-CD) were prepared according to Garcia et al.[15] in a 1:1 molar ratio. To prepare the ABZ-CD complex, ABZ (0.565 mmol, 150 mg) was solubilized in 15 mL of acetic acid, and C-β-CD (0.565 mmol) was solubilized in 60 mL of bidistilled water. To prepare the MBZ-CD complex, MBZ (0.508 mmol, 150 mg) and C-β-CD (0.508 mmol) were solubilized in formic acid (15 mL) and bidistilled water (70 mL), respectively. Drug and C-β-CD solutions were mixed under stirring and immediately dried using a Büchi Mini Spray Dryer B-290 under the following conditions: temperature 130°C, flow rate 5 mL/min, and aspirator set at 100%. The solid product obtained was kept in an oven at 40°C for 24 h.

Particle Size Determination

The particle size of the APIs, CH microcrystals, and inclusion complexes was determined by imaging, using scanning electron microscopy (Leitz AMR 1600 T [Amray, Bedford, MA]), with an acceleration potential of 20 kV. Samples were sputter-coated with a gold layer to make them conductive. Scanning electron microscopy images were analyzed using the ImageJ software to estimate particle size. Particle size of nanosuspensions was determined by using a Nano Particle Analyzer Horiba SZ-100 (Germany). Samples were diluted (1:30) in filtered distilled water before measuring.

Table 1
Composition of the ABZ and MBZ Formulations

Formulations	Sample Name	Composition	w/w Proportion	% Drug in Sample
Nanoparticles	ABZ-PVA	ABZ/PVA/MD	1:1:1	33
	MBZ-PVA	MBZ/PVA/MD	1:1:1	33
	ABZ-P80	ABZ/P80/MD	1:0.275:1	44
Microcrystals	ABZ-CH	ABZ/CH	1:0.25	80
	MBZ-CH	MBZ/CH	1:0.25	80
			Molar proportion	
Inclusion complexes	ABZ-CD	ABZ/C-β-CD	1:1	15.2
	MBZ-CD	MBZ/C-β-CD	1:1	18.2

Solubility and Dissolution Studies

The solubility of ABZ and MBZ in the different formulations was determined adding an excess amount (corresponding to 25 mg of API) in sealed vials with 5 mL of 0.1 N HCl, in an orbital shaker at 180 rpm for 72 h. Afterward, the solutions were filtered through 0.45 μm PVDF filters and the concentration of API was determined by UV spectroscopy at 290.8 nm (ABZ formulations) and at 285.0 nm (MBZ formulations) in a Shimadzu spectrophotometer.

Dissolution studies of APIs and ABZ or MBZ formulations were performed in a Hanson Research, SR8 8-Flask Bath equipment as described.[22-24] The conditions were as follows: rotating paddle (apparatus II) speed of 50 rpm (ABZ formulations) and 75 rpm (MBZ formulations), dissolution medium HCl 0.1 N (900 mL), and temperature of 37.0 ± 0.1°C.

Powdered samples of each formulation, equivalent to 100 mg of API, were spread on the surface of the dissolution media. Aliquots of 5 mL were withdrawn at different time intervals (10, 20, 30, 45, 60, 90, 120, 240, and 300 min) and filtered, and the percentage of drug dissolved was calculated from concentrations obtained by spectrophotometry. Dissolution efficiency of the dosage forms was calculated following the procedure proposed by Khan.[25] For each formulation, the dissolution efficiency was calculated as the percentage ratio of the area under the dissolution curve up to time t to that of the area of the rectangle described by 100% dissolution in the same time (Q_{100}), using the following equation[26]:

$$\text{Dissolution efficiency } (\%) = \frac{AUC_0^t}{Q_{100} \cdot t} \times 100 \quad (1)$$

The area under the dissolution curve was performed using GraphPad Prism 7.00 (GraphPad Software, San Diego, CA). Solubility and dissolution experiments were carried out in triplicate.

In accordance to USP procedures,[22] the dissolution medium for MBZ is 0.1 N HCl containing 1% sodium lauryl sulfate, an anionic surfactant. This amount of surfactant produces an extremely rapid dissolution of the API that makes it impossible to detect differences in the DR of pure drug respect to the improved formulations. For that reason, we decided to carry out the dissolution studies without sodium lauryl sulfate.[27]

Animals and Parasites

The complete life cycle of *H. polygyrus* is maintained at Swiss TPH. *H. polygyrus* is an excellent model for hookworm infections.[28] All animal experiments were authorized by the Canton Basel-Stadt, Switzerland (license number 2070). During the experiment, mice were kept in the Swiss TPH animal facilities at 22°C, 50% humidity, with a 12-h light/dark cycle, and water and rodent food (KLIBA NAFAG, Switzerland) were available for them *ad libitum*. Three-week-old female NMRI mice were ordered from Charles River (Sulzfeld, Germany) and were allowed to acclimatize to the new environment for 1 week before being manipulated. During the acclimatization period, from day 2 after arrival and until 2 days before treatment, the animals received dexamethasone (Sigma-Aldrich, Buchs, Switzerland) in the drinking water at a concentration of 0.25 mg/L to immunosuppress them and support parasite establishment. Mice were infected via oral gavage with 90 *H. polygyrus* L3 stage larvae on day 7 after arrival and treated with the drugs by oral gavage on days 21 or 22 from arrival (14 days after infection). The control group consisted of 4 mice following the same procedure but remained untreated.

In Vitro *Activity Testing Against* H. polygyrus

For the *in vitro* studies, the adult worms were harvested from the infected mice by dissection. The worms were maintained at 37°C and 5% CO_2 in a medium until use (always within a period not longer than 2 days after being collected). The assay medium pH 7.2 consisted of RPMI 1640 (Sigma-Aldrich) supplemented with 6 g/L Hepes buffer, 2.6 g/L sodium bicarbonate, 500 U/mL penicillin, 500 mg/mL streptomycin (LubioScience, Switzerland), and 2.5 mg/mL amphotericin B (Sigma-Aldrich).

The acidic mediums were prepared using RPMI, 500 U/mL penicillin, 500 mg/mL streptomycin, and 2.5 mg/mL amphotericin B and buffered to pH 4, 5, and 6 using the McIlvaine buffer. The pH was finally adjusted to the desired level using a Mettler FiveEasy pH meter®.

ABZ, MBZ, and the formulations were prepared as 10 mM stock solutions regarding the content of API in dimethyl sulfoxide (Sigma-Aldrich), and diluted in culture medium to 200, 100, and 50 μM in a final volume of 2.0 mL. Three to 4 worms per well were added into a plate and incubated for 72 h.

When preparing the 10 mM stock solutions in dimethyl sulfoxide for the *in vitro* studies, the drugs and excipients were in all cases perfectly dissolved and the solution was transparent, but when diluting the stock solutions with culture medium, different amounts of crystals precipitated after some minutes. The precipitate formation was proportional to the concentration used and in all cases the crystals of the improved formulations were smaller and more uniformly distributed than the crystals formed from the pure drugs, according to microscopy observation.

To increase the worms' motility at the end point, the viability scoring was performed after addition of 500 μL water at 80 ± 3°C. The viability was determined using a phenotypic readout evaluating parasite's motility, transparency, and morphology on a scale between 3 (normal phenotype) and zero (highly impaired phenotype; dead parasite).[29] All *in vitro* experiments were performed in duplicates and repeated 3 times. The drug effect *in vitro* was obtained by applying the following formula to normalize the viability scores of the treated worms to the controls:

$$Effect = 1 - Average\ Score\ \text{treatment} / Average\ score\ \text{control} \quad (2)$$

In Vivo *Studies*

All drugs were suspended in 7% Tween 80, 3% ethanol, and 90% water (v/v/v). ABZ was administered to the animals at doses of 3.125, 6.25, 12.5, 25, 50, and 100 mg/kg. The ABZ improved formulations were administered at doses of 6.25, 12.5, 25, 50, and 100 mg/kg, whereas MBZ and its improved formulations were given at doses of 150 and 300 mg/kg. Six to 8 days after treatment, the animals were euthanized by the CO_2 method, dissected, and the worms were picked from the whole *lumen* of the gastrointestinal tract and counted. Drug activity, defined as the reduction in the worm burden (WBR%), was calculated according to the following formula:

$$WBR\% = \frac{(WB_{Ctrl} - WB_{Tmt}) \times 100}{WB_{Ctrl}} \quad (3)$$

WB_{Ctrl}: Worm burden of the controls, WB_{Tmt}: worm burden of the treated group.

Table 2
Particle Size, Solubility, Dissolution Efficiency, and *In Vitro* IC_{50} Values After 72 h of Exposure to the Different ABZ and MBZ Formulations in the Medium pH 7.2

Formulation	Particle Size (μm)	Solubility in HCl 0.1 N (mg/mL)	Solubility Increase (Fold)	Dissolution Efficiency (%)	Dissolution Efficiency Increase (Fold)	IC_{50} (μM)
ABZ	22.2 ± 8.8	0.274 ± 0.006	–	10.3 ± 0.2	–	158
ABZ-PVA	0.472 ± 0.097	0.788 ± 0.001	3	89.8 ± 0.2	9	198
ABZ-P80	0.321 ± 0.007	1.08 ± 0.07	4	101.1 ± 0.5	10	111
ABZ-CH	2.5 ± 1.4	0.38 ± 0.003	1.4	70.9 ± 0.8	7	152
ABZ-CD	4.1 ± 2.3	3.22 ± 0.08	12	94.5 ± 0.5	9	>200
MBZ	10.4 ± 6.9	0.025 ± 0.003	–	20.6 ± 0.1	–	>200
MBZ-PVA	0.106 ± 0.004	0.53 ± 0.04	21	74.2 ± 0.5	7	>200
MBZ-CH	4.9 ± 2.9	0.173 ± 0.001	7	43.4 ± 0.2	4	>200
MBZ-CD	4.2 ± 2.1	2.015 ± 0.009	81	87.4 ± 0.3	8	>200

IC50, half-maximal inhibitory concentration.

Calculation of Significance, ED_{50}, and IC_{50} Values

For testing the significance, we used the Software R, applying the Kruskal-Wallis test.

For the determination of ED_{50} and IC_{50} values, we used the amount of API present in the formulation. The software used was CompuSyn version 1.0 (ComboSyn Inc., 2007).

Results

Particle Size, Solubility, and Dissolution Studies

All formulations were subjected to physicochemical characterization and their particle size, solubility, and DR were determined (Table 2, Figs. 1 and 2).

The novel formulations (microcrystals, nanoparticles, and CD inclusion complexes) showed a decreased particle size and improved solubility and DR compared with the respective pure APIs. Particle size of ABZ and MBZ decreased 5-69 and 2-98 times, respectively. Microcrystals and CD complexes exhibited particles with less than 5 μm and nanoparticles were under 500 nm and monodispersed.

The formulation that most improved the solubility of ABZ was the C-β-CD formulation, followed by P80 and PVA formulations. Among the ABZ formulations, the one that showed the highest dissolution efficiency was ABZ-P80. The CH-based microcrystals increased both solubility and DR of ABZ and MBZ but in a much lower extent when compared with the other excipients. Regarding MBZ formulations, the CD inclusion complexes presented the best dissolution profile followed by PVA nanoparticles. The excipient that most increased the solubility of MBZ was the C-β-CD formulation. We did not prepare P80 formulations with MBZ because nanoparticles were not stabilized with this surfactant.

For comparison, ABZ commercial tablets (Zentel®) showed ~55% of ABZ dissolved at a time point of 10 min,[30] and five different commercial tablets exhibited no more than 30% (between 5% and 30%) of drug dissolved at 10 min in 0.1N HCl.[31]

In Vitro *Studies*

H. polygyrus were incubated in a culture medium containing the drugs at different concentrations. In the case of ABZ, a correlation between dose and effect was observed, but this was not the case for MBZ (Figs. 3a and 3b).

In vitro, none of the formulations or pure drugs was 100% active (all worms dead) within 72 or 120 h (data not shown) of exposure at the highest concentration tested, and the effects were negligible by doses below 50 μM. Only ABZ-CH and ABZ-P80 showed a slightly higher activity (lower IC_{50} values) than pure ABZ. In all other cases (in ABZ and in MBZ formulations), the IC_{50} values of the improved formulations were higher than the standard drugs (Table 2).

Considering that the worms dwell in the intestine, and here the pH in mice ranks from 4 to 6,[32] we evaluated the response in the medium set to pH 4, 5, and 6. Although, at pH 4 and 5 the worms were still alive after 72 h, the viability of the control worms was not high enough to establish appropriate assumptions about the drug's activity. By pH 6.0 instead, the worms tolerated the medium, but we could not evidence an increase in the API's activity respect to the neutral pH. In none of the cases we observed a total effect (all worms dead) at any concentration. (Supplemental files, Fig. S4).

In Vivo *Assays*

The worm burden (WB) of mice treated with all formulations and the pure drugs were statistically different from the untreated mice at all doses tested ($p < 0.05$) with the exception of some of the

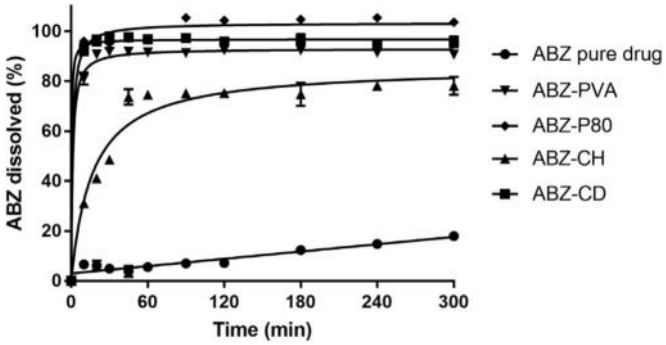

Figure 1. Drug release profiles of ABZ systems and pure ABZ in HCl 0.1N.

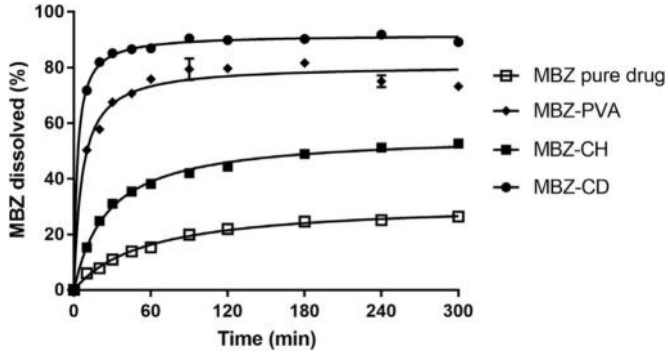

Figure 2. Drug release profiles of MBZ systems and pure MBZ in HCl 0.1N.

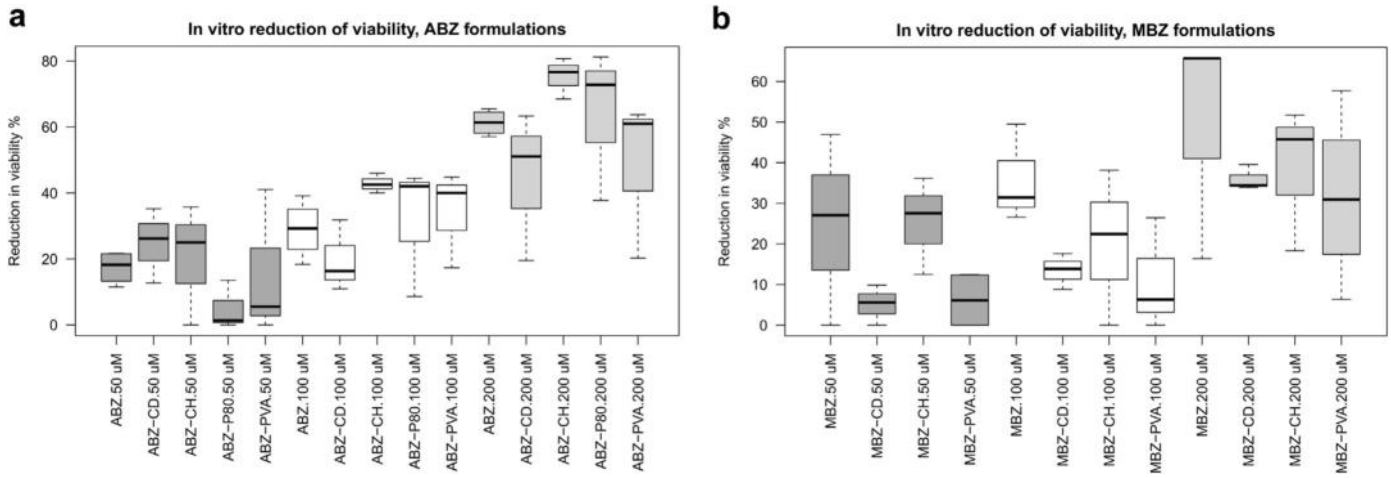

Figure 3. Studies on *H. polygyrus:* Reduction of the worms' viability after 72 h of exposure to the different ABZ (a) and MBZ (b) formulations at 3 different concentrations in the medium pH 7.2.

lowest ABZ doses (3.125 mg/kg for ABZ, 12.5 mg/kg for ABZ-P80), where the WBR was below 50% (Table 3). We found that even when containing less amount of API, in most cases, the ABZ and MBZ formulations showed higher reduction of the WB than the respective pure drug (Table 3), a finding that is reflected by the lower ED_{50} values. The ABZ formulations based on CH and P80 showed the highest activity, revealing the lowest ED_{50} values of 3.09 mg/kg and 4.08 mg/kg, respectively. In the case of MBZ, the ED_{50} values of the improved formulations were over 10 times lower than the pure MBZ (20 mg/kg for MBZ-PVA, 8 mg/kg for MBZ-CH, and 17 mg/kg for MBZ-CD compared with 203 mg/kg for MBZ pure drug). The highest effect of a MBZ formulation we observed was the CH microcrystals, which achieved a 99% WBR, at a dose of 300 mg/kg (corresponding to 240 mg/kg of API). This formulation showed a significant better activity compared with standard MBZ ($p = 0.019$ at 300 mg/kg).

Discussion

Although many efforts have focused on increasing the bioavailability of anthelmintic drugs in the treatment of the cestode *Echinococcus multilocularis*,[33-35] this is the first study to compare the effect of different drug formulations with improved solubility in the treatment of hookworm infections. We developed β-cyclodextrin inclusion complexes, CH-based microcrystals, and PVA and P80-based nanoparticles of ABZ and MBZ for this study. Different

Table 3
Summary of Drug Administered, Worm Burden Reduction, and ED_{50} Values

Drug Tested	Dose (mg/kg)	Content of Drug in Dose (mg/kg)	WBR%	ED_{50} Value (mg/kg)
ABZ	100	100	83.1[b]	7.0
	50	50	63.5[b]	
	25	25	87.5[b]	
	12.5	12.5	89.3[b]	
	6.25	6.25	54.8[b]	
	3.125	3.125	19.5	
Nano ABZ-PVA	100	33	91.2[b]	4.7
	50	16.5	83.0[b]	
	25	8.25	35.2[b]	
ABZ-CH Microcrystals	100	80	91.9[b]	3.1
	50	40	93.9[b]	
	25	20	89.1[b]	
	12.5	10	78.1[b]	
	6.25	5	52.6[b]	
Nano ABZ-P80	100	44	88.5[b]	4.1
	50	22	96.4[b]	
	25	11	67.2[b]	
	12.5	5.5	21.9	
ABZ-CD	100	15.24	76.0[b]	7.7
	50	7.62	35.7[b]	
MBZ	300	300	63.5[b]	203
	150	150	37.8[b]	
Nano MBZ-PVA	300	100	79.8[b]	20.1
	150	50	66.2[b]	
MBZ-CH Microcrystals	300	240	99.0[b,a]	8.0
	150	120	66.2[b]	
MBZ-CD	300	54.6	81.7[b]	16.7
	150	27.3	46.9[b]	

ED_{50}, effective dose 50.
[a] Significantly different from MBZ, $p < 0.05$.
[b] Significantly different from control.

groups have been working on the synthesis of ABZ and MBZ salts with increased solubility[13,36]; however, in a recent study, Kourentas et al.[37] found that this strategy is unlikely to lead to a higher absorption and bioavailability and we therefore decided not to include salt derivatives in this work. We found that all formulations tested were more active *in vivo* than the standard formulations except for ABZ-CD. When compared to ABZ, ABZ-CH revealed the highest improvement in terms of *in vivo* activity (2.25-fold ED_{50} decrease) and *in vitro* activity (IC_{50} value of 158 μM for ABZ and of 111 μM for ABZ-CH). The ABZ-P80 and ABZ-PVA nanoparticles performed also very well, increasing the *in vivo* activity of the API 1.7 and 1.5 times, respectively. ABZ-CD surprisingly, despite presenting an improved solubility profile (Fig. 1), resulted in a higher ED_{50} value than the pure drug (10% less active).

For all improved formulations as for the standard formulation, the doses needed to reach high reductions of the WB (>75% WBR) were substantially higher for MBZ than for ABZ. Despite this, the increased *in vivo* activity of the MBZ formulations compared with standard MBZ was more marked than the improved activity of ABZ's improved formulations. The highest improvement was documented for the microcrystals of MBZ-CH, which decreased the ED_{50} value 25-fold followed by MBZ-CD (12 times ED_{50} decrease) and MBZ-PVA (10-fold ED_{50} decrease).

Our results using a hookworm infection model are consistent with previous studies confirming higher activity of improved formulations of ABZ when compared with pure ABZ. Most studies were oriented to *Echinococcus* spp,[20,33] for which the absorption and bioavailability are critical factors and, because of the parasitostatic and not parasiticidal effect and the difficulty to reach the cysts, long-term treatments are required.[33,38] However, our *in vivo* results slightly differ from those obtained by Cowan et al.,[29] who observed 100% WBR with an ABZ dose of 100 mg/kg and 68% WBR after an administration of 150 mg/kg MBZ to *H. polygyrus*-infected mice. A slightly lower activity of both drugs was observed in the present study (Table 3).

In terms of pharmaceutical characterization, a significant decrease of particle size was observed for both APIs in all formulations (Table 2); however, the smallest particles were not correlated with the highest solubility, dissolution, or ED_{50}, indicating that other factors such as drug crystallinity, polymorphism, and type of excipient also influence the performance of the formulations. It is well known that in CD-drug complexes prepared by cogrinding, spray-drying, and freeze-drying, an amorphous state of the drug is reached[39] and transformation of the crystalline drug into amorphous drug is widely used for increasing solubility.[40] Therefore, we would expect higher drug solubility in CD complexes than in CH microcrystals, which was demonstrated in our formulations. The fact that ED_{50} is lower in CH microcrystals than CD complexes responds to different polymers' characteristics. Microcrystals are formulated with CH that has bioadhesive properties and binds to the intestinal mucosa or could bind to the parasite itself maintaining the drug near to the site of action, leading to a higher ABZ and MBZ activity *in vivo*.[41]

Based on ATR-FTIR spectra (Supplementary material, Fig. S2), MBZ-CH microcrystals consisted of MBZ polymorph C, whereas commercial MBZ tablets tested consisted of polymorph A (less soluble than C). This finding and the CH properties could explain the better performance of MBZ-CH (lowest ED_{50}), although this formulation exhibited the highest particle size.

Comparing the nanoparticles ABZ-PVA and ABZ-P80, the smallest particles (ABZ-P80) had both higher solubility and dissolution and lower ED_{50} (Table 2), demonstrating that the decrease of particle size of poorly water-soluble drugs is important to improve *in vivo* activity. The particle size of the formulations stabilized with PVA was smaller for MBZ than ABZ, which may be either due to a different surface interaction of PVA molecules with the APIs' molecules or differences in precipitation or both, because ABZ and MBZ are solubilized in acetic acid and formic acid, respectively, before precipitation.

The affinity between ABZ or MBZ and CDs decreases in acidic pH and increases at higher pH values[42]; therefore, the interaction between CDs and drugs is high in the intestine and results in a small free fraction of drug available for acting on the parasites; a situation that could explain the high ED_{50} observed with CD formulations. Our results are comparable with those observed by Pacheco et al.[43] who developed similar CD formulations and detected slight but not significant increase of the activity of the formulations with respect to the pure drug in lambs infected with naturally gastrointestinal nematodes. However, several groups have been working on CD-based formulations with promising results.[15,44] Nonetheless, one of the limitations of the use of CDs is that the efficiency in the complex formation for many drugs is low and the comparative molecular weight of the CD to the drug molecule is very high. Therefore, a high amount of CD is needed and the relative content of API becomes very low (15.2% ABZ and 18.2% MBZ in our final formulation), even in the case of ABZ, which has a high binding constant.[45] Hence, the other compared formulations were superior in terms of bulk needed to achieve a proper drug concentration to exert its action.

One limitation of our study might be that we predissolved the formulations in Tween alcohol for the oral administration and future studies should explore the use of drug-loaded microcapsules to study the dissolution of the formulations in the stomach or intestine. Moreover, solubility and dissolution studies were performed following USP conditions, instead of biorelevant dissolution media, because the aim of this study was to test the formulations against intestine-dwelling STH, for which to date no correlation between *in vivo* activity and plasma concentrations could be demonstrated.[29] It might nonetheless be worth highlighting that during the last decade, a range of biorelevant media have been developed to simulate conditions in the stomach and small intestine before and after meals. Using appropriately designed dissolution media and experiments, bioavailability problems and the *in vivo* performance of drug formulations can be identified.[46] Although of less relevance for the intestine-dwelling STH, further studies targeted to the lead candidate ABZ-P80 should include dissolution assays in simulated intestinal fluids, which will give a closer insight to the theoretic bioavailability of the drugs.[46,47] These studies should be accompanied by PK evaluation.

The *in vitro* performance of the APIs and improved formulations was suboptimal, we therefore raised the question if the *in vitro* activity could be increased when considering the more water-soluble metabolite ABZSO or changing the medium pH conditions mimicking intestinal conditions, given ABZ's highly variable pH-dependent solubility, which is 900 times higher by pH 1.2 than pH 6.8.[48] The role of the parent ABZ and its main active metabolite ABZSO in the treatment of intestinal helminths and the site of drug action (need of absorption or direct activity in the intestine) is still under debate.[29] ABZSO showed the best solubility in the assay medium particularly at the highest concentration of 200 μM, when compared to ABZ and the novel formulations, but despite its improved solubility *in vitro,* ABZSO did not reveal higher activity than ABZ, and the effect was negligible even at a 200 μM concentration (data not shown). Our results slightly differ from those of Cowan et al.[29] who observed an effect of 60% on the viability reduction after 72 h of exposure to ABZSO but are in accordance with the low *in vitro* activity of both ABZ and MBZ observed in that study.

In conclusion, the microcrystals formed of ABZ and MBZ and CH (ABZ-CH, MBZ-CH) and the ABZ-P80 nanoparticles offered a

considerable advantage over the standard drug *in vivo* and among these, the formulation of ABZ-P80 is the one that showed the best compromise among physicochemical properties (drug release and dissolution efficiency) and *in vivo* activity (low ED_{50}) and could be recommended as lead formulation for further studies.

Further evaluation should include PK studies in rodents to investigate the *in vivo* behavior of the ABZ−P80 formulation as a function of time and evaluate the correlation between dissolution in biorelevant media, intestinal absorption, and therapeutic efficacy on internal parasites. Additional preclinical studies would not only increase our knowledge on the treatment of STH but might also predict whether this lead formulation could play a role in the treatment of other helminth infections and finally whether to progress into further development.

Acknowledgments

J.P. is grateful to CONICET for a doctoral fellowship. V.B. is grateful to the Swiss government excellence scholarships for his doctoral fellowship (Personal ESKAS-Nr: 2017.0801). J.K. would like to thank the European Research Council, European Union [grant number ERC-2013-CoG 614739-A_HERO] for financial support. The funding organizations did not have any influence in the study design, data collection, analysis of data, writing of the report, or decision to submit the article for publication.

References

1. Jourdan PM, Lamberton PHL, Fenwick A, Addiss DG. Soil-transmitted helminth infections. *Lancet*. 2018;391(10117):252-265.
2. World Health Organization. Model list of essential medicines - 21st list 2019 [11.12.19]. Available at: https://apps.who.int/iris/bitstream/handle/10665/325771/WHO-MVP-EMP-IAU-2019.06-eng.pdf?ua=1.
3. World Health Organization. *Investing to overcome the global impact of neglected tropical diseases Third WHO report on neglected tropical diseases*. Geneva, Switzerland: World Health Organisation; 2015.
4. Moser W, Schindler C, Keiser J. Efficacy of recommended drugs against soil transmitted helminths: systematic review and network meta-analysis. *BMJ*. 2017;358:j4307.
5. Keiser J, Utzinger J. Efficacy of current drugs against soil-transmitted helminth infections: systematic review and meta-analysis. *JAMA*. 2008;299(16):1937-1948.
6. World Health Organization. *Guideline: Preventive Chemotherapy to Control Soil-Transmitted Helminth Infections in At-Risk Population Groups Guideline: Preventive Chemotherapy to Control Soil-Transmitted Helminth Infections in At-Risk Population Groups*. Geneva: WHO; 2017.
7. Priotti J, Leonardi D, Pico G, Lamas MC. Application of fluorescence emission for characterization of albendazole and ricobendazole micellar systems: elucidation of the molecular mechanism of drug solubilization process. *AAPS PharmSciTech*. 2018;19(3):1152-1159.
8. Calvo NL, Kaufman TS, Maggio RM. Mebendazole crystal forms in tablet formulations. An ATR-FTIR/chemometrics approach to polymorph assignment. *J Pharm Biomed Anal*. 2016;122:157-165.
9. Amidon GL, Lennernäs H, Shah VP, Crison JR. A theoretical basis for a biopharmaceutic drug classification: the correlation of *in vitro* drug product dissolution and *in vivo* bioavailability. *Pharm Res*. 1995;12(3):413-420.
10. Jung H, Medina L, García L, Fuentes I, Moreno-Esparza R. Biopharmaceutics: absorption studies of albendazole and some physicochemical properties of the drug and its metabolite albendazole sulphoxide. *J Pharm Pharmacol*. 1997;50(1):43-48.
11. Tsume Y, Mudie DM, Langguth P, Amidon GE, Amidon GL. The Biopharmaceutics Classification System: subclasses for *in vivo* predictive dissolution (IPD) methodology and IVIVC. *Eur J Pharm Sci*. 2014;57:152-163.
12. European Medicines Agency (EMA). *List of Nationally Authorised Medicinal Products*. EMA; 2016.
13. Paulekuhn GS, Dressman JB, Saal C. Salt screening and characterization for poorly soluble, weak basic compounds: case study albendazole. *Pharmazie*. 2013;68(7):555-564.
14. García A, Leonardi D, Lamas MC. Promising applications in drug delivery systems of a novel â-cyclodextrin derivative obtained by green synthesis. *Bioorg Med Chem Lett*. 2016;26(2):602-608.
15. García A, Leonardi D, Salazar MO, Lamas MC. Modified β-cyclodextrin inclusion complex to improve the physicochemical properties of albendazole. Complete *in vitro* evaluation and characterization. *PLoS One*. 2014;9(2):e88234.
16. Kang B-S, Lee S-E, Ng CL, Kim J-K, Park J-S. Exploring the preparation of albendazole-loaded chitosan-tripolyphosphate nanoparticles. *Materials*. 2015;8(2):486-498.
17. Hattori Y, Haruna Y, Otsuka M. Dissolution process analysis using model-free Noyes-Whitney integral equation. *Colloids Surf B Biointerfaces*. 2013;102:227-231.
18. Dokoumetzidis A, Macheras P. A century of dissolution research: from Noyes and Whitney to the biopharmaceutics classification system. *Int J Pharm*. 2006;321(1-2):1-11.
19. Ji L, Shi B. A novel method for determining surface free energy of powders using Washburn's equation without calculating capillary factor and contact angle. *Powder Technol*. 2015;271:88-92.
20. Torabi N, Dobakhti F, Haniloo A. Albendazole and praziquantel chitosan nanoparticles: preparation, characterization, and *in vitro* release study. *Iran J Sci Technol Trans Sci*. 2017;42:1269-1275.
21. Bai F, Wang D, Huo Z, et al. A versatile bottom-up assembly approach to colloidal spheres from nanocrystals. *Angew Chem Int Ed Engl*. 2007;46(35):6650-6653.
22. *United States Pharmacopeia and National Formulary (USP 30-NF 25)*. Rockville, MD: Pharmacopeia Convention; 2006.
23. Narayan R, Pednekar A, Bhuyan D, Gowda C, Koteshwara KB, Nayak UY. A top-down technique to improve the solubility and bioavailability of aceclofenac: *in vitro* and *in vivo* studies. *Int J Nanomed*. 2017;12:4921-4935.
24. Ullrich A, Schiffter HA. The influence of polymer excipients on the dissolution and recrystallization behavior of ketoconazole: application, variation and practical aspects of a pH shift method. *Eur J Pharm Biopharm*. 2018;133:20-30.
25. Khan KA. The concept of dissolution efficiency. *J Pharm Pharmacol*. 1975;27(1):48-49.
26. Simionato LD, Petrone L, Baldut M, Bonafede SL, Segall AI. Comparison between the dissolution profiles of nine meloxicam tablet brands commercially available in Buenos Aires, Argentina. *Saudi Pharm J*. 2018;26(4):578-584.
27. García-Rodriguez JJ, de la Torre-Iglesias PM, Vegas-Sánchez MC, Torrado-Durán S, Bolás-Fernández F, Torrado-Santiago S. Changed crystallinity of mebendazole solid dispersion: improved anthelmintic activity. *Int J Pharm*. 2011;403(1-2):23-28.
28. Reynolds LA, Filbey KJ, Maizels RM. Immunity to the model intestinal helminth parasite *Heligmosomoides polygyrus*. *Semin Immunopathol*. 2012;34(6):829-846.
29. Cowan N, Meier C, Neodo A, Keiser J. Exposure of *Heligmosomoides polygyrus* and *Trichuris muris* to albendazole, albendazole sulfoxide, mebendazole and oxantel pamoate *in vitro* and *in vivo* to elucidate the pathway of drug entry into these gastrointestinal nematodes. *Int J Parasitol Drugs Drug Resist*. 2017;7(2):159-173.
30. Sawatdee S, Atipairin A, Sae Yoon A, Srichana T, Changsan N, Suwandecha T. Formulation development of albendazole-loaded self-microemulsifying chewable tablets to enhance dissolution and bioavailability. *Pharmaceutics*. 2019;11(3):1-20.
31. Garbuio AP, Hanashiro T, Markman BO, Fonseca FA, Perazzo FF, Rosa PP. Evaluation and study of mebendazole polymorphs present in raw materials and tablets available in the Brazilian pharmaceutical market. *J Appl Pharm Sci*. 2014;4:1-7.
32. McConnell EL, Basit AW, Murdan S. Measurements of rat and mouse gastrointestinal pH, fluid and lymphoid tissue, and implications for *in-vivo* experiments. *J Pharm Pharmacol*. 2007;60(1):63-70.
33. Abulaihaiti M, Wu X-W, Qiao L, et al. Efficacy of albendazole-chitosan microsphere-based treatment for alveolar echinococcosis in mice. *PLoS Negl Trop Dis*. 2015;9(9):e0003950.
34. Torabi N, Dobakhti F, Faghihzadeh S, Haniloo A. *In vitro* and *in vivo* effects of chitosan-praziquantel and chitosan-albendazole nanoparticles on *Echinococcus granulosus* metacestodes. *Parasitol Res*. 2018;117:2015-2023.
35. García A, Barrera MG, Piccirilli G, et al. Novel albendazole formulations given during the intestinal phase of *Trichinella spiralis* infection reduce effectively parasitic muscle burden in mice. *Parasitol Int*. 2013;62(6):568-570.
36. Gutiérrez EL, Souza MS, Diniz LF, Ellena J. Synthesis, characterization and solubility of a new anthelmintic salt: mebendazole nitrate. *J Mol Struct*. 2018;1161:113-121.
37. Kourentas A, Vertzoni M, Stavrinoudakis N, et al. An *in vitro* biorelevant gastrointestinal transfer (BioGIT) system for forecasting concentrations in the fasted upper small intestine: design, implementation, and evaluation. *Eur J Pharm Sci*. 2016;82:106-114.
38. Brunetti E, Kern P, Vuitton DA. Expert consensus for the diagnosis and treatment of cystic and alveolar echinococcosis in humans. *Acta Trop*. 2010;114(1):1-16.
39. Ogawa N, Takahashi C, Yamamoto H. Physicochemical characterization of cyclodextrin−drug interactions in the solid state and the effect of water on these interactions. *J Pharm Sci*. 2015;104(3):942-954.
40. Karagianni A, Kachrimanis K, Nikolakakis I. Co-amorphous solid dispersions for solubility and absorption improvement of drugs: composition, preparation, characterization and formulations for oral delivery. *Pharmaceutics*. 2018;10(3):1-26.
41. Barbosa MA, Gonçalves IC, Moreno PMD, et al. *Chitosan. Comprehensive Biomaterials*. 2nd ed. Oxford: Elsevier; 2017:279-305.

42. García A, Priotti J, Codina AV, et al. Synthesis and characterization of a new cyclodextrin derivative with improved properties to design oral dosage forms. *Drug Deliv Transl Res*. 2018;9:273-283.
43. Pacheco PA, Rodrigues LNC, Ferreira JFS, et al. Inclusion complex and nano-clusters of cyclodextrin to increase the solubility and efficacy of albendazole. *Parasitol Res*. 2018;117(3):705-712.
44. Ehteda A, Galettis P, Chu SWL, Pillai K, Morris DL. Complexation of albendazole with hydroxypropyl-β-cyclodextrin significantly improves its pharmacokinetic profile, cell cytotoxicity and antitumor efficacy in nude mice. *Anticancer Res*. 2012;32(9):3659-3666.
45. Carrier RL, Miller LA, Ahmed I. The utility of cyclodextrins for enhancing oral bioavailability. *J Control Release*. 2007;123(2):78-99.
46. Klein S. The use of biorelevant dissolution media to forecast the *in vivo* performance of a drug. *AAPS J*. 2010;12(3):397-406.
47. Rosenberger J, Butler J, Muenster U, Dressman J. Application of a refined developability classification system. *J Pharm Sci*. 2019;108(3):1090-1100.
48. Kohri N, Yamayoshi Y, Iseki K, Sato N, Todo S, Miyazaki K. Effect of gastric pH on the bioavailability of albendazole in rabbits. *Pharm Pharmacol Commun*. 1998;4(5):267-270.

Chapter III

Characterization of moxidectin against *Strongyloides ratti*: *in vitro* and *in vivo* activity and pharmacokinetics in the rat model

ACS Infectious Diseases

pubs.acs.org/journal/aidcbc Article

Characterization of Moxidectin against *Strongyloides ratti*: In Vitro and In Vivo Activity and Pharmacokinetics in the Rat Model

Valentin Buchter, Daniela Hofmann, Cécile Häberli, and Jennifer Keiser*

Cite This: https://dx.doi.org/10.1021/acsinfecdis.0c00435 Read Online

ACCESS | Metrics & More | Article Recommendations | Supporting Information

ABSTRACT: *Strongyloides stercoralis* is a soil-transmitted helminth affecting an estimated 30−100 million people. Since the infection may be severe and life-threatening, accessible and effective treatment is pivotal. Currently, ivermectin is the drug of choice but has limitations. Moxidectin, a veterinary anthelminthic approved for use in human onchocerciasis, is a promising drug alternative against strongyloidiasis. In this study, we evaluated the in vitro activity of moxidectin on *Strongyloides ratti* larvae (L_3) and adult females and the activity as well as the pharmacokinetics of moxidectin in *S. ratti* infected rats. In vitro, moxidectin had an activity that was similar to that of ivermectin, with median lethal concentration values for L_3 and adults in the range of 0.08−1.44 μM, after 72 h of exposure. In vivo, doses of 250, 500, and 750 μg/kg of moxidectin resulted in a reduction of the worm burden ranging from 48.5 to 75%. At the highest dose (750 μg/kg) we observed a maximal blood concentration of 50.3 ng/mL and an area under the curve of 895.2 ng × h/mL. The half-life in rats was 9 h, and moxidectin was cleared to undetectable blood levels within 7 d (<10 ng/mL). No exposure-response relationship was observed. This work contributes to the characterization of moxidectin in the treatment of *S. ratti* as a model of *Strongyloides spp*. and, as such, supports moving moxidectin further along the drug development pipeline in the treatment of human strongyloidiasis.

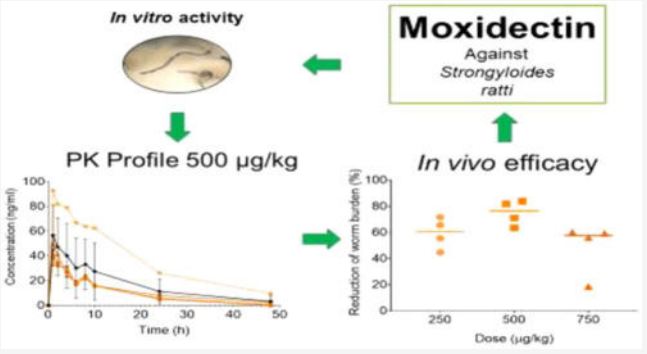

KEYWORDS: *Strongyloides stercoralis, Strongyloides ratti, moxidectin, pharmacokinetics, in vitro, in vivo*

Soil transmitted helminthiasis is a neglected tropical disease caused by the chronic infection with one or more of the soil-transmitted helminths (STHs): the hookworms (*Ancylostoma duodenale, Necator americanus*), the whipworm (*Trichuris trichiura*), the roundworm (*Ascaris lumbricoides*), and the threadworm (*Strongyloides stercoralis*). According to the World Health Organization (WHO) these parasites affect worldwide 1.5 billion people or 24% of the world's population,[1] and among them, *S. stercoralis* is the most underdiagnosed, with estimates of 30−100 million people affected.[2,3] STH infections occur mainly in rural areas, where sanitation is poor, causing nutritional, physical, and cognitive impairment, contributing this way to the vicious cycle of poverty and disease of deprived communities.[4]

Control strategies for hookworm, whipworm, and roundworm rely mainly on periodical drug-based deworming campaigns with albendazole or mebendazole. However, no public health strategy for controlling strongyloidiasis exists so far.[1] This is despite, the parasite's unique ability to multiply and spread in the host, which can cause long-lasting and even fatal complications.[2] Treatment of strongyloidiasis currently relies on ivermectin, which shows excellent activity;[5] however, its availability is limited,[6] being mostly accessible through donations by onchocerciasis and lymphatic filariasis programs.[7] Additionally, authors suggest that ivermectin presents variable outcomes, reporting cure rates ranging from 55 to 100%[8] and, thus, raising uncertainty in the treatment of strongyloidiasis. Last but not least, given its widespread use against different parasitic infections, drug resistance might become a problem.[7,9] Hence, new drugs or drug combinations for strongyloidiasis are necessary. Among new human anthelminthic candidates, evidence suggests that moxidectin, an antiparasitic drug with more than 30 years of use in veterinary medicine,[10] might be an appropriate alternative for the treatment of *S. stercoralis*.[11] Moxidectin harbors beneficial attributes including a lower neurotoxic potential than ivermectin[12] and its successful use in veterinary medicine against some ivermectin-resistant strains.[13] Additionally, while its efficacy against STHs in humans has still not been fully established, in the treatment of onchocerciasis, moxidectin is applied independently of weight (unique dose of 8 mg), which renders the administration easier to handle, especially when treating large communities.[14] Moxidectin's

Special Issue: Gut Pathogens

Received: June 18, 2020
Published: September 29, 2020

https://dx.doi.org/10.1021/acsinfecdis.0c00435
ACS Infect. Dis. XXXX, XXX, XXX−XXX

mechanism of action has been studied in nematodes, and moxidectin is suggested to act by binding a nematode-specific glutamate-gated chloride channel (GluCl), leading to increased permeability, influx of chloride ions, neuronal inhibition, and final muscle paralysis, thus killing the parasite.[15] Moxidectin has been safely used since its development in the treatment of parasitic diseases of horses,[10] sheep,[16] cattle,[17] and dogs.[18] Just recently, in 2018 the United States Food and Drug Administration (FDA) approved the human use of moxidectin in the treatment of river blindness.[19] Clinical trials on onchocerciasis proved moxidectin to be a safe and well-tolerated drug.[20]

Because of moxidectin's long-term use in animals and its beneficial properties in the treatment of river blindness, there is growing interest to extend its applicability to STHs. A first exploratory clinical study of moxidectin against *S. stercoralis* showed very promising outcomes with cure rates higher than 90%.[11] Yet, the underlying preclinical studies are missing, and the pharmacokinetic (PK) characteristics of moxidectin treating STH infections are in a large part unexplored. Few studies exist that have evaluated the pharmacokinetic/-dynamic (PK/PD) behavior of moxidectin in different healthy or infected animal species,[10,16,18,21] but none of them evaluated its application against soil-transmitted helminthiasis.

The main objective of this work was to investigate for the first time the in vitro and in vivo activity of ascending doses of moxidectin against *S. ratti* and describe the underlying PK/PD behavior in rats. The in vitro activity of moxidectin was investigated on *S. ratti* against third-stage larvae (L_3) and adult females. Moreover, three different doses (250, 500, 750 μg/kg) were administered to *S. ratti*-infected rats, and the reduction of the worm burden was determined 7 d after treatment. Finally, we characterized the drug's PK profile in rats using an adapted and revalidated liquid chromatography-tandem mass spectrometry (LC-MS/MS) method.[22]

RESULTS AND DISCUSSION

In Vitro Activity of Moxidectin Versus Ivermectin. The activity of moxidectin against *S. ratti* L_3 and female adults was evaluated in vitro after 24, 48, and 72 h of incubation and compared to the activity of ivermectin, the current gold-standard therapy against strongyloidiasis.[5] The results are summarized in Table 1.

On L_3 and adults, both ivermectin and moxidectin performed similarly at the final evaluation point of 72 h of exposure, and the median lethal concentration (LC_{50}) values were similar: 0.15 and 0.08 μM for the larval stage for moxidectin and ivermectin, respectively, and 1.44 and 0.47 μM for the adult stage. On L_3, there was almost no difference in the onset of activity between moxidectin and ivermectin, showing excellent in vitro performance of both drugs at all time points and confirming previous studies on *S. ratti* exposed to ivermectin.[23−25] On adults, instead, we observed a faster onset of activity for moxidectin than for ivermectin, resulting in 24 h in LC_{50} values of 10.7 μM and more than 100 μM, respectively, confirming previous studies on the time dependency in the in vitro activity of ivermectin on the treatment of *Strongyloides spp.*[24,25]

Compared to the recently published data on emodepside,[26] moxidectin performed slightly better in terms of activity against L_3; however, it was not as fast-acting as emodepside in the killing of adult parasitic stages. The activity of emodepside on *S. ratti* ranged from 0.25 to 0.73 μM against L_3 and from 0.21 to 0.75 μM against adults after 24−72 h of exposure, respectively.[26] Compared to thiabendazole, moxidectin showed a far more potent profile, since the experimentally found paralysis concentration 50% (PC_{50}) for thiabendazole on *S. ratti* L_3 was 140 μM after 24 h of exposure,[23] 2000-fold higher than the LC_{50} of moxidectin at the same time of exposure.

Our in vitro results confirm that the *S. ratti* drug sensitivity assays are an excellent tool for drug discovery against strongyloidiasis. A study published in 2000[23] found very similar activities of ivermectin against *S. ratti* and *S. venezuelensis* L_3 underlying a similar in vitro susceptibility across *Strongyloides* species and supporting the use of these models in drug discovery for *Strongyloides spp*.

In Vivo Activity of Moxidectin. We next evaluated the activity of moxidectin at three dosages (250, 500, and 750 μg/kg) in *S. ratti*-infected rats (Table 2).

As shown in Table 2, we observed a significant difference in the worm burden after treatment with all three doses when compared to the respective untreated control animals. Overall, 500 μg/kg was the most effective dose, achieving a WBR of 75.0% after one single drug administration; however, this reduction of worm burden was not statistically different from the higher and lower doses (Kruskal Wallis test $\chi^2 = 5.3$, degrees of freedom = 2, $p = 0.07$). We calculated a 50% efficacy dose (ED_{50}) of 152.4 μg/kg. Since, at a dose of 750 μg/kg, no raise in activity (WBR = 48.5, SD, 20.0) was observed, increasing the dose above 500 μg/kg seems to provide no benefit in the treatment of rats infected with *S. ratti*. On the one hand, when compared to published in vivo activity data on *S. ratti*, ivermectin[27] showed a better outcome than moxidectin, achieving a worm burden reduction (WBR) of 100% at a dose of 500 μg/kg. Similarly, in previous studies with emodepside in *S. ratti*-infected rats, a dose of 1 mg/kg was enough to cure an adult infection.[28] On the other hand, when considering tribendimidine in this model, a high dose of 25 mg/kg was necessary to cure all rats.[27]

LC-MS/MS Method Partial Validation. We performed a partial validation, to apply a liquid chromatography-mass spectrometry (LC-MS/MS) method validated for the quantification of moxidectin in human blood[22] to rat blood, following and in agreement with the FDA guidelines for method validation.[29] We analyzed three independent full validation sets, one of them composed of three subsets, to compare interday and intraday variability. The method was partially validated in terms of linearity, sensitivity, accuracy, precision, recovery rate, and matrix effect, as described below.

Linearity. Throughout the three full validation sets and sample analyses, the calibration line (CL) fitted to a regression

Table 1. In Vitro Studies[a]

	S ratti adult		*S. ratti* L_3	
	moxidectin	ivermectin	moxidectin	ivermectin
time (h)	LC_{50} (SD) (μM)	LC_{50} (SD) (μM)	LC_{50} (SD) (μM)	LC_{50} (SD) (μM)
24	10.69 (5.57)	>100	0.07 (0.00)	0.06 (0.03)
48	3.34 (2.54)	14.21 (17.06)	0.06 (0.04)	0.03 (0.03)
72	1.44 (0.29)	0.47 (0.19)	0.15 (0.19)	0.08 (0.07)

[a]LC_{50} of moxidectin and ivermectin against *S ratti* female adult and L_3 larval stages. Abbreviations: LC_{50}, lethal concentration 50%; SD standard deviation.

https://dx.doi.org/10.1021/acsinfecdis.0c00435
ACS Infect. Dis. XXXX, XXX, XXX−XXX

Table 2. Activity and PK Parameters[a]

	treatment group			control A[b]	control B[b]
dose (μg/kg)	250	500	750		
WB (SD) (count)	60.2 (17.6)[c]	37.0 (14.1)[c]	113.7 (44.3)[c]	148.2 (13.0)	221.2 (81)
WBR (SD) (%)	59.4 (11.8)	75.0 (9.49)	48.5 (20.0)		
$AUC_{0\text{-}t}$ (SD) (ng·h/ml)	233.96 (82.2)	873.3 (717)[d]	895.18 (205)[d]		
C_{max} (SD) (ng/mL)	29.93 (8.2)	56.5 (24.6)[d]	50.31 (6.3)[d]		
T_{max} (SD) (h)	1 (0)	1 (0)	5.25 (2.98)		
$T_{1/2}$ (SD) (h)	5.38 (2.6)	10.41 (5.05)	9.0 (2.6)		
MRT $_{0\text{-inf\_obs}}$ (SD) (h)	8.4 (3.9)	15.2 (5.0)	14.0 (3.2)		
Vz/F (SD) (μg/kg)/(ng/mL)	8.3 (1.9)	10.5 (5.8)	11.0 (2.2)		
Cl/F (SD) ((μg/kg)/(ng/mL)/h)	1.2 (0.4)	0.8 (0.8)	0.87 (0.2)		

[a]Activity and PK parameters of oral moxidectin in *S. ratti*-infected rats, stratified by dose. Abbreviations: AUC: area under the concentration−time curve, Cl/F: total body clearance, MRT: mean residence time, SD standard deviation, Vz/F: apparent volume of distribution based on the terminal phase, WB: worm burden, WBR%: worm burden reduction in percentage. [b]WBR of 250 and 500 μg/kg calculated on base of untreated control group A. WBR of 750 μg/kg calculated on base of the untreated control group B. [c]Significantly different from the respective control. [d]Significantly different from the lowest dose.

coefficient of $R^2 \geq 0.997$ along the full linearity range, which covered the concentrations from 10 (lowest limit of quantification, LLOQ) to 2500 ng/mL. The CL was formed out of eight points, where at least six values (75%) fitted the nominal value with an accuracy of ±15% (and 20% for the LLOQ). Sensitivity: the lowest limit of quantification was found to be 10 ng/mL, the concentration at which the signal obtained was at least 5 times the background noise and could be determined with an accuracy of a deviation of not more than 20% of the nominal value and a precision fitting a coefficient of variation less than or equal to 20%[29] (range of 4−13%) among the three full validation sets. The blank's background noise for the internal standard (IS) (m/z^+ = 531.6) was (average ± standard deviation (AVG ± SD)) 30.7 ± 13.6, and for moxidectin (m/z^+= 528.6) it was 7.4 ± 2.2, while at the LLOQ level the signal was, for the IS, 6025 ± 1386, and for moxidectin the signal was 107.1 ± 27.9, fitting the requirements along the three validation sets.

Accuracy and Precision. (AVG ± SD%) 85 ± 3.7% of each of the quality controls (QC) among the five validation sets successfully passed the accuracy conditions described by the FDA guidelines for method validation (a minimum of 67% surpassing deviation not more than 20% from the nominal value for the LLOQ and 15% for all other QCs). The intraday accuracy was 95 ± 5%, and the interday accuracy was 76 ± 8%. Precision: the coefficient of variation of the QCs was 9.0 ± 3.3% at the LLOQ level (10 ng/mL); 7.6 ± 2.7 at the low calibrator (25 ng/mL) level, 10.4 ± 2.3 at the mid calibrator (500 ng/mL) level, and 9.4 ± 3.5% at the high calibrator (500 ng/mL) level, fulfilling the FDA recommendation.

The values for the recovery rate (RR %) and matrix effect (ME %) for the low (25 ng/mL), mid (100 ng/mL), and high (500 ng/mL) concentrations were calculated in triplicate: RR_{low}: 75.3 ± 0.4%, RR_{mid}: 104.0 ± 0.2%, RR_{high}: 83.4 ± 0.2%, ME_{low}: 105.4 ± 0.3%, ME_{mid}: 93.4 ± 0.08%, ME_{high}: 103.9 ± 0.06%.

Pharmacokinetics of Moxidectin. The PK profile of oral moxidectin at three different doses was evaluated along the full time of the experiment, between administration on day 0 and dissection on day 7. The main PK parameters are displayed in Table 2, and the corresponding blood concentration versus time (0 h−7 d post treatment) profiles are plotted in Figure 1. An increase in maximal concentration (C_{max}) and area under the curve ($AUC_{0\text{-}t}$) was observed in rats following ascending doses of 250 and 500 μg/kg. The dosing of rats with 750 μg/kg of moxidectin provided a slightly, yet nonsignificant greater increase in $AUC_{0\text{-}t}$, and no further increase in C_{max}.

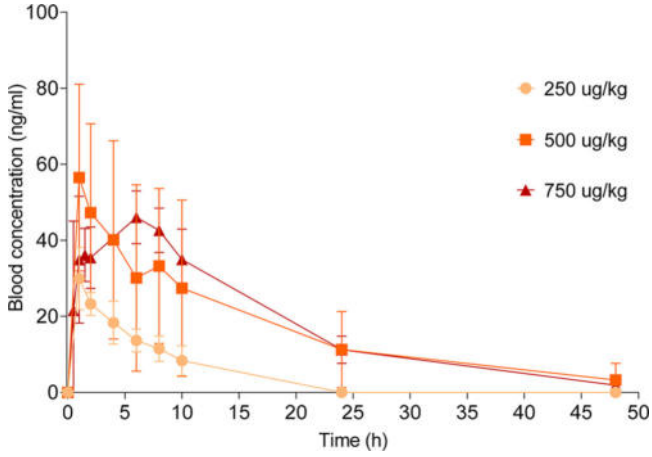

Figure 1. Moxidectin blood concentration vs time profiles in *S. ratti*-infected rats following oral administration of 250, 500, and 750 μg/kg doses of moxidectin (n = 4).

Moreover, while doses of 250 and 500 μg/kg reached the mean peak concentration at 1.0 ± 0.0 h after drug administration, the T_{max} for the 750 μg/kg dose was detected at 5.25 ± 2.98 h. The mechanism of absorption of moxidectin has not been fully elucidated; however, according to the predictions of drug solubility and permeability described by Lipinski et al.,[30] the rather large molecule (molecular weight (MW) > 500 Da) moxidectin could result in limited passive absorption and/or the need of an active transporter for membrane passage.[30] A possible saturation of the transporters might further explain the lack of increase of AUC or C_{max} at the highest dose tested (750 μg/kg) but not a delay of the T_{max}. Moreover, given that moxidectin is only slightly soluble in water (0.51 mg/L),[31] solubility issues, translating into lower absorption, could as well explain the lack of increase of the C_{max} and AUC at the highest dose and a delayed T_{max}.

It is worthwhile mentioning that differences in the bioavailability of moxidectin are strongly correlated to a food effect, with an increase in absorption when administered together with fatty meals.[20] However, since all rats were treated under fed conditions, there is no reason to suggest differences

https://dx.doi.org/10.1021/acsinfecdis.0c00435
ACS Infect. Dis. XXXX, XXX, XXX−XXX

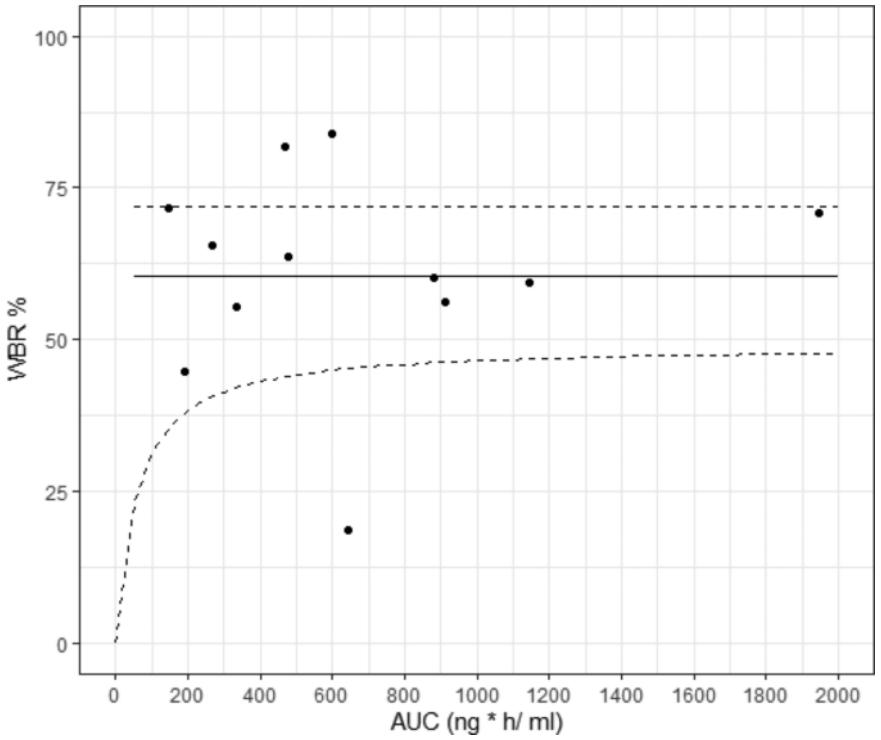

Figure 2. Reduction of the worm burden as a function of exposure ($AUC_{0\text{-}t}$). The correlation plot shows a linear prediction of reduction of worm burden as a function of exposure (solid line). Dotted lines represent the 95% CI. Solid black dots are individual rat data.

in the feeding state among different dosing groups that could explain differences in the C_{max} or AUC.

Analysis of PK/PD Relationship. With significant differences in AUC and small differences in the reduction of the worm burden between the three doses, we analyzed the exposure-response correlation, which is presented in Figure 2, as the WBRs of individual rats as a function of AUC (WBR as a function of dose and C_{max} are shown in Figures S2 and S3 in the Supporting Information). The exposure−response curve shows a slope equal to 0; hence, there was no relationship between AUC and WBR, and the maximal predicted activity could not be accurately determined by means of an maximum effect E_{max} model.

As a limitation of our study it is worth mentioning that a small number of animals was used per group, which revealed a high variation in the individual worm burden. However, given the broad range of exposure (AUC) observed among our animals it is unlikely that an exposure-response correlation would have been detected if a larger number of animals had been studied.

Table 3 shows the main PK parameters of four studies published, following an oral administration of different doses of moxidectin in different large animals, and preclinical data in uninfected rats, obtained from drug approval documents for the treatment of human onchocerciasis.[32] Of note, several other studies investigated the PK parameters of moxidectin using different formulations and other routes of administrations.[33−35] Additionally, our study evaluated PK parameters in blood sampled with the Mitra®® sampling device, while the compared studies worked with plasma. This method difference, however, should not significantly influence the results, as shown by a recent study comparing Mitra®® with plasma sampling.[36]

The half-life observed in rats in our study was relatively short compared to previous studies. For a drug to be active, it should be present within the therapeutic window for a sufficient time to exert its activity.[38,39] As concluded from the in vitro studies (Table 1), there is a time dependency on the activity of moxidectin (though less pronounced as in the case of ivermectin) in the treatment of adult females. This might explain why a maximum WBR of 75% and a flat exposure response curve was observed, uncovering a limitation of the rat as a model system, compared to larger animal species (Table 3). This observation might have been expected, given the inversely proportional relationship of metabolic rate and species body weight. To overcome this limitation, a multiple dose schedule of moxidectin in rats should be considered in future studies to control for species-to-species translatability.

Interestingly, there is a considerable difference in $T_{1/2}$ and AUC between our study and the previous PK study in rats.[32] This finding might be explained by the different vehicles (corn oil vs Tween 80 -ethanol) used. A higher solubility of moxidectin in corn oil might have resulted in increased absorption and thus higher AUC and tissue distribution,[10] thus extending its half-life.

CONCLUSION

Moxidectin might be an aspiring alternative medication to ivermectin to be integrated in the depleted anthelmintic drug repertoire. We evaluated the activity of moxidectin in vitro and in vivo against *S. ratti* infections and observed that moxidectin shows excellent in vitro activity, comparable to that of ivermectin, and in vivo, moxidectin was similarly active at all tested dose levels. A flat dose and exposure-response correlation was evaluated.

In summary, our findings support efforts to determine the efficacy and safety of moxidectin in the treatment of human

https://dx.doi.org/10.1021/acsinfecdis.0c00435
ACS Infect. Dis. XXXX, XXX, XXX−XXX

Table 3. Comparison[a]

	Alvinerie et al., 1998[16]	Escudero et al., 1999[37]	Al-Azzam et al., 2007[18]	Cobb et al., 2009[10]	FDA, 2017[32]		this study	
species	sheep	goat	beagle dog	horse	Sprague−Dawley rat		Wistar rat	
parasite	uninfected	uninfected	*Brugia pahangi*	mixed nematodes infection	uninfected		*Strongyloides ratti*	
dose (μg/kg)	200	200	250	400	3′000	10′000	250	500	750
T_{max} (h)	5.28	9.12 ± 0.5	2.0 ± 1.0	8.88 ± 4.56	2	2	1	1	5.25 ± 2.99
C_{max} (ng/mL)	28.07	15.5 ± 1.3	234.0 ± 64.3	70 400 ± 10 700	562 ± 172	2513 ± 221	29.9 ± 8.1	56.5 ± 24.6	50.3 ± 6.2
$T_{1/2}$ (h)	505 ± 48	288 ± 14.4	621 ± 149	555 ± 264	20.5 ± 2.4	18.6 ± 2.0	5.38 ± 2.6	10.4 ± 5.0	9.01 ± 2.6
AUC (ng·h/ml)	2373 ± 837.6	881 ± 96	11′800 ± 2′300	872′640 ± 158′400	8′022 ± 2′731	42′114 ± 5′205	234.0 ± 82.2	873 ± 717	895 ± 205
MRT (h)	301.2	247.2 ± 19.2	696.6 ± 188.9	ND	ND	ND	8.4 ± 3.9	15.2 ± 5.0	14.04 ± 3.2
formulation/vehicle	oral Cydectin	oral Cydectin	oral Cydectin	oral gel	corn oil suspension		Tween 80 - ethanol - water		

[a]Comparison of doses used and main PK parameters of moxidectin following oral administration to veterinary and laborarory animals. Abbreviations: AUC: area under the concentration−time curve, C_{max}: maximal concentration reached, FDA: Food and Drug Administration, MRT: mean residence time, T_{max}: time to peak concentration, $T_{1/2}$: half-life, ND: not detected.

strongyloidiasis, yet further efforts are needed to characterize drug dosing.

METHODS

Animals and Parasites. All animal experiments were performed in compliance with the regulations of the canton Basel Stadt, Switzerland, and in the framework of license No. 2070.

The studies were performed in male Wistar rats purchased from Janvier at the age of three weeks. Upon arrival, rats were kept for one week in the animal facility with food and tap water ad libitum (22 °C, 50% humidity, with a 12 h light/dark cycle, 6 AM to 6 PM). Following the adaption period, all rats were infected via oral gavage with 800 *S. ratti* L_3, obtained from our established in-house life cycle. The studies were performed in biosecurity-level 2 (BSL-2) laboratories.

In Vivo Studies. Eight days after infection, the rats were randomly assigned and treated in two series of experiments: four infected rats per arm were treated with either 250 (low dose), 500 (medium dose), or 750 (high dose) μg/kg of moxidectin (Livzon New North River Pharmaceutical Co. Ltd.), and four untreated animals served as a control in each experiment.

For the oral administration via gavage, the drugs were first dissolved in a mixture of 70% Tween 80 (Sigma-Aldrich) with 30% ethanol (Merck), corresponding to 10% of the final volume, and then tap water was added under constant agitation using a magnetic stirrer until completion of the necessary volume. The doses of 250 and 500 μg/kg were prepared as a suspension of 0.2 mg/mL moxidectin, while the 750 μg/kg dose was prepared at a concentration of 0.4 mg/mL due to limitations on the administration volume specified by the animal regulations. After the last PK sampling point, 7 d after administration, the rats were euthanized in CO_2, and the hosting worms were counted following the procedure described below.

In Vitro Studies. Female adult *S. ratti* for the in vitro studies were collected from the control rats as follows: after death, the intestines were opened longitudinally, drained in phosphate base saline (PBS) buffer (ingredients from Sigma-Aldrich, prepared in-house), and placed in Petri dishes containing PBS buffer with 1% pen/strep (penicillin 100 U/ml−streptomycin 0.1 mg/mL, BioConcept). Plates were kept for 4 h in the incubator (37 °C, 5% CO_2) (Innova CO-48, New Brunswick scientific) for the worms to get loose from the intestines and intestinal material. Afterward the worms were picked out and counted while being sucked out using a pipet and placed into a second Petri dish containing clean PBS + 1% pen/strep. This step was repeated twice for washing. Afterward the worms were placed in an incubation medium (RPMI 1640 (Gibco-Thermofisher) supplemented with 1% pen/strep and 5% fetal calf serum (FCS) (BioConcept)). Subsequently, the intestines were incubated overnight in PBS buffer, and additional worms were collected on the following day, following the same procedure. The in vitro assays were prepared in duplicate in standard 24-well plates, where 8−10 worms were placed into each well. The worms were incubated for 24, 48, and 72 h in incubation medium containing 0.5, 1, 5, 10, and 20 μM moxidectin or ivermectin (Sigma-Aldrich). The control condition consisted of medium containing 0.5% dimethyl sulfoxide (DMSO) (Sigma-Aldrich), which is the content of DMSO present in the highest assay concentration. For scoring, 200 μL of water, 80 °C, were added to each well

https://dx.doi.org/10.1021/acsinfecdis.0c00435
ACS Infect. Dis. XXXX, XXX, XXX−XXX

to stimulate worm motility and permit the scoring, which was done using a bright field inverted microscope (Carl Zeiss, magnifications ×4 and ×10), and a visual scale ranging from 0 to 3, where 0 corresponds to dead worms (no motion within 5 s) and 3 is the maximal motility.[26]

Blood Sampling. Animals were sampled in the first experiment (250 and 500 μg/kg) at 0, 1, 2, 4, 6, 8, 10, 24, 48, and 72 h and also at 7 d. Taking into account the PK data from the two first doses, we performed a second experiment (with the dose 750 μg/kg) using the following time points: 0, 30, 60, 90, and 120 min, 6, 8, 10, 24, 48, and 72 h, and 7 d.

For the sample collection of two replicates per rat and time point, the rats were anesthetized with isoflurane (MinRad Inc.), and the blood was taken from the sublingual vein using the 10 μL microsampling device, Mitra®® (Neoteryx). After collection, the Mitra®® samples were kept in the fridge (4 °C) until analysis within 7 d.

Sample Extraction and LC-MS/MS. The extraction and quantification of moxidectin using the microsampling device Mitra®® were validated for its use in human blood[22] following the FDA guidelines for industry.[29] For this study, the method was further adapted for its application to rat blood and partially validated in terms of linearity, sensitivity, accuracy, precision, recovery rate, and matrix effect following the FDA guidelines for method validation 2018.[29]

A 1 mg/mL stock solution of moxidectin was prepared in DMSO and serially diluted in acetonitrile (ACN) (LC-MS grade, Merck) to prepare the working solutions, which were 24-fold more concentrated than the calibration line. For the preparation of the CL, 92 μL of naïve fresh full blood were spiked with 4 μL of working solution, and the 10 μL Mitra®® device was soaked for three seconds. The Mitra®® were left to dry in the fridge, subsequently extracted, and run in the LC-MS/MS within a period of 7 d.

The extraction solution consisted of a 4:1 mixture of methanol (MeOH)/ACN (LC-MS grade Merck) and 20 ng/mL of trideuterated moxidectin (moxidectin-d_3, Sigma-Aldrich), which served as internal standard. Samples were first sonicated for 60 min in 300 μL of extraction solution in a 1 mL 96-well plate (Phenomenex AH-8636 Stratz 96 well plate 2 mL round 8 mm Phenomenex) and agitated for 1 h at room temperature by shaking at 1200 rpm (Eppendorf Thermomixer C) without passing by a water washing step. The Mitra®® devices were afterward removed from the plate, and the extracted samples were vacuum-dried for 2 h at 45 °C in a speed-vacuum instrument (SPD 111 V, Thermo Scientific).

For the LC-MS/MS analysis, the samples were reconstituted in 100 μL of methanol supplemented with 0.5 mM ammonium formate (Sigma-Aldrich), and 10 μL aliquots were injected in the LC-MS/MS.

Each measurement set consisted of a calibration line covering the range from 10 (LLOQ) to 2500 ng/mL, and the quality controls were prepared in sextuplicate, including the concentrations LLOQ (10 ng/mL), low (25 ng/mL), mid (100 ng/mL), and high (500 ng/mL), consisting of blood prepared out of six different hematocrit values (30−55%).

The LC separation was accomplished using an Agilent 1200 series high-performance liquid chromatograph (HPLC) coupled to an Agilent 6460 triple quadrupole analyzer (Agilent). The software Mass Hunter Workstation (Agilent Technologies, ver. B.06.00) was used to operate the instrument and for data analysis. The LC column was a Phenomenex Luna 5 μm C8(2), 50 × 2 mm (Phenomenex Helvetia GmbH, catalog No. 00B-4249-B0).

The mobile phases A and B consisted of Milli-Q water (in-house production, Merk Millipore, advantage A10) and MeOH (LC-MS grade Sigma-Aldrich), respectively, both supplemented with formic acid LC-MS grade (Sigma-Aldrich) to a final concentration of 0.05%. The elution gradient was defined as follows: 0−3 min, B = 80 → 100%; 3−4 min, B = 100%; 4−7 min, B, 100 → 80%; 7−7.8 min, B, 80%. The flow rate was set to 0.4 mL/min. The injector temperature was set to 4 °C, and the injection volume was 10 μL for all samples, followed by a needle wash step in pure isopropyl alcohol after each sampling. The ionization mode was set to positive, and the ions were tracked in multiple reaction monitoring at 531.6 and 528.6 m/z^+ for moxidectin-D3 and moxidectin, respectively.

Data Analysis. The drug's effect in vitro was calculated by normalizing the viability (for LC_{50} calculation) to the condition of the control worms. The inhibitory concentration 50% (LC_{50}) and effective dose 50% (ED_{50}) were calculated using Calcusyn software (Biosoft).

The significance of in vivo studies was evaluated by application of a Kruskall Wallis test for non-parametric multiple comparisons and applying the Dunn test with Bonferroni correction for identifying the individual differences. The cutoff for significance was $p < 0.05$.

PK data were analyzed using the software PK-Solver[40] applying a noncompartmental model. Statistical tests for significance were performed in RStudio,[41] using a non-parametric Kruskal−Wallis test.

For estimating the exposure-response, the E_{max} model was applied using the nonlinear least-squares (nls2) and nlstools packages in RStudio. The formula used to estimate the E_{max} and E_{50} parameters was "nonlinear least square estimate = WBR ~ (AUC*E_{MAX})/(E_{50}+AUC)" within the nls2 package, while confint2, level = 0.90 was used to estimate the confidence interval (CI) of the curve. The figure was made by including these parameters in the ggplot2 package.

Figures 2 and S3 where created using the software RStudio, while Figures 1, S1, and S2 were created using the software GraphPad Prism version 8.0.

■ ASSOCIATED CONTENT

Supporting Information

The Supporting Information is available free of charge at https://pubs.acs.org/doi/10.1021/acsinfecdis.0c00435.

Individual PK curves of each of the doses used. WBR% as a function of dose administered. Reduction of the worm burden as a function of Cmax (PDF)

■ AUTHOR INFORMATION

Corresponding Author

Jennifer Keiser − *Swiss Tropical and Public Health Institute, CH-4002 Basel, Switzerland; University of Basel, CH-4001 Basel, Switzerland;* orcid.org/0000-0003-0290-3521; Phone: +41 (0)61 284 8218; Email: jennifer.keiser@swisstph.ch

Authors

Valentin Buchter − *Swiss Tropical and Public Health Institute, CH-4002 Basel, Switzerland; University of Basel, CH-4001 Basel, Switzerland*

Daniela Hofmann − *Swiss Tropical and Public Health Institute, CH-4002 Basel, Switzerland; University of Basel, CH-4001 Basel, Switzerland*

Cécile Häberli − *Swiss Tropical and Public Health Institute, CH-4002 Basel, Switzerland; University of Basel, CH-4001 Basel, Switzerland*

Complete contact information is available at: https://pubs.acs.org/10.1021/acsinfecdis.0c00435

Author Contributions

V.B. designed the study, performed the in vivo experiments, MS analysis, and partial validation and the wrote first draft of the manuscript. D.H. validated the MS human blood analytic method, supplied technical guidance to V.B., and corrected the manuscript. C.H. performed the in vitro studies and contributed to the in vivo experiments. J.K. designed the study, supervised the work, and corrected the manuscript.

Notes

The authors declare no competing financial interest.

■ ACKNOWLEDGMENTS

V.B. is thankful to the Swiss government excellence scholarships for financial support (Scholarship No. 2017.0801). J.K. and D.H. are grateful to the European Research Council for financial support (Grant No. 614739-A_HERO).

■ ABBREVIATIONS

AUC, Area under the curve; AVG, average; Cl/F, total body clearance; CV, coefficient of variation; ED_{50}, effective dose 50%; LC_{50}, lethal concentration 50%; IVM, ivermectin; LCMS/MS, liquid chromatography−tandem mass spectrometry; LLOQ, Lowest limit of quantification; ME, and matrix effect MIC, minimal inhibitory concentration; MOX, moxidectin; MRT, Mean residence time; PC_{50}, Paralysis concentration 50%; QC, quality control; RR, recovery rate; STH, soil transmitted helminth; Vz/F, apparent volume of distribution based on the terminal phase; WB, worm burden; WBR, worm burden reduction

■ REFERENCES

(1) WHO. Soil-transmitted helminth infections 2020 [updated 2020-02-03. Available from: https://www.who.int/news-room/fact-sheets/detail/soil-transmitted-helminth-infections. Date accessed 2020-08-21.

(2) Schär, F., Trostdorf, U., Giardina, F., Khieu, V., Muth, S., Marti, H., Vounatsou, P., and Odermatt, P. (2013) *Strongyloides stercoralis*: Global Distribution and Risk Factors. *PLoS Neglected Trop. Dis. 7* (7), e2288−e2288.

(3) Bethony, J., Brooker, S., Albonico, M., Geiger, S. M., Loukas, A., Diemert, D., and Hotez, P. J. (2006) Soil-transmitted helminth infections: ascariasis, trichuriasis, and hookworm. *Lancet 367* (9521), 1521−1532.

(4) Gazzinelli, A., Correa-Oliveira, R., Yang, G.-J., Boatin, B. A., and Kloos, H. (2012) A research agenda for helminth diseases of humans: social ecology, environmental determinants, and health systems. *PLoS Neglected Trop. Dis. 6* (4), e1603−e1603.

(5) Hurlimann, E., and Keiser, J. (2019) A single dose of ivermectin is sufficient for strongyloidiasis. *Lancet Infect. Dis. 19* (11), 1150−1151.

(6) WHO (2019) in *2030 targets for soil-transmitted helminthiases control programmes* WHO, Geneva, Switzerland; Available from: https://apps.who.int/iris/bitstream/handle/10665/330611/9789240000315-eng.pdf?ua=1.

(7) WHO. African Programme for Onchocerciasis Control (APOC) 2020. Available from: https://www.who.int/apoc/cdti/ivermectin/en/. Date accessed 2020-08-21.

(8) Mendes, T., Minori, K., Ueta, M., Miguel, D. C., and Allegretti, S. M. (2017) Strongyloidiasis current status with emphasis in diagnosis and drug research. *J. Parasitol. Res. 2017*, 5056314.

(9) WHO (2006) in *Preventive Chemotherapy in Human Helminthiasis: Coordinated Use of Anthelminthic Drugs in Control Interventions - A Manual for Health Professionals and Programme Managers* World Health Organization

(10) Cobb, R., and Boeckh, A. (2009) Moxidectin: a review of chemistry, pharmacokinetics and use in horses. *Parasites Vectors 2*, S5.

(11) Barda, B., Sayasone, S., Phongluxa, K., Xayavong, S., Keoduangsy, K., Odermatt, P., Puchkov, M., Huwyler, J., Hattendorf, J., and Keiser, J. (2017) Efficacy of moxidectin versus ivermectin against *Strongyloides stercoralis* infections: A Randomized, Controlled Noninferiority Trial. *Clin. Infect. Dis. 65* (2), 276−281.

(12) Janko, C., and Geyer, J. (2013) Moxidectin has a lower neurotoxic potential but comparable brain penetration in P-glycoprotein-deficient CF-1 mice compared to ivermectin. *J. Vet. Pharmacol. Ther. 36* (3), 275−284.

(13) Barnes, E. H., Dobson, R. J., Stein, P. A., Le Jambre, L. F., and Lenane, I. J. (2001) Selection of different genotype larvae and adult worms for anthelmintic resistance by persistent and short-acting avermectin/milbemycins. *Int. J. Parasitol. 31* (7), 720−727.

(14) Opoku, N. O., Bakajika, D. K., Kanza, E. M., Howard, H., Mambandu, G. L., Nyathirombo, A., Nigo, M. M., Kasonia, K., Masembe, S. L., Mumbere, M., Kataliko, K., Larbelee, J. P., Kpawor, M., Bolay, K. M., Bolay, F., Asare, S., Attah, S. K., Olipoh, G., Vaillant, M., Halleux, C. M., and Kuesel, A. C. (2018) Single dose moxidectin versus ivermectin for *Onchocerca volvulus* infection in Ghana, Liberia, and the Democratic Republic of the Congo: a randomised, controlled, double-blind phase 3 trial. *Lancet 392* (10154), 1207−1216.

(15) Shoop, W. L., Mrozik, H., and Fisher, M. H. (1995) Structure and activity of avermectins and milbemycins in animal health. *Vet. Parasitol. 59* (2), 139−156.

(16) Alvinerie, M., Escudero, E., Sutra, J. F., Eeckhoutte, C., and Galtier, P. (1998) The pharmacokinetics of moxidectin after oral and subcutaneous administration to sheep. *Vet Res. 29* (2), 113−118.

(17) Zulalian, J., Stout, S. J., daCunha, A. R., Garces, T., and Miller, P. (1994) Absorption, Tissue Distribution, Metabolism, and Excretion of Moxidectin in Cattle. *J. Agric. Food Chem. 42* (2), 381−387.

(18) Al-Azzam, S. I., Fleckenstein, L., Cheng, K.-J., Dzimianski, M. T., and McCall, J. W. (2007) Comparison of the pharmacokinetics of moxidectin and ivermectin after oral administration to beagle dogs. *Biopharm. Drug Dispos. 28* (8), 431−438.

(19) WHO. First new treatment for river blindness approved by U.S. FDA in 20 years 2018 [updated 2018-06-18]. Available from: https://www.who.int/tdr/news/2018/moxidectin-approved-as-treatment-for-river-blindness/en/. Date accessed 2020-08-24.

(20) Cotreau, M. M., Warren, S., Ryan, J. L., Fleckenstein, L., Vanapalli, S. R., Brown, K. R., Rock, D., Chen, C. Y., and Schwertschlag, U. S. (2003) The antiparasitic moxidectin: safety, tolerability, and pharmacokinetics in humans. *J. Clin. Pharmacol. 43* (10), 1108−1115.

(21) Perez, R., Cabezas, I., Sutra, J. F., Galtier, P., and Alvinerie, M. (2001) Faecal excretion profile of moxidectin and ivermectin after oral administration in horses. *Vet. J. 161* (1), 85−92.

(22) Hofmann, D., Sayasone, S., and Keiser, J. (2020) Development and validation of a LC-MS/MS method for the quantification of the anthelmintic drug moxidectin in Mitra®, blood and plasma: Application to a pharmacokinetic study of adults infected with strongyloides in Laos. [Analytical method]. To be submitted.

(23) Satou, T., Koga, M., Koike, K., Tada, I., and Nikaido, T. (2001) Nematocidal activities of thiabendazole and ivermectin against the larvae of *Strongyloides ratti* and *S. venezuelensis*. *Vet. Parasitol. 99* (4), 311−322.

(24) Kotze, A. C., O'Grady, J., Behnke, J. M., McCarthy, J. S., and Clifford, S. (2004) An in vitro larval motility assay to determine

anthleminthic sensitivity for human hookworm and strongyloides species. *Am. J. Trop. Med. Hyg. 71* (5), 608−616.
(25) Smout, M. J., Kotze, A. C., McCarthy, J. S., and Loukas, A. (2010) A novel high throughput assay for anthelmintic drug screening and resistance diagnosis by real-time monitoring of parasite motility. *PLoS Neglected Trop. Dis. 4* (11), e885−e885.
(26) Karpstein, T., Pasche, V., Häberli, C., Scandale, I., Neodo, A., and Keiser, J. (2019) Evaluation of emodepside in laboratory models of human intestinal nematode and schistosome infections. *Parasites Vectors 12* (1), 226−226.
(27) Keiser, J., Thiemann, K., Endriss, Y., and Utzinger, J. (2008) *Strongyloides ratti*: in vitro and in vivo activity of tribendimidine. *PLoS Neglected Trop. Dis. 2* (1), e136.
(28) Harder, A., and Samson-Himmelstjerna, G. (2001) Activity of the cyclic depsipeptide emodepside (BAY 44−4400) against larval and adult stages of nematodes in rodents and the influence on worm survival. *Parasitol. Res. 87* (11), 924−928.
(29) FDA (2018) Bioanalytical Method Validation Guidance for Industry U.S. Food & Drug Administration
(30) Lipinski, C. A., Lombardo, F., Dominy, B. W., and Feeney, P. J. (1997) Experimental and computational approaches to estimate solubility and permeability in drug discovery and development settings. *Adv. Drug Delivery Rev. 23* (1), 3−25.
(31) FDA (2018) Moxidectin prescribing information [2020-08-24]. Available from: https://www.accessdata.fda.gov/drugsatfda_docs/label/2018/210867lbl.pdf. Date accessed [2020-08-24].
(32) FDA (2017) Moxidectin non-clinical report [2020-08-24]. Available from: https://www.accessdata.fda.gov/drugsatfda_docs/nda/2018/210867Orig1s000PharmR.pdf. Date accessed [2020-08-21].
(33) Fazzio, L., Moreno, L., Galvan, W., Canton, C., Alvarez, L., Streitenberger, N., Sánchez, R., Lanusse, C., and Sanabria, R. (2019) Pharmacokinetic profile and anthelmintic efficacy of moxidectin administered by different doses and routes to feedlot calves. *Vet. Parasitol. 266*, 73−79.
(34) Hooke, F. G., Clement, P., Dell'Osa, D., Porter, R. M., MacColl, D., and Rew, R. S. (1997) Therapeutic and protective efficacy of doramectin injectable against gastrointestinal nematodes in cattle in New Zealand: A comparison with moxidectin and invermectin pour-on formulations. *Vet. Parasitol. 72* (1), 43−51.
(35) Sallovitz, J., Lifschitz, A., Imperiale, F., Pis, A., Virkel, G., and Lanusse, C. (2002) Breed Differences on the Plasma Availability of Moxidectin Administered Pour-on to Calves. *Vet. J. 164* (1), 47−53.
(36) Schulz, J. D., Neodo, A., Coulibaly, J. T., and Keiser, J. (2019) Pharmacokinetics of Albendazole, Albendazole Sulfoxide, and Albendazole Sulfone Determined from Plasma, Blood, Dried-Blood Spots, and Mitra® Samples of Hookworm-Infected Adolescents. *Antimicrob. Agents Chemother. 63* (4), e02489−02418.
(37) Escudero, E., Carceles, C. M., Diaz, M. S., Sutra, J. F., Galtier, P., and Alvinerie, M. (1999) Pharmacokinetics of moxidectin and doramectin in goats. *Res. Vet. Sci. 67* (2), 177−181.
(38) Levison, M. E., and Levison, J. H. (2009) Pharmacokinetics and pharmacodynamics of antibacterial agents. *Infect Dis Clin N Am 23* (4), 791−vii.
(39) White, N. J. (2013) Pharmacokinetic and Pharmacodynamic Considerations in Antimalarial Dose Optimization. *Antimicrob. Agents Chemother. 57* (12), 5792.
(40) Zhang, Y., Huo, M., Zhou, J., and Xie, S. (2010) PKSolver: An add-in program for pharmacokinetic and pharmacodynamic data analysis in Microsoft Excel. *Computer Methods and Programs in Biomedicine. 99* (3), 306−314.
(41) R Core Team (2018) RFfSC. R: A Language and Environment for Statistical Computing [Available from: https://www.R-project.org/. Date accessed 2020-08-21.

https://dx.doi.org/10.1021/acsinfecdis.0c00435
ACS Infect. Dis. XXXX, XXX, XXX−XXX

Chapter IV

Oxamniqune derivatives

Chapter IV-A

Assessment of tegumental damage to *Schistosoma mansoni* and *S. haematobium* after *in vitro* exposure to ferrocenyl, ruthenocenyl and benzyl derivatives of oxamniquine using scanning electron microscopy

Buchter et al. Parasites & Vectors (2018) 11:580
https://doi.org/10.1186/s13071-018-3132-x

Parasites & Vectors

RESEARCH Open Access

Assessment of tegumental damage to *Schistosoma mansoni* and *S. haematobium* after *in vitro* exposure to ferrocenyl, ruthenocenyl and benzyl derivatives of oxamniquine using scanning electron microscopy

Valentin Buchter[1,2], Jeannine Hess[3], Gilles Gasser[4] and Jennifer Keiser[1,2*]

Abstract

Background: Schistosomiasis is one of the most harmful parasitic diseases worldwide, praziquantel being the only drug in widespread use to treat it. We recently demonstrated that ferrocenyl, ruthenocenyl and benzyl derivatives of oxamniquine (Fc-OXA, Rc-OXA and Bn-OXA) are promising antischistosomal drug candidates.

Methods: In this study we assessed the tegumental damage of these three derivatives of oxamniquine using scanning electron microscopy. Adult *Schistosoma mansoni* and *S. haematobium* were exposed to a concentration of 100 μM of each drug and incubated for 4–120 h, according to their onset of action and activity.

Results: While on *S. mansoni* the fastest acting compound was Fc-OXA, which revealed high activity after 4 h of incubation, on *S. haematobium*, Rc-OXA revealed the quickest onset, being lethal on all males within 24 h. In both species studied, the three derivatives showed the same patterns of tegumental damage consisting of blebs, sloughing and tegument rupturing all over the body. Additionally, on *S. mansoni* distinct patterns of tegumental damage were observed for each of the compounds: tissue ruptures in the gynaecophoric canal for Fc-OXA, loss of spines for Rc-OXA and oral sucker rupture for Bn-OXA.

Conclusions: Our study confirmed that Fc-OXA, Rc-OXA and Bn-OXA are promising broad spectrum antischistosomal drug candidates. All derivatives show fast *in vitro* activity against *S. mansoni* and *S. haematobium* while validating the previous finding that the parent drug oxamniquine is less active *in vitro* under the conditions described. This work sets the base for further studies on the identification of a lead oxamniquine derivative, with the aim of identifying a molecule with the potential to become a new drug for human use.

Keywords: Schistosomiasis, Organometallic derivatives, Oxamniquine, *Schistosoma mansoni*, *Schistosoma haematobium*, Scanning electron microscopy

* Correspondence: jennifer.keiser@swisstph.ch
[1]Department of Medical Parasitology and Infection Biology, Swiss Tropical and Public Health institute, Socinstrasse 57, 4051 Basel, CH, Switzerland
[2]University of Basel, P.O. Box, 4003 Basel, CH, Switzerland
Full list of author information is available at the end of the article

Background

Schistosomiasis is a human parasitic disease that affected 230 million people worldwide in 2014 [1] and is caused by the infection with one or more of the six *Schistosoma* species: *Schistosoma mansoni*, *S. haematobium*, *S. japonicum*, *S. mekongi*, *S. intercalatum* and *S. guineensis*; the first three are the most important human species [1]. Because no vaccine is available, and the use of molluscicides to control the intermediate host is difficult to conduct, the most commonly used strategy to control the disease is preventative chemotherapy through large-scale administration of praziquantel [2]. Praziquantel, developed in the 1970's, is safe and effective, but has some shortcomings: the tablets are big because of the large dose needed, it is very bitter [3] and the drug is not active against juvenile forms of the parasite [4]. Frequent retreatment of patients is therefore required to target all parasite stages. Oxamniquine (OXA) is a drug that was developed in the 1960's [5] and proved to be effective and safe, but has two shortcomings: it is only active against *S. mansoni* [5–7] and resistance developed quickly due to punctual mutations to the enzyme's active site [8]. OXA is a pro-drug that for activation needs to be taken up by the worm and sulfonated by a sulfotransferase (SmSULT) to an unstable intermediate that spontaneously decays to a highly electrophilic molecule that alkylates DNA, proteins and macromolecules, thus interfering with its metabolic functions and killing the parasite [9]. Enzyme orthologs are present also in *S. japonicum* and *S. haematobium* and in mammalian cells, but differences in the interaction in the active site prevent the activation of the molecule (70% protein sequence homology between *S. haematobium* and *S. mansoni*) [9]; therefore the drug is not active against *S. haematobium* [6]. The SmSULT expression in juvenile stages of the parasite has not yet been studied; however, OXA is known to be only slightly active against larval stages of *S. mansoni* [10]. Aiming to overcome this species and stage specificity through improved interaction with the target enzyme, we previously tested six OXA derivatives primarily based on organometallic derivatization due to its medicinal potential [11, 12] and identified three molecules (ferrocenyl, ruthenocenyl and benzyl derivatives of oxamniquine, named Fc-OXA, Rc-OXA and Bn-OXA, respectively) (Fig. 1) with a promising *in vivo* and *in vitro* activity profile against *S. mansoni.* Importantly, these compounds also displayed activity *in vitro* against *S. haematobium* [11].

The aim of the present study was to assess the damage to the tegument of *S. mansoni* and *S. haematobium*, evidenced by scanning electron microscopy (SEM) following incubation with Fc-OXA, Rc-OXA and Bn-OXA at the time points where the *in vitro* viability of the worms was markedly affected. Considering the importance of the tegument for schistosomes, which allows them to evade the immune response of the host, SEM is a valuable approach to identify whether the molecules can induce damage to this critical structure [13], and hence expose immune-reactive molecules and trigger an immune response in the host.

Methods

Adult *S. mansoni* worms

Three week-old female NMRI mice (n = 7) were purchased from Charles River and were allowed to acclimatize for one week. They were infected by a subcutaneous injection in the back of the neck with approximately 100 cercariae and kept in the animal facility of the Swiss TPH for 49 days to allow the infection to develop into the adult stage. Mice were then euthanized by the CO_2 method and worms were collected by picking them from the hepatic portal system and mesenteric veins. Worms were washed in culture medium at room temperature and incubated at 37 °C with 5% CO_2 until use (no longer than 2 days). The medium consisted of RPMI 1640 culture medium (Gibco - Thermofisher, Waltham, MA USA) supplemented with 1% penicillin/streptomycin (BioConcept, Allschwil, Switzerland) and 5% Fetal Calf Serum (FCS) (BioConcept). Eight to ten worms of both sexes per time

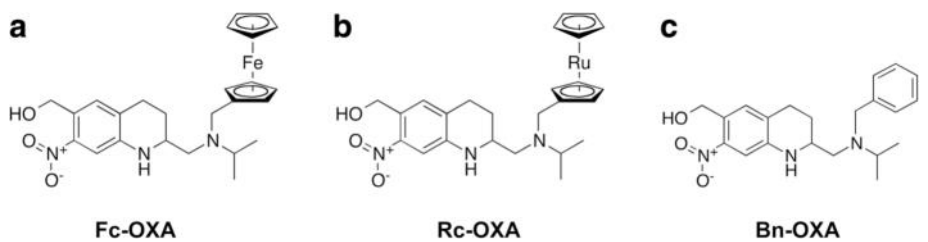

Fig. 1 Molecular structure of the derivatives of oxamniquine. **a** Ferrocenyl oxamniquine. **b** Ruthenocenyl oxamniquine. **c** Benzyl oxamniquine

point were incubated in the described medium, in the presence of 100 μM [11] of each of the three derivatives (Fc-OXA, Rc-OXA, Bn-OXA) and oxamniquine. The control consisted of 8–10 worms incubated in culture medium spiked with dimethyl sulfoxide (DMSO) at a concentration of 1%, equivalent to the content of DMSO present in the wells of treated worms. Worms were monitored daily, scoring motility, viability and morphological alterations under a bright field inverted microscope (Carl Zeiss Oberkochen, Germany, magnification ×4 and ×10) as described elsewhere [14]. The scoring scale ranges from 3 to 0 with a 0.25 interval. The score 3 corresponds to fully vital worms showing normal movement and activity, and no morphological changes; 2 is assigned to slowed worm activity, first morphological changes (loss of attachment to the well plate, suckers deformity) and visible granularity; 1 is given if minimal activity, severe morphological changes (change of the color, loss of transparency, rounded body disposition) and marked granularity is observed; and 0 refers to dead worms revealing severe granularity.

Worms were collected for SEM analysis at the time point when the average viability of the worms was visibly affected. For each compound the onset of action was different, therefore the time points range from 4 h for Fc-OXA, to 24 h for Rc-OXA, to 72 h for Bn-OXA and 120 h for OXA.

Adult *S. haematobium* worms

One month-old male LVG hamsters (Charles River, NY) (n = 4) were exposed to 350 *S. haematobium* cercariae at the Biomedical Research Institute in Rockville, USA (NR-21964), and shipped to the Swiss TPH where the infection was allowed to develop for three months until chronic infections had been established. The animals were kept in the animal facility until use, for a maximum of four months. Hamsters were euthanized by the CO_2 method and worms picked from hepatic portal system and mesenteric veins. Briefly, 8–10 adult *S. haematobium* were exposed to a 100 μM concentration for 24 h for ruthenocenyl oxamniquine, 48 h for ferrocenyl and benzyl oxamniquine and 120 h for oxamniquine, depending on the time needed for the worms to show a marked decrease in viability. Media used and scoring procedure were conducted as described for *S. mansoni* worms.

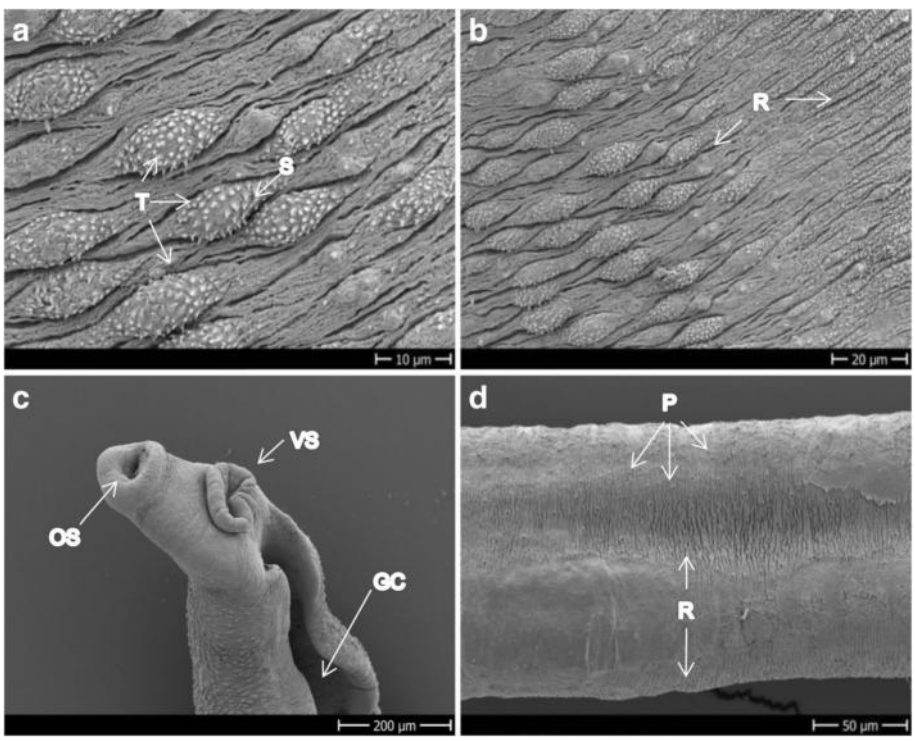

Fig. 2 SEM images of *S. mansoni* control worms incubated with 1% DMSO. **a** Tubercles of dorsal mid-part of a male. **b** Lateral mid-part of a male showing the transition between the tubercles of the dorsal side to the spiny ridges of the ventral side of the body. **c** Head of a male showing the oral and ventral suckers and the gynaecophoric canal. **d** Mid-part of the body of a female showing the ridges and pores in a context of a smooth tegument. *Abbreviations*: GC, gynaecophoric canal; OS/VS, oral/ventral sucker; P, pores; R, ridges; S, spines; T, tubercles. *Scale-bars*: **a**, 10 μm; **b**, 20 μm; **c**, 200 μm; **d**, 50 μm

Oxamniquine derivatives

Oxamniquine was kindly donated by Pfizer (New York City, USA) while the Fc-OXA, Rc-OXA and Bn-OXA were prepared starting from oxamniquine, as described previously [11].

SEM images

Following the *in vitro* cultivation of the worms with the compounds as described above, *S. mansoni* and *S. haematobium* worms were rinsed twice in PBS, and fixed in 1 ml glutaraldehyde 2.5% for 4 h at room temperature. Worms were then sequentially dehydrated by incubation for 30 min in increasing concentrations of ethanol in deionized water (30, 50, 70, 90 and 100%) and kept in the fridge in 100% ethanol until use. For imaging, worms were critically point-dried (Bomar SPC-900, Washington, USA), mounted on aluminum stubs and sputter-coated with gold of 20 nm particle size (Leica EM ACE 600, Heerbrugg, Switzerland). Samples were visualized using a high-resolution SEM accelerating voltage of 5 kV (Philips XL30 ESEM, Bruchsal, Germany). Control worms were prepared and visualized in the same manner. All images were taken in the Nano Imaging Lab, SNI, University of Basel.

IC_{50} value calculations

The IC_{50} values of each of the derivatives against *S. haematobium* were calculated using the software CompuSyn 1.0 (ComboSyn Inc, 2007) after 72 h of incubation with the following concentrations of each drug: 100, 50, 25, 12.5 and 6.25 μM. The equation to normalize the score of the treated worms to the controls and calculate the effect was:

$$\text{Effect} = 1 - \left(\text{Average score}_{\text{treatment}} / \text{Average score}_{\text{control}}\right)$$

The IC_{50} values obtained for the drugs on *S. mansoni* are described elsewhere [11].

Results and discussion

Studies on *S. mansoni*

Figure 2a and b shows the tegument of healthy adult *S. mansoni* males depicting ridges and tubercles covered

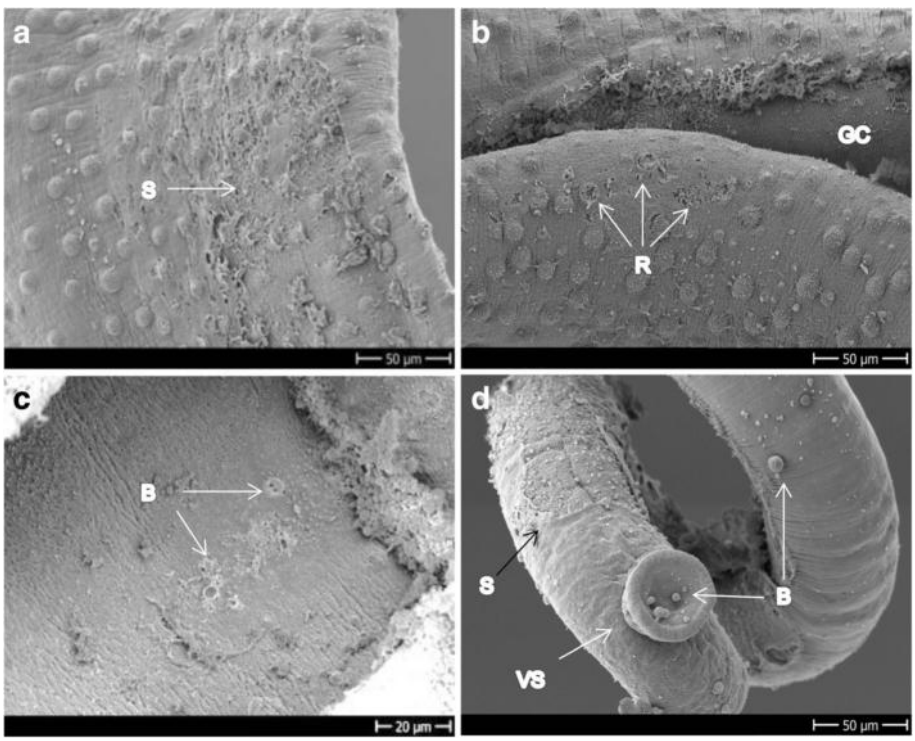

Fig. 3 Adult *S. mansoni* exposed to 100 μM Fc-OXA incubated for 4 h. **a** Tissue sloughing from the lateral side of the mid-part of the body of a male and exposure of sub-tegumental tissue. **b** Mid-part of the body of a male showing the lateral side with ruptures, the gynaecophoric canal and ruptured tissue on the other side of the canal. **c** Blebs and ruptures in the inner side of the gynaecophoric canal, mid-part of the body. **d** Upper part of the body of a female showing tissue sloughing off and blebs on the tegument and ventral sucker. *Abbreviations*: B, blebs; GC, gynaecophoric canal; R, rupturing; S, sloughing off; VS, ventral sucker. *Scale-bars*: **a**, **b**, **d**, 50 μm; **c**, 20 μm

by spines that are more or less uniformly distributed. In Fig. 2c the oral and ventral suckers and the gynaecophoric canal of control worms are shown. Ridges are also present on females, but no tubercles or spines; instead, the teguments of the female look more porous and smooth (Fig. 2d).

After 24 h and 48 h of exposure to a 100 μM concentration of oxamniquine, the worms were alive and phenotypically in a good shape (score above 2) and we did not evidence any damage to the tegument by means of SEM (not shown). After exposure for 120 h we observed loss of attachment to the well, slight blebbing on the tegument and reduction of movement of the treated worms when compared to the control group. Since the controls also showed mild blebbing and sloughing tissue after this long incubation, we were not able to correlate a certain pattern of damage with the exposure of the worms to OXA. Our data confirm previous findings of OXA being only slightly active *in vitro* [11] and the difficulties to maintain the worms for long incubation periods where they start revealing tegument damage [15].

Fc-OXA produced after four hours of exposure at a 100 μM concentration extensive blebs, sloughing and rupture of the tegument along the whole dorsal body surface on all worms examined (Fig. 3a–c). Along the gynaecophoric canal blebbing and sloughing tissue was evident (Fig. 3c). On the males, no damage to the suckers was observed and the spines did not look significantly damaged (not shown), but were partially covered by the tissue that was detaching, as can be seen in Fig. 3a. On the females, the damage was principally focused on the upper part of the body, where Fc-OXA produced sloughing off and blebbing on the tegument and the ventral sucker (Fig. 3d).

Four hours after exposure to Rc-OXA, the phenotypic score of the worms averaged 0.81 ± 0.15 (n = 8, all worms alive) yet only mild tegumental damage was observed by means of SEM, which consisted of loss of spines and mild blebs in the male, but no damage was evidenced in the females (not shown). After 24 h of incubation, the male worms had died and the females showed significant morphological changes, very low motility and the maximum score observed was 0.25. Tegumental damage of the males consisted of increased loss of spines (Fig. 4a) accompanied by tegument sloughing, blebs and vesicle formation all over the body surface (Fig. 4a–c). Although the viability score of the females was below 0.5, no pronounced tegumental damage could be evidenced using

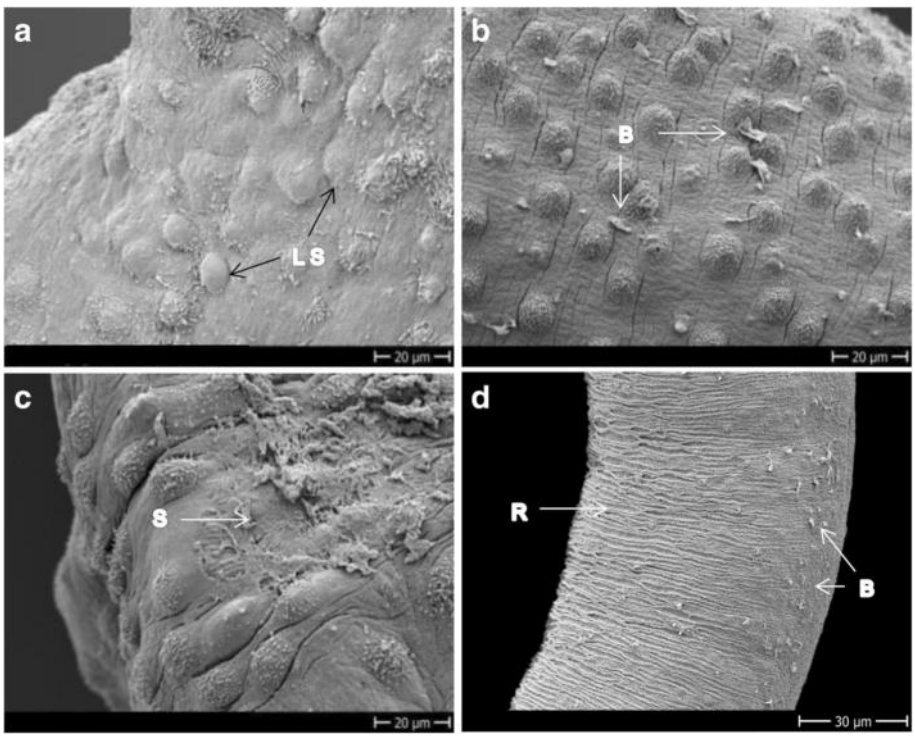

Fig. 4 Adult *S. mansoni* exposed to 100 μM Rc-OXA for 24 h. **a**–**c** Dorsal mid-part of males showing blebs, sloughing tissue and loss of spines. **d** Mid-part of the body of a female showing undamaged ridges and very mild damage characterized by blebs along the body. *Abbreviations*: B, blebs; LS, loss of spines; R, ridges; S, sloughing off. *Scale-bars*: **a**–**c**, 20 μm; **d**, 30 μm

SEM (Fig. 4d). The oral and ventral suckers did not show significant damage and most couples stayed together during drug exposure (not shown) despite death of the male worms. We have no explanation for this observation, but it is possible that the females showed very low vitality and eventually were not able to dissociate from the dead male.

Bn-OXA produced minor damage to the tegument 24 h after incubation, which consisted of small dimples (Fig. 5a). Only after 72 h of drug exposure the tegumental damage became evident and consisted, similar to Fc-OXA and Rc-OXA, of blebs (Fig. 5b), sloughing and tegumental rupture distributed all over the dorsal surface (not shown). At this time point, eight worms were dead (5 females, 3 males) while five were still alive but highly affected (scoring below 1). Of the three candidates tested, Bn-OXA was the one which showed the most visible damage to the females, which consisted of tegumental rupture (Fig. 5c) and loss of uniformity on the ridges (Fig. 5d), and surprisingly was the only compound with slightly more activity on females than on males within 72 h of drug exposure. Additionally, Bn-OXA was the only compound that produced loss of spines from the ventral sucker and erosion in the oral sucker of *S. mansoni* (Fig. 5e, f).

Table 1 summarizes IC_{50} values [11], onset of action and key tegumental changes for all compounds examined on *S. mansoni*. Bn-OXA had the slowest onset

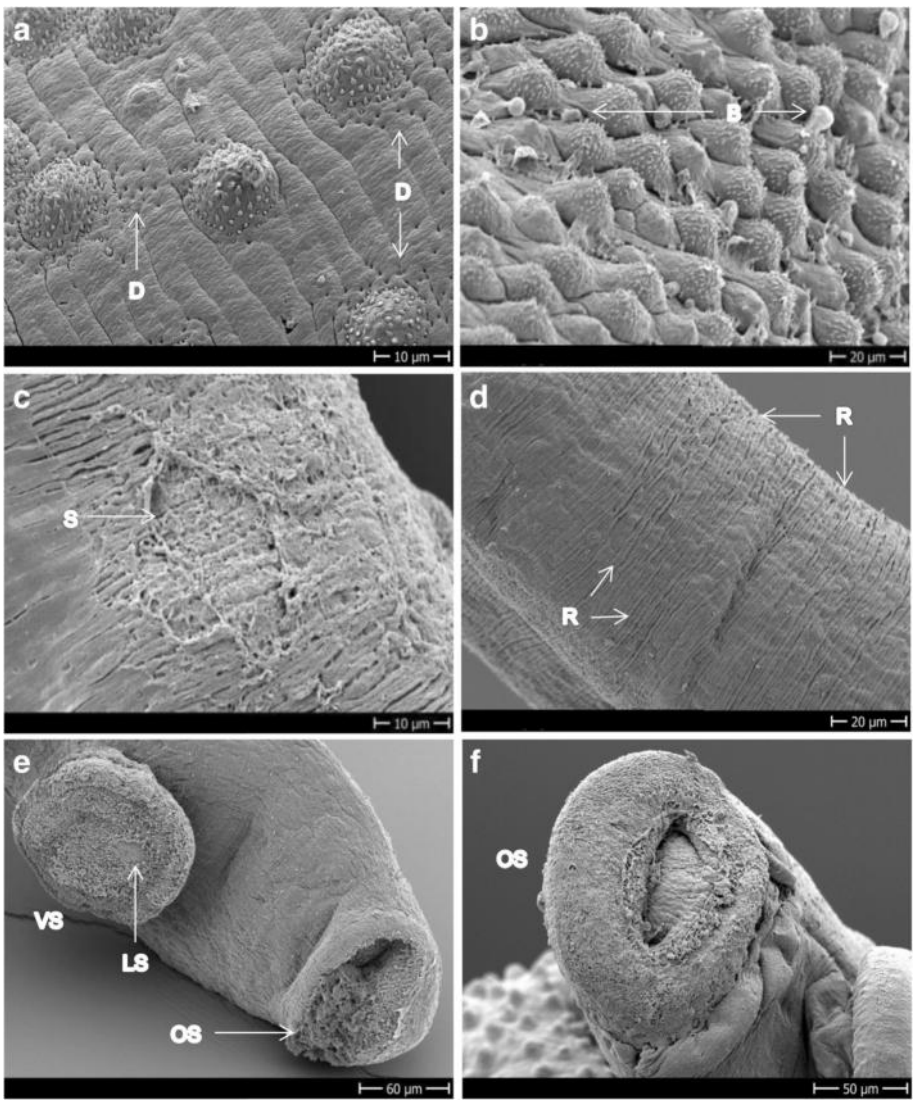

Fig. 5 Adult *S. mansoni* exposed to 100 µM Bn-OXA. **a** Dorsal mid-part of a male exposed for 24 h showing very mild damage. **b** Dorsal mid-part of a male's body incubated for 72 h. **c**, **d** Mid-part of female exposed for 72 h showing tegument ruptures and loss of uniformity of the ridges. **e**, **f** Head of males exposed for 72 h showing loss of spines from the ventral sucker and rupture and occlusion of the oral sucker. *Abbreviations*: B, blebs; D, dimples; LS, loss of spines; OS/VS, oral/ventral sucker; R, ridges; S, sloughing off; *Scale-bars*: **a**, **c**, 10 µm; **b**, **d**, 20 µm; **e**, 60 µm; **f**, 50 µm

Table 1 Comparative activity and effect of the OXA derivatives against *S. mansoni*

Compound	*S. mansoni* adult 72 h IC_{50} (μM)	Onset of action 100 μM (h)	Most affected sex	Tegumental damage		
				Blebbing	Sloughing off	Specific damage pattern/organ
Fc-OXA	11.4[a]	4	Males	+	++	Gynaecophoric canal
Rc-OXA	8.7 [a]	24	Males	++	+	Loss of spines
Bn-OXA	11.1 [a]	72	Females	+	+++	Suckers
OXA	> 100	120	Both	β	β	β

Abbreviation: β, no difference was observed to control group
[a]Hess et al. [11]

of action, which slightly contradicts the results presented by Hess et al. [11] who described 80% reduction in viability already after 24 h and 100% effect (all worms dead) in 72 h. The qualitative changes observed differ between the compounds studied and between males and females, a finding which is not uncommon for antischistosomal drugs. Artemether for example, causes extensive peeling in females but not in males [16]. Overall, the tegumental changes observed resemble findings from previous studies with praziquantel and other lead candidates, which also mention loss of spines, blebs and sloughing tissue with exposure of sub-tegumental tissue [17, 18].

Studies on *S. haematobium*

Figure 6 depicts images of control *S. haematobium*. Ridges and tubercles with spines on the dorsal side of the tegument and spines uniformly distributed in the gynaecophoric canal are visible (Fig. 6a, b). The apexes of the tubercles of male *S. haematobium* are free of spines (Fig. 6c). The tegument of the females also presents ridges, looks smoother than the males

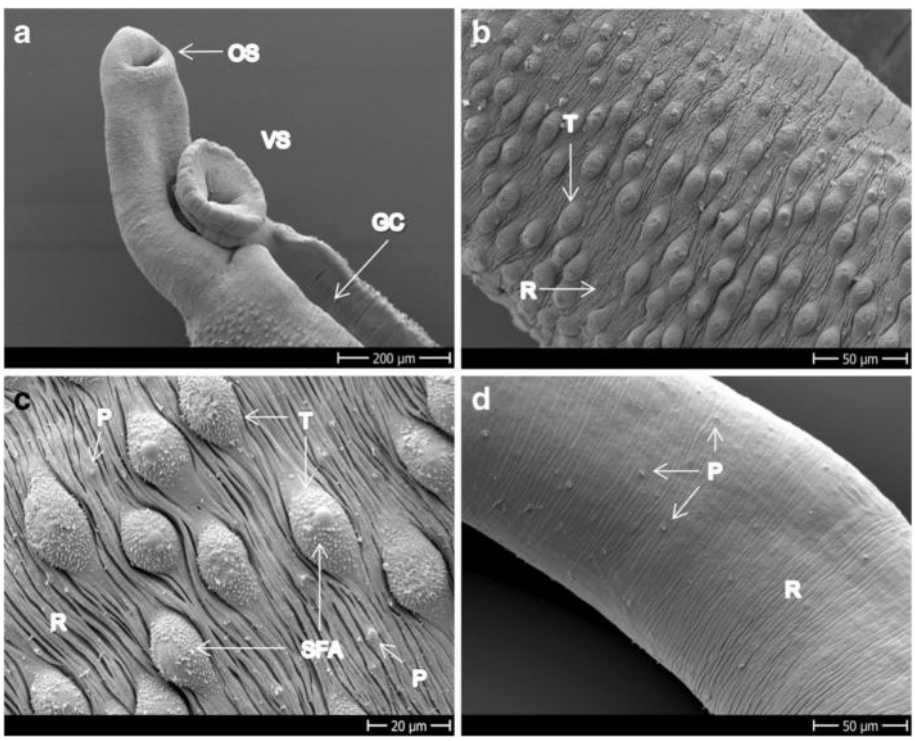

Fig. 6 Control group of adult *S. haematobium*. **a** Head of a male showing oral and ventral suckers and the gynaecophoric canal. **b** Dorsal and lateral side of a male with tubercles and ridges. **c** Dorsal side of the mid-part of male showing ridges, sensory papillae and apex-spine-free tubercles. **d** Mid-part of the body of a female revealing the smooth tegument with ridges and sensory papillae. *Abbreviations*: GC, gynaecophoric canal; OS/VS, oral/ventral sucker; P, papillae; R, ridges; SFA, spine free apex; T, tubercles. *Scale-bars*: **a**, 200 μm; **b**, 50 μm; **c**, 20 μm; **d**, 50 μm

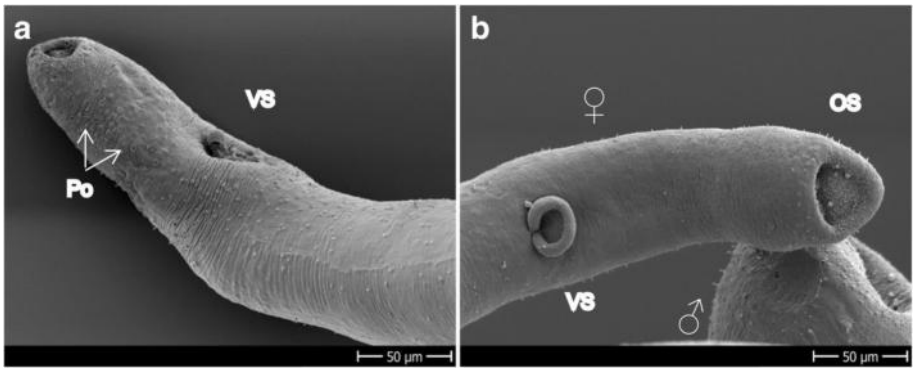

Fig. 7 *Schistosoma haematobium* exposed to 100 µM OXA for 120 h. **a** Head of a female showing the invaginated ventral sucker. **b** Head of a female showing the invaginated ventral sucker and mild damage to the oral sucker consisting of blebs and the oral sucker of a male, also showing small ruptures and blebs. *Abbreviations*: OS, oral sucker; Po, pores; VS, ventral sucker. *Scale-bars*: 50 µm

and the sensory papillae are uniformly distributed all over the body (Fig. 6d).

As observed for *S. mansoni*, *S. haematobium* incubated for 120 h in 1% DMSO also showed slight tegumental damage, characterized by blebs and sloughing tissue (not shown). Therefore few conclusions can be drawn with regard to the damage of 100 µM OXA incubated for 120 h. However one sign of damage could be related to OXA, due to the fact it was not evidenced in any of the controls: worms incubated with OXA for 120 h showed invagination of the ventral sucker in females and erosion of the oral sucker in both sexes (Fig. 7a, b).

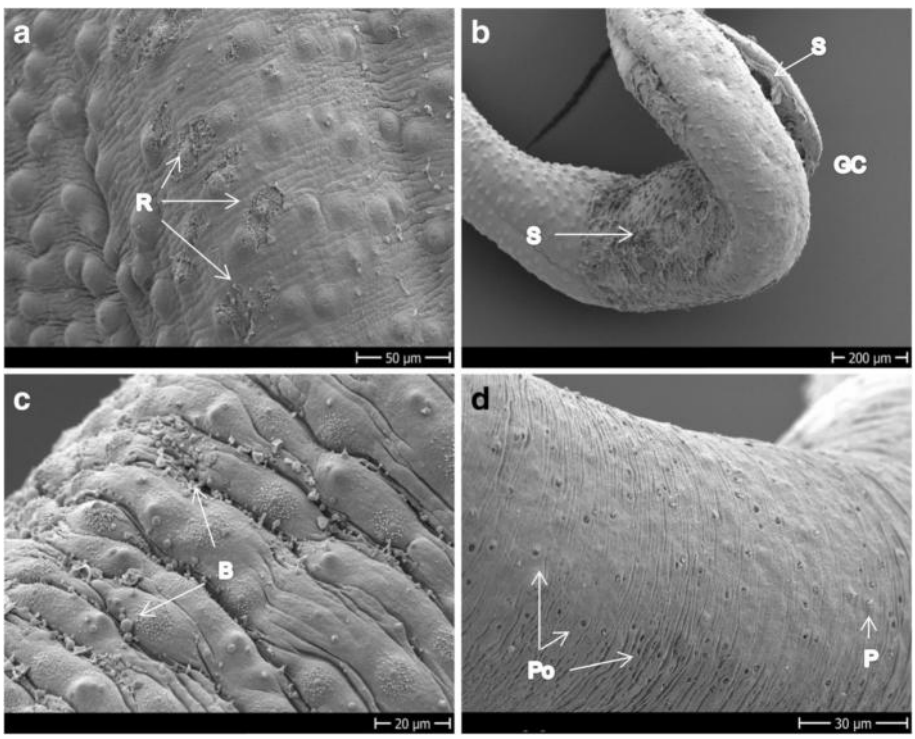

Fig. 8 Adult *S. haematobium* exposed to 100 µM Fc-OXA for 48 h. **a** Dorsal mid-part of the body of a male showing early rupturing around the tubercles. **b** Tegument sloughing at the dorsal mid-part of the body and the gynaecophoric canal. **c** Blebs on the dorsal mid-part of the body of a male. **d** Tegument of a female showing normal ridges and papillae, but also pores; pores seem to be present in higher quantity than in the control group. *Abbreviations*: B, blebs; GC, gynaecophoric canal; P, papillae; Po, pores; R, rupturing; S, sloughing off. *Scale-bars*: **a**, 50 µm; **b**, 200 µm; **c**, 20 µm; **d**, 30 µm

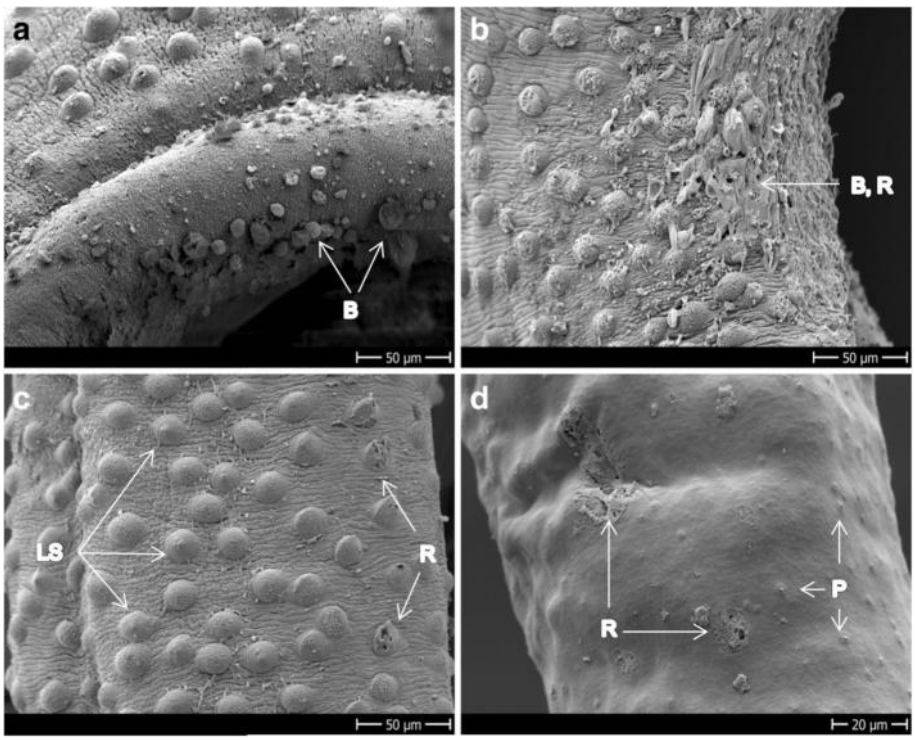

Fig. 9 Adult *S. haematobium* exposed to 100 μM Rc-OXA for 24 h. **a**–**c** Dorsal mid part of the body of a male showing blebs, tissue rupture and loss of spines. **d** Mid-part of the body of a female showing the tegument rupture. *Abbreviations*: B, blebs; LS, loss of spines; P, papillae; R, ruptures. *Scale-bars*: **a**–**c**, 50 μm; **d**, 20 μm

Additionally, we observed a higher number of pores in both sexes of the treated worms with respect to the controls (Fig. 7a).

After 48 h of exposure to 100 μM Fc-OXA we observed damage to the tegument and the gynaecophoric canal along the entire body, which, as in *S. mansoni*, consisted of blebbing and sloughing off (Fig. 8a–c). The sloughing tissue started its rupture from the areas surrounding the tubercles (Fig. 8a). Compared to the damage of this compound to the gynaecophoric canal in *S. mansoni*, the damage to this part of the body in *S. haematobium* was more pronounced (Fig. 8b). In females, appearance of pores over all the tegument (Fig. 8d), sporadic blebs and sloughing tissue (not shown) was visible. Damage to the oral or ventral suckers was not seen for Fc-OXA and the overall damage observed was more evident in males than in females.

The treatment of *S. haematobium* with Rc-OXA produced, as in *S. mansoni,* rupture of the tegument, with blebs and sloughing of tissue, and loss of spines within 24 h of incubation (Fig. 9a–c). In the females (Fig. 9d) we observed damage limited to small ruptures not related to any specific section or structure of the body despite that the viability of both male and female worms had decreased to a score below 0.5, revealing high activity of the drug. We could not evidence damage to the suckers or gynaecophoric canal following exposure to this compound either in males or in females.

Following incubation of *S. haematobium* males with Bn-OXA, creases of the inner and outside of the body were visible after 48 h of exposure and there was a tendency of the worms to die in a circular body disposition (Fig. 10a). As in *S. mansoni* and Fc-OXA and Rc-OXA on *S. haematobium*, bleb/vesicles formation was a common phenomenon that appeared in large quantities on the entire surface of the tegument (Fig. 10b, c). With regard to tegumental sloughing, the effect of Bn-OXA against *S. haematobium* was much milder (Fig. 10b, c) when compared to the other compounds (Figs. 8b, 9b) and exposure of *S. mansoni* to Bn-OXA (Fig. 5c, f). We did not evidence damage to the suckers of the males following exposure to Bn-OXA. However, in females, the erosion and deformity to both oral and ventral suckers was significant (Fig. 10d) and was also accompanied by sloughing tissue.

Different from the activity of Bn-OXA against *S. mansoni*, in *S. haematobium* this compound was more active against males than against females, but as for *S. mansoni*, Bn-OXA seemed to reveal the highest activity of the three derivatives against females.

Table 2 summarizes *in vitro* effects of the three compounds on *S. haematobium*. After exposure to a 100 μM

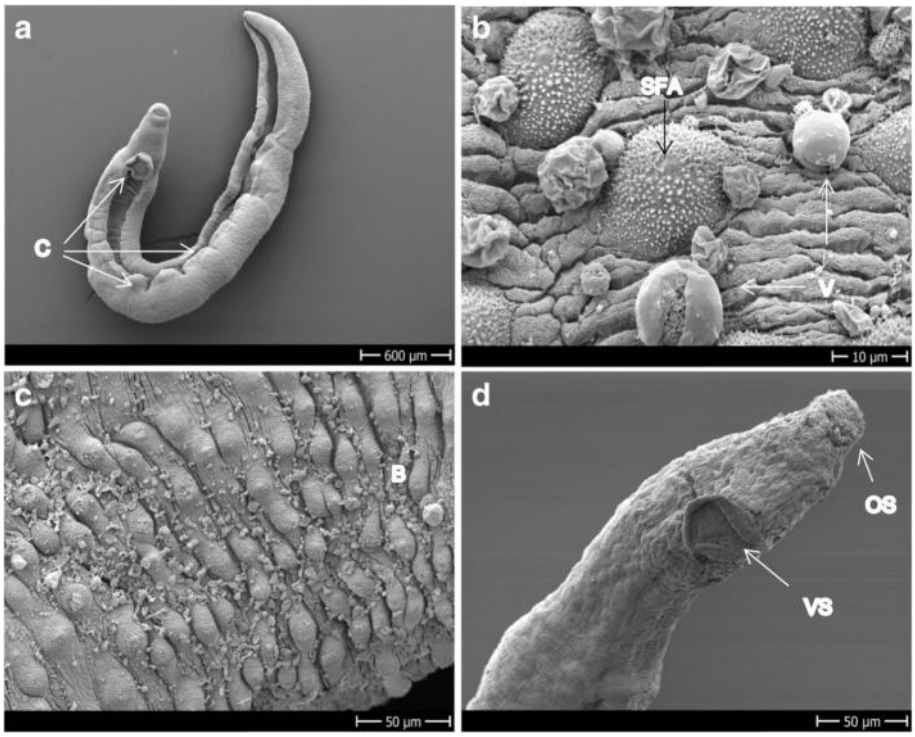

Fig. 10 Adult *S. haematobium* exposed to 100 µM Bn-OXA for 48 h. **a** Male showing creases of the tegument and the circular disposition of the body before dying. **b**, **c** Dorsal mid-part of male's tegument showing the extensive distribution of blebs, vesicles and mild sloughing off. **d** Head of a female showing extensive erosion of the oral sucker and extensive deformity of the ventral sucker. *Abbreviations*: B, blebs; C, creases; OS/VS, oral/ventral sucker; SFA, spine free apex; V, vesicles. *Scale-bars*: **a**, 600 µm; **b**, 10 µm; **c**, **d**, 50 µm

concentration, Fc-OXA needed 48 h to trigger a reduction in viability of 75–85% on *S. haematobium*, while Rc-OXA was lethal for all males and reduced the viability of the females to a score lower than 0.5 within 24 h. Rc-OXA also had the lowest IC_{50} value of the three compounds. Bn-OXA reduced the viability of males and females by 70% within 48 h. All derivatives were more active on males than on females, while in the case of oxamniquine no difference of sex susceptibility could be determined. Also, for *S. haematobium* we observed loss of spines and sloughing tissue, which are signs of drug activity that have been described before, for example for artemisinins against *S. haematobium* [19]. Other studies reported the damage of active compounds to *S. haematobium* to be characterized by edematous intertubercular spaces and collapse of tubercles, signs that were not observed in our compounds [20].

Comparison of oxamniquine derivatives

While the fastest and most active compound against *S. mansoni* was Fc-OXA, Rc-OXA was the most promising compound for *S. haematobium* with regard to *in vitro* activity and tegumental damage. Surprisingly, Fc-OXA had the highest IC_{50} value against *S. haematobium.* Bn-OXA was the compound with the slowest visible effect against both species, but was active against both species as well, in a timeframe of 48–72 h, depending on the species. Overall, a higher activity of the derivatives was observed against *S. mansoni* than against *S. haematobium.*

Table 2 Comparative activity and effect of the derivatives against *S. haematobium*

Compound	*S. haematobium* adult 72 h IC_{50} (µM)	Onset of action 100 µM (h)	Most affected sex	Tegumental damage		
				Blebbing	Sloughing off	Specific damage pattern/organ
Fc-OXA	68.1	48	Males	+	++	Gynaecophoric canal
Rc-OXA	24.5	24	Males	++	++	Loss of spines
Bn-OXA	38.6	48	Males	+	+++	Body creases
OXA	> 100	120	Both	+	β	VS invagination

Abbreviations: VS, ventral sucker; β, no difference was observed to control group

For both species, and all three derivatives investigated, we could observe common patterns of damage to the tegument, which consisted of extensive blebs and considerable tegument rupture and sloughing off along the whole body, with exposure of sub-tegumental tissue. The sub-tegument might expose antigens and therefore trigger an immune response attack, commonly observed for antischistosomal drugs [17–19].

Differences in the damage distribution cannot be explained, but might be due to a differential distribution of the activating enzyme in the body of the parasites or additional mechanisms of action for the individual derivatives supporting the antiparasitic effect.

Conclusions

Our study confirmed that Fc-OXA, Rc-OXA and Bn-OXA are promising broad spectrum antischistosomal drug candidates. All derivatives showed high *in vitro* activity against *S. mansoni* and *S. haematobium*, while validating the previous finding that the parent drug oxamniquine is less active *in vitro* under the conditions described. Future studies should aim to further characterize these compounds, taking into account the *in vivo* activity on juvenile stages of development and activity against *S. haematobium in vivo*.

Abbreviations

OXA: Oxamniquine; Fc-OXA: Ferrocenyl oxamniquine; Rc-OXA: Ruthenocenyl oxamniquine; Bn-OXA: Benzyl oxamniquine; SEM: Scanning electron microscopy; SmSULT: *Schistosoma mansoni* sulfotransferase; DMSO: Dimethyl sulfoxide

Acknowledgments

We kindly acknowledge the help and expertise from Eva Bieler from the Swiss Nano science Institute.

Funding

We gratefully acknowledge financial support from the Swiss National Science Foundation (Professorships No. PP00P2_133568 and PP00P2_157545 to GG), the University of Zurich (GG) and the Swiss excellence scholarships for foreign students (ESKAS to VB). This work has received support under the program "Investissements d'Avenir" launched by the French Government and implemented by the ANR with the reference ANR-10-IDEX-0001-02 PSL (GG). JK and GG are grateful to the European Research Council (ERC-2013-CoG 614739-A_HERO to JK and ERC-2015-CoG 681679-PhotoMedMet to GG) for financial support.

Availability of data and materials

The data supporting the conclusions of this article are included within the article. Raw data are available upon request from the corresponding author.

Authors' contributions

JK and VB designed the studies and collected and analysed the data. VB took the images with the assistance of a professional technician in the imaging facilities and drafted the first version of the manuscript that JK supervised. GG and JH designed and synthetized the derivatives of oxamniquine and revised the manuscript. All authors read and approved the final manuscript.

Ethics approval

All animal experiments were authorized by the veterinary office from Canton Basel Stadt (Authorization No. 2070) based on the Swiss national and cantonal regulations.

Consent for publication

Not applicable.

Competing interests

The authors declare that they have no competing interests.

Publisher's Note

Author details

[1]Department of Medical Parasitology and Infection Biology, Swiss Tropical and Public Health institute, Socinstrasse 57, 4051 Basel, CH, Switzerland. [2]University of Basel, P.O. Box, 4003 Basel, CH, Switzerland. [3]Department of Chemistry, University of Zurich, Winterthurerstrasse 190, 8057 Zurich, CH, Switzerland. [4]Chimie ParisTech, PSL University, Laboratory of Inorganic Chemical Biology, F-75005 Paris, France.

Received: 9 July 2018 Accepted: 2 October 2018
Published online: 06 November 2018

References

1. Colley DG, Bustinduy AL, Secor WE, King CH. Human schistosomiasis. Lancet. 2014;383:2253–64.
2. Bergquist R, Utzinger J, Keiser J. Controlling schistosomiasis with praziquantel: how much longer without a viable alternative? Infect Dis Poverty. 2017;6:74.
3. Stothard JR, Sousa-Figueiredo JC, Betson M, Bustinduy A, Reinhard-Rupp J. Schistosomiasis in African infants and preschool children: Let them now be treated! Trends Parasitol. 2013;29:197–205.
4. Cioli D, Pica-Mattoccia L, Basso A, Guidi A. Schistosomiasis control: praziquantel forever? Mol Biochem Parasitol. 2014;195:23–9.
5. Lago EM, Xavier RP, Teixeira TR, Silva LM, da Silva Filho AA, de Moraes J. Antischistosomal agents: state of art and perspectives. Future Med Chem. 2017;10:89–120.
6. Pica-Mattoccia L, Novi A, Cioli D. Enzymatic basis for the lack of oxamniquine activity in *Schistosoma haematobium* infections. Parasitol Res. 1997;83:687–9.
7. Sabah AA, Fletcher C, Webbe G, Doenhoff MJ. *Schistosoma mansoni*: chemotherapy of infections of different ages. Exp Parasitol. 1986;61:294–303.
8. Chevalier FD, Le Clec'h W, Eng N, Rugel AR, Assis RR de, Oliveira G, et al. Independent origins of loss-of-function mutations conferring oxamniquine resistance in a Brazilian schistosome population. Int J Parasitol. 2016;46:417–424.
9. Valentim CLL, Cioli D, Chevalier FD, Cao X, Taylor AB, Holloway SP, et al. Genetic and molecular basis of drug resistance and species-specific drug action in schistosome parasites. Science. 2013;342:1385–9.
10. Manneck T, Braissant O, Haggenmüller Y, Keiser J. Isothermal microcalorimetry to study drugs against *Schistosoma mansoni*. J Clin Microbiol. 2011;49:1217–25.
11. Hess J, Panic G, Patra M, Mastrobuoni L, Spingler B, Roy S, et al. Ferrocenyl, ruthenocenyl, and benzyl oxamniquine derivatives with cross-species activity against *Schistosoma mansoni* and *Schistosoma haematobium*. ACS Infect Dis. 2017;3:645–52.
12. Hess J, Keiser J, Gasser G. Toward organometallic antischistosomal drug candidates. Future Med Chem. 2015;7:821–30.
13. Jones MK, Gobert GN, Zhang L, Sunderland P, McManus DP. The cytoskeleton and motor proteins of human schistosomes and their roles in surface maintenance and host-parasite interactions. BioEssays. 2004;26:752–65.
14. Keiser J. *In vitro* and *in vivo* trematode models for chemotherapeutic studies. Parasitology. 2010;137:589–603.
15. Gobert GN, Schulte L, Jones MK. Tegument and external features of *Schistosoma* (with particular reference to ultrastructure). In: Jamieson BGN, editor. *Schistosoma*: Biology, Pathology, and Control. Boca Raton: CRC Press; 2017. p. 213–38.
16. Abdul-Ghani R, Loutfy N, Sheta M, Hassan A. Artemether shows promising female schistosomicidal and ovicidal effects on the Egyptian strain of *Schistosoma mansoni* after maturity of infection. Parasitol Res. 2011;108:1199–205.
17. Silva A, Oliveira S, Oliveira J, Santiago E, Júnior A, Jacobi Í, et al. Tegumental changes in adult *Schistosoma mansoni* induced by a new imidazolidinic derivative. Br J Pharm Res. 2014;4:1988–2005.
18. de Oliveira SA, de Oliveira Barbosa M, Filho CALM, Oliveira AR, de Sousa FA, de Farias Santiago E, et al. Phthalimido-thiazole as privileged scaffold:

activity against immature and adult worms of *Schistosoma mansoni*. Parasitol Res. 2018;117:2105–15.
19. El-Beshbishi SN, El Bardicy S, Tadros M, Ayoub M, Taman A. Efficacy of artemisinin-naphthoquine phosphate against *Schistosoma haematobium* adult flukes: dose-effect relationship and tegumental alterations. J Helminthol. 2018. https://doi.org/10.1017/S0022149X18000421.
20. Eraky MA, Aly NSM, Selem RF, El-Kholy AAE-M, Rashed GAE-R. *In vitro* schistosomicidal activity of phytol and tegumental alterations induced in juvenile and adult stages of *Schistosoma haematobium*. Korean J Parasitol. 2016;54:477–84.

Chapter IV-B

Multidisciplinary preclinical investigations on three oxamniquine analogues as new drug candidates for schistosomiasis

Full Paper
doi.org/10.1002/chem.202002856

Medicinal Organometallic Chemistry

Multidisciplinary Preclinical Investigations on Three Oxamniquine Analogues as New Drug Candidates for Schistosomiasis**

Valentin Buchter[+],[a, b] Yih Ching Ong[+],[c] François Mouvet[+],[d] Abdallah Ladaycia,[e] Elise Lepeltier,[e] Ursula Rothlisberger,*[d] Jennifer Keiser,*[a, b] and Gilles Gasser*[c]

Abstract: Schistosomiasis is a disease of poverty affecting millions of people. Praziquantel (PZQ), with its strengths and weaknesses, is the only treatment available. We previously reported findings on three lead compounds derived from oxamniquine (OXA), an old antischistosomal drug: ferrocene-containing (Fc-CH_2-OXA), ruthenocene-containing (Rc-CH_2-OXA) and benzene-containing (Ph-CH_2-OXA) OXA derivatives. These derivatives showed excellent in vitro activity against both *Schistosoma mansoni* larvae and adult worms and *S. haematobium* adult worms, and were also active in vivo against adult *S. mansoni*. Encouraged by these promising results, we conducted additional in-depth preclinical studies and report in this investigation on metabolic stability studies, in vivo studies on *S. haematobium* and juvenile *S. mansoni*, computational simulations, and formulation development. Molecular dynamics simulations supported the in vitro results on the target protein. Though all three compounds were poorly stable within an acidic environment, they were only slightly cleared in the in vitro liver model. This is likely the reason why the promising in vitro activity did not translate into in vivo activity on *S. haematobium*. This limitation could not be overcome by the formulation of lipid nanocapsules as a way to improve the in vivo activity. Further studies should focus on increasing the compound's bioavailability, to reach an active concentration in the microenvironment of the parasite.

Introduction

Schistosoma mansoni, S. haematobium, and *S. japonicum* account for over 90% of the cases of schistosomiasis, an acute and chronic parasitic disease that affects over 200 million people worldwide[1–3] and threatens more than 700 million people who are at risk of infection.[4] In children, schistosomiasis stunts physical growth and the ability to learn, while in adults, the disease affects the ability to work and can cause organ failure and, ultimately, death; a situation that causes an enormous socioeconomic burden for developing communities.[5] Praziquantel (PZQ) is the only drug being used for periodic mass drug administration to control the disease. Considering the imminent threat of resistance[6] and considering other drawbacks that PZQ presents, our efforts are oriented towards identifying and developing a new molecule with the potential to become an alternative therapeutic option in the treatment of this disease.

Oxamniquine (OXA, Figure 1) is an anthelmintic drug developed in the 1960s[7] that showed high activity and a very convenient drug profile in terms of safety and ease of administration. It became the cornerstone of the schistosomiasis eradication program in Brazil in the past and at the beginning of the 21st century, but fell into disuse for two main reasons: it was only active against adult *S. mansoni*[7–9] and resistance was clinically confirmed. The drug was therefore no longer commercialized after 2010 and replaced by PZQ.[7] OXA is a prodrug that needs to be activated by the sulfotransferase of *S. mansoni* (SmULT) to an alkylating molecule that binds proteins and DNA, consequently killing the parasite.[10] Different enzyme or-

[a] V. Buchter,[+] Prof. Dr. J. Keiser
Swiss Tropical and Public Health Institute
Socinstrasse 57, P.O. box, 4002 Basel (Switzerland)
E-mail: jennifer.keiser@swisstph.ch
Homepage: https://www.swisstph.ch/en/about/mpi/helminth-drug-development/

[b] V. Buchter,[+] Prof. Dr. J. Keiser
University of Basel, Petersplatz 1, P.O. Box, 4001 Basel (Switzerland)

[c] Dr. Y. C. Ong,[+] Dr. G. Gasser
Chimie ParisTech, PSL University
CNRS, Institute of Chemistry for Life and Health Sciences
Laboratory of Inorganic Chemical Biology
75005 Paris (France)
E-mail: gilles.gasser@chimeparistech.psl.eu
Homepage: www.gassergroup.com

[d] F. Mouvet,[+] Prof. Dr. U. Rothlisberger
Laboratory of Computational Chemistry and Biochemistry, EPFL
1015 Lausanne (Switzerland)
E-mail: ursula.roethlisberger@epfl.ch
Homepage: https://www.epfl.ch/labs/lcbc/roethlisberger/

[e] A. Ladaycia, Dr. E. Lepeltier
MINT, UNIV Angers, INSERM 1066, CNRS 6021
Université Bretagne Loire, 4 rue Larrey, 49933 Angers Cedex 9 (France)

[+] These authors contributed equally to this work.

[**] A previous version of this manuscript has been deposited on a preprint server (https://doi.org/10.26434/chemrxiv.12102894.v1).

Supporting information and the ORCID identification number(s) for the author(s) of this article can be found under: https://doi.org/10.1002/chem.202002856.

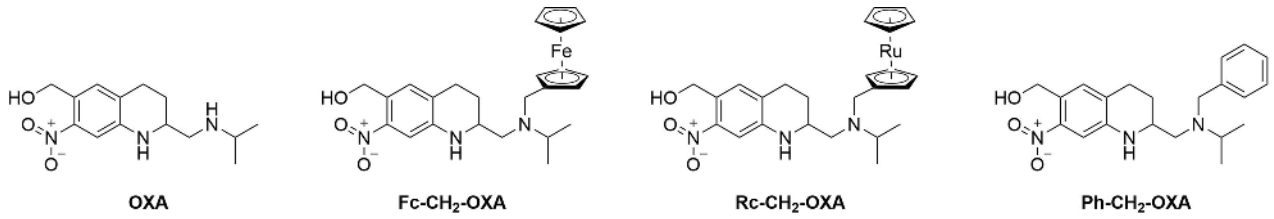

Figure 1. Structures of the compounds investigated in this study.

thologues are present in all *Schistosoma* species, but only the active site of the sulfotransferase of *S. mansoni* can activate OXA.[11]

OXA was commercialized as a 1:1 racemic mixture, with both enantiomers having antiparasitic activity, although the (*S*)-OXA contributes the most. Crystal structures of (*R*)-OXA and (*S*)-OXA complexes with SmSULT target show similarities in the modes of OXA binding, but only the (*S*)-OXA enantiomer is observed in the structure of the enzyme exposed to racemic OXA.[12]

The mechanism of resistance and lack of activity against some schistosome species has been well studied. Resistance is based in one or more point mutations in the enzyme's active site that prevent the molecule from being sulfonated.[13] Taking into account that there is a 70% homology between the amino acid sequences of the sulfotransferases of *S. mansoni* and *S. haematobium*,[11] we derivatized OXA based on the hypothesis that modification of OXA could overcome the species and stage specificity.[14]

Previous studies by Jaouen and co-workers on the anticancer drug candidate ferrocifen[15–17] and Brocard, Biot and co-workers on the anti-malarial drug candidate ferroquine showed that the ferrocenyl analogues of tamoxifen and chloroquine, respectively, have improved bioactivity compared to the original organic drug compounds.[18,19] This was due to several factors: the ferrocenyl component acted as a producer of reactive oxygen species (ROS), increased the lipophilic character of the molecule, and provided a mechanism of action different to that of the original drug.[20–22] With this concept in mind, we developed several metal-containing derivatives of OXA that were studied in vitro and in vivo against *Schistosoma spp.*[23–25] Among others, we demonstrated that the three derivatives of OXA, namely a ferrocene- (Fc-CH_2-OXA), ruthenocene- (Rc-CH_2-OXA), and benzene-containing (Ph-CH_2-OXA) derivative (Figure 1), showed promising in vitro results, where all three OXA derivatives caused death of *S. mansoni* and *S. haematobium* adult worms[25] and worm burden reductions of 76 to 93% against adult *S. mansoni* in vivo.[23] Encouraged by our promising preliminary results, we decided to go further in the development and to fully characterize these three OXA analogues. In vitro studies were conducted against *S. mansoni* juvenile worms, and *S. japonicum* and *S. haematobium* adult worms. In vivo studies were carried out against adult *S. haematobium* and juvenile *S. mansoni* including studies with Ph-CH_2-OXA encapsulated in Lipid NanoCapsules (LNC). Only racemic mixtures were tested, as we focused on determining the presence of activity for the OXA derivatives in vivo with *S. mansoni* and *S. haematobium*, rather than on each of the enantiomers. As these drugs are intended to be administered orally, we evaluated the stability of the derivatives under acidic conditions. Our work was complemented by computational models and molecular dynamics simulations as well as microsomal stability and albumin binding studies.

Results and Discussion

In vitro studies

Fc-CH_2-OXA, Rc-CH_2-OXA, and Ph-CH_2-OXA were previously demonstrated to have promising activity as drug candidates in vitro against adult *S. mansoni* and S. *haematobium* and first stage of the larval development (NTS: newly transformed schistosomula) and in vivo against adult *S. mansoni*.[23,25] To test the full potential of our compounds, we first elucidated the in vitro activity of the OXA derivatives against 28-day-old juvenile *S. mansoni* worms, because one of the important drawbacks of PZQ is its low activity against this developmental stage. All three compounds killed all the worms within 24 h of incubation at a concentration of 100 μM (Table 1). Against juvenile *S. mansoni*, Fc-CH_2-OXA had the lowest IC_{50} (0.5 μM) while

Table 1. In vitro activity of Fc-CH_2-OXA, Rc-CH_2-OXA, and Ph-CH_2-OXA versus OXA against *S. mansoni*, *S. haematobium*, and *S. japonicum*.

	S. mansoni				*S. haematobium*		*S. japonicum*
Compd	IC_{50} adults 72 h [μM]	IC_{50} adults in medium 45 g L^{-1} albumin 72 h [μM]	Onset of action on juveniles 100 μM [h]	IC_{50} 28 day juveniles 72 h [μM]	IC_{50} adults 72 h [μM]	IC_{50} adults in medium with albumin 72 h [μM]	IC_{50} adults 72 h [μM]
Fc-CH_2-OXA	9.0	28.1	<24	0.5	52.3	55.7	22.7
Rc-CH_2-OXA	6.0	NC	<24	1.3	15.5	25.0	30.9
Ph-CH_2-OXA	13.5	90.7	<24	26.7	32.6	70.6	39.8
OXA	>100	>100	72	>100	>100[a]	ND	>100

[a] Hess et al.;[23] NC: no correlation, ND: not done.

Ph-CH_2-OXA was the drug with the highest IC_{50} value (26.7 μM), i.e., the compound with the lowest activity. Interestingly, in the case of Ph-CH_2-OXA, the effect of the molecules on the juveniles was faster than against the adults: on adult *S. mansoni*, Ph-CH_2-OXA needed 72 h to exert its maximal activity, whereas against juvenile stages, we observed a total lethal effect within 24 h of incubation at a dose of 100 μM. For comparison, in the same incubation time, juvenile *S. mansoni* exposed to OXA showed an IC_{50} of >100 μM, confirming previous studies of OXA being only slightly active in vitro and against juvenile stages of the parasite.[9,25] Only after 72 h of incubation at 100 μM, where the derivatives had long exerted their activity, a 48% reduction of the viability of OXA with respect to the control worms was found (Table S3).

Against *S. japonicum* adult worms, we observed the same behavior: while OXA was not active even with 100 μM after 3 days (Table 1 and Table S3), our derivatives showed considerable activity. Of the three derivatives tested, Fc-CH_2-OXA proved to be the most active of all three derivatives, killing all the parasites within 24 h at a concentration of 100 μM and having the lowest IC_{50} value (22.6 μM). On *S. haematobium* instead, the most active compound was Rc-CH_2-OXA, also killing all parasites at a concentration of 100 μM and revealing the lowest IC_{50} value (15.5 μM).

Moreover, we incubated adult *S. mansoni* in medium containing albumin and compared the activity determined to our standard assay. A lower activity of the three drugs was observed in the enriched medium, with Fc-CH_2-OXA showing the least loss of activity of the three derivatives (Table 1). The albumin binding experiment was also performed for adult *S. haematobium*. Also in this case, the three compounds showed a reduction of the activity. These results are comparable to those obtained by Pasche et al.[26] who also identified a significant decrease in drug activity incubating antischistosomal drug candidates in vitro in the presence of albumin. PZQ also presents a high percentage (ca. 80%) of drug bound to protein[27] and this might be a reason for the high doses needed to reach a significant effect. Protein binding is a major issue in drug development, since only the free fraction of the drug is able to interact with the target.[28]

Studies on juvenile *S. mansoni* in the mouse model

In terms of activity against juvenile parasites in vivo, we identified a lower activity of all three compounds in respect to the results on adult parasites.[23] Although the drug showed moderate activity, as shown by their shift to the liver due to the loss of vein attachment (data not shown), worm burden reductions were low, ranging from 39 to 47% (Table 2). When considering the gender of the surviving worms, we found that there was no gender difference in susceptibility (binomial test, $p > 0.77$).

In vivo studies on adult *S. haematobium*

Table 3 shows the worm burden reduction of the three compounds against *S. haematobium*: none of the compounds affected *S. haematobium* in vivo, contradicting the findings observed in vitro.

Table 3. Change in the worm burden of *S. haematobium* infected hamsters after treatment with 200 mg kg^{-1} of the OXA derivatives.

Compd	No. of mice	Worm burden (SD)		WBR %
		Females	Total	
control group	4	18.5 (8.3)	40 (13.6)	–
Fc-CH_2-OXA	4	25.8 (7.5)	54 (16.2)	0
Rc-CH_2-OXA	3[a]	55 (16.1)	108 (28.9)	0
Ph-CH_2-OXA	4	19 (3.7)	51 (18.9)	0

[a] One animal died during the experiment.

Computational studies

To understand the interaction between OXA analogues and the sulfotransferase proteins from *S. mansoni* (SmSULT) and *S. haematobium* (ShSULT), we performed classical molecular dynamics simulations of OXA, Fc-CH_2-OXA, Ph-CH_2-OXA, and Fc-CO-OXA to determine their binding poses within the active site of the two sulfotransferases at body temperature. Fc-CO-OXA was added to the comparison to include the case of a derivative that was shown to be less active against *S. mansoni* in vitro than the other compounds considered in the present study.[23]

We did not consider Rc-CH_2-OXA explicitly because, both from a geometrical and electrostatic point of view, the force field models for ferrocenyl and ruthenocenyl compounds are very similar and would likely yield comparable behavior at this simplified level of theory.

Table 2. Reduction of the juvenile worm burden in *S. mansoni* infected mice after treatment with 200 mg kg^{-1} of the OXA derivatives and after treatment with the nanoencapsulated Ph-CH_2-OXA.

Compd	No. of mice	Worm burden (SD)		WBR % pure drug (SD)[a]		WBR % nanocapsule[a]	
		Females	Total	Females	Total	Females	Total
control group	8	6.5 (1.6)	12.3 (2.5)	–	–	–	–
Fc-CH_2-OXA	4	3.8 (1.0)	7.5 (2.7)	42.3 (14.7)	38.8 (21.6)	ND	ND
Rc-CH_2-OXA	4	3.0 (2.5)	6.5 (4.4)	53.8 (7.7)	46.9 (36.2)	ND	ND
Ph-CH_2-OXA	4	4.3 (0.5)	7.5 (0.6)[b]	34.6 (7.7)	38.8 (4.7)[b]	0	0

[a] ND: Not done; WBR: worm burden reduction. [b] Statistically different from control on $p < 0.05$.

The free-energy difference between bound and unbound states of a receptor-ligand complex is a direct measure of the binding affinity. To estimate this quantity from our trajectories, we used the MM/PBSA (Table 4) and MM/GBSA methods (Table S1). All binding free energies are negative, meaning that the bound state is energetically favorable for all compounds. No systematic difference can be noted between the two proteins and all modified OXA compounds show a higher binding affinity than OXA itself. This is probably due to their larger size, forcing a tighter fit inside the protein and increasing the number of interactions with the binding pocket. Consequently, all analogues are strongly bound to their target proteins.

Since the drugs are supposed to react with PAPS within the target protein, the distance between the closest oxygen of the sulfate group of PAPS and the hydrogen in the hydroxyl group of each drug was measured every 40 ps. These distances are represented as histograms in Figure 2 and their average is shown in Table 5. The near-attack configurations (NAC), i.e., those with shorter distances between the reactive groups, are more likely to result in the activation of the compounds.

For OXA in SmSULT, the sulfate-hydroxyl distance is short and stable for both enantiomers, with an average slightly above 3 Å. The relative orientation of the reactive groups is fixed through their mutual interaction with ASN230, thus promoting the interaction (Figure S2). The chain of residues 19 to 23 also binds to PAPS and OXA at different places, stabilizing the configuration. For OXA, the difference between *R*- and *S*-enantiomers is very small, which is consistent with previous experimental works that reported that both enantiomers bind in a similar fashion and that the activity difference originates from their binding kinetics.[12]

Both enantiomers of Ph-CH_2-OXA and Fc-CH_2-OXA show a very strong interaction with PAPS within SmSULT. Residues 18 to 21 bind both ligands in several places, highly stabilizing their binding (Figures S4 and S6). Moreover, the residue ASN230 also binds to PAPS and to the chain of residues 18–21, further increasing the stability. This may explain the high activity of these compounds in vitro. On the other hand, the *R*-enantiomer of Fc-CH_2-OXA seems to drift slowly away from PAPS and a proper equilibrium is never reached within our simulation time. The distance increases over time, which suggests that the final configuration will not be active. Strikingly, Ph-CH_2-OXA does not seem to be impacted by the enantiomer selectivity observed for all other derivatives.

Fc-CH_2-OXA, which was the most active against *S. mansoni* according to the in vitro experimental studies, shows short

Table 4. Estimated binding free-energies computed by the MM/PBSA method [kcal mol^{-1}].

Compd	*S. mansoni*		*S. haematobium*	
	R	*S*	*R*	*S*
Fc-CH_2-OXA	−39.3	−41.9	−36.3	−39.9
Fc-CO-OXA	−36.3	−29.9	−26.4	−32.0
Ph-CH_2-OXA	−30.3	−35.0	−36.6	−18.3
OXA	−12.5	−8.0	−17.1	−22.8

Table 5. Average O–H distance with standard deviation (Å).

Compd	*S. mansoni*		*S. haematobium*	
	R	*S*	*R*	*S*
Fc-CH_2-OXA	5.1 ± 1.1	1.8 ± 0.1	11.8 ± 0.7	6.1 ± 0.8
Fc-CO-OXA	12.2 ± 1.2	10.0 ± 0.9	12.8 ± 1.9	6.2 ± 0.7
Ph-CH_2-OXA	2.2 ± 0.7	2.0 ± 0.7	14.5 ± 1.1	4.3 ± 0.5
OXA	3.3 ± 0.4	3.5 ± 0.3	9.5 ± 1.6	6.1 ± 0.8

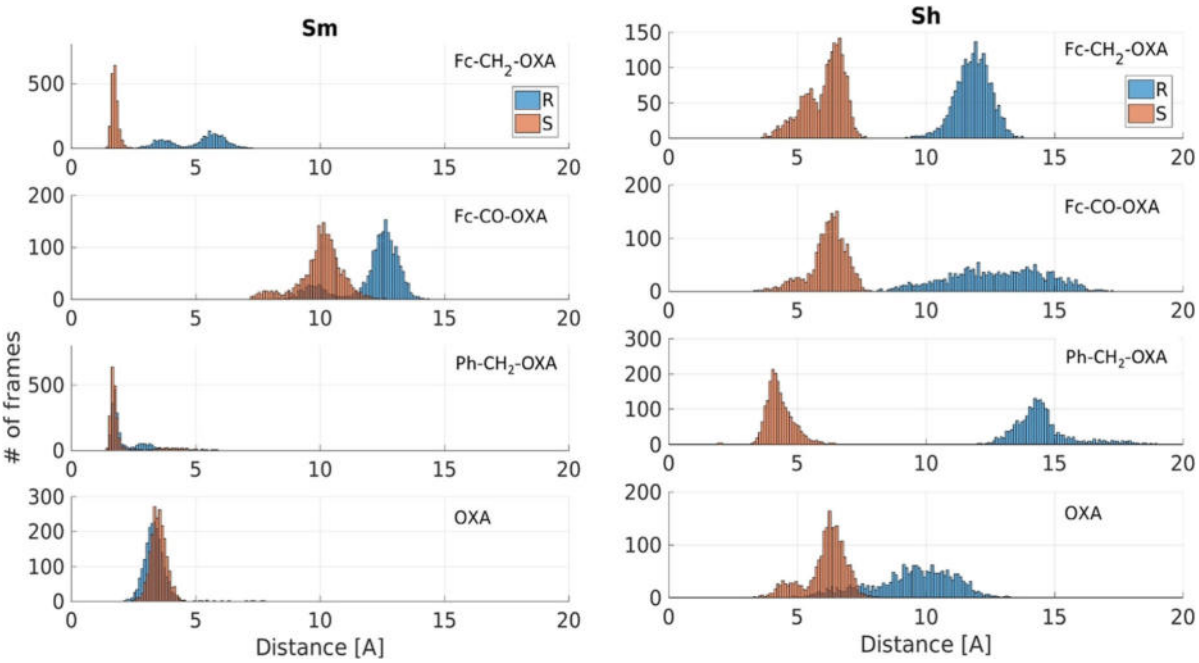

Figure 2. Distance between the closest oxygen of PAPS and the hydroxyl group of the analogues; (*R*)-enantiomers in blue and (*S*)-enantiomers in orange.

average distance to PAPS. In *S. haematobium* instead, the shortest distance to PAPS is observed for the *S*-enantiomer of Ph-CH_2-OXA, which also shows a lower IC_{50} against this species when compared to Fc-CH_2-OXA. Furthermore, our simulations of Fc-CO-OXA in SmSULT show NAC distributions in which the reactants are about three times more distant than in OXA, with averages above 10 Å. These configurations are very unlikely to activate the drug, which is again consistent with experimental results.

In practice, OXA is not active on *S. haematobium*. In simulations in which OXA is docked into ShSULT, we observe that the distance between the reactive groups is much larger than in SmSULT, by more than 6 Å on average. Furthermore, we observe a large difference between enantiomers, where the *R*-enantiomer shows a broad distribution of NAC distances with an average of 9.5 Å. This strong enantiomer dependence is present for all compounds and is more pronounced than in SmSULT with all *R*-enantiomers adopting less reactive configurations. The residue ASP80 seems to have a negative impact, forming a stable bond with the drug's hydroxyl group (Figures S3, S5, S7). This bond is far from PAPS, leading to unreactive geometries shown by a widening of the distance distributions between the compounds and PAPS. This residue is conserved in SmSULT but stays at larger distances (more than 4.5 Å from the hydroxyl group of all considered compounds).

In ShSULT, the *S*-enantiomer of Ph-CH_2-OXA shows the most promising results. Our in vitro experiments showed that this compound was active against *S. haematobium* and our structures show significant improvements over OXA. The distances between reactant groups are significantly smaller, at about 4.3 Å on average and only slightly larger than for OXA in SmSULT, indicating that the compound could be activated. We also noted that the difference between enantiomers is much larger in ShSULT than in SmSULT, suggesting that using enantiopure samples of Ph-CH_2-OXA instead of a racemic mixture may significantly improve the drug's efficacy against *S. haematobium*. However, given the overall low activity of the racemate in vivo, this specific point was not further evaluated.

Stability of OXA Analogues in acidic environments and in the presence of microsomes

We further investigated whether the limited in vivo activity on juvenile *S. mansoni* and adult *S. haematobium* could be explained by physiological stability issues. We therefore evaluated two different conditions: an acidic environment and the co-incubation in the presence of liver microsomes, to simulate the environments within the stomach and the liver, respectively.

Simple HPLC methods with a short run time were used to visually check the elution of the fragments before and after exposure to 1 M HCl (Figure S8). Since all compounds after 24 h incubation with 1 M HCl produce completely different elution peaks after incubation, all three compounds have little stability in acidic media.

We conducted the metabolic stability assays using commercially available human liver microsomes, which are specific for Phase I processes catalyzed by cytochrome P450 (CYP) monooxygenases and flavin containing monooxygenases (FMO). We selected human instead of murine microsomes because the human is the final species of interest. Nonetheless, the results of these metabolic studies can give us an inference of the behavior in our mouse experiments.

The metabolic stability results are summarized in Table 6. The stability of the compounds decreased exponentially with $>40\,\%$ compound remaining after 24 h, with similar half-life values ranging from 2.2 to 3.8 h. The intrinsic clearance of the compounds was low and intermediate, ranging from 7.5 to 13.3 $\mu L\,min^{-1}\,mg^{-1}$.[29]

Table 6. Metabolic stability in human microsomes.

Compd	$t_{1/2}$ [h]	k [min^{-1}]	CL_{int} [$\mu L\,min^{-1}\,mg^{-1}$]
Fc-CH_2-OXA	3.8	0.003	7.5
Rc-CH_2-OXA	2.2	0.0053	13.3
Ph-CH_2-OXA	2.4	0.0048	12.0
OXA	3.1	0.0037	9.3

From the values of intrinsic clearance in Table 6, according to McNaney et al., Fc-CH_2-OXA could be categorized as "low" clearance, whereas Rc-CH_2-OXA, Ph-CH_2-OXA, and OXA would be categorized as "intermediate".[30,31]

The elution peaks showed (Figure S9, S10 and S11) for Fc-CH_2-OXA, Rc-CH_2-OXA, and Ph-CH_2-OXA that only the Ph-CH_2-OXA derivative remained unchanged in an acceptable 56% after 24 h of incubation in the presence of microsomes, which indicates that the Ph-CH_2-OXA derivative was more resistant to microsomal oxidation, hydroxylation and reduction compared to its metallocenyl analogues, Fc-CH_2-OXA and Rc-CH_2-OXA.

We previously reported[23] excellent in vivo efficacy in the *S. mansoni* murine model at 100 $mg\,kg^{-1}$. At that time, the stability of the compounds was unknown. Based on the stability results we obtained, it is entirely possible to attribute some activity of the derivatives to OXA itself, in addition to the derivatives' own bioactivity. Furthermore, we could infer that the factors of poor metabolic stability, solubility, and permeability of the compound to the membrane contributed to the poor in vivo results. To have a better idea of the permeability of Ph-CH_2-OXA (deemed the most stable candidate based on stability testing), we proceeded to calculate the MW, log*P* value, and the number of hydrogen-bond donors and hydrogen-bond acceptors, by using the software Molinspiration[32] to estimate its theoretical solubility and membrane permeability. These values gave us a rational basis for selecting a compound for formulation studies aimed at improving bioavailability. Traditionally, therapeutics have been small molecules that fall within Lipinski's rule of five[33] (i.e.; a molecule with a molecular mass ≤ 500 Da, ≤ 5 hydrogen bond donors, ≤ 10 hydrogen bond acceptors, and an octanol-water partition coefficient log$P \leq 5$). Molecules violating more than one of these rules may exhibit limited bioavailability. Ph-CH_2-OXA has a molecular mass of 369 Da, 6 H-bond acceptors, 2 H-bond donors, and a calculated log*P* value of 4.26 with 7 rotatable bonds, which were well

within the parameters of being an ideally permeable small molecule (Table S2).

It is important to note that it is solubility, permeability, and metabolic stability, collectively that have a bearing on the bioavailability of oral drugs. Ph-CH_2-OXA was active in vitro, and the in silico studies also predicted a very promising interaction with the parasite's active site on both evaluated species. Additionally, since Ph-CH_2-OXA was metabolically the most stable compound and with predicted acceptable permeability according to Lipinski's criteria, we proceeded with Ph-CH_2-OXA for further nanoencapsulation formulation studies on the hypothesis that the nanoencapsulated compound would have increased overall solubility and reduced degradation within the acidic environment of the stomach, a new panorama, which would allow better delivery of the compound to its parasitic target.

Lipid nanocapsules loaded with Ph-CH_2-OXA

Lipid nanocapsules (LNC) are the vector of choice to encapsulate lipophilic molecules.[34] LNC present an oily core formed of medium-chain triglycerides covered by a membrane made from a mixture of lecithin and a PEGylated surfactant[34] (Figure 3): this core is able to encapsulate various lipophilic compounds and LNC have already been intensively used for in vivo administration of ferrocifens.[35–38]

Ph-CH_2-OXA was encapsulated at a concentration of 32.35 mg per mL of LNC, representing a drug loading of 4.35% w/w. The physicochemical parameters (characterized by dynamic light scattering analysis), of blank LNC and Ph-CH_2-OXA loaded LNC were the same: diameters of approximately 50 nm, a pdi value below 0.2, which demonstrates a monodispersed population of nanoobjects, and a zeta potential close to neutrality as shown in Table 7.

The in vivo activity of the drug loaded nanocapsules was evaluated in mice harboring a 21-day *S. mansoni* infection, but this improvement in formulation was not translated into a increase in the activity, as summarized in Table 2. The low activity could be the result of a slow or even an absence of drug release, and/or a limited pathogen LNC internalization. In a study instigating the release of different dyes from LNC to a lipophilic compartment mimicking the cells lipid membrane, lipophilic indocarbocyanine dyes were reported to stay entrapped in the surfactant shell of the LNC and no transfer was observed.[39] In a similar paper, studying the transfer in vivo of different dyes from LNC to different lipophilic acceptors, the absence of release of lipophilic indocarbocyanine from LNC was confirmed.[40] For Ph-CH_2-OXA, being similar in terms of hydrophobicity, the same behavior could be hypothesized and explain the lack of increase of activity of the LNC in comparison to the pure compound.

Table 7. Physicochemical parameters characterized by DLS of empty LNC (blank) and Ph-CH_2-OXA loaded LNC.

Sample	Diameter [nm]	pdi[a]	Zeta potential [mV]
Blank LNC	57.4 ± 0.9	0.07 ± 0.02	−3.9 ± 0.7
Ph-CH_2-OXA LNC	53.0 ± 0.5	0.04 ± 0.02	−3.1 ± 0.1

[a] pdi = polydispersity index.

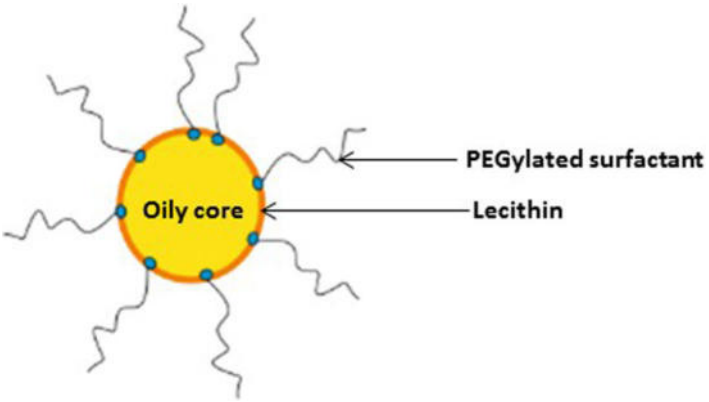

Figure 3. Schematic representation of LNC.

Conclusion

We followed up on three OXA analogues that had shown promising antischistosomal activity. The computational models forecast that the ferrocene- and benzene-containing analogues sample far more near attack configurations with the target sulfotransferase than the parent compound (OXA) for *S. mansoni*. In contrast, in *S. haematobium*, only the *S*-enantiomer of Ph-CH_2-OXA shows the most significant improvement over OXA and could be active against this species. In vitro, the derivatives showed improved activity compared to OXA, against adult worms of all three species evaluated (*S. mansoni, S. haematobium* and *S. japonicum)* and against juvenile *S. mansoni*. When considering the in vivo studies instead, we measured a lack of activity for all three derivatives against juvenile *S. mansoni* and adult *S. haematobium*. We found that all three compounds were only slightly cleared in the in vitro liver model but were poorly stable within an acidic environment. This is likely the reason why the promising in vitro results did not translate into in vivo activity. We further evaluated whether lipid nanoencapsulation of the lead compound (Ph-CH_2-OXA) could overcome this limitation, but unfortunately the formulated compound was also inactive. Since the stability and not the activity on the target seems to be the main limitation of these molecules, further steps should include additional strategies for improved drug formulation, to establish whether an enhanced bioavailability can overcome the loss of in vivo activity.

Experimental Section

^{1}H and ^{13}C NMR spectra: All chemicals were either commercially available or were prepared by following standard procedures. Solvents were used as received or distilled using standard procedures. All preparations were carried out using standard Schlenk techniques.

^{1}H and ^{13}C NMR spectra were recorded in deuterated solvents with a Bruker 400 or 500 MHz spectrometer at RT. The chemical shifts, δ, are reported in ppm (parts per million). The residual solvent peaks have been used as internal references. The abbreviations for the peak multiplicities are as follows: s (singlet), d (doublet), t (triplet), m (multiplet). ESI mass spectrometry was performed with an LTQ-Orbitrap XL from Thermo Scientific. Elemental analysis was performed at Science Centre, London Metropolitan University with a Thermo Fisher (Carlo Erba) Flash 2000 Elemental Analyser, configured for % CHN. The scanned spectra of the compounds are available in the Supporting Information.

OXA-Derivatives preparation: The OXA derivatives were prepared starting from the parent compound oxamniquine (Pfizer) as described previously.[23] The analytical data matched that previously reported and is available in the Supporting Information for further reference.[23]

Animals and parasites: All animal experiments were conducted at the Swiss Tropical and Public Health Institute (Swiss TPH) and authorized by the animal welfare office Kanton Basel Stadt, Switzerland (Authorization no. 2070).

NMRI female mice were purchased from Charles River (Sulzfeld, Germany) at the age of three weeks and were left without intervention for one week of acclimatization. Mice were infected with a subcutaneous infection of around 100 cercariae in the back of the neck by following the procedure described by Lombardo et al.[41]

For the *S. haematobium* chronic infection, one-month old LVG hamsters (Charles River, NY) were provided by the National Institutes of Health (NIH)-National Institute of Allergy and Infectious Diseases (NIAID) Schistosomiasis Resource Center (SRC) for distribution by the Biomedical Research Institute in Rockville, USA, which were pre-infected with 350 *S. haematobium* cercariae. The animals were kept in the animal facility with humidity and light control (50% −12/12) for three months.

Swiss Webster mice infected with *S. japonicum* (Philippine strain) were also obtained from NIH NIAID SRC for our in vitro studies.

In vitro studies: Adult *S. mansoni*, *S. haematobium* and *S. japonicum* worms were collected by dissection from the mesenteric veins. Until use (within 24 h after dissection) and during the experiments, the worms were kept in an incubator at 37 °C and 5% CO_2 and the culture medium consisted of RPMI 1640 (Gibco–Thermofisher, Waltham, MA USA) supplemented with 1% penicillin/streptomycin (BioConcept, Allschwil, Switzerland) and 5% Fetal Calf Serum (FCS) (BioConcept). The control groups consisted of culture medium spiked with dimethyl sulfoxide (DMSO) at a concentration of 1% or 0.5%, equivalent to the content of DMSO present in the wells of worms treated with the highest drug concentration for that assay. The concentrations evaluated were 100, 50, 25, 12.5, and 6.25 μM. The studies on *S. mansoni* and *S. japonicum* were performed as duplicates and repeated once, while the studies on *S. haematobium* were performed in duplicate. Every study condition included at least three worms.

We further evaluated the effect of the addition of albumin (AlbuMAX II, Gibco) to the culture medium to investigate if the activity of the derivatives was different. For this we set the same assay design as described before and added 45 g L^{-1} albumin to the culture medium, corresponding to the content of albumin within the range of human plasma.[42] We performed the study with medium containing albumin on adult *S. mansoni* (duplicate and repeated once), and on adult *S. haematobium* (in duplicate). To assign a score to the viability, we used a previously described method[43] scoring motility, viability, and morphological alterations using a bright field inverted microscope (Carl Zeiss Oberkochen, Germany, magnification ×4 and ×10).

***S. mansoni* juvenile worms for in vitro studies**: 28 days after infection, mice were euthanized and juvenile worms were obtained by blood perfusion. The perfusion solution consisted of 8.5 g L^{-1} NaCl, 7.5 g L^{-1} Na-citrate in distilled water. Parasites were in different stages of development, as reported elsewhere.[44] All juvenile worms were kept in culture medium as described before for adult *S. mansoni* until use within 24 h. To test the activity of the derivatives against the juvenile stages, we incubated the worms with a 100 μM concentration of each of the derivatives in duplicate and at least two worms per well. Duplicates of 100 μM OXA and 1% DMSO served as control conditions.

Calculation of IC_{50} values: CompuSyn 1.0 (ComboSyn Inc, 2007) was used to calculate the IC_{50} values of each of the derivatives after an incubation period of 72 h. Equation (1) was used to normalize the scores of the treated worms to the controls:

$$\text{Effect} = 1 - \frac{\text{average score treatment}}{\text{average score control}} \quad (1)$$

Statistical analysis: All statistics were performed using RStudio version 3.5.1.[45] For evaluating significance in the in vivo studies we applied the non-parametric Kruskall Wallis test for multiple comparisons, and the Dunn test with Bonferronni correction for individual differences. Significance was defined as an adjusted p value <0.05. To evaluate whether there was difference in gender susceptibility we applied the binomial test.

Drug suspension for oral administration: The derivatives were administered to the animals in the form of an oral suspension. The compounds were first dissolved in DMSO (Sigma–Aldrich, Buchs, Switzerland) corresponding to 10% of the total volume, and then a mixture of Tween 80 and ethanol in a proportion of 70:30 was added, also corresponding to 10% of the final volume. The remaining 80% of the volume consisted of distilled water, which was added under stirring in small aliquots.

In vivo activity on juvenile *S. mansoni*: 21 days after infection, mice were treated orally with each of the derivatives and the nanocapsules loaded with Ph-CH_2-OXA at a concentration of 200 mg kg^{-1}. The control group consisted of four mice, which were infected on the same day and under the same conditions as the treatment arm, but were not treated, avoiding additional stress, in accordance to animal welfare regulations. Four weeks after treatment (seven weeks after infection), when the worms reached the adult stage of development, the mice were euthanized with CO_2, dissected, and the remaining live worms were picked out from the mesenteric veins and liver, sexed and counted.

In vivo activity on adult *S. haematobium*: The hamsters harboring an adult infection were treated with a dose of 200 mg kg^{-1} of the compounds. Three weeks after treatment, the hamsters were euthanized with CO_2, dissected, and the worms were picked out from the mesenteric veins and liver, sexed and counted. The control group consisted of four untreated hamsters.

Computational studies: Classical molecular dynamics simulations were performed on the target proteins, that is, the sulfotransferase of *S. mansoni* (SmSULT) and of *S. haematobium* (ShSULT), in complex with OXA, Fc-CH_2-OXA and Ph-CH_2-OXA. Since the two enantiomers of OXA show different activities against schistosomes,[12,46] we performed separate simulations for both enantiomeric forms of all molecules.

To develop force field parameters for the drugs, the geometry of all compounds was optimized in the gas phase with the Gaussi-

an 16 software package,[47] using DFT with B3LYP functional and a 6–31+G* basis set for non-metallic atoms and LANL2DZ pseudopotential for the iron atom. The initial geometries were taken from crystallized (*S*)-OXA complexed to SmSULT (PDB: 4MUB[11]). Hess et al. crystallized in 2017 the (*R*)-enantiomer of Fc-CO-OXA[23] and we used this structure as a starting point for all (*R*)-isomers. The electrostatic potential was computed with the same functional and basis set to estimate the effective atomic point charges through RESP fitting.[48]

Classical molecular dynamics simulations were performed using Amber16.[49] The protein was modeled using the FF14SB force field and the Generalized Amber Force Field 2 (*gaff2*) was used as a base for the ligands. The ferrocenyl group was modeled using the force field published by Doman et al.[50] To estimate the missing dihedral parameters between the ferrocenyl group and the rest of the molecule, we scanned the angles of interest and performed DFT single-point energy calculations for all angles, using the same functional, basis set and pseudopotential as for the geometry optimization. We then used the software *paramfit* from AmberTools16[49] to estimate the parameters. To prevent clashes between nuclei during the rotation, we performed these computations on subsystems containing solely atoms that are relevant for these parameters (e.g., Fc-CH_2-NH_2, Fc-CH_2-*N*-$(CH_3)_2$, Fc-CO-NH_2 and Fc-CO-*N*-$(CH_3)_2$). All parameters determined in this way accurately reproduce the corresponding ab initio energy profiles (Figure S5).

The crystallographic structures of SmSULT and ShSULT with OXA and the cofactor 3′-phosphoadenosine-5′-phosphate (PAP) served as a starting point for our simulations (PDB: 4MUB and 5TIY,[46] respectively). OXA was replaced by its derivatives through alignment of their shared atomic groups. 3′-Phosphoadenosine-5′-phosphosulfate (PAPS), the active version of PAP, was inserted in the same way by minimizing the distance between shared PAP atoms. Missing loops of the protein were added using the ModLoop web server.[51] Using *tleap*, the resulting system was put in an 84×84×84 $Å^3$ periodic box filled with explicit TIP3P water molecules. Finally, the total charge was neutralized by adding Na^+ counterions. The resulting systems consisted of about 50,000 atoms.

Classical trajectories were computed using Amber's CUDA version of the PMEMD program. After minimization, the SHAKE algorithm[52] was used to constrain covalent bonds involving hydrogen atoms and the system was heated to body temperature ($T=310$ K) in two steps using a Langevin thermostat. First, the water molecules were heated to the target temperature while restraining the positions of the ligand and protein during 50 ps with a time step of 1 fs. Then, the restraints were released and the whole system was thermalized in the NPT ensemble for 400 ps, with a time step of 1 fs and a pressure relaxation time of 3 ps. We then performed NPT simulations for 40 ns with a time step of 2 fs to reach an equilibrium state of the system. We finally performed 80 ns NPT production runs that were used for analysis.

The binding free-energy of the ligands inside the protein was estimated based on the MD trajectories using two methods available in Amber16: Generalized Born Surface Area (MM/GBSA) and Poisson Boltzmann Surface Area (MM/PBSA).[53]

pH and metabolic stability studies: The stability of the three OXA derivatives was studied by in vitro co-incubation in acidic environment. To 200 μL of HPLC grade MeCN in a 1.5 mL Eppendorf, 2 μL of 37% HCl were added to form a final 0.1 M HCl solution. Test compound (10 μL; 5 mM in HPLC MeCN) was then added to this acidic solution. For the non-acidic control samples, test compound (10 μL; 5 mM in HPLC MeCN) was added to 200 μL of HPLC grade MeCN. The compounds were then incubated for 24 h at 37 °C and assessed at $t=0$ h and $t=24$ h.

Analytical HPLC measurement was performed with a 1260 Infinity HPLC System (Agilent Technology) comprising: 2 × Agilent G1361 1260 Prep Pump system with Agilent G7115A 1260 DAD WR Detector equipped with an Agilent Pursuit XRs 5C18 (100 Å, C18 5 μm 250×4.6 mm) Column. The solvents were acetonitrile (HPLC grade) and purified water (Pacific TII) with flow rate 1 mL min^{-1}. Detection was performed at 215, 250, 350, 450, 550, and 650 nm with a slit of 4 nm. The flow rate was 1 mL min^{-1} and the max pressure was set 200 bar. Run parameters were as follows: 0 min 85% acetonitrile (MeCN) 15% H_2O; 3 min 85% MeCN 15% H_2O; 7 min 100% MeCN; 9 min 100% MeCN, 11 min 85% MeCN 15% H_2O.

The metabolic stability of the three OXA derivatives was studied by in vitro co-incubation with human liver microsomes. All three compounds were incubated in the presence of NADPH at 37 °C. The protocol was adapted from previous studies:[54,55] 10 μL of 20 mg mL^{-1} microsomes (GIBCO, 50 pooled), 463 μL of PBS (GIBCO, 1× PBS) and 2 μL of 40 mM NADPH (Sigma) were added to 1.5 mL Eppendorf tubes and incubated at 37 °C for 10 min to prime the microsomes. Following this, 10 μL of 50 mM test compound and an additional 15 μL of NADPH were added (1 mM final concentration of test compound in 500 μL total volume). The samples were incubated at 37 °C, and quenched at the desired time points of 1, 4 and 24 h by adding 2 mL of dichloromethane (DCM) or any other organic solvent. 2.5 μL of 5 mM caffeine (TCI Chemicals) in HPLC MeCN as internal standard were added during the quenching process. The mixture was shaken for 10 min to ensure complete extraction. The DCM layer was carefully removed and then evaporated to provide residues that were analyzed by LC-MS (HPLC Waters 2525/Mass Spectrometry Waters ZQ 2000) using a pure acetonitrile–water system with the same column as above. The residues were dissolved in 100 μL HPLC grade acetonitrile. 20 μL from each MeCN residue sample was injected manually by using the following run parameters: 3 min 5% MeCN 95% H_2O; 13 min 40% MeCN 60% H_2O; 14 min 100% MeCN 0% H_2O; 20 min 100% MeCN 0% H_2O; 23 min 5% MeCN 95% H_2O. UV spectra were analyzed and compared at different time points.

By comparing the differences in respective *m/z* values in the MS spectra, *m/z* values for the parent compound and OXA could be identified. Semiquantitative analysis of the ratio of parent compound and different metabolites present in the mixture after incubation with human liver microsomes was achieved by comparing the areas under the respective peaks of different compounds visible in the UV traces of the LC analysis at 245 nm. To determine the in vitro half-life ($t_{1/2}$), the following process was derived from Tan et al.[56]

The peak areas of the compounds at different time points are expressed first as a percentage of the internal standard, caffeine [Eq. (2)]:

$$\text{Ratio at timepoint} = \frac{\text{Area under curve of compound}}{\text{Area under curve of internal standard}} \quad (2)$$

Following this, normalized ratios were calculated using the ratio of peak area of the test compounds to caffeine at $t=0$ h. Normalized ratios were calculated at each assessed timepoint of $t=1$ h, 4 h and 24 h [Eq. (3)]:

$$\text{Normalized ratio} = \frac{\text{Ratio at timepoint} \neq 0}{\text{Ratio at timepoint} = 0} \quad (3)$$

The normalized ratio values are then plotted against incubation time. The $t_{1/2}$ values calculated via analyses methods in GraphPad

Prism 8 (nonlinear regression, exponential one phase decay). The degradation rate constant, k was then calculated using the $t_{1/2}$ values (converted from hours into minutes).

The predicted in vitro intrinsic clearance values (expressed as $\mu L\,min^{-1}\,mg^{-1}$ protein) were then calculated as a ratio of the degradation rate constant k (expressed as min^{-1}) and the microsomal protein concentration ($mg\,\mu L^{-1}$) [Eq. (4)]:

$$\text{in vitro intrinsic clearance values } CL_{int} = \frac{k}{\text{microsomal protein content } (0.4\,mg/mL \text{ protein})} \quad (4)$$

Ph-CH_2-OXA loaded lipid nanocapsules: Lipid nanocapsules (LNC) were formulated by the phase inversion method.[57] Briefly, to prepare blank LNC, Labrafac® (Gattefossé SAS, France, 20.6% w/w), Lipoid® S 100 (Ludwigshafen, Germany 1.5% w/w), Kolliphor HS 15 (Florham Park, USA 17% w/w), NaCl (Sigma–Aldrich, USA 1.3% w/w) and water (59.6% w/w) were mixed and homogenized under magnetic stirring at 80 °C. Three cycles of progressive heating and cooling between 90 and 50 °C were then performed. During the last cooling cycle, the mixture was diluted by adding 2 °C purified water (28.7% v/v) in order to induce an irreversible shock and formulate LNC. To encapsulate Ph-CH_2-OXA inside the LNC, some slight changes to this protocol have been applied. The Ph-CH_2-OXA (4.35% w/w) was mixed with Labrafac®, Lipoid® S 100 and ethanol (Fisher, USA) to help the solubilization of the molecule in the lipid phase. This mixture was put under agitation at 50 °C until total solubilization of the Ph-CH_2-OXA. The ethanol was then evaporated under argon. Once the ethanol evaporated, Kolliphor HS 15, NaCl and water were added and three heating and cooling cycles were performed as prescribed for formulating blank LNC. During the last cooling cycle, the mixture was diluted by adding 2 °C purified water. Empty LNC and Ph-CH_2-OXA loaded LNC were characterized using dynamic light scattering (DLS) to determine their size, polydispersity index (pdi), and zeta potential.

NMRI female mice were purchased from Charles River (Sulzfeld, Germany) at the age of three weeks and were left without intervention for one week of acclimatization. Mice were infected with a subcutaneous infection of around 100 cercariae in the back of the neck, by following the procedure described by Lombardo et al.[42]

For the *S. haematobium* chronic infection, one-month old LVG hamsters (Charles River, NY) were provided by the National Institutes of Health (NIH)–National Institute of Allergy and Infectious Diseases (NIAID) Schistosomiasis Resource Center (SRC) for distribution by the Biomedical Research Institute in Rockville, USA, which were pre-infected with 350 *S. haematobium* cercariae. The animals were kept in the animal facility with humidity and light control (50 % - 12/12) for three months.

Swiss Webster mice infected with *S. japonicum* (Philippine strain) were also obtained from NIH NIAID SRC for our in vitro studies.

All animal experiments were conducted at the Swiss Tropical and Public Health Institute (Swiss TPH) and authorized by the animal welfare office Kanton Basel Stadt, Switzerland (Authorization no. 2070).

Acknowledgements

This work was financially supported by the Swiss National Science Foundation (Grant Sinergia CRSII5_173718 and 320030_175585) and has received support under the program «Investissements d'Avenir» launched by the French Government and implemented by the ANR with the reference ANR-10-IDEX-0001–02 PSL (G.G.). We are grateful for the loan of analytical instruments by Agilent Technologies and CEA Saclay to Chimie ParisTech. V.B. is grateful to the Swiss excellence scholarships for financial support, scholarship number 2017.0801.

Conflict of interest

The authors declare no conflict of interest.

Keywords: bioinorganic chemistry · drug delivery · drug discovery · medicinal chemistry · molecular dynamics · schistosomiasis

[1] D. G. Colley, A. L. Bustinduy, W. E. Secor, C. H. King, *Lancet* **2014**, *383*, 2253 – 2264.
[2] M. Rotger, T. Serra, M. G. de Cárdenas, A. Morey, M. A. Vicente, *Eur. J. Clin. Microbiol. Infect. Dis.* **2004**, *23*, 855 – 856.
[3] A. Berry, H. Moné, X. Iriart, G. Mouahid, O. Aboo, J. Boissier, J. Fillaux, S. Cassaing, C. Debuisson, A. Valentin, G. Mitta, A. Théron, J.-F. Magnaval, *Emerging Infect. Dis.* **2014**, *20*, 1595 – 1597.
[4] P. Steinmann, J. Keiser, R. Bos, M. Tanner, J. Utzinger, *Lancet Infect. Dis.* **2006**, *6*, 411 – 425.
[5] R. Bergquist, X.-N. Zhou, D. Rollinson, J. Reinhard-Rupp, K. Klohe, *Infect. Dis. Povert.* **2017**, *6*, 158.
[6] S. Geerts, B. Gryseels, *Clin. Microbiol. Rev.* **2000**, *13*, 207 – 222.
[7] E. M. Lago, R. P. Xavier, T. R. Teixeira, L. M. Silva, A. A. da Silva Filho, J. de Moraes, *Fut. Med. Chem.* **2018**, *10*, 89 – 120.
[8] L. Pica-Mattoccia, A. Novi, D. Cioli, *Parasit. Res.* **1997**, *83*, 687 – 689.
[9] A. A. Sabah, C. Fletcher, G. Webbe, M. J. Doenhoff, *Exper. Parasitol.* **1986**, *61*, 294 – 303.
[10] L. Pica-Mattoccia, D. Carlini, A. Guidi, V. Cimica, F. Vigorosi, D. Cioli, *Mem. Inst. Oswaldo Cruz* **2006**, *101*, 307 – 312.
[11] C. L. L. Valentim, D. Cioli, F. D. Chevalier, X. Cao, A. B. Taylor, S. P. Holloway, L. Pica-Mattoccia, A. Guidi, A. Basso, I. J. Tsai, M. Berriman, C. Carvalho-Queiroz, M. Almeida, H. Aguilar, D. E. Frantz, P. J. Hart, P. T. LoVerde, T. J. C. Anderson, *Science* **2013**, *342*, 1385 – 1389.
[12] A. B. Taylor, L. Pica-Mattoccia, C. M. Polcaro, E. Donati, X. Cao, A. Basso, A. Guidi, A. R. Rugel, S. P. Holloway, T. J. C. Anderson, P. J. Hart, D. Cioli, P. T. LoVerde, *PLoS Neglected Trop. Dis.* **2015**, *9*, e0004132.
[13] F. D. Chevalier, W. Le Clec'h, N. Eng, A. R. Rugel, R. R. Assis, G. Oliveira, S. P. Holloway, X. Cao, P. J. Hart, P. T. LoVerde, T. J. C. Anderson, *Int. J. Parasitol.* **2016**, *46*, 417 – 424.
[14] A. Rugel, R. S. Tarpley, A. Lopez, T. Menard, M. A. Guzman, A. B. Taylor, X. Cao, D. Kovalskyy, F. D. Chevalier, T. J. C. Anderson, P. J. Hart, P. T. LoVerde, S. F. McHardy, *ACS Med. Chem. Lett.* **2018**, *9*, 967.
[15] E. A. Hillard, A. Vessières, G. Jaouen in *Ferrocene Functionalized Endocrine Modulators as Anticancer Agents in Medicinal Organometallic Chemistry* (Eds.: G. Jaouen, N. Metzler-Nolte), Springer, Berlin, **2010**, pp. 81 – 117.
[16] C. Biot, D. Dive in *Bioorganometallic Chemistry and Malaria in Medicinal Organometallic Chemistry* (Eds.: G. Jaouen, N. Metzler-Nolte), Springer, Berlin, **2010**, pp. 155 – 193.
[17] G. Gasser, N. Metzler-Nolte, *Curr. Opin. Chem. Biol.* **2012**, *16*, 84 – 91.
[18] M. Patra, G. Gasser, *Nat. Rev. Chem.* **2017**, *1*, 0066.
[19] Y. C. Ong, S. Roy, P. C. Andrews, G. Gasser, *Chem. Rev.* **2019**, *119*, 730 – 796.
[20] F. Dubar, T. J. Egan, B. Pradines, D. Kuter, K. K. Ncokazi, D. Forge, J.-F. Paul, C. Pierrot, H. Kalamou, J. Khalife, E. Buisine, C. Rogier, H. Vezin, I. Forfar, C. Slomianny, X. Trivelli, S. Kapishnikov, L. Leiserowitz, D. Dive, C. Biot, *Chem. Biol.* **2011**, *18*, 275 – 287.
[21] J. Keiser, M. Vargas, R. Rubbiani, G. Gasser, C. Biot, *Parasit Vectors* **2014**, *7*, 424.
[22] C. Biot, D. Taramelli, I. Forfar-Bares, L. A. Maciejewski, M. Boyce, G. Nowogrocki, J. S. Brocard, N. Basilico, P. Olliaro, T. Egan, *J. Mol. Pharm.* **2005**, *2*, 185 – 193.

[23] J. Hess, G. Panic, M. Patra, L. Mastrobuoni, B. Spingler, S. Roy, J. Keiser, G. Gasser, *ACS Infect. Dis.* **2017**, *3*, 645 – 652.
[24] J. Hess, J. Keiser, G. Gasser, *Fut. Med. Chem.* **2015**, *7*, 821 – 830.
[25] V. Buchter, J. Hess, G. Gasser, J. Keiser, *Parasites Vectors* **2018**, *11*, 580.
[26] V. Pasche, B. Laleu, J. Keiser, *Parasites Vectors* **2018**, *11*, 298.
[27] P. Olliaro, P. Delgado-Romero, J. Keiser, *J. Antimicr. Chemother.* **2014**, *69*, 863 – 870.
[28] P. Keen, *Effect of Binding to Plasma Proteins on the Distribution, Activity and Elimination of Drugs in Concepts in Biochemical Pharmacology: Part 1* (Eds.: B. B. Brodie, J. R. Gillette, H. S. Ackerman), Springer, Berlin, **1971**, pp. 213 – 233.
[29] Measurement of in vitro intrinsic clearance using microsomes. Available from: https://www.cyprotex.com/admepk/in vitro-metabolism/microsomal-stability. Date accessed [04.06.2020].
[30] C. A. McNaney, S. Y. Hnatyshyn, T. A. Zvyaga, J. O. Knipe, J. V. Belcastro, M. Sanders, *Assay Drug Dev. Technol.* **2008**, *6*, 121 – 129.
[31] K. Słoczyńska, A. Gunia-Krzyżak, P. Koczurkiewicz, K. Wójcik-Pszczoła, D. Żelaszczyk, J. Popiół, E. Pękala, *Acta Pharm.* **2019**, *69*, 345 – 361.
[32] Cheminformatics, M. 2001 (cited 2020 05.06.2020). Available from: https://www.molinspiration.com/about.html. Date accessed [05.06.2020].
[33] C. A. Lipinski, F. Lombardo, B. W. Dominy, P. J. Feeney, *Adv. Drug Delivery Rev.* **1997**, *23*, 3 – 25.
[34] N. T. Huynh, C. Passirani, P. Saulnier, J. P. Benoit, *Int. J. Pharm.* **2009**, *379*, 201 – 209.
[35] A. L. Laine, N. T. Huynh, A. Clavreul, J. Balzeau, J. Bejaud, A. Vessieres, J. P. Benoit, J. Eyer, C. Passirani, *Eur. J. Pharm. Biopharm.* **2012**, *81*, 690 – 693.
[36] E. Allard, D. Jarnet, A. Vessieres, S. Vinchon-Petit, G. Jaouen, J P. Benoit, C. Passirani, *Pharm. Res.* **2010**, *27*, 56 – 64.
[37] R. Karim, E. Lepeltier, L. Esnault, P. Pigeon, L. Lemaire, C. Lepinoux-Chambaud, N. Clere, G. Jaouen, J. Eyer, G. Piel, C. Passirani, *Nanoscale* **2018**, *10*, 13485 – 13501.
[38] A. L. Lainé, E. Adriaenssens, A. Vessieres, G. Jaouen, C. Corbet, E. Desruelles, P. Pigeon, R. A. Toillon, C. Passirani, *Biomaterials* **2013**, *34*, 6949 – 6956.
[39] G. Bastiat, C. O. Pritz, C. Roider, F. Fouchet, E. Lignières, A. Jesacher, R. Glueckert, M. Ritsch-Marte, A. Schrott-Fischer, P. Saulnier, J. P. Benoit, *J. Controlled Release* **2013**, *170*, 334 – 342.
[40] C. Simonsson, G. Bastiat, M. Pitorre, A. S. Klymchenko, J. Béjaud, Y. Mély, J. P. Benoit, *J. Arbeitsgem. Pharm. Verfahrenstechn.* **2016**, *98*, 47 – 56.
[41] F. C. Lombardo, V. Pasche, G. Panic, Y. Endriss, J. Keiser, *Nat. Protocols* **2019**, *1*.
[42] Human Albumin, Hemotherapy TMa, Chapter 5, editor 36, 4th ed., S. Karger GmbH, Freiburg: *Cross-Sectional Guidelines for Therapy with Blood Components and Plasma Derivatives*, **2009**, pp. 399 – 407.
[43] J. Keiser, *Parasitology* **2010**, *137*, 589 – 603.
[44] E. C. Faust, C. A. Jones, *Proc. Soc. Experim. Biol. Med.* **1934**, *31*, 478 – 479.
[45] Team, R. RStudio: Integrated Development for, R. 3.5.1 ed: RStudio Inc.; Boston, MA **2016**.
[46] A. B. Taylor, K. M. Roberts, X. Cao, N. E. Clark, S. P. Holloway, E. Donati, C. M. Polcaro, L. Pica-Mattoccia, R. S. Tarpley, S. F. McHardy, D. Cioli, P. T. LoVerde, P. F. Fitzpatrick, P. J. Hart, *J. Biol. Chem.* **2017**, *292*, 11154 – 11164.
[47] Gaussian 16, Revision A.03, M. J. Frisch, G. W. Trucks, H. B. Schlegel, G. E. Scuseria, M. A. Robb, J. R. Cheeseman, G. Scalmani, V. Barone, G. A. Petersson, H. Nakatsuji, X. Li, M. Caricato, A. V. Marenich, J. Bloino, B. G. Janesko, R. Gomperts, B. Mennucci, H. P. Hratchian, J. V. Ortiz, A. F. Izmaylov, J. L. Sonnenberg, D. Williams-Young, F. Ding, F. Lipparini, F. Egidi, J. Goings, B. Peng, A. Petrone, T. Henderson, D. Ranasinghe, V. G. Zakrzewski, J. Gao, N. Rega, G. Zheng, W. Liang, M. Hada, M. Ehara, K. Toyota, R. Fukuda, J. Hasegawa, M. Ishida, T. Nakajima, Y. Honda, O. Kitao, H. Nakai, T. Vreven, K. Throssell, J. A. Montgomery, Jr., J. E. Peralta, F. Ogliaro, M. J. Bearpark, J. J. Heyd, E. N. Brothers, K. N. Kudin, V. N. Staroverov, T. A. Keith, R. Kobayashi, J. Normand, K. Raghavachari, A. P. Rendell, J. C. Burant, S. S. Iyengar, J. Tomasi, M. Cossi, J. M. Millam, M. Klene, C. Adamo, R. Cammi, J. W. Ochterski, R. L. Martin, K. Morokuma, O. Farkas, J. B. Foresman, D. J. Fox, Gaussian Inc., Wallingford CT, **2016**.
[48] C. I. Bayly, P. Cieplak, W. Cornell, P. A. Kollman, *J. Phys. Chem.* **1993**, *97*, 10269 – 10280.
[49] AMBER 2016, D. A. Case RMB, D. S. Cerutti, T. E. Cheatham III, T. A. Darden, R. E. Duke, T. J. Giese, H. Gohlke, A. W. Goetz, N. Homeyer, S. Izadi, P. Janowski, J. Kaus, A. Kovalenko, T. S. Lee, S. LeGrand, P. Li, C. Lin, T. Luchko, R. Luo, B. Madej, D. Mermelstein, K. M. Merz, G. Monard, H. Nguyen, H. T. Nguyen, I. Omelyan, A. Onufriev, D. R. Roe, A. Roitberg, C. Sagui, C. L. Simmerling, W. M. Botello-Smith, J. Swails, R. C. Walker, J. Wang, R. M. Wolf, X. Wu, L. Xiao, P. A. Kollman, University of California, San Francisco, **2016**.
[50] T. N. Doman, C. R. Landis, B. Bosnich, *J. Am. Chem. Soc.* **1992**, *114*, 7264 – 7272.
[51] A. Fiser, R. K. Do, A. Sali, *Protein Sci.* **2000**, *9*, 1753 – 1773.
[52] J.-P. Ryckaert, G. Ciccotti, H. J.C. Berendsen, *J. Computat. Phys.* **1977**, *23*, 327 – 341.
[53] B. R. Miller, T. D. McGee, J. M. Swails, N. Homeyer, H. Gohlke, A. E. Roitberg, *J. Chem. Theory Comput.* **2012**, *8*, 3314 – 3321.
[54] M. Patra, K. Ingram, A. Leonidova, V. Pierroz, S. Ferrari, M. N. Robertson, M. H. Todd, J. Keiser, G. Gasser, *J. Med. Chem.* **2013**, *56*, 9192 – 9198.
[55] S. Keller, Y. C. Ong, Y. Lin, K. Cariou, G. Gasser, *J. Organometallic Chem.* **2020**, *906*, 121059.
[56] J. Tan, H. Sivaram, H. V. Huynh, *Appl. Organometal. Chem.* **2018**, *32*, e4441
[57] B. Heurtault, P. Saulnier, B. Pech, J.-E. Proust, J.-P. Benoit, *Pharm. Res.* **2002**, *19*, 875 – 880.

Manuscript received: June 13, 2020
Revised manuscript received: August 24, 2020
Accepted manuscript online: August 27, 2020
Version of record online: ■■ ▮▮, 0000

FULL PAPER

Testing alternatives: Schistosomiasis is a disease of poverty affecting millions of people. In this investigation, in-depth preclinical studies on three lead compounds derived from oxamniquine were conducted with respect to pH and metabolic stability, in vivo studies on *S. haematobium* and juvenile *S. mansoni*, computational simulations, and formulation development.

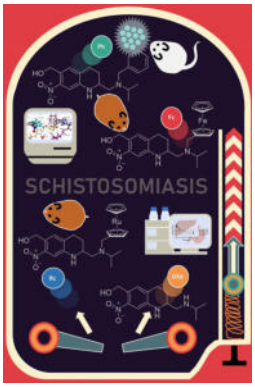

Medicinal Organometallic Chemistry

V. Buchter, Y. C. Ong, F. Mouvet, A. Ladaycia, E. Lepeltier, U. Rothlisberger, J. Keiser,* G. Gasser**

■■ – ■■

Multidisciplinary Preclinical Investigations on Three Oxamniquine Analogues as New Drug Candidates for Schistosomiasis

Chapter V

Validation of a human-serum-based *in vitro* growth method for drug screening on juvenile development stages of *Schistosoma mansoni*

PLOS NEGLECTED TROPICAL DISEASES

RESEARCH ARTICLE

Validation of a human-serum-based *in vitro* growth method for drug screening on juvenile development stages of *Schistosoma mansoni*

Valentin Buchter[1,2], **Pierre H. H. Schneeberger**[1,2], **Jennifer Keiser**[1,2]*

1 Swiss Tropical and Public Health Institute, Basel, Switzerland, **2** University of Basel, Basel, Switzerland

* jennifer.keiser@swisstph.ch

OPEN ACCESS

Citation: Buchter V, Schneeberger PHH, Keiser J (2021) Validation of a human-serum-based *in vitro* growth method for drug screening on juvenile development stages of *Schistosoma mansoni*. PLoS Negl Trop Dis 15(3): e0009313. https://doi.org/10.1371/journal.pntd.0009313

Editor: Winka Le Clec'h, Texas Biomedical Research institute, UNITED STATES

Received: September 12, 2020

Accepted: March 17, 2021

Published: March 30, 2021

Data Availability Statement: All relevant data are within the manuscript and its Supporting Information files.

Funding: This study was funded by the Schweizerischer Nationalfonds zur Förderung der Wissenschaftlichen Forschung 320030_175585 (to JK). The funders had no role in study design, data collection and analysis, decision to publish, or preparation of the manuscript.

Competing interests: The authors have declared that no competing interests exist.

Abstract

Background

Schistosomiasis affects over 200 million people worldwide but only praziquantel is available for treatment and control. Drug discovery is often based on phenotypic drug screening, involving different parasite stages retrieved from infected mice. Aiming to reduce animal use, we validated an *in vitro* growth method for juvenile *Schistosoma mansoni* for the purpose of drug sensitivity assays.

Methodology/Principal findings

We compared inter–batch variability of serum, worm size and organ development, gender distribution, and drug sensitivity between *in vitro* and *in vivo* grown worms over different life stages. *In vitro* developed *S. mansoni* in Hybridoma medium supplemented with 20% human serum were similar in size as *in vivo* worms until 28 days of incubation (males 1.4 ± 0.2 mm, females 1.1 ± 0.5 mm long). qPCR analysis revealed similar gender distribution both on newly transformed schistosomula and worms grown for 21 days. Worms developed *in vitro* and *in vivo* were similarly sensitive to praziquantel from 7 to 35 days of development with the exception of 21 days of development, where a slightly lower activity was observed for the *in vitro* grown worms (IC_{50}: 0.54 μM *in vitro*, 0.14 μM *in vivo* 72 hours post-incubation). The evaluation of five additional drugs revealed a similar sensitivity on worms developed for 21 days, with the exception of mefloquine, where we observed a 10-fold lower sensitivity on *in vitro* developed schistosomes when compared to *in vivo* grown (IC_{50}: 4.43 μM *in vitro*, 0.48 μM *in vivo*).

Conclusion

A large number of juvenile *S. mansoni* worms can be grown *in vitro*, which show similar drug sensitivity, gender distribution, size and morphology as the worms recovered from rodents, supporting the use of this method in drug screening efforts.

Author summary

Schistosomiasis is a water-borne disease affecting over 200 million people worldwide and praziquantel is the only drug available for treatment. Although this drug is effective on all *Schistosoma* species on the adult stage of development, its activity is only partial against early infection stages. In addition, this has been the only drug in use for over 40 years, a situation that poses selective pressure towards resistant worms and highlights the urgent need of new drugs. The discovery and development of new drugs is often based on drug screenings, performed on worms collected from infected mammals. In line with animal welfare recommendations and aiming to increase throughput and reduce the assay costs, we validated a recently established *in vitro* method to grow juvenile *S. mansoni* as a drug screening tool. The *in vitro* established worms have similar gender distribution, size and drug sensitivity as worms collected from mice.

Introduction

Schistosomiasis is a human acute and chronic parasitic disease caused by five different trematode species (*Schistosoma haematobium*, *S. intercalatum*, *S. japonicum*, *S. mansoni and S. mekongi)* that affected over 229 million people in 2018, in 78 countries [1]. Despite all efforts to control the disease, which include large-scale population treatment with the only available drug praziquantel [1], the disease remains a significant public health problem [1,2]. Although drug resistance has not yet been documented in human medicine, treatment failures have been observed [3], and resistance to praziquantel could readily be induced in the laboratory [4]. Considering the high selective pressure due to a continuous and unique use of praziquantel in the treatment of schistosomiasis, and the fact that the efficacy of praziquantel is limited and inconsistent against immature worms [3], the development of alternative broad spectrum drugs is an urgent need [3].

One of the strategies used in drug discovery and development for schistosomiasis is the screening of drug libraries on different parasite stages *in vitro*. While drug screening on the larval stage (newly transformed schistosomula, NTS) [5,6] can be performed fully *in vitro*, infected mice or hamster are needed, when compounds need to be tested on juvenile and adult worms. Working with the juvenile stages of the parasites is particularly cumbersome, since the collection of worms by blood perfusion is a time intense process with low recovery rates and high costs. Moreover, because only few worms per animal can be collected, the use of juvenile worms collected from rodents is not in line with the 3R principle (reduce, replace, refine) for animal welfare in science [5,7].

Hence, a reliable and robust *in vitro* growing procedure for juvenile *S. mansoni* generating a large number of worms is required. During the 1960 and 70's Clegg [8] and Basch [9] developed techniques for *in vitro* development for *S. mansoni*, that are still used today [10,11]. These methods rely on the addition of red blood cells (RBC) [8,9] or complex culture media and are therefore subject to high variability, are time consuming and due to the presence of the red blood cells in the medium, the phenotypic microscopy readout becomes imprecise [12,13]. Additionally, the success rate of development is as low as 10% of the original number of larvae incubated [14], the size of the worms is 20 to 40% smaller, and development is slower when compared to the *in vivo* counterparts [9]. Frahm *et al.* recently described a novel, cell-free method to grow *S. mansoni* cercariae into juvenile worm stages, thus decreasing the hurdles associated with previous methods [13]. However, a systematic comparison of

developmental bias between this method and *in vivo* grown schistosomes, which is considered the gold standard [15], has not been conducted to date.

The aim of our study was to evaluate the reproducibility of a cell-free method to grow juvenile *S. mansoni* [13] and to validate its applicability for drug screening assays, comparing the assay results with worms developed *in vivo*. We evaluated the parasites' development in medium containing serum of five different human donors individually, and as a pool of sera. Next, we compared the size, organ development and morphology of the worms developed i*n vitro* and *in vivo*. To avoid gender bias in the drug assays, we evaluated by means of qPCR and microscopy, the gender of the NTS which gave origin to the juvenile worms, the gender of developed worms as well as the gender of non-developing worms. Finally, to evaluate the applicability of this method for drug screening purposes, we quantitatively compared the sensitivity of the *in vitro* developed worms to six different drugs, with the sensitivity of the worms developed *in vivo*.

Methods

Ethics statement

All animal experiments were authorized by the Canton Basel Stadt, Switzerland (license number 2070).

Parasites

The life cycle of *S. mansoni* is established at Swiss TPH [5]. Briefly, *Biomphalaria glabrata* (Egypt) snails were infected with 6–8 *S. mansoni*–Liberian Strain miracidia and 6 weeks after infection, the cercariae shed from the snails were used for animal infection or mechanically transformed to newly transformed schistosomula (NTS) [5] and used for *in vitro* growing.

Human serum

Human serum (HSe) was collected at the blood donation center in Basel, Switzerland, from five anonymous and randomly chosen donors. Parasite growth was tested with each serum sample, individually, or with a pool of all sera, composed by the mixture of equal parts of each of these sera. The effect of heat inactivation of the complement proteins in the serum was evaluated. Two batches of developing worms were incubated with heat inactivated serum and two with normal serum. Inactivation was achieved by placing serum samples in a 56˚C water bath for 30 minutes.

In vitro growing assay

For the *in vitro* growth procedure, 30 to 50 NTS were placed into each well of 96 well transparent polystyrene flat bottom plates containing 100 μl medium. We compared the growth of the schistosomes in both Dulbecco's modified eagle's medium (DMEM, Sigma-Aldrich, Buchs, Switzerland) and HybridoMed (HM) DIF1000 serum-free medium (VWR international, Dietikon, Switzerland) both supplemented with 20% HSe and 500 U/mL penicillin, 500 mg/mL streptomycin (LuBioScience, Switzerland) [13]. The plates were kept in the incubator with 5% CO_2 and at 37˚C. To avoid evaporation and keep humidity and temperature constant, the outer rows of the plate were filled with culture medium, but no NTS were added. The medium was changed twice a week until use. Pictures of the worms were taken weekly, using a Canon photo camera EOS digital mounted on a Carl Zeiss Primovert microscope and using 200x, 100x and 40x magnifications.

Table 1. Assignment of developmental stage according to morphology and organ formation.

Stage		Time in mouse model (d)	Description
Lung stage	Larvae	7–8	Elongated schistosomula, without specific gender differentiation and increased movement. Suckers are hardly visible and there is no evidence of digestive system formation.
Gut development stage	Juvenile	15	Considerable increase in volume takes place and the gut ceca turns visible and united behind the ventral sucker. Males, thicker and longer, can be differentiated from females, which are thinner and still elongated. While in males the ventral and oral sucker are clearly evidenced, this is not the case for females. Defined as liver stage by Frahm *et al*. [13]
Organogeny stage	Juvenile	21	Growing continues in length and the gut ceca elongates. Male schistosomes start to develop the lateral extensions of the body and two testicles are visible.
Gametogeny stage	Juvenile	28	Males develop 8 testes while females have a small ovary. Mating occurs for the first time and the females are enclosed by the lateral extensions of the males' body.
Adult stage	Adult	35–55	First eggs from *in vivo* developed *S. mansoni* are produced 34–35 days after infection. Despite highly variable, the size of females ranges from 5.1 to 9.4 mm and males from 5.0 to 8.8 mm. The vitellaria are well developed. Spermatozoa can be seen in all 8 testes of the male, and a seminal vesicle is present. By day 55 day post infection all worms have matured. While the tegument of females is smooth, the tegument of males is covered by spines.

https://doi.org/10.1371/journal.pntd.0009313.t001

We compared the schistosome development in five different batches of sera and a pool of these sera. We incubated two wells with each of the sera, and allowed the worms to develop for 21 days. After this period we took pictures of the wells and counted the number of dead and alive worms in each well and the number of worms which had reached the organogeny stage (Table 1). The incubation with the pool of sera was repeated once. For subsequent experiments this batch of pooled sera was used.

In vivo developed worms

Three-week-old female NMRI mice were ordered from Charles River (Sulzfeld, Germany) and were allowed to acclimatize to the new environment for one week before being manipulated. After this time, the mice were infected subcutaneously with 1000 cercariae for the 7 and 14 day time point and with 300 cercariae for the remaining time points, following a procedure described elsewhere [5]. Seven, 14, 21, 28 and 35 days after infection, the mice were euthanized and the worms were collected by blood perfusion. The perfusion solution (PS) consisted of 8.5 g NaCl and 7.5 g sodium citrate (Sigma Aldrich, Buchs, Switzerland) per liter of distilled water. The PS was sterile filtered and used at 4˚C. For euthanasia, we injected a solution containing 87 μl of Esconarkon (sodium pentobarbital 300 mg/ml, Streuli Pharma, Uznach, Switzerland) and 13 μl of sodium heparin at 5.000 U.I./ml(Braun Medical AG, Sempach, Switzerland) subcutaneously in the third quadrant of the abdomen. Cervical dislocation was performed as second killing method, in line with the Swiss animal regulations. Afterwards, an incision in the abdomen was done and extended to the chest, removing the ribs, yet taking care not to damage the blood vessels.

The seven day-old worms were collected from the lungs as follows: the descendant thoracic portion of the aorta was cut with a scissor, to allow the blood to flow out by heart pressure. Later, 10 to 20 ml PS supplemented with 10 units heparin/ml were injected into the right ventricle of the heart to flush the blood from the lungs. The blood was discarded. The lungs were further removed from the chest, placed in glass beakers with 1–2 ml culture medium and minced into small pieces, transferred in 50 ml falcon tubes, filled with culture medium and incubated for 3 hours at 37˚C and 5% CO_2 to allow the worms to leave the tissue. Afterwards, the suspension was filtered through a 30-mesh screen and the filtrate was centrifuged 3 min at 100 g. The supernatant was removed and replaced with 10 ml fresh medium and transferred to a 24 well plate. The well plate was kept in the incubator at 37˚C and 5% CO_2 until use for the

assays within 24 hours. For drug sensitivity assays the worms were collected using a 10 μl pipet.

For the 14 day-old worms and later development time points, we applied the following protocol: An incision was made in the portal vein and the blood was allowed to flow into a cylindrical glass container (23 cm diam. 3500 ml, Cat No.AYH0.1, Roth AG, Switzerland) placed below the mouse. The PS was used to rinse the area around the incision in the portal vein and thus prevent worms adhering to abdominal viscera. Next, 20 ml of PS were injected into the cava vein to retro-perfuse the liver and remove the worms contained in this organ. The full perfusate fluid from the glass container was collected into 50 ml falcon tubes and centrifuged for 3 minutes by 100 g. Next, the supernatant was removed and replaced with fresh PS. The centrifugation and clean up procedure was repeated three times until a transparent fluid was obtained. Finally, the PS was replaced by 10 ml culture medium (HM + HSe + Pen/Strep) and the worms placed in 24 well plates. Worms were kept in these plates in the incubator at 37˚C and 5% CO_2until use, within 24 hours after collection. At the 14 days p.i. time point, additional worms harbored in the lungs were collected following the procedure described for the 7 day p.i. perfusion.

Assessment of development

To evaluate the development of the worms grown *in vitro* or *in vivo* we adapted the description of Clegg [8] for *S. mansoni* developed in mice. In brief, we evaluated growth (increase in size), development (organ formation and tissue differentiation) and maturation (sexual organ formation) as summarized in Table 1.

Size determination

For the calculation of the parasite's size we used the software Fiji–Image J [16]. Pictures with 100x and 200x magnification were taken after 0, 7, 14, 21, 28, 35 days of *in vitro* development and the length of 11 males and females was measured per time point. From the worms developed *in vivo*, we measured the size at days 14, 21, 28, 35 as well as at day 49 post infection.

Gender determination

DNA from individual worms was extracted using DNeasy PowerSoil Pro Kit (Qiagen, Hilden, Germany) extraction kits. We extracted DNA from NTS, 21 and 28 day old juvenile *S. mansoni* grown *in vitro*, both developed and undeveloped as determined by morphological assessment, and matured adult worms which were grown *in vivo*.

We used a qPCR assay described by Chevalier *et al.* [17] to unambiguously determine the gender of the worms at each developmental stage. Briefly, this qPCR assay was designed to target two gender-specific regions of the chromosomal DNA, namely region W6 for females, and region Z for males. Accordingly, samples were classified as females if positive solely for region W6, and as males if positive only for region Z. For samples amplifying both regions, we measured the cycle threshold difference between both amplification targets (Δ Cq = Cq_{W6} –Cq_Z), allowing for the unambiguous classification as females (high W6 / low Z) or males (high Z / low W6).

To amplify the Z marker we used the primers described elsewhere [17] Smp 011570.1 (Eurofins genomics, Ebersberg, Germany, sequence F (5'–3' orientation): TGGATGTTGGATAAGCTGGG, sequence R: TGGATCTGGATATCGAATGGTC) while for the W6 marker we used the primer Sm_W6 (Eurofins genomics, Ebersberg, Germany, sequence F: TGTGAAGCAAAGTGTTCACTG, sequence R: TTCATCAAGTCAATCACAGCTC) used at a final concentration of 0.3 μM for each reaction. Each reaction also contained 2 μl of 5x HOT

FIREPol Eva Green qPCR Supermix (Solis BioDyne, Tartu, Estonia), 5.4 μl DNA free water (Thermo Scientific, Allschwill, Switzerland), and 2 μl DNA template for a reaction volume of 10 μl. The DNA was amplified with the following program: 95˚C for 12 min, [95˚C for 15 s, 60˚C for 1 min] × 40 cycles using a Bio-Rad CFX96 qPCR instrument (Bio-Rad Hungary Ltd., Budapest, Hungary). A melting curve (60–95˚C) at the end of the program was added to check specificity of amplification. qPCR data analysis was performed with the software CFX Maestro version 4.0 (Bio-Rad, Hercules, California, USA).

Drug sensitivity assays and IC_{50} calculations

We evaluated the viability of the worms after 24, 48, and 72 hours of continuous drug exposure by means of visual microscopy. The worms' viability was evaluated assigning a score ranging from 0 to 3, with 0.25 unit intervals. A score of 0 was given to dead worms, while a score of 3 was assigned to fully vital worms. The criteria used to score the viability were movement, frequency of body contractions, granularity and transparency and tegument morphology.

The activity of six drugs, namely auranofin (Enzo Life Sciences AG, Lausen, Switzerland), mefloquine (Sigma-Aldrich, Buchs, Switzerland), nicardipine (Sigma-Aldrich, Buchs, Switzerland), oxamniquine (kindly donated by Pfizer, NY, USA), oxethazaine (Sigma-Aldrich, Buchs, Switzerland) and praziquantel (Sigma-Aldrich, Buchs, Switzerland) was evaluated against both *in vitro* and *in vivo* developed *S. mansoni* by 21 days of development. For praziquantel, we additionally compared the drug sensitivity of worms developed for 7, 14, 28 and 35 days *in vitro* and *in vivo*. The concentrations used to calculate the IC_{50} values were: for praziquantel: 2.5, 1.25 and 0.625 μM, for oxamniquine: 50, 25, 12.5 μM, for auranofin, mefloquine, nicardipine and oxethazaine: 10, 5, 2.5, 1.25 μM. The selection of the dose range was based on previous published studies describing the sensitivity of different stages of development to these drugs [13,18–20]. The experiments were performed in duplicate using at least three worms per well and were repeated once. The drug effect was calculated by normalizing the viability of the worms exposed to the drugs, to the viability score of the control wells. The control wells consisted of worms incubated in the same culture media as the test conditions, and had the amount of DMSO corresponding to highest concentration of the assay (0.5% V/V). IC_{50} values were calculated using the software Graph Pad Prism V8.0 (San Diego, CA, USA).

Statistical analysis

We analyzed the gender distribution of NTS and juvenile developed and undeveloped worms using binomial tests for dichotomous non-parametric comparisons in R, version 3.5.1 (2018-07-02) [21]. By PCR we investigated the gender of 18 randomly selected NTS provided by three different batches and 26 worms incubated *in vitro* for 21 days from which the gender could not be determined by microscopy (undeveloped worms), also provided by three different batches. For data interpretation, we applied the binomial test assigning a success to "female" and a fail to "male". The null hypothesis was "the probability of success is equal to 0.5". The null hypothesis was rejected if $\rho<0.05$.

Kruskal-Wallis tests were used to compare the length between *in vivo* and *in vitro* grown worms. In each case we compared the length of worms among the week development group. *P*-values were adjusted for multiple testing bias using the Bonferroni procedure. For comparison of the 35 days of development, we additionally performed a Student's t-Test to focus on single comparisons of males and females *in vitro* versus *in vivo*.

Results

Assay establishment

NTS incubated in HM + 20% HSe showed weekly changes in morphology, bigger size and higher viability scores and movement than those incubated in DMEM + 20% HSe, in line with developmental phases described in the literature [8,13] (S1–S5 Figs). Based on these findings, we continued our study using HM medium + 20% HSe. The overall survival by means of this cultivation method was 99% within 21 days of development.

Subsequently we evaluated the reproducibility of the incubation conditions by testing five serum batches consisting of individual serum samples from different donors and a pool of all five sera mixed in equal parts. Although all individual batches of serum were able to promote the development of the parasites to further stages than the gut development stage (described as early liver stage by Frahm *et al.* [13]) after 21 days of incubation, the highest survival rate and rate of worms reaching the organogeny stage of development, was observed by the pool of sera (Table 2 and S6 Fig).

Additionally, the complement system, tested by adding untreated or heat-inactivated serum, had no influence on the development of the parasites, judged by the size, survival rate and morphology of the parasites.

Size comparison

We next evaluated the length of the *S. mansoni* grown *in vitro* and compared it to that of the worms developed *in vivo* (Fig 1). We found that the length of the worms developed *in vitro* correlated very well with the length of the worms developed *in vivo* for both genders until 28 days of development (S1 Table). After this time, the growth of the *in vitro* cultivated schistosomes reached a plateau and no further significant growth was detected, while the *in vivo* developed worms continued growing in length and reached sexual maturity. As a result, both males and females developed for 35 days *in vitro* were significantly shorter than those developed *in vivo* ($\rho<0.01$) (S7 Fig). For comparison, we also depict the adult worms retrieved from mice 49 days after infection, which had increased considerably in size (males: 7.2 ± 1.0 mm, females: 5.3 ± 0.9 mm).

Gender determination

Under the described medium conditions, we were able to determine the gender by microscopy, from day 13 onwards and to keep the *in vitro* growing worms alive for at least 56 days. However, sexual maturity was not evident in any experiment and worms did not couple and therefore did not lay any eggs.

Table 2. Comparison of the promotion of development to the organogeny stage, by each of the sera added to HM.

Serum #	N	% survival	% developed organogeny
1	71	85.9 (0.3)	54.4 (1.6)
2	62	80.6 (0.9)	48.7 (15.9)
3	70	67.1 (7.1)	16.8 (2.5)
4	58	55.6 (9.9)	25.0 (3.2)
5	73	67.3 (3.0)	37.3 (20.6)
6	151	98.7 (1.3)	71.8 (9.4)

Serum 6 is the mixture of equal parts of sera 1 to 5.

The table shows the average and standard deviation (SD) of experimental duplicates by 21 days of *in vitro* incubation. The experiment on the pool of sera was repeated once.

https://doi.org/10.1371/journal.pntd.0009313.t002

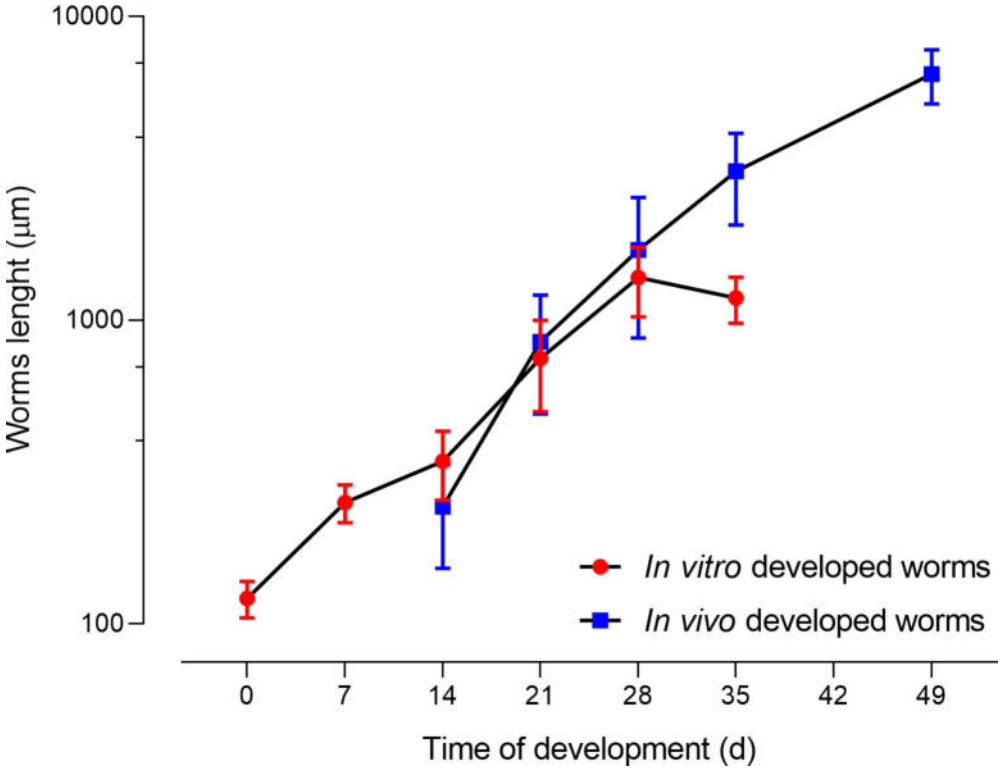

Fig 1. Comparison of the length of *S. mansoni* developed *in vitro* with those developed *in vivo*. Each point represents the average length of 22 worms including males and females.

https://doi.org/10.1371/journal.pntd.0009313.g001

As described by Chevalier *et al.* [17], males present high levels of Z marker, while females present high expression of the W6 region. For worms expressing both markers, at any developmental stage, we calculated the Δ Cq ($Cq_{W6} - Cq_{Z}$) value and found a difference of -9.21 ± 1.31 cycles for female *S. mansoni* and a positive Δ Cq for male worms (Fig 2), allowing us to unambiguously assign a gender to each worm. When considering the adult worms only, we observed that all samples amplified both markers. In males the ΔCq was 9.4 ± 2.2 (mean ± SD), while in females the ΔCq was -9.6 ± 0.3 (Fig 2A). We found a 100% agreement between morphology gender assignment and qPCR (Figs 2A and S8) when looking at a subset (n = 12) of adult worms (developed *in vivo*).

We were interested in identifying a possible bias in the gender distribution of the worms grown *in vitro*, which might influence results of the drug sensitivity assays. We first evaluated the gender distribution of the NTS by qPCR and found 50% of the parasites to be females (n = 18, $p = 1$) (Fig 2B). Subsequently, we evaluated the gender of parasites that were undeveloped by day 21 (worms that are not growing and for which no gender can be assigned by morphological assessment), and found that 65.4% of these were females. This difference was not significant (n = 26, $p = 0.17$) (Fig 2C). When considering the developed worms by 21 days of *in vitro* cultivation, by optical microscopy, no significant difference in the number of males compared to females was observed (males = 52%, $p = 0.47$, $n_{total} = 193$).

Comparison of drug sensitivity

We evaluated the activity of praziquantel on NTS and 7-to-35-day old *S. mansoni*, cultured *in vitro* and collected *in vivo*. As a reference, the activity of praziquantel on adult *S. mansoni* (grown *in vivo* for 49 days) was also evaluated (Fig 3).

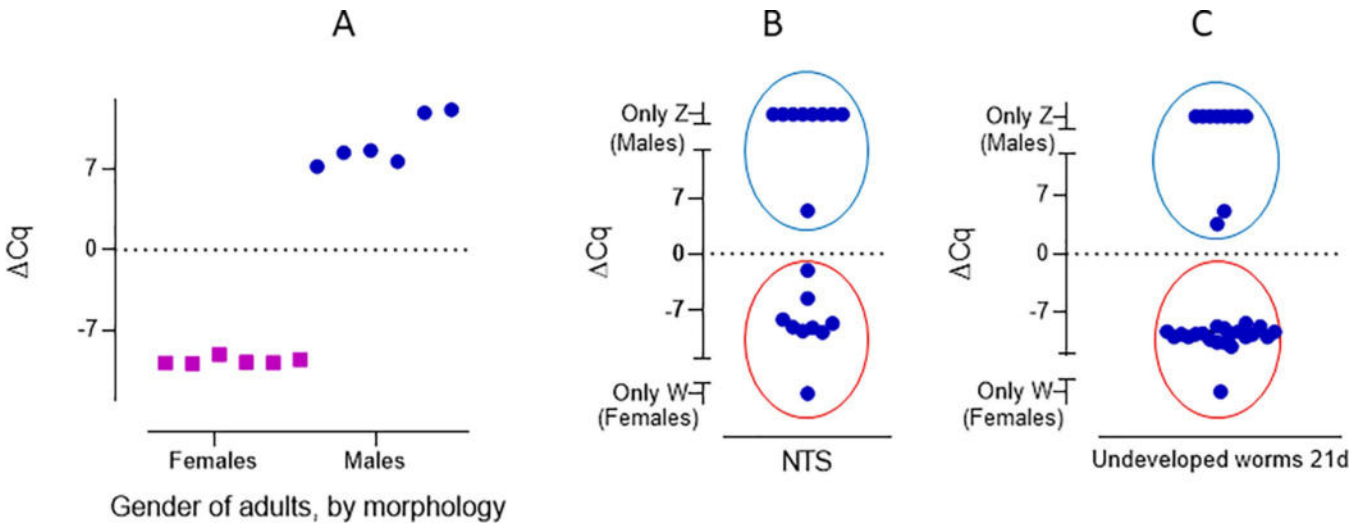

Fig 2. Comparison of the morphology and ΔCq of adult *S. mansoni* (A) NTS (B) and undeveloped worms by 21 days (C). A: adult worms, collected from mice 49 days post infection, classified as females (squares) and males (circles) by morphology, compared to ΔCq. B: gender distribution observed in NTS by means of qPCR. C: gender distribution of undeveloped worms, incubated for 21 days. The ΔCq for female worms was negative (red circle) and positive for males (blue circle), allowing unequivocal gender identification.

https://doi.org/10.1371/journal.pntd.0009313.g002

Next, we exposed worms grown *in vitro* and *in vivo* to five additional marketed drugs with known antischistosomal activity and different mechanisms of action [20] and compared sensitivities after 21 days of development (Table 3). The drugs used were auranofin [22], mefloquine [23], nicardipine [20,24], oxamniquine [25] and oxethazaine [20,26]. Oxamniquine was not lethal against worms grown either *in vivo* or *in vitro*, resulting in IC_{50} values above the range of concentrations used. Despite considerable differences at early evaluation time points (24 and 48 hours) for auranofin, nicardipine and oxethazaine all drugs evaluated showed similar IC_{50} values at the 72 hours evaluation time. In contrast, we observed a different sensitivity among both growing methods, resulting in a 10-fold lower sensitivity to mefloquine for *in vitro* developed worms, compared to those developed *in vivo* at 72 hours post-incubation.

Discussion

Our aim was to validate the application of a method to grow *S. mansoni in vitro* [13] for drug sensitivity assays. We first evaluated the reproducibility of different batches of sera to promote the parasite growth, and once the method was established, we evaluated the length, gender distribution and drug sensitivity of the worms grown under *in vitro* conditions and compared them to *in vivo* collected worms.

As also described by Basch *et al.* [9], we found differences in worm development between sera provided by different donors, while complement inactivation did not influence worm development. The highest survival and development rates at 21 and 28 days of development were observed while using the pool of sera when compared to the serum of individual donors. In the previous study by Frahm *et al.* [13], serum provided by six different donors was evaluated, but inter-batch variability was not reported.

In mice, the full life cycle and an established infection takes from 5 to 8 weeks [5,8]. By this time in the mouse model, adults would have developed, coupled in the liver, moved to the mesenteric veins and the females started shedding eggs. We did not observe sexual maturity and pairing of the worms using the *in vitro* culture. This is a limitation when compared to the method described by Basch and colleagues, who managed to culture mature egg laying worms.

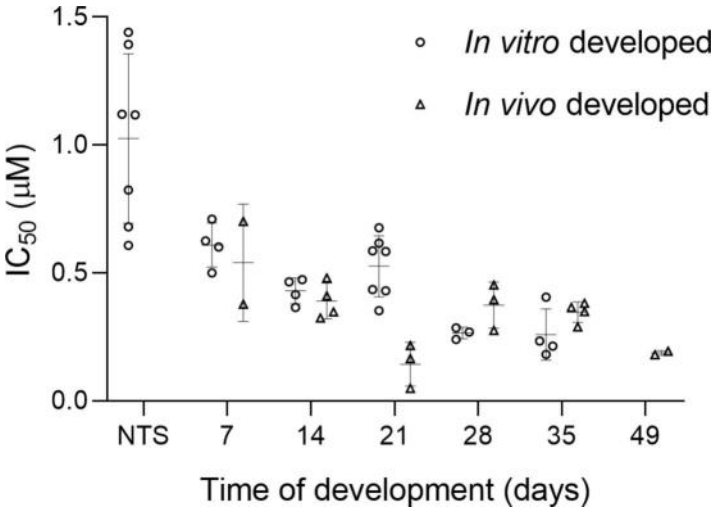

Fig 3. Sensitivity (IC_{50} values) of *S. mansoni* grown *in vivo* and developed *in vitro* exposed to praziquantel for 72 hours as a function of time. Each point in the figure represents an IC_{50} value, calculated from a full assay including four concentrations, three worms per concentration and conducted in duplicate.

https://doi.org/10.1371/journal.pntd.0009313.g003

However, these eggs were not viable, and the full life cycle could not be established until today [14,27,28]. In our study, no worms coupled even after 56 days of *in vitro* incubation, suggesting that sexual maturity is not only a matter of time, but more a factor of parasites/environment interaction, that triggers development, and future research could be oriented to identify these factors.

As known from previous studies [9], the development of schistosomes is subject to great variability [8] and we also observed it in worms grown both *in vitro* and *in vivo*. For example,

Table 3. Sensitivity (IC_{50} (SD)) comparison of *S. mansoni* incubated *in vitro* for 21 days compared to *S. mansoni* developed in mice for 21 days (μM).

		In vitro	*In vivo*
Auranofin	24 h	6.02 (12.35)	>100
	48 h	3.85 (3.64)	12.05 (6.30)
	72 h	3.93 (6.92)	5.31 (1.59)
Mefloquine	24 h	24.26 (0.00)	5.64 (0.79)
	48 h	9.31 (1.91)	11.67 (9.44)
	72 h	4.43 (0.20)	0.48 (0.20)
Oxamniquine	24 h	>100	>100
	48 h	>100	>100
	72 h	>100	>100
Praziquantel	24 h	0.74 (1.55)	0.54 (0.04)
	48 h	0.75 (0.71)	0.09 (0.09)
	72 h	0.54 (0.12)	0.14 (0.09)
Oxethazaine	24 h	>100	>100
	48 h	2.52 (0.14)	>100
	72 h	8.32 (10.32)	3.26 (3.23)
Nicardipine	24 h	6.87 (6.73)	12.45 (10.68)
	48 h	12.66 (20.48)	2.30 (3.24)
	72 h	2.09 (0.67)	2.05 (0.80)

https://doi.org/10.1371/journal.pntd.0009313.t003

in our experiments on 21-day old *in vivo* worms, 47.4% of the worms were not sufficiently developed to unambiguously assign a gender and there was also great variability in the parasites lengths (Figs 1 and S7 and S9). This finding is in line with the descriptions by Clegg *et al*. on *in vivo* grown juvenile *S. mansoni*, who also reported variability in the size of the worms, as well as in the time needed to progress from one stage to the next [8]. Although by 28 days of *in vivo* development we also found marked variability in their length (Fig 1), all worms could be morphologically classified either as males or females (S10 Fig), and a few worms had coupled.

The size determined for 7–14 day old worms grown *in vitro* are in line with findings described by Clegg *et al* [8]. For example, Clegg noted the size of the 7 day old (lung stage) worms to be 252 x 25 μm, similar to our study (*in vitro* grown worms: mean (SD): 251.1 (35.5) μm). However, contradictory findings were observed for the worms collected from day 28 to 49. In the aforementioned study, worms reached a maximum of 4.8 mm [8], which represented more than double the size of the largest worm (2.1 mm) observed in our study, after an incubation period of 28 days.

There is clear evidence of differential praziquantel sensitivity along the life cycle in infected animals [29–31] and humans [32], showing lower sensitivity to praziquantel in the juvenile stages of development. However, the differential sensitivity *in vitro* is under discussion [31,33]. Overall, studies agree that the highest sensitivity to praziquantel is observed in the adult stage [33,34] but the results on juveniles are diverse, showing reduced sensitivity until day 7 of development [13,29,35] or day 28 [33] and recovery of sensitivity by day 37 [33]. This was confirmed by our study as well, as we observed the highest activity of praziquantel on adults, low activity against NTS and moderate activity for the juvenile stages. The sensitivity to praziquantel along the life cycle was similar among the worms obtained by both growing methods, with the exception of the 21 days old stage, where we observed differences at the 48 and 72 hour IC_{50} values despite the similar sensitivity at the 24 hours evaluation time. The stage-specific sensitivity found in our studies *in vitro* is slightly different from studies evaluating the sensitivity to praziquantel in *S. mansoni* infected mice, where the lowest activity was observed against juvenile 28 day-old worms [36].

We also included oxamniquine as a negative control, since it is a pro-drug [25] that shows excellent clinical efficacy against chronic infections [32] and is also active on adult worms in *in vivo* models [37], but has limited activity against any of the developmental stages *in vitro* [38,39]. As expected, oxamniquine was inactive in both the *in vivo* and *in vitro* developed worms ($IC_{50} > 100$ μM).

We observed a slight difference in the sensitivity to mefloquine particularly at the 72 hour evaluation time point. The exact mechanism of action of mefloquine on schistosomes has not been elucidated yet. On *Plasmodium* spp. mefloquine is suggested to act via the inhibition of the hemoglobin detoxification mechanisms, causing an accumulation of toxic hem inside the parasite, leading to its death [40]. In *S. mansoni*, the same hemoglobin degradation products were found, suggesting a similar detoxification mechanism [41]. However, previous studies showed that although mefloquine was more active on *S. mansoni* in the presence of hemin [42], the drug was also active on the parasites in absence of blood or hemin itself [43], suggesting multiple mefloquine targets or mechanisms of action. Both our *in vitro* developed worms and those obtained by perfusion were incubated in blood-free medium; however, the worms collected from the mice still had blood remaining in the gut at the beginning of the assay, and this could explain the slightly higher activity of mefloquine on the *in vivo* worms compared to the ones grown *in vitro*, which have never had contact with hemoglobin. However, it is not clear why a difference in sensitivity to mefloquine was only observed 72 hours post-incubation. We also observed considerable difference in the activity of auranofin, oxethazaine and nicardipine, hinting to differences in the onset of action of the drugs between the *in vitro* and *in vivo*

developed worms. Further studies are necessary to understand the underlying reasons for these results. Nonetheless, with exception of mefloquine, a good correlation between the assays was observed at the most commonly used, recommended 72 hours evaluation time point [5].

Conclusion

We evaluated the size, gender, and drug susceptibility of juvenile *in vitro* developed *S. mansoni* and compared them to parasites grown *in vivo*. Overall, the size of the worms and gender was similar between both growing techniques until 28 days of development. Additionally, we observed similarity in sensitivity to auranofin, nicardipine, oxamniquine, oxethazaine and praziquantel, after 72 hours of incubation between the worms developed *in vitro* and the worms grown *in vivo* for 21 days. Despite the slightly different sensitivity to mefloquine at the 72-hour evaluation time point and considering the highly laborious method to collect juvenile *S. mansoni* from infected mice, this method is an excellent alternative to the development of juvenile *S. mansoni* in mice, as it allows the production of a much higher number of juvenile worms in an ethical manner and under very simple assay conditions, which can be used for drug screening on juvenile worms.

Supporting information

S1 Table. *S. mansoni* length (μm) according to time of development (in days) either *in vitro* or *in vivo*.
(XLSX)

S1 Fig. *S. mansoni* developed *in vitro* for 7 days. No gender identification possible. Amplification: A: 100x, B:200x. Scale bar: 200 μm.
(TIF)

S2 Fig. *S. mansoni* developed *in vitro* for 14 days By 14 days of development, the males are distinguishable from females. Amplification: A: 100x, B:200x. Scale bar: 200 μm.
(TIF)

S3 Fig. *S. mansoni* developed *in vitro* for 21 days Amplification: 200x. U: undeveloped worm. Scale bar: 200 μm.
(TIF)

S4 Fig. *S. mansoni* developed *in vitro* for 28 days. U: undeveloped worm. Amplification: A: 200x, B: 100x. Scale bar: 200 μm.
(TIF)

S5 Fig. *S. mansoni* developed *in vitro* for 35 days. Amplification: 100x. Scale bar: 200 μm.
(TIF)

S6 Fig. Comparison of five individual batches of sera and the pool of all of them. Comparison of the development of *in vitro* grown *S. mansoni* using HM + 20% HSe from five different donors by 21 days of development. Serum 6 is the combination of the other five sera mixed together in equal parts. Scale bar: 200 μm.
(TIF)

S7 Fig. Comparison of the length of worms grown by both methods as a function of time, split by gender. By means of either growing technique the worms' gender is only to be identified after 10–13 days of development. Each point represents one worm. Abbreviations: ND: not done, undef: undefined: the gender of the worms cannot be determined by optical

microscopy.
(TIF)

S8 Fig. Adult couples of *S. mansoni* developed *in vivo* for 49 days and incubated free of drugs for 24 hours. Amplification: 40x. Scale bar: 1 mm.
(TIF)

S9 Fig. *S. mansoni* developed *in vivo* for 21 days A: male and two undeveloped worms 100X, B: undeveloped worms100X. U: undeveloped worm. Scale bar: 200 μm.
(TIF)

S10 Fig. *S. mansoni* developed *in vivo* for 28 days. Amplification: 100x. Scale bar: 200 μm.
(TIF)

Author Contributions

Conceptualization: Valentin Buchter, Jennifer Keiser.

Formal analysis: Valentin Buchter.

Funding acquisition: Jennifer Keiser.

Investigation: Valentin Buchter, Pierre H. H. Schneeberger.

Methodology: Valentin Buchter, Pierre H. H. Schneeberger.

Project administration: Jennifer Keiser.

Supervision: Pierre H. H. Schneeberger, Jennifer Keiser.

Visualization: Valentin Buchter.

Writing – original draft: Valentin Buchter.

Writing – review & editing: Pierre H. H. Schneeberger, Jennifer Keiser.

References

1. WHO. Schistosomiasis 2020 [updated 02.03.20]. Available from: https://www.who.int/news-room/fact-sheets/detail/schistosomiasis.
2. Colley DG, Bustinduy AL, Secor WE, King CH. Human schistosomiasis. Lancet. 2014; 383 (9936):2253–64. https://doi.org/10.1016/S0140-6736(13)61949-2 PMID: 24698483
3. Cioli D, Pica-Mattoccia L, Basso A, Guidi A. Schistosomiasis control: praziquantel forever? Molecular & Biochemical Parasitology. 2014; 195(1):23–9. https://doi.org/10.1016/j.molbiopara.2014.06.002 PMID: 24955523
4. Couto FF, Coelho PMZ, Araújo N, Kusel JR, Katz N, Jannotti-Passos LK, et al. *Schistosoma mansoni*: a method for inducing resistance to praziquantel using infected *Biomphalaria glabrata* snails. Memórias do Instituto Oswaldo Cruz. 2011; 106:153–7. https://doi.org/10.1590/s0074-02762011000200006 PMID: 21537673
5. Lombardo FC, Pasche V, Panic G, Endriss Y, Keiser J. Life cycle maintenance and drug-sensitivity assays for early drug discovery in *Schistosoma mansoni*. Nature Protocols. 2019:1. https://doi.org/10.1038/s41596-018-0101-y PMID: 30610241
6. Pasche V, Laleu B, Keiser J. Screening a repurposing library, the Medicines for Malaria Venture Stasis Box, against *Schistosoma mansoni*. Parasites & Vectors. 2018; 11:298. https://doi.org/10.1186/s13071-018-2855-z PMID: 29764454
7. Fenwick N, Griffin G, Gauthier C. The welfare of animals used in science: how the "Three Rs" ethic guides improvements. Canadian Veterinary Journal. 2009; 50(5):523–30. PMID: 19436640
8. Clegg JA. *In vitro* cultivation of *Schistosoma mansoni*. Experimental Parasitology. 1965; 16(2):133–47. https://doi.org/10.1016/0014-4894(65)90037-8 PMID: 14281210

9. Basch PF. Cultivation of *Schistosoma mansoni in vitro*. I. Establishment of cultures from cercariae and development until pairing. Journal of Parasitology. 1981; 67(2):179–85. PMID: 7241277
10. Reimers N, Homann A, Höschler B, Langhans K, Wilson RA, Pierrot C, et al. Drug-induced exposure of *Schistosoma mansoni* antigens SmCD59a and SmKK7. PLOS Neglected Tropical Diseases. 2015; 9 (3):e0003593. https://doi.org/10.1371/journal.pntd.0003593 PMID: 25774883
11. Štefanić S, Dvořák J, Horn M, Braschi S, Sojka D, Ruelas DS, et al. RNA interference in *Schistosoma mansoni* schistosomula: selectivity, sensitivity and operation for larger-scale screening. PLOS Neglected Tropical Diseases. 2010; 4(10):e850. https://doi.org/10.1371/journal.pntd.0000850 PMID: 20976050
12. Paveley RA, Mansour NR, Hallyburton I, Bleicher LS, Benn AE, Mikic I, et al. Whole organism high-content screening by label-free, image-based bayesian classification for parasitic diseases. PLOS Neglected Tropical Diseases. 2012; 6(7):e1762. https://doi.org/10.1371/journal.pntd.0001762 PMID: 22860151
13. Frahm S, Anisuzzaman A, Prodjinotho UF, Vejzagić N, Verschoor A, Costa CPd. A novel cell-free method to culture *Schistosoma mansoni* from cercariae to juvenile worm stages for *in vitro* drug testing. PLOS Neglected Tropical Diseases. 2019; 13(1):e0006590. https://doi.org/10.1371/journal.pntd.0006590 PMID: 30689639
14. Clegg MAS J. A. B. Culture of vertebrate host stages. In: Baker TAERaJR, editor. *In vitro* methods for parasite cultivation—Culture of *S mansoni*. 1: Academic Press; 1987. p. 258–61.
15. Farah IO, Kariuki TM, King CL, Hau J. An overview of animal models in experimental schistosomiasis and refinements in the use of non-human primates. Laboratory animals. 2001; 35(3):205–12. https://doi.org/10.1258/0023677011911570 PMID: 11463066
16. Schindelin J, Arganda-Carreras I, Frise E, Kaynig V, Longair M, Pietzsch T, et al. Fiji: an open-source platform for biological-image analysis. Nature Methods. 2012; 9(7):676–82. https://doi.org/10.1038/nmeth.2019 PMID: 22743772
17. Chevalier FD, Le Clec'h W, Alves de Mattos AC, LoVerde PT, Anderson TJ. Real-time PCR for sexing *Schistosoma mansoni* cercariae. Molecular & Biochemical Parasitology. 2016; 205(1–2):35–8. https://doi.org/10.1016/j.molbiopara.2016.03.010 PMID: 27021570
18. Pasche V, Laleu B, Keiser J. Early antischistosomal leads identified from *in vitro* and *in vivo* screening of the medicines for malaria venture pathogen box. ACS infectious diseases. 2019; 5(1):102–10. https://doi.org/10.1021/acsinfecdis.8b00220 PMID: 30398059
19. Ingram K, Ellis W, Keiser J. Antischistosomal activities of mefloquine-related arylmethanols. Antimicrobial Agents and Chemotherapy. 2012; 56(6):3207. https://doi.org/10.1128/AAC.06177-11 PMID: 22470113
20. Panic G, Vargas M, Scandale I, Keiser J. Activity profile of an FDA-approved compound library against *Schistosoma mansoni*. PLOS Neglected Tropical Diseases. 2015; 9(7):e0003962. https://doi.org/10.1371/journal.pntd.0003962 PMID: 26230921
21. RStudio Team (2016). RStudio: Integrated Development for R. RStudio ed.3.5.1, PBC, Boston, MA
22. Angelucci F, Sayed AA, Williams DL, Boumis G, Brunori M, Dimastrogiovanni D, et al. Inhibition of *Schistosoma mansoni* thioredoxin-glutathione reductase by auranofin: structural and kinetic aspects. Journal of Biological Chemistry. 2009; 284(42):28977–85. https://doi.org/10.1074/jbc.M109.020701 PMID: 19710012
23. Xiao SH. Mefloquine, a new type of compound against schistosomes and other helminthes in experimental studies. Parasitol Res. 2013; 112(11):3723–40. https://doi.org/10.1007/s00436-013-3559-0 PMID: 23979493
24. Pica-Mattoccia L, Orsini T, Basso A, Festucci A, Liberti P, Guidi A, et al. *Schistosoma mansoni*: lack of correlation between praziquantel-induced intra-worm calcium influx and parasite death. Expermental Parasitology. 2008; 119(3):332–5. https://doi.org/10.1016/j.exppara.2008.03.012 PMID: 18456260
25. Pica-Mattoccia L, Carlini D, Guidi A, Cimica V, Vigorosi F, Cioli D. The schistosome enzyme that activates oxamniquine has the characteristics of a sulfotransferase. Memórias do Instituto Oswaldo Cruz. 2006; 101:307–12. https://doi.org/10.1590/s0074-02762006000900048 PMID: 17308787
26. Ravaynia PS, Lombardo FC, Biendl S, Dupuch MA, Keiser J, Hierlemann A, et al. Parallelized impedance-based platform for continuous dose-response characterization of antischistosomal drugs. Advanced Biosystems. 2020; 4(7):1900304. https://doi.org/10.1002/adbi.201900304 PMID: 32510834
27. Wang J, Chen R, Collins JJ, III. Systematically improved *in vitro* culture conditions reveal new insights into the reproductive biology of the human parasite *Schistosoma mansoni*. PLOS Biology. 2019; 17(5): e3000254. https://doi.org/10.1371/journal.pbio.3000254 PMID: 31067225

28. Doenhoff MJ, Modha J, Walker AJ. Failure of *in vitro*-cultured schistosomes to produce eggs: how does the parasite meet its needs for host-derived cytokines such as TGF-β? International Journal for Parasitology. 2019; 49(10):747–57. https://doi.org/10.1016/j.ijpara.2019.05.004 PMID: 31348959

29. Andrews P. A summary of the efficacy of praziquantel against schistosomes in animal experiments and notes on its mode of action. Arzneimittelforschung. 1981; 31(3a):538–41. PMID: 7016122

30. Sabah AA, Fletcher C, Webbe G, Doenhoff MJ. *Schistosoma mansoni*: chemotherapy of infections of different ages. Experimental Parasitology. 1986; 61(3):294–303. https://doi.org/10.1016/0014-4894(86)90184-0 PMID: 3086114

31. Pica-Mattoccia L, Cioli D. Sex- and stage-related sensitivity of *Schistosoma mansoni* to *in vivo* and *in vitro* praziquantel treatment. International Journal of Parasitology. 2004; 34(4):527–33. https://doi.org/10.1016/j.ijpara.2003.12.003 PMID: 15013742

32. Lago EM, Xavier RP, Teixeira TR, Silva LM, da Silva Filho AA, de Moraes J. Antischistosomal agents: state of art and perspectives. Future Medicinal Chemistry. 2017; 10(1):89–120. https://doi.org/10.4155/fmc-2017-0112 PMID: 29235368

33. Aragon AD, Imani RA, Blackburn VR, Cupit PM, Melman SD, Goronga T, et al. Towards an understanding of the mechanism of action of praziquantel. Molecular and biochemical parasitology. 2009; 164(1):57–65. https://doi.org/10.1016/j.molbiopara.2008.11.007 PMID: 19100294

34. Kasinathan RS, Sharma LK, Cunningham C, Webb TR, Greenberg RM. Inhibition or knockdown of ABC transporters enhances susceptibility of adult and juvenile schistosomes to praziquantel. PLOS Neglected Tropical Diseases. 2014; 8(10). https://doi.org/10.1371/journal.pntd.0003265 PMID: 25330312

35. Xiao SH, Catto BA, Webster LT Jr., Effects of praziquantel on different developmental stages of *Schistosoma mansoni in vitro* and *in vivo*. Journal of Infectious Diseases. 1985; 151(6):1130–7.

36. Utzinger J, Xiao SH, Tanner M, Keiser J. Artemisinins for schistosomiasis and beyond. Current Opinion on Investigative Drugs. 2007; 8(2):105–16. PMID: 17328226

37. Hess J, Panic G, Patra M, Mastrobuoni L, Spingler B, Roy S, et al. Ferrocenyl, ruthenocenyl, and benzyl oxamniquine derivatives with cross-species activity against *Schistosoma mansoni* and *Schistosoma haematobium*. ACS infectious diseases. 2017; 3(9):645–52. https://doi.org/10.1021/acsinfecdis.7b00054 PMID: 28686009

38. Doenhoff MJ. The immune-dependence of chemotherapy in experimental schistosomiasis. Memórias do Instituto Oswaldo Cruz. 1989; 84 Suppl 1:31–7. https://doi.org/10.1590/s0074-02761989000500004 PMID: 2517867

39. Buchter V, Hess J, Gasser G, Keiser J. Assessment of tegumental damage to *Schistosoma mansoni* and *S. haematobium* after *in vitro* exposure to ferrocenyl, ruthenocenyl and benzyl derivatives of oxamniquine using scanning electron microscopy. Parasites & Vectors. 2018; 11(1):580. https://doi.org/10.1186/s13071-018-3132-x PMID: 30400935

40. Zhang J, Krugliak M, Ginsburg H. The fate of ferriprotorphyrin IX in malaria infected erythrocytes in conjunction with the mode of action of antimalarial drugs. Molecular and Biochemical Parasitology. 1999; 99(1):129–41. https://doi.org/10.1016/s0166-6851(99)00008-0 PMID: 10215030

41. Oliveira MF, d'Avila JC, Torres CR, Oliveira PL, Tempone AJ, Rumjanek FD, et al. Haemozoin in *Schistosoma mansoni*. Molecular Biochemistry and Parasitology. 2000; 111(1):217–21. https://doi.org/10.1016/s0166-6851(00)00299-1 PMID: 11087932

42. Manneck T, Braissant O, Ellis W, Keiser J. *Schistosoma mansoni*: antischistosomal activity of the four optical isomers and the two racemates of mefloquine on schistosomula and adult worms *in vitro* and *in vivo*. Experimental Parasitology. 2011; 127(1):260–9. https://doi.org/10.1016/j.exppara.2010.08.011 PMID: 20732321

43. Manneck T, Keiser J, Müller J. Mefloquine interferes with glycolysis in schistosomula of *Schistosoma mansoni* via inhibition of enolase. Parasitology. 2012; 139(4):497–505. https://doi.org/10.1017/S0031182011002204 PMID: 22309769

Chapter VI

Discussion and conclusion

The drugs used as first line in the treatment of the three diseases described in this thesis, namely praziquantel (PZQ), albendazole (ABZ), mebendazole (MBZ) and ivermectin (IVM), expose limitations in the efficacy profile or are strongly challenged by the emergence of resistance. Therefore, new drugs, or improved alternatives of them are urgently needed (Olsen, 2007, Mendes *et al.*, 2017, Moser *et al.*, 2017, Panic *et al.*, 2018). My research was oriented to the development of new molecules and the improvement of the formulations of existing drugs, with the final goal of improving the treatment of these diseases.

The amount of knowledge available on STH infections and schistosomiasis, and the fact that a key strategy for their control is MDA (WHO, 2020b), allow for a clear definition of the characteristics that ideal drugs to treat these diseases should fulfil. I collected the most important characteristics of an ideal drug, to define a target product profile (TPP) of the drugs to be developed for STH infections and schistosomiasis (Figure 1). In the further sections I will discuss the contributions of my research towards the development of drugs for each of the diseases covered in this thesis and how my projects related to the development of this TPP.

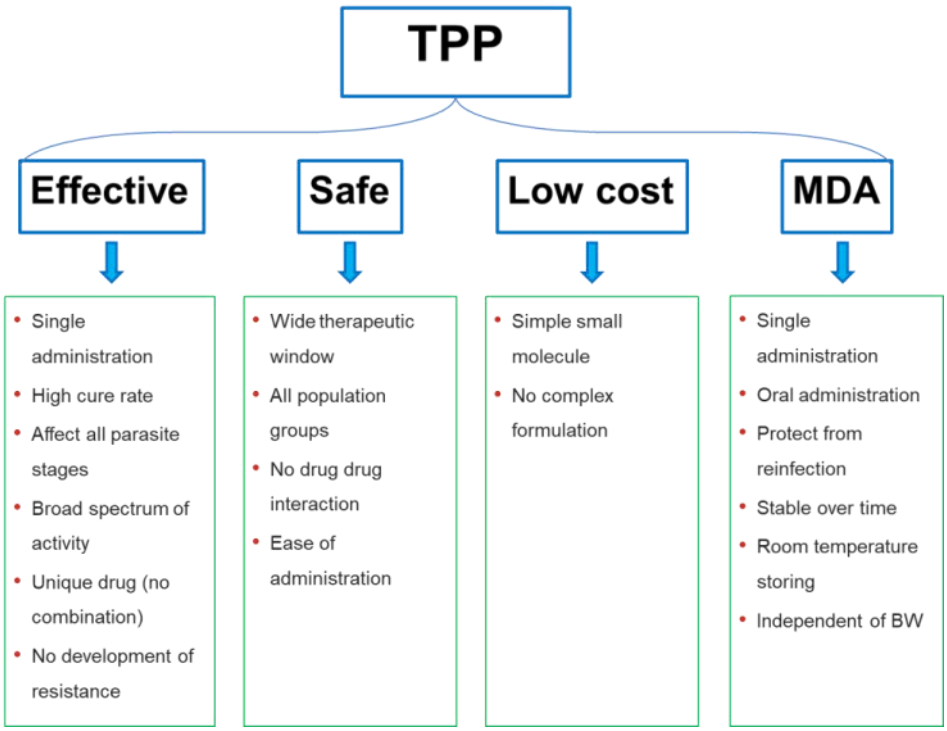

Figure 1: Characteristics of ideal drugs for the control of STH infections and schistosomiasis, to be administered in the frame of mass drug administration programs (MDA). As must criteria, the drugs need

to be effective, safe, low cost, and need to be able to be administered in the frame of MDA. Abbreviations: BW: body weight, MDA: Mass drug administration, TPP: target product profile.

To be applied in the frame of MDA campaigns, an ideal drug needs to be effective after one, single and oral administration (Keiser *et al.*, 2008b, WHO, 2017). In this frame, drugs need to be safe to all target populations including children and pregnant women, making it necessary to the drug to have a wide therapeutic window (Keiser *et al.*, 2010, Stothard *et al.*, 2013). In addition, a wide therapeutic window allows for the administration of a drug independent of body weight. This not only narrows down the chance of dosing errors, but also allows low-trained staff (e.g. teachers) to administer the drugs, saving time and resources. Considering the chronic underfunding of the health systems towards these diseases, the drug needs to reach the population by incurring low costs (Lo *et al.*, 2015). A limitation of PZQ is that is low active against juvenile stages of the parasite (Cioli *et al.*, 2014). In parallel, oxamniquine (OXA) is restricted in the sense of only being active against *S. mansoni* (Pica-Mattoccia *et al.*, 1997). Both benzimidazoles show limited efficacy in the treatment of *T. trichiura*, while MBZ's performance is suboptimal in the treatment of hookworm infections (WHO, 2006, Moser *et al.*, 2017). To overcome these limitations, an ideal drug should be active against all stages of parasite's development and all targeted species. Additional desirable characteristics would be: no drug-drug interactions, a long half-life providing a preventive effect, and long term stability under room temperature conditions.

Albendazole and mebendazole

Considering the high costs and time needed to develop a new drug and the fact that the drugs are urgently needed (Moser *et al.*, 2017, WHO, 2020b), my research was oriented to the development of four formulations to raise the efficacy of the benzimidazoles in the treatment of STH infections.

The benzimidazoles have many advantages in terms of safety and tolerability (Keiser *et al.*, 2008b), cost-effectiveness (Lo *et al.*, 2015), and can be administered in the frame of MDA programs (WHO, 2017). Both MBZ and ABZ achieve high cure rates in the treatment of *A. lumbricoides* infections. However, only ABZ is sufficiently effective against hookworm

infections, and none of the drugs is effective enough in the treatment of *T. trichiura* (Keiser *et al.*, 2008b, Moser *et al.*, 2017). It was hypothesized that it is the solubility of the benzimidazoles, and not necessarily the permeability or the intrinsic activity, the main reason of the reduced efficacy (Jung *et al.*, 1997). Based on this hypothesis, the second chapter of this thesis focused on our efforts to improve the water solubility of the drugs, and how the enhanced solubility led to the raise of the drugs activity.

The activity of a drug depends fundamentally on two aspects: the concentration at which the drug is present at the target microenvironment, and the time the drug is in contact with the target and can exert its action (Levison *et al.*, 2009, White, 2013). In addition, only solubilized molecules can be absorbed by the body of the host, or penetrate the parasite's cuticle and exert its activity (Alvarez *et al.*, 2007, Savjani *et al.,* 2012). In consequence, it could be hypothesized that the different drug sensitivities against the individual species is based on the worms' exposure, which is linked to the location within the body, and/or the feeding mechanism.

Adult *A. lumbricoides* live in the upper small intestine's lumen and feed on pre-digested food (Despommier, 2017d) and are probably the most exposed parasites and therefore the most affected by the drugs. Secondly, hookworms are attached to the small intestine's wall and feed on blood (Despommier, 2017b). Last but not least, adult *T. trichiura* find their niche in the large intestine, with the anterior third part of the body embedded in the columnar cells and two thirds of the body moving freely in the intestine's lumen (Tilney *et al.*, 2005, Despommier, 2017a). The feeding mechanism of *T. trichiura* is suggested to be from the cytoplasm of epithelial cells (Tilney *et al.*, 2005) while it was proved not to be based on blood digestion (Despommier, 2017a). The differences in location, feeding mechanisms and cuticle permeation properties (Mottier *et al.*, 2006) have an influence in drug's activity, but we hypothesized that all differences can be faced, if the drug is better solubilized.

The difference in drug efficacy could additionally be explained by the drug's reactive and metabolic properties, already studied on *H. polygyrus* and *T. muris* (Cowan *et al.*, 2017). In the

case of ABZ, because of the reversible Red-ox reactions of the parent drug, uptake by the parasite seems to be a result of passive permeation through the cuticle, in addition to an indirect way via blood meal (Mottier *et al.*, 2006, Alvarez *et al.*, 2007, Cowan *et al.*, 2017). Different is the entering mechanism of MBZ into both *T. muris* and *H. polygyrus*. MBZ forms no metabolites, and the permeation mechanism is passive, through the worm's cuticle (Mottier *et al.*, 2006, Cowan *et al.*, 2017). In our experiments, the MBZ – chitosan formulation (MBZ-CH) showed the highest raise of activity despite not dramatically increasing the solubility, (20 fold ED_{50} reduction compared to pure MBZ). We observed the same behavior for the ABZ – CH formulation, resulting as well in the lowest ED_{50} value despite not accounting on the highest solubility improvement. Chitosan is a polymer with bio adhesive properties (Kang *et al.*, 2015), and could enhance the drugs' activity mediated by a longer contact between the drug and the parasite and allowing the drug to exert its activity. Our findings are in line with previous research showing chitosan as useful formulation component to improve ABZ activity (Abulaihaiti *et al.*, 2015). Further research on these improved formulations could include PK/PD studies on infected mice, to evaluate the exposure-response correlation and quantify the contribution of the direct permeation of the worm, compared to the drug intake via blood meal.

In contrast to the chitosan formulations, cyclodextrin complexes (CD) seem not to be an alternative strategy to improve the activity of ABZ in the treatment of STH, even after reaching the maximal dissolution rate among the formulations. Despite research showing advantages in the solubility of the CD formulation (Ehteda *et al.*, 2012, García *et al.*, 2014, Pacheco *et al.*, 2018), our *in vitro* and *in vivo* results showed no great advantage in the activity of these formulations, compared to the pure drugs. Similar as in our study, Pacheco *et al.* observed no raise in activity on infected lambs, despite reaching an improved solubility *in vitro* (Pacheco *et al.*, 2018). A possible explanation is the high binding constant of ABZ with CD (Carrier *et al.*, 2007), suggesting a too intense interaction within the complex, which makes the free fraction availability too low to interact with the target. CD complexes are not a unique case where the

lack of drug release can be observed, as it could also happen with other drugs when formulated within lipid nanocapsules (Huynh *et al.*, 2009).

There is much evidence on improved formulations of ABZ showing an enhanced bioavailability for the drugs, when compared to the drugs administered pure, both in animal species (Ravichandran, 2010, García *et al.*, 2013, Abulaihaiti *et al.*, 2015, Paredes *et al.*, 2018) and humans (Rigter *et al.*, 2004). Independent of the mechanism of drug uptake by the worms, a raise in the bioavailability provided by the improved formulations might have a benefit in the cure rates considering the MDA campaigns in clinical settings. The life cycle of hookworms and *A. lumbricoides* include a larval migration phase in the blood compartment of the host (Despommier, 2017d). Importantly, larval stages of development were also found to be sensitive to ABZ (Tritten *et al.*, 2011, Hajaji *et al.*, 2019). As a result, it can be hypothesized that the improved formulations also provide a positive effect in the fight against the larval stages of the parasites, especially important in high transmission areas (Loukas *et al.*, 2016).

From our studies, the best strategy for formulation improvement, indicated for further research on STH, are the chitosan ABZ and MBZ microcrystal formulations. Additionally, the ABZ-P80 formulation also reveals an optimal compromise among drug release properties, drug content in formulation and *in vivo* efficacy. Further steps in this line of research could include the evaluation of the formulations on other STH models with lower drug sensitivity, like *T. muris*, a model organism of *T trichiura* (Cowan *et al.*, 2017). As mentioned before, PK-PD studies on animal models could help to understand the relationship between the direct uptake by the worm, and the need of drug absorption and access via blood meal. Despite the great efforts to improve the efficacy of ABZ and MBZ in animal models, formulations with enhanced water solubility have been investigated in few clinical studies, and showed enhanced bioavailability on healthy volunteers (Rigter *et al.*, 2004). This situation highlights a knowledge gap, and makes the topic suitable for further research on STH infected patients, where improved ABZ and MBZ formulations might be advantageous. An enhanced bioavailability profile would be

specifically relevant in the treatment of recent infections, when the larvae are found in the blood.

Moxidectin

It is important to remember that no public health approach currently exists for controlling strongyloidiasis (WHO, 2020c). Considering the geographical overlapping (Jourdan *et al.*, 2018), the ideal scenario for STH control would include drugs that affect classical STH but are also effective in the treatment of *Strongyloides sp.* Currently, this is not the case, since the benzimidazoles are not sufficiently active against *S. stercoralis* infections (Jourdan *et al.*, 2018) and therefore *S. stercoralis* are not strongly affected by MDA campaigns targeting STH (Olsen *et al.*, 2009). Inversely, IVM, the gold standard treatment for human strongyloidiasis (Jourdan *et al.*, 2018, Hürlimann *et al.*, 2019), showed to be highly effective in the treatment of *A. lumbricoides*, but is not an alternative for the treatment of *T. trichiura* and hookworm infections (Wimmersberger *et al.*, 2018).

My research regarding strongyloidiasis was oriented to the characterization of moxidectin (MOX) in the frame of a drug repurposing strategy. What makes MOX interesting for its investigation as a possible human nematodes treatment is its wide and longstanding use in veterinary medicine as broad-spectrum, safe antiparasitic drug (Shoop *et al.*, 1995) and its molecular similarity, but still existing differences with IVM (Prichard *et al.*, 2012). There are some characteristics of MOX and IVM that I would like to expand on: (I) their transport mechanisms and safety profile, (II) the much longer half-life of moxidectin, (III) moxidectin administration independent of body weight, (IV) the ability of these drugs to avoid cross resistance.

(I) transport mechanisms and safety profile of moxidectin and ivermectin

We evaluated the PK-PD profile of MOX in rats infected with *S. ratti* after administration of three different doses in form of a water-based suspension. While the elimination and export mechanisms have been widely investigated, there is little knowledge available about the absorption, but our rat model could help clarifying open questions.

MOX is a lipophilic molecule (logP = 6 (Ménez *et al.*, 2012)) with fast absorption, classified as class II in the BCS, presenting low solubility and high permeability (Amidon *et al.*, 1995). In our experiments, despite observing an increase in Cmax and AUC from the 250 to the 500 µg/kg dose, no significant change in AUC or Cmax was observed by the higher dose of 750 µg/kg. In addition, there is a delay in the Tmax after the highest dose administration when compared to the low and mid doses. Given the low water solubility of MOX (0.51 mg/L (FDA, 2018)), solubility issues, translating into lower and slower absorption, could explain the lack of increase of the Cmax and AUC at the highest dose and a delayed Tmax (Figure 2). This PK profile is compatible with a passive absorption mechanism, where it could be hypothesized that the ceiling effect on the total exposition (AUC) is explained with a fraction of the drug not being dissolved and therefore excreted via faeces.

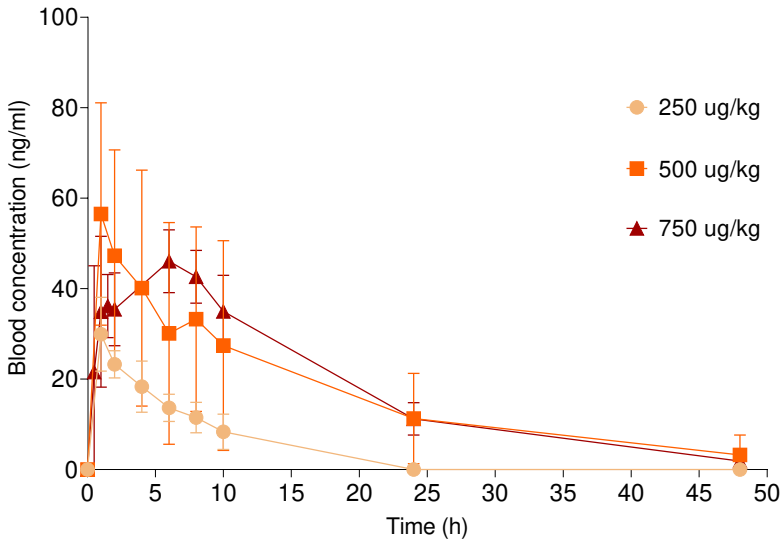

Figure 2. Profiles of moxidectin blood concentration vs time following an oral administration of 250, 500, and 750 µg/kg, in rats (n = 4). Despite observing an increment in Cmax and AUC from the 250 to the 500 µg/kg dose, no significant change in AUC or Cmax was observed by the higher dose of 750 µg/kg. There is a delay in the Tmax after the highest dose administration when compared to the low and mid dose (peak at 1 h vs peak at 5.25 h).

Different to our experiments, a study on uninfected rats did not observe a clear AUC ceiling effect: much higher doses than in our study were used, but the PK profile resulted in a much higher AUC (FDA, 2017). In that case, the vehicle used for drug administration was corn oil,

instead of a water - tween 80 - ethanol suspension used in our study, which could be better to solubilize a low polar drug (FDA, 2017). The reason to choose a water-based suspension in our studies instead of corn oil, is because this is our standard vehicle, which is more compatible with human administration than the use of an oily vehicle. This observation suggests that the vehicle used for administration, in addition to the increased absorption by concomitant ingestion of a fatty meal (Korth-Bradley *et al.*, 2012) would have a significant influence on the bioavailability of MOX. This finding opens the discussion if a formulation to improve the water solubility, as was done with ABZ and MBZ, would also be worth for MOX.

Both macrocyclic lactones (MLs: IVM and MOX) have in common that are mainly eliminated from the body by faeces, with only mild liver metabolism (Perez *et al.*, 2001, Prichard *et al.*, 2012). However, the active excretion mechanisms differ. Although there is clear evidence of IVM being exported from the digestive tract by the Pgp protein, this is not the case for MOX, which only showed negligible variation in the total drug exposure when administered together with the Pgp inhibitor, verapamil (Molento *et al.*, 2004, Kiki-Mvouaka *et al.*, 2010, Prichard *et al.*, 2012).

Different is the situation in the central nervous system (CNS) where both molecules are actively exported. Due to the existence of ABC transporters in the blood-brain-barrier (BBB), MOX and IVM are found in very low concentrations in the cerebrospinal fluid (Janko *et al.*, 2013). However, in Pgp deficient mice, both drugs managed to enter the CNS compartment, but MOX was less neurotoxic than IVM (Janko *et al.*, 2013). This difference in toxicity is important in the frame of MDA, where the drugs are administered without prior diagnosis and concomitant medicines consumption is rarely investigated. As a result, a potential drug-drug-interaction is important to consider when administering IVM or MOX in combination with PZQ, which is also transported by the Pgp protein (Messerli *et al.*, 2009). An example of this combined treatment is observed in the frame of joint campaigns against schistosomiasis and lymphatic filariasis (LF). In these campaigns, ABZ + IVM, followed by PZQ one week later are administered as the preferred regimen (Olsen *et al.*, 2009).

(II) Moxidectin has a longer half-life than ivermectin

A very important difference between IVM and MOX is the higher lipophilicity of MOX ($LogP_{IVM}$ = 4.8, $LogP_{mox}$= 6 (Prichard *et al.*, 2012)), what results in a bigger volume of distribution (Vd) and a longer half-life (Cobb *et al.*, 2009). While the half-life of IVM in humans is 1 day, for MOX the half-life is 20 – 35 days (Cotreau *et al.*, 2003, Prichard *et al.*, 2012), probably due to the larger tissue distribution and accumulation in the fat tissue (Cobb *et al.*, 2009). Another factor with a positive effect on the half-life of MOX when compared to IVM is the lower affinity of MOX towards the export protein Pgp, explained before (Prichard *et al.*, 2012). In consequence, the longer $T_{1/2}$ of MOX seems to result from a combination of both, a higher lipophilicity and distribution to fat tissue, and a lower Pgp affinity, which reduces its active export to the faeces (Prichard *et al.*, 2012).

Given the long half-life demonstrated in healthy humans (Cotreau *et al.*, 2003) and the efficacy of MOX observed in the treatment of L3 larvae (chapter 3 of this thesis), it would be interesting to investigate if MOX could provide a re-infection protective effect. A long-term protective effect was already suggested in the treatment of the nematode *O. volvulus*, where skin microfilaria loads were lower after treatment with MOX than IVM, on the 12 months follow up investigation (Opoku *et al.*, 2018).

To close this section, I would like to discuss on the rat as a model of human *Strongyloides spp.* infection and the treatment with MOX. We observed a shorter $T_{1/2}$ in rats when compared to studies in healthy humans and other species bigger in size. In our study as well as additional studies on rats, the $T_{1/2}$ was in the range of 9-20 h (chapter 3 of this thesis, (Cotreau *et al.*, 2003, FDA, 2017)). For different animal species and humans, this time was much longer: beagle dogs: 621 h (Al-Azzam *et al.*, 2007), horses: 555 h (Cobb *et al.*, 2009), humans: 480 – 700 h (Cotreau *et al.*, 2003). Given the time dependency of MOX to kill *S. ratti in vitro* (described in chapter three), and the need of a drug concentration to be above the effective concentration to exert its activity (Levison *et al.*, 2009), it can be hypothesized that the drug effect in humans is higher than in rats, given the longer time of exposure. The efficacy of MOX in the treatment of human strongyloidiasis has been recently investigated (Hofmann *et al.*, in

press 2020). A single dose of MOX led to a larvae reduction rate of 97.8 – 100% in *S. stercoralis* infected humans, higher than the reduction of the worm burden in our rat model (Hofmann *et al.*, in press 2020).

(III) Moxidectin administration independent of body weight

MOX has been approved for human onchocerciasis, administered as a single dose of 8 mg (FDA, 2018, Opoku *et al.*, 2018). In addition, a recent study proved no advantage in using doses higher than 8 mg in the treatment of *T. trichiura* infected patients (Keller *et al.*, 2019). In our experiments, we demonstrated the independence of exposure and effect in the rat model, showing that big differences in the exposure (AUC) correlate with small differences in the effect (reduction of the worm burden). This finding uncovers a great advantage over IVM, which is administered as a 200 µg/kg dose (Hürlimann *et al.*, 2019). The combination of a broad safety window (Cotreau *et al.*, 2003) and the independence of exposure and effect allows for the simplification of the treatment, making it possible to administer a unique dose to the targeted population, independent of the body weight. This observation was proved in a very recent study, which demonstrated similar cure rates between patients infected with *S. stercoralis,* who received doses from 2 to 12 mg MOX (Hofmann *et al.*, in press 2020).

As a closing note, it is important to mention that the bioavailability of MOX is highly dependent on a fatty meal (Korth-Bradley et al., 2012) and/or the vehicle used for drug administration. A phase I clinical study identified a 44% higher AUC in the fed cohort, when compared to the fasted cohort (Korth-Bradley *et al.*, 2012). In addition, in our experiments in rats, we identified a lower drug absorption when administered as a water-suspension, when compared to the absorption using corn oil as a vehicle for drug administration (FDA, 2017). Despite the wide therapeutic window explained before, it is important to consider this fast - fed state dependency and the fact that the drug needs to be well solubilized, to warrant the sufficient absorption of the drug.

(IV) The ability of moxidectin to overcome a specific resistance towards ivermectin and vice versa

The resistance profile of MOX and IVM in the treatment of nematodes infections in veterinary medicine was thoroughly reviewed by Prichard *et al*. (Prichard *et al*., 2012). Resistance is an existing risk in the treatment with both drugs (Mendes *et al*., 2017), therefore caution in the treatment and avoiding the use of sub-lethal doses is highly encouraged.

Overall, IVM seems to be more prone to resistance, with examples in cattle and horses, among others (Prichard *et al*., 2012). In veterinary medicine, both situations were observed: cross resistance in the treatment with both drugs, but also a much higher efficacy for MOX when compared to IVM (Prichard *et al*., 2012). Two mechanisms are suggested to modulate the parasite's sensitivity: on the one hand, the affinity of the drugs for the glutamate-gated-chloride channels where both ML exert their activity and are different between parasite species. On the other hand, the large and diverse number of ABC transporters present in the different nematode species, specifically the Pgp protein, which have an influence in the systemic exposure (Prichard *et al*., 2012). Overall, considering the many factors influencing the emergence of resistance to each of these drugs, it is impossible to predict the resistance profile in the treatment of human strongyloidiasis. It is therefore worth to invest efforts in the research of these two drugs that, despite the risk of resistance, are still in use and remain effective.

Drugs in development for strongyloidiasis

Two promising drugs under investigation for *Strongyloides sp.* are emodepside and tribendimidine (Mendes *et al*., 2017, Karpstein *et al*., 2019). Similar to MOX, emodepside is active against *Onchocerca volvulus*, and is used as anthelmintic in veterinary medicine (Karpstein *et al*., 2019). A recent study showed the drug to be effective against L_3 larvae and adult parasites of *S. ratti in vitro*, in a similar concentration as MOX and IVM in our study, and was active in *S. ratti* infected rats (Karpstein *et al*., 2019). In addition, the safety of emodepside has been tested on healthy volunteers in a phase I clinical trial (trials.gov, 2017), but the results have not been published yet.

Tribendimidine is also being investigated for strongyloidiasis, and is active against *S. ratti in vitro,* and *in vivo* (Keiser *et al.*, 2008a). Unfortunately, when investigated in humans, it failed to cure patients infected with *S. stercoralis*, with cure rates as low as 54% (Steinmann *et al.*, 2008, Mendes *et al.*, 2017). A possible explanation could be that the doses used to cure mice infections, 25 mg/kg (Keiser *et al.*, 2008a) were higher than the doses used in humans (5 – 10 mg/kg) (Steinmann *et al.*, 2008). Overall, the doses used in these studies were much higher than the ones used in our experiments, showing an advantage of MOX in comparison to tribendimidine in terms of dose needed.

Closing remarks on *Strongyloides stercoralis*

Overall, to combat strongyloidiasis, new diagnostic tools, as well as efficient control strategies based on robust and effective drugs are needed. To prevent the emergence of resistance, it is necessary that routine MDA campaigns for STH and LF, which include ABZ and IVM (Djune-Yemeli *et al.*, 2020), consider the usual geographical overlapping of *Strongyloides*, as the doses used of these drugs might not be enough to completely cure the *S. stercoralis* infections, therefore selecting the less sensitive parasites (Olsen *et al.*, 2009). While IVM is effective against *Strongyloides spp.*, but has limitations and could lead to severe adverse events (Prichard *et al.*, 2012), MOX is an excellent candidate for further clinical research on the treatment of *S. stercoralis,* supported by evidence showing its safe use in humans (Cotreau *et al.*, 2003, Prichard *et al.*, 2012, Barda *et al.*, 2017, Keller *et al.*, 2019, Hofmann *et al.*, in press 2020).

Oxamniquine and the derivatives

The ultimate goal of this research project was to develop an alternative to PZQ, with activity on all *Schistosoma* species and all parasite stages of development. The main limitation of oxamniquine (OXA) is the specific efficacy against adult *S. mansoni* and the lack of efficacy against juvenile stages of development (Lago *et al.*, 2017). Additionally, as a limitation within the research tools used in schistosomiasis, OXA is active *in vivo*, but shows only limited activity *in vitro* (Hess *et al.*, 2017). We hypothesized that the organometallic derivatization of OXA is a good strategy to overcome this limited activity scope, as described in the introduction. The

third objective of my thesis was to evaluate the drug-ability potential of three promising derivatives, which in early phases of research had demonstrated advantage over OXA. The derivatives were active *in vitro* against adult *S. mansoni* and *S. haematobium* and *in vivo* towards *S. mansoni* infected mice (Hess *et al*., 2017). From this previous work, open questions remained, principally on behalf of the full scope of schistosome activity, but also on the mode of action.

Aiming to identify a lead candidate for further research, we followed a rational drug discovery strategy to fully characterize these molecules (Figure 3). First experiments followed the cascade described by Lombardo & Pasche *et al*. (2019), where the candidates were successfully tested *in vitro* against NTS and adult *S. mansoni* and *S. haematobium* worms, followed by efficacy on adult *S. mansoni* infected mice (Hess *et al*., 2017). Already at this stage of research, the derivatives were more efficacious than OXA, since they were active *in vitro*. We further characterized the *in vitro* activity of all three derivatives on *S. haematobium* and *S. japonicum* adult worms, as well as on juvenile *S. mansoni,* obtaining also promising results, resulting in IC_{50} values in the range of 3 to 39 µM. Our *in vitro* results were confirmed by *in silico* simulations, which showed interaction distances between the molecules and the enzyme's active site, compatible with drug activation for both *S. mansoni* and *S. haematobium*. Limitations appeared when testing the derivatives *in vivo* against adult *S. haematobium* and juvenile *S. mansoni.* At this stage, we investigated the pH and metabolic stability, which in all derivatives resulted in degradation, highlighting a possible explanation for the lack of *in vivo* activity observed. However, also when encapsulating the derivative in a lipid nanocapsule, which should protect against these forms of degradation and provide improved delivery, the efficacy was insufficient and we decided to stop the development at this point.

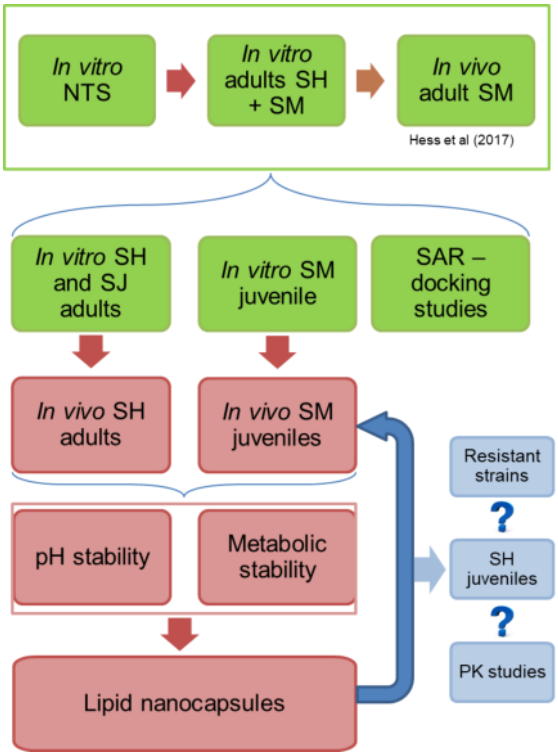

Figure 3: Drug development cascade followed for the oxamniquine derivatives characterization.

Legend: Boxes in green represent the steps of the drug development cascade where the derivatives were a hit, whereas the red boxes represent the steps where the derivatives faced a limitation. Blue boxes contain possible future steps we could have continued with, if solved the issues in the red boxes. Abbreviations: SAR: structure-activity relationship. SH: *Schistosoma haematobium,* SJ*: S. japonicum,* SM: *S. mansoni.*

This project is an example of lessons learned during drug discovery research. The first question that arises is why the OXA derivatives were active *in vivo* against an adult *S. mansoni* infection, but were not active against juveniles *in vivo*, considering the fact that the *in vitro* sensitivities are similar for both stages? A possible explanation was found during the stability assays, where we observed that all three derivatives were in a higher or lower extend, degraded to OXA + metallocene group, suggesting the fact that the *in vivo* activity is guided by the parent OXA. Additionally, a critical issue when considering the treatment of juvenile infections is the location of the worms in the body. The life cycle of *Schistosoma spp.* includes a migration phase through the lungs, where most worms are found from day 5 to 7 (Clegg, 1965) and this could affect the efficacy of drugs that are highly affected by a first pass effect. However, we performed our experiments on mice 21-day post infection, when the worms are found in the liver (Clegg, 1965, Andrews, 1981). Thus, the distribution in the body seems not to be a suitable explanation for the reduced activity on 21-day-old juvenile infections, highlighting the low pH and metabolic stability as principal limitations.

In addition, I also would like to discuss the transition from *in vitro*, to *in vivo* settings. Many drugs fail in this step, due to many reasons, and this was not the exception. At this stage of development, it is convenient to investigate the drug candidates in terms of solubility, stability and predicted permeability (Lipinski *et al.*, 1997) as early as possible, being able discard inviable molecules. Specifically the solubility is a point to make special attention since this has a great impact in the bioavailability and consequent efficacy, as previously discussed for the benzimidazoles and MOX. In this regard, *in silico* tools will be further and further implemented in drug discovery settings, as they allow, despite limitations, to predict the permeability of some drug candidates (Winiwarter *et al.*, 1998), even in the CNS (Bendels *et al.*, 2008). We used *in silico* simulations for the prediction of the activation distances within the active site of the enzyme and found a 1 to 1 correlation between the *in silico* prediction and the *in vitro* studies. The shorter simulated activation distance of the derivatives inside the active pocket correlated with the lowest IC_{50} value, both on *S. mansoni* and *S. haematobium*. This finding opens the door for discussion of future in research, where the research tools will include less animals and will be more and more replaced by *in vitro* and *in silico* strategies, as I will discuss later, in the frame of the *in vitro* growing validation.

From my point of view and experience, the decision of stopping the research on these derivatives in early phases was correct. Proceeding on these derivatives would have meant the investment of time, resources and animals, in compounds that from early phases are known not to be sufficiently soluble and stable to be considered as realistic drug candidates. However, one additional step could be worth to investigate: the specific application of the organometallic derivatives to kill mutated, OXA-resistant *S. mansoni* worms. Further research should investigate the activity of the derivatives against OXA-resistant worms, either on the worms *in vitro*, or *in silico,* given the fact that the structure of the mutated enzyme is known (Valentim *et al.*, 2013). This research would provide very important knowledge into overcoming drug resistance based on target mutation, and give an insight whether organometallic derivatization could be transferred to other organisms showing mutations in an active site.

Juvenile *S. mansoni*

There is plenty of evidence indicating the sensitivity to PZQ is reduced against juvenile infections (Sabah *et al.*, 1986, Pica-Mattoccia *et al.*, 2004, Greenberg, 2013, Despommier, 2017c). However, the *in vitro* sensitivity is under discussion, with studies showing only slight differences along the life cycle (Andrews, 1981, Xiao *et al.*, 1985, Aragon *et al.*, 2009). In contrast to PZQ, the artemisinin derivatives (artemether and artesunate) and mefloquine (MFQ) are more active against juvenile stages of development (Pérez del Villar *et al.*, 2012, Cioli *et al.*, 2014). It is important to target these juvenile infections, since they represent a reservoir that allows the life cycle in recently infected patients and the transmission chain at a community level, to continue (Colley *et al.*, 2014). In this sense, many efforts were oriented to investigate the differential drug sensitivity on *S. mansoni* along the life cycle (Greenberg, 2013), but given the difficulty to collect the worms in sufficient quantities from the mice, these stages are frequently overlooked in routine screening settings (Lombardo *et al.*, 2019). Our contribution to the research on the juvenile stages of *S. mansoni*, was to validate an *in vitro* growing method for juvenile worms, which can be applied to drug screening purposes.

Several differences with the adult worms and the NTS make the juvenile worms a very interesting stage of development to investigate, since these differences could lead to differential target expression and have an impact on drug efficacy, as is the example for PZQ and the antimalarials (Cioli *et al.*, 2014). As described in chapter five, juvenile worms are different from NTS in size and tegument morphology, movement, presence of digestive organs, including oral and ventral suckers and ceca development. From day 13 onwards, we were able to differentiate between male and female by visual assessment. Compared to adults, juvenile worms are smaller, are not sexually mature, and do not mate nor lay eggs. In addition, the nutritional requirement are different between NTS, juveniles and adults, judged by the different media that provide the highest viability, being respectively, M199, hybridoma medium and RPMI (chapter five, (Lombardo *et al.*, 2019)). Our objective was to investigate if the worms grown *in vitro* can replace the experiments on worms collected from mice, for drug sensitivity assays.

The reduced susceptibility to PZQ could be linked in the first days after infection (Xiao *et al.*, 1985) to the organ distribution of the worms, which in the first 5 - 7 days post infection are found in the lungs (Clegg, 1965). Given the fast and extensive metabolism of PZQ (Dayan, 2003, Kovač *et al.*, 2017) and the fact that the worms are harbored in the lungs, these worms could be less exposed to the drug, and so explain the reduced cure rate at this time (Xiao *et al.*, 1985, Sabah *et al.*, 1986). In this sense, the *in vitro* screening assays (independent of the method used to grow the worms) are limited when compared to the *in vivo* models. However, it would be unethical and too expensive to screen early drug candidates on infected animals (Fenwick *et al.*, 2009) and therefore *in vitro* assays remain a good alternative.

In addition to the distribution throughout the body, an enhanced expression of export proteins could explain the reduced sensitivity of juvenile worms exposed to PZQ. At least two proteins from the ABC superfamily, namely SmMRP1 and SmMDR2 (the homolog of human Pgp protein) show increased expression in the juvenile stages of development and adult worms with reduced PZQ sensitivity (Kasinathan *et al.*, 2010). There are arguments to suggest that this higher expression could lead to the increased export of PZQ from the parasite and so reduce the drug's effect (Messerli *et al.*, 2009, Kasinathan *et al.*, 2010, Kasinathan *et al.*, 2014). Based on this hypothesis, we investigated whether the activity of PZQ can be enhanced on our juvenile worms grown *in vitro* if combined with different molecules known to interact with the Pgp protein. We tested the lethal concentration 50% (LC_{50}) of PZQ combined with IVM, omeprazole, elacridar and digoxin, used in sub-lethal concentrations (unpublished research). The worms seemed to be more affected as by PZQ alone, but not in a significant magnitude (Figure 4). These findings suggest that a combination of a single Pgp inhibitor with PZQ is not a good strategy to fight these stages, possibly due to the existence of alternative transporters or limited transporters inhibition, which allow for parasite survival. To observe a significant increase in sensitivity to PZQ, mediated by Pgp inhibition, a cocktail of inhibitors could be administered to fully inhibit the export mechanisms of *S. mansoni* (Kasinathan *et al.*, 2014), but this is not feasible on *in vivo* or clinical settings because of the complex DDI that should be considered.

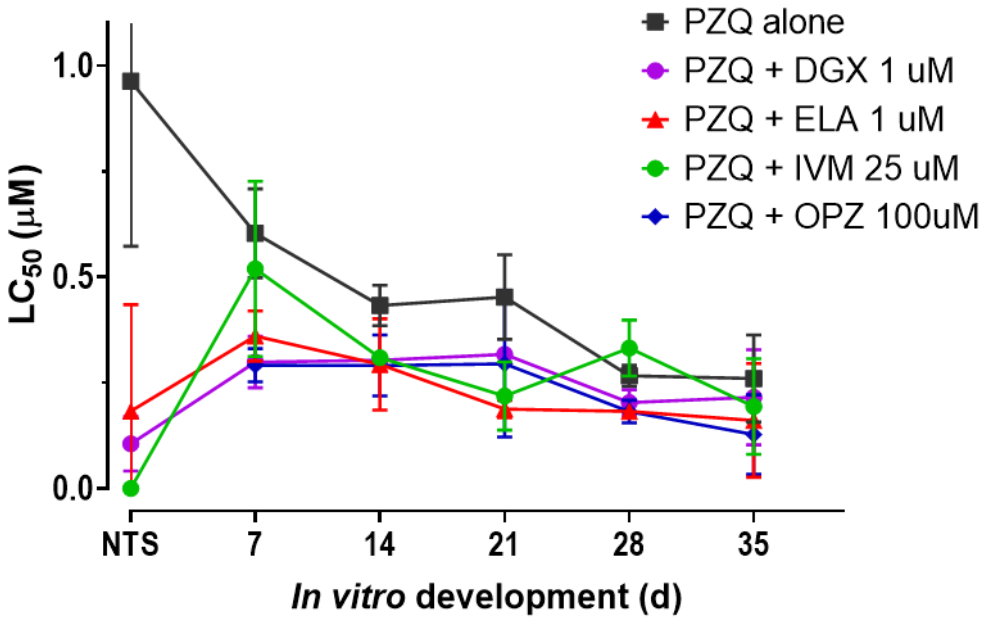

Figure 4: Comparison of the sensitivity of *in vitro* developed juvenile worms exposed to praziquantel alone and in combination with molecules interacting with the Pgp protein.

Note: Due to differential viability in different media, the NTS assay was performed in medium M199 while the additional time points were performed on hybridoma medium. Abbreviations: d: days, digoxin (DGX), elacridar (ELA), ivermectin (IVM), omeprazole (OPZ), praziquantel (PZQ), LC50: lethal dose 50%.

As part of the validation of the *in vitro* growing method for juvenile *S. mansoni*, we included OXA as a test drug for the characterization of the worm's drug susceptibility. This drug was a negative control, since the same profile as PZQ is observed for OXA, where the drug is only slightly active against juvenile *S. mansoni* infections (Sabah *et al.*, 1986, Cioli *et al.*, 2014). Additionally, OXA is only active *in vivo,* while it shows limited activity *in vitro* (Hess *et al.*, 2017). In our experiments, we also found low activity of the drug on juvenile worms, both grown *in vitro* and perfused from infected mice. Today, no evidence exists that supports a differential expression of the activating enzyme of OXA (SmSULT) (Pica-Mattoccia *et al.*, 2006) along the life cycle. Therefore, the stage specificity of OXA remains an open question. However, it has been suggested that the drug requires a contribution from the immune system of the host to exert its full activity (Doenhoff, 1989, Reimers *et al.*, 2015) and this could explain the lack of *in vitro* efficacy of OXA (Hess *et al.*, 2017). In more detail, the exposure to OXA would promote the presentation of the surface antigens SmCD59a and SmKK7, making them accessible to

antibody recognition and enhancing the intrinsic activity of the drug *in vivo* (Reimers *et al.*, 2015). Despite happening in a smaller scale, the antigen exposure in presence of a drug was also observed for PZQ and artemether (Reimers *et al.*, 2015).

On the juvenile worms we also tested the activity of mefloquine. After drug exposure, as expected (Manneck *et al.*, 2011, Cioli *et al.*, 2014), mefloquine was active on both the worms developed *in vivo*, as on the worms developed *in vitro*. However, the worms developed *in vivo* were slightly more sensitive. On *Plasmodium spp.*, mefloquine is suggested to act via the inhibition of hemoglobin detoxification mechanisms that cause an accumulation of toxic hem inside the parasite, leading to its death (Zhang *et al.*, 1999). The same detoxification products were also observed in schistosomes, suggesting a similar detoxification mechanism (Oliveira *et al.*, 2000). Additionally, interference in the glycolysis process has been suggested as alternative or additional mechanism of action of mefloquine on schistosomes (Manneck *et al.*, 2012). As shown in the supplemental information of the paper in chapter five, the worms collected *in vivo* still contain residual amounts of red blood cells in the gut, while the *in vitro* developed worms don't, because of the absence of these cells in the medium. As a result, the *in vivo* developed worms might have been affected by both mechanisms of action proposed for mefloquine, while the *in vitro* grown only by the inhibition of the glycolysis process. This difference in the toxic mechanisms of mefloquine affecting the worms obtained by the different techniques might explain the slightly different sensitivity of worms obtained by either growing strategy.

Remarks on study strategies

On different stages of drug development, *in silico, in vitro,* and *in vivo* approaches can be applied for different purposes (Figure 5). Each tool accounts on strengths and weaknesses, and this defines its applicability to each phase of discovery or development of new chemical entities.

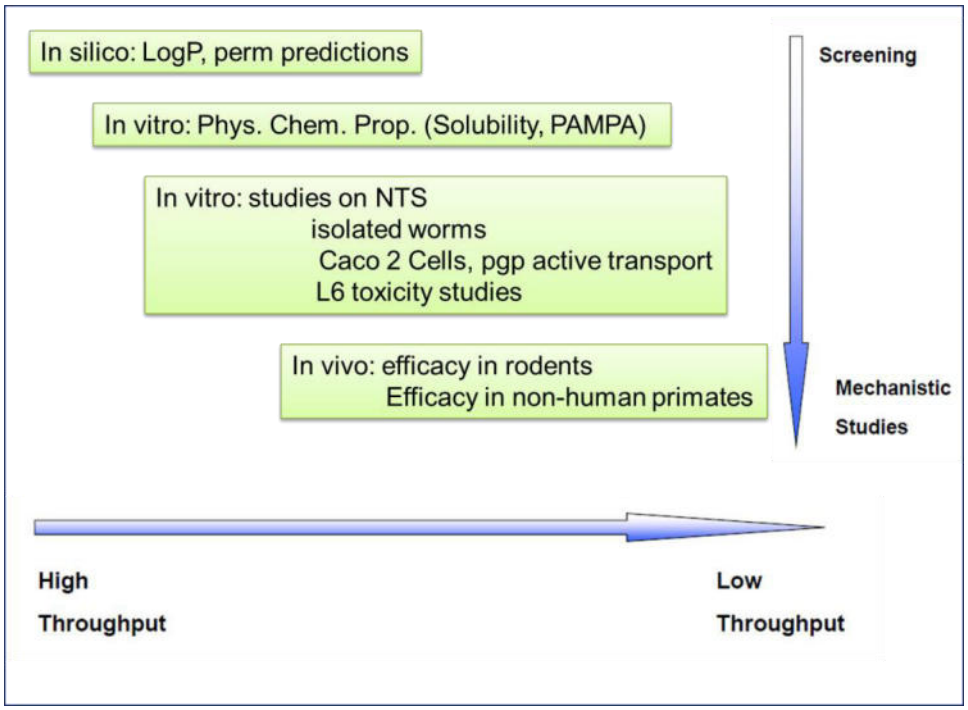

Figure 5: Schematic representation of the main tools used in drug discovery and development and its applicability from screening to mechanistic studies. Abbreviations: PAMPA: Parallel artificial membrane permeability assay. Adapted from: "Drug delivery and targeting" lecture, Unibasel, J. Hüwyler, 2019.

In silico prediction can be applied as a first high throughput tool, to screen large libraries of molecules (Singh *et al.*, 2020). This approach allows researchers to estimate the polarity, lipophilicity, and molecular weight of new molecules (Schwab, 2010) and make a first selection for further experiments, based on predicted permeability (Lipinski *et al.*, 1997) and basic ADME/toxicity properties (Sacan *et al.*, 2012). These tools are also useful to predict these physicochemical properties on a new derivate of a known drug (Schwab, 2010, Sacan *et al.*, 2012), while the most modern software providers even allow for target interaction predictions (Singh *et al.*, 2020), as was done in our OXA derivatives project (chapter four). We successfully applied different software tools to investigate the interaction distances and free binding energies of the OXA derivatives with the active site of the sulfotransferase of *S. mansoni* and *S. haematobium.* The predictions made *in silico* correlated very well with the activity observed in the *in vitro* studies on adult worms. However, as limitation of the *in silico* tools, it is necessary to mention that many parameters still need to be considered in a model before reaching a concrete conclusion (Sacan *et al.*, 2012) and the predicted properties still need to be validated

experimentally (Singh *et al.*, 2020). Parameters that are still not considered in the simulations are active transport mechanisms that affect drug absorption, the drug excipients used to modulate the solubility, protein binding properties, chemical and metabolic stability, diet interference, etc. (Singh *et al.*, 2020), that still have to be determined experimentally, as done in our study (Chapter four).

Contributions to reduce the use of animals in science

The reduction of the number of animals over the last years in Switzerland despite the great increase in research articles published highlights a transition on the research strategies (Figure 6). Animal experimentation is being reduced, refined and replaced (Fenwick *et al.*, 2009, SAP, 2017) by alternative methods, as *in silico* and *in vitro* experimentation, which become more and more sophisticated, reliable (Xie *et al.*, 2016) and accessible to non-informatics users (Singh *et al.*, 2020). However, animal experimentation remains the gold standard compared to *in vitro* studies and a requirement in drug development as prior step to clinical trials. Applied to the drug development for helminth infections, animals are still needed to keep the full life cycle of the parasites, which still today could not be fully kept in the lab (Frahm *et al.*, 2019, Lombardo *et al.*, 2019). In line with this trend, in chapter five, I described the assay conditions that allow to screen high number of compounds on juvenile worms in an animal-free setting and describe as well the limitations of this approach, compared to the *in vivo* development.

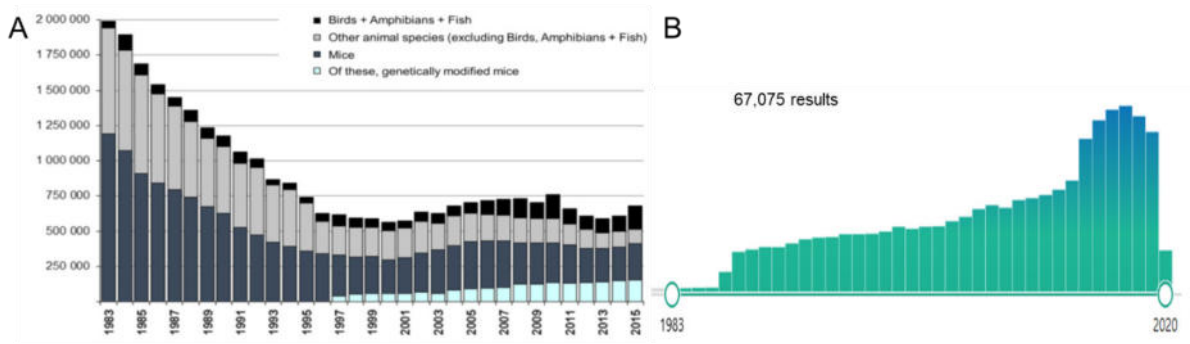

Figure 6: A: Number of animals used in Switzerland for research purposes from 1983 to 2015 (SAP, 2017). B: number of research articles including animals where Switzerland is given as affiliation from 1983 to 2020 (Source: Pubmed, 23.10.2020). This figure serves to show that the number of animals used in science was constant despite the higher number of publications in the last years. Consider also that the animals used by industry in drug discovery and development do not impact on the number of publications.

Note: the Y axis is not the same for both panels. The search terms were: "(Switzerland[Affiliation]) AND (animal[Filter])" in PubMed on the 23.10.2020.

Disease eradication: a realistic goal if tackled from multiple approaches

Success stories of different countries as Japan and China reflect the benefit of integrated and time sustained efforts towards the control of schistosomiasis (Bergquist *et al.*, 2017). In addition, some authors suggest that schistosomiasis eradication is not realistic if based only on PZQ treatment and water-based interventions are not considered (Secor, 2014). In this regard, WHO published the strategy 2015 – 2020 "Water, Sanitation and Hygiene for accelerating and sustaining progress on Neglected Tropical Diseases", to respond to the growing support for intersectoral approaches and the need for guidance towards reaching the NTD roadmap milestones (WHO, 2015). Given the overlapping distribution of the NTDs, efforts are oriented to integrate the control programs (schistosomiasis, onchocerciasis, LF, STH), being currently implemented in many countries and principally oriented to drug co-administrations (Olsen, 2007, Olsen *et al.*, 2009). Drug therapy remains the major aspect of helminth infection control (WHO, 2020a, b) and drugs need to remain effective, while efforts should be made to improve treatment and to develop new drugs prior to the appearance of resistance. In addition, health education, usually included in the WASH strategy, is an additional pillar that should not be underestimated when considering NTD control strategies, since it allows for long-term behavioral changes (Secor, 2014).

Conclusion

The main objective of this thesis was to investigate on improved drug alternatives for the treatment of STHs, strongyloidiasis and schistosomiasis. In addition, I validated the application of a method to provide high number of juvenile *S. mansoni* worms, suitable for drug screening assays.

Moxidectin is a drug with a very promising activity profile on *S. ratti* and has the potential to be considered as an alternative to IVM, therefore clinical investigations should continue.

The development of juvenile *S. mansoni* in a full *in vitro* setting allows for the collection of a high number of worms in a very simple and ethical manner to be used for screening assays. Given some limitations on the *in vitro* setting, and slight differences in drug sensitivity, the *in vivo* studies remain the first line tool for further characterization steps.

The improved solubility of the formulations of ABZ and MBZ enhanced the activity of the respective drugs in the treatment of mice infected with adult *H. polygyrus*. Further research should investigate if this improved solubility leads to an enhanced systemic exposure and evaluate if this has an impact on the larval stages. Studies on *T. muris*, as a model organism of *T. trichiura* would show if our findings can also increase the efficacy on this species. In addition, bioequivalence studies on these formulations could evaluate if the inclusion of these formulations into clinical trials would improve the systemic exposure and lead to an enhanced effect in humans infected with STH.

On behalf of the OXA derivatives, further research could investigate the interaction between the derivatives and the *S. mansoni* mutated enzyme and build knowledge on its applicability to overcome resistance, to further extrapolate this strategy to other pathogens with similar drug-target interactions.

References

Abulaihaiti, M., Wu, X.-W., Qiao, L., Lv, H.-L., Zhang, H.-W., Aduwayi, N.*, et al.* 2015. Efficacy of albendazole-chitosan microsphere-based treatment for alveolar echinococcosis in mice. PLOS Neglected Tropical Diseases, 9.

Al-Azzam, S. I., Fleckenstein, L., Cheng, K.-J., Dzimianski, M. T. and McCall, J. W. 2007. Comparison of the pharmacokinetics of moxidectin and ivermectin after oral administration to beagle dogs. Biopharmaceutics & Drug Disposition, 28**,** 431-438.

Alvarez, L. I., Mottier, M. L. and Lanusse, C. E. 2007. Drug transfer into target helminth parasites. Trends in Parasitology, 23**,** 97-104.

Amidon, G. L., Lennernäs, H., Shah, V. P. and Crison, J. R. 1995. A theoretical basis for a biopharmaceutic drug classification: the correlation of *in vitro* drug product dissolution and *in vivo* bioavailability. Pharmaceutical Research, 12**,** 413-420.

Andrews, P. 1981. A summary of the efficacy of praziquantel against schistosomes in animal experiments and notes on its mode of action. Arzneimittelforschung, 31**,** 538-41.

Aragon, A. D., Imani, R. A., Blackburn, V. R., Cupit, P. M., Melman, S. D., Goronga, T.*, et al.* 2009. Towards an understanding of the mechanism of action of praziquantel. Molecular and biochemical parasitology, 164**,** 57-65.

Barda, B., Sayasone, S., Phongluxa, K., Xayavong, S., Keoduangsy, K., Odermatt, P.*, et al.* 2017. Efficacy of moxidectin versus ivermectin against *Strongyloides stercoralis* infections: a randomized, controlled noninferiority trial. Clinical Infectious Diseases, 65**,** 276-281.

Bendels, S., Kansy, M., Wagner, B. and Huwyler, J. 2008. *In silico* prediction of brain and CSF permeation of small molecules using PLS regression models. European Journal of Medicinal Chemistry, 43**,** 1581-92.

Bergquist, R., Zhou, X.-N., Rollinson, D., Reinhard-Rupp, J. and Klohe, K. 2017. Elimination of schistosomiasis: the tools required. Infectious diseases of poverty, 6**,** 158-158.

Carrier, R. L., Miller, L. A. and Ahmed, I. 2007. The utility of cyclodextrins for enhancing oral bioavailability. Journal of Controlled Release, 123**,** 78-99.

Cioli, D., Pica-Mattoccia, L., Basso, A. and Guidi, A. 2014. Schistosomiasis control: praziquantel forever? Molecular and Biochemical Parasitology, 195**,** 23-29.

Clegg, J. A. 1965. *In vitro* cultivation of *Schistosoma mansoni*. Experimental Parasitology, 16**,** 133-147.

Cobb, R. and Boeckh, A. 2009. Moxidectin: a review of chemistry, pharmacokinetics and use in horses. Parasites & Vectors, 2**,** S5.

Colley, D. G., Bustinduy, A. L., Secor, W. E. and King, C. H. 2014. Human schistosomiasis. Lancet (London, England), 383**,** 2253-2264.

Cotreau, M. M., Warren, S., Ryan, J. L., Fleckenstein, L., Vanapalli, S. R., Brown, K. R.*, et al.* 2003. The antiparasitic moxidectin: safety, tolerability, and pharmacokinetics in humans. Journal of Clinical Pharmacology, 43**,** 1108-15.

Cowan, N., Meier, C., Neodo, A. and Keiser, J. 2017. Exposure of *Heligmosomoides polygyrus* and *Trichuris muris* to albendazole, albendazole sulfoxide, mebendazole and oxantel pamoate *in vitro* and *in vivo* to elucidate the pathway of drug entry into these gastrointestinal nematodes. International Journal for Parasitology: Drugs and Drug Resistance, 7**,** 159-173.

Dayan, A. D. 2003. Albendazole, mebendazole and praziquantel. Review of non-clinical toxicity and pharmacokinetics. Acta Tropica, 86**,** 141-159.

Despommier, D., Griffin, D, Gwadz, R, Hotez, P, Knirsch, C. 2017a. Chapter 17: *Trichuris trichiura* Parasitic Diseases Sixth Edition. New York, US: Parasites Without Borders**,** p: 209 -216.

Despommier, D., Griffin, D, Gwadz, R, Hotez, P, Knirsch, C. 2017b. Chapter 19: The Hookworms. Parasitic Diseases Sixth Edition. Sixth ed. New York, US: Parasites Without Borders**,** p: 227 -240.

Despommier, D., Griffin, D, Gwadz, R, Hotez, P, Knirsch, C. 2017c. Chapter 33: The Schistosomes. Parasitic Diseases Sixth Edition. 6 ed. New York, US: Parasites Without Borders**,** p: 391 - 418.

Despommier, D., Griffin, D, Gwadz, R, Hotez, P, Knirsch, C. 2017d. Parasitic Diseases Sixth Edition, New York, US, Parasites Without Borders.
Djune-Yemeli, L., Nana-Djeunga, H. C., Lenou-Nanga, C. G., Donfo-Azafack, C., Domche, A., Fossuo-Thotchum, F.*, et al.* 2020. Serious limitations of the current strategy to control Soil Transmitted Helminths and added value of ivermectin/Albendazole mass administration: A population-based observational study in Cameroon. PLoS Negl Trop Dis, 14**,** e0008794.
Doenhoff, M. J. 1989. The immune-dependence of chemotherapy in experimental schistosomiasis. Memórias do Instituto Oswaldo Cruz, 84 Suppl 1**,** 31-7.
Ehteda, A., Galettis, P., Chu, S. W. L., Pillai, K. and Morris, D. L. 2012. Complexation of albendazole with hydroxypropyl-β-cyclodextrin significantly improves its pharmacokinetic profile, cell cytotoxicity and antitumor efficacy in nude mice. Anticancer Research, 32**,** 3659-3666.
FDA. 2017. Non-clinical reviews on Moxidectin [Online]. Available: https://www.accessdata.fda.gov/drugsatfda_docs/nda/2018/210867Orig1s000PharmR.pdf [Accessed 21.08.2020].
FDA. 2018. Moxidectin prescribing information [Online]. Available: https://www.accessdata.fda.gov/drugsatfda_docs/label/2018/210867lbl.pdf [Accessed 24.08.2020].
Fenwick, N., Griffin, G. and Gauthier, C. 2009. The welfare of animals used in science: how the "Three Rs" ethic guides improvements. The Canadian veterinary journal, 50**,** 523-530.
Frahm, S., Anisuzzaman, A., Prodjinotho, U. F., Vejzagić, N., Verschoor, A. and Costa, C. P. d. 2019. A novel cell-free method to culture *Schistosoma mansoni* from cercariae to juvenile worm stages for *in vitro* drug testing. PLOS Neglected Tropical Diseases, 13**,** e0006590.
García, A., Barrera, M. G., Piccirilli, G., Vasconi, M. D., Di Masso, R. J., Leonardi, D.*, et al.* 2013. Novel albendazole formulations given during the intestinal phase of *Trichinella spiralis* infection reduce effectively parasitic muscle burden in mice. Parasitology International, 62**,** 568-570.
García, A., Leonardi, D., Salazar, M. O. and Lamas, M. C. 2014. Modified β-cyclodextrin inclusion complex to improve the physicochemical properties of albendazole. Complete *in vitro* evaluation and characterization. PLOS ONE, 9.
Greenberg, R. M. 2013. New approaches for understanding mechanisms of drug resistance in schistosomes. Parasitology, 140**,** 1534-1546.
Hajaji, S., Jabri, M.-A., Alimi, D., Rekik, M. and Akkari, H. 2019. Chamomile methanolic extract mitigates small bowel inflammation and ROS overload related to the intestinal nematodes infection in mice. Acta Parasitologica, 64**,** 152-161.
Hess, J., Panic, G., Patra, M., Mastrobuoni, L., Spingler, B., Roy, S.*, et al.* 2017. Ferrocenyl, ruthenocenyl, and benzyl oxamniquine derivatives with cross-species activity against *Schistosoma mansoni* and *Schistosoma haematobium*. ACS infectious diseases, 3**,** 645-652.
Hofmann, D., Sayasone, S., Sengngam, K., Chongvilay, B., Hattendorf, J. and Keiser, J. in press 2020. Efficacy and safety of ascending dosages of moxidectin against *Strongyloides stercoralis* infections in adults: a randomized, blinded, placebo-controlled, dose-ranging, phase 2a trial. Accepted: The Lancet Infectious Diseases.
Hürlimann, E. and Keiser, J. 2019. A single dose of ivermectin is sufficient for strongyloidiasis. Lancet Infectious Diseases, 19**,** 1150-1151.
Huynh, N. T., Passirani, C., Saulnier, P. and Benoit, J. P. 2009. Lipid nanocapsules: a new platform for nanomedicine. International Journal of Pharmaceutics, 379**,** 201-9.
Janko, C. and Geyer, J. 2013. Moxidectin has a lower neurotoxic potential but comparable brain penetration in P-glycoprotein-deficient CF-1 mice compared to ivermectin. Journal of Veterinary Pharmacology and Therapeutics, 36**,** 275-84.
Jourdan, P. M., Lamberton, P. H. L., Fenwick, A. and Addiss, D. G. 2018. Soil-transmitted helminth infections. Lancet, 391**,** 252-265.

Jung, H., Medina, L., García, L., Fuentes, I. and Moreno-Esparza, R. 1997. Biopharmaceutics: absorption studies of albendazole and some physicochemical properties of the drug and its metabolite albendazole sulphoxide. Journal of Pharmacy and Pharmacology, 50**,** 43-48.

Kang, B.-S., Lee, S.-E., Ng, C. L., Kim, J.-K. and Park, J.-S. 2015. Exploring the preparation of albendazole-loaded chitosan-tripolyphosphate nanoparticles. Materials, 8**,** 486-498.

Karpstein, T., Pasche, V., Häberli, C., Scandale, I., Neodo, A. and Keiser, J. 2019. Evaluation of emodepside in laboratory models of human intestinal nematode and schistosome infections. Parasites & Vectors, 12**,** 226-226.

Kasinathan, R. S., Morgan, W. M. and Greenberg, R. M. 2010. *Schistosoma mansoni* express higher levels of multidrug resistance-associated protein 1 (SmMRP1) in juvenile worms and in response to praziquantel. Molecular and Biochemical Parasitology, 173**,** 25-31.

Kasinathan, R. S., Sharma, L. K., Cunningham, C., Webb, T. R. and Greenberg, R. M. 2014. Inhibition or knockdown of ABC transporters enhances susceptibility of adult and juvenile schistosomes to praziquantel. PLOS Neglected Tropical Diseases, 8.

Keiser, J., Thiemann, K., Endriss, Y. and Utzinger, J. 2008a. *Strongyloides ratti*: *in vitro* and *in vivo* activity of tribendimidine. PLOS Neglected Tropical Diseases, 2**,** e136.

Keiser, J. and Utzinger, J. 2008b. Efficacy of current drugs against soil-transmitted helminth infections: systematic review and meta-analysis. JAMA, 299**,** 1937-1948.

Keiser, J. and Utzinger, J. 2010. Chapter 8 - The drugs we have and the drugs we need against major helminth infections. *In:* Zhou, X.-N., Bergquist, R., Olveda, R. & Utzinger, J. (eds.) Advances in Parasitology. Academic Press**,** p: 197-230.

Keller, L., Palmeirim, M. S., Ame, S. M., Ali, S. M., Puchkov, M., Huwyler, J.*, et al.* 2019. Efficacy and safety of ascending dosages of moxidectin and moxidectin-albendazole against *Trichuris trichiura* in adolescents: a randomized controlled trial. Clinical Infectious Diseases.

Kiki-Mvouaka, S., Menez, C., Borin, C., Lyazrhi, F., Foucaud-Vignault, M., Dupuy, J.*, et al.* 2010. Role of P-glycoprotein in the disposition of macrocyclic lactones: a comparison between ivermectin, eprinomectin, and moxidectin in mice. Drug Metabolism and Disposition, 38**,** 573-80.

Korth-Bradley, J. M., Parks, V., Chalon, S., Gourley, I., Matschke, K., Cailleux, K.*, et al.* 2012. The effect of a high-fat breakfast on the pharmacokinetics of moxidectin in healthy male subjects: a randomized phase I trial. The American Journal of Tropical Medicine and Hygiene, 86**,** 122-125.

Kovač, J., Vargas, M. and Keiser, J. 2017. *In vitro* and *in vivo* activity of R- and S- praziquantel enantiomers and the main human metabolite trans-4-hydroxy-praziquantel against *Schistosoma haematobium*. Parasites & Vectors, 10.

Lago, E. M., Xavier, R. P., Teixeira, T. R., Silva, L. M., da Silva Filho, A. A. and de Moraes, J. 2017. Antischistosomal agents: state of art and perspectives. Future Medicinal Chemistry, 10**,** 89-120.

Levison, M. E. and Levison, J. H. 2009. Pharmacokinetics and pharmacodynamics of antibacterial agents. Infectious Disease Clinics of North America, 23**,** 791-vii.

Lipinski, C. A., Lombardo, F., Dominy, B. W. and Feeney, P. J. 1997. Experimental and computational approaches to estimate solubility and permeability in drug discovery and development settings. Advanced Drug Delivery Reviews, 23**,** 3-25.

Lo, N. C., Bogoch, II, Blackburn, B. G., Raso, G., N'Goran, E. K., Coulibaly, J. T.*, et al.* 2015. Comparison of community-wide, integrated mass drug administration strategies for schistosomiasis and soil-transmitted helminthiasis: a cost-effectiveness modelling study. Lancet Global Health, 3**,** e629-38.

Lombardo, F. C., Pasche, V., Panic, G., Endriss, Y. and Keiser, J. 2019. Life cycle maintenance and drug-sensitivity assays for early drug discovery in *Schistosoma mansoni*. Nature Protocols**,** 1.

Loukas, A., Hotez, P. J., Diemert, D., Yazdanbakhsh, M., McCarthy, J. S., Correa-Oliveira, R.*, et al.* 2016. Hookworm infection. Nature Reviews Disease Primers, 2**,** 16088.

Manneck, T., Braissant, O., Ellis, W. and Keiser, J. 2011. *Schistosoma mansoni*: antischistosomal activity of the four optical isomers and the two racemates of

mefloquine on schistosomula and adult worms *in vitro* and *in vivo*. Experimental Parasitology, 127**,** 260-269.
Manneck, T., Keiser, J. and Müller, J. 2012. Mefloquine interferes with glycolysis in schistosomula of *Schistosoma mansoni* via inhibition of enolase. Parasitology, 139**,** 497-505.
Mendes, T., Minori, K., Ueta, M., Miguel, D. C. and Allegretti, S. M. 2017. Strongyloidiasis current status with emphasis in diagnosis and drug research. Journal of Parasitology Research, 2017**,** 5056314.
Ménez, C., Sutra, J.-F., Prichard, R. and Lespine, A. 2012. Relative neurotoxicity of ivermectin and moxidectin in Mdr1ab (−/−) mice and effect on mammalian GABA(A) channel activity. PLOS Neglected Tropical Diseases, 6**,** e1883.
Messerli, S. M., Kasinathan, R. S., Morgan, W., Spranger, S. and Greenberg, R. M. 2009. *Schistosoma mansoni* P-glycoprotein levels increase in response to praziquantel exposure and correlate with reduced praziquantel susceptibility. Molecular & Biochemical Parasitology, 167**,** 54-9.
Molento, M. B., Lifschitz, A., Sallovitz, J., Lanusse, C. and Prichard, R. 2004. Influence of verapamil on the pharmacokinetics of the antiparasitic drugs ivermectin and moxidectin in sheep. Parasitology Research, 92**,** 121-127.
Moser, W., Schindler, C. and Keiser, J. 2017. Efficacy of recommended drugs against soil transmitted helminths: systematic review and network meta-analysis. BMJ**,** j4307.
Mottier, L., Alvarez, L., Ceballos, L. and Lanusse, C. 2006. Drug transport mechanisms in helminth parasites: passive diffusion of benzimidazole anthelmintics. Experimental Parasitology, 113**,** 49-57.
Oliveira, M. F., d'Avila, J. C., Torres, C. R., Oliveira, P. L., Tempone, A. J., Rumjanek, F. D.*, et al.* 2000. Haemozoin in *Schistosoma mansoni*. Molecular Biochemistry and Parasitology, 111**,** 217-21.
Olsen, A. 2007. Efficacy and safety of drug combinations in the treatment of schistosomiasis, soil-transmitted helminthiasis, lymphatic filariasis and onchocerciasis. Transactions of The Royal Society of Tropical Medicine and Hygiene, 101**,** 747-758.
Olsen, A., van Lieshout, L., Marti, H., Polderman, T., Polman, K., Steinmann, P.*, et al.* 2009. Strongyloidiasis – the most neglected of the neglected tropical diseases? Transactions of The Royal Society of Tropical Medicine and Hygiene, 103**,** 967-972.
Opoku, N. O., Bakajika, D. K., Kanza, E. M., Howard, H., Mambandu, G. L., Nyathirombo, A.*, et al.* 2018. Single dose moxidectin versus ivermectin for *Onchocerca volvulus* infection in Ghana, Liberia, and the Democratic Republic of the Congo: a randomised, controlled, double-blind phase 3 trial. The Lancet, 392**,** 1207-1216.
Pacheco, P. A., Rodrigues, L. N. C., Ferreira, J. F. S., Gomes, A. C. P., Veríssimo, C. J., Louvandini, H.*, et al.* 2018. Inclusion complex and nanoclusters of cyclodextrin to increase the solubility and efficacy of albendazole. Parasitology Research, 117**,** 705-712.
Panic, G. and Keiser, J. 2018. Acting beyond 2020: better characterization of praziquantel and promising antischistosomal leads. Current Opinion in Pharmacology, 42**,** 27-33.
Paredes, A. J., Bruni, S. S., Allemandi, D., Lanusse, C. and Palma, S. D. 2018. Albendazole nanocrystals with improved pharmacokinetic performance in mice. Therapeutic Delivery, 9**,** 89-97.
Pérez del Villar, L., Burguillo, F. J., López-Abán, J. and Muro, A. 2012. Systematic review and meta-analysis of artemisinin based therapies for the treatment and prevention of schistosomiasis. PLOS ONE, 7**,** e45867.
Perez, R., Cabezas, I., Sutra, J. F., Galtier, P. and Alvinerie, M. 2001. Faecal excretion profile of moxidectin and ivermectin after oral administration in horses. The Veterinary Journal, 161**,** 85-92.
Pica-Mattoccia, L., Carlini, D., Guidi, A., Cimica, V., Vigorosi, F. and Cioli, D. 2006. The schistosome enzyme that activates oxamniquine has the characteristics of a sulfotransferase. Memórias do Instituto Oswaldo Cruz, 101**,** 307-312.

Pica-Mattoccia, L. and Cioli, D. 2004. Sex- and stage-related sensitivity of *Schistosoma mansoni* to *in vivo* and *in vitro* praziquantel treatment. International Journal of Parasitology, 34**,** 527-33.
Pica-Mattoccia, L., Novi, A. and Cioli, D. 1997. Enzymatic basis for the lack of oxamniquine activity in *Schistosoma haematobium* infections. Parasitology Research, 83**,** 687-689.
Prichard, R., Ménez, C. and Lespine, A. 2012. Moxidectin and the avermectins: consanguinity but not identity. International journal for parasitology: Drugs and drug resistance, 2**,** 134-153.
Ravichandran, R. 2010. *In vivo* pharmacokinetic studies of albendazole nanoparticulate oral formulations for improved bioavailability. International Journal of Green Nanotechnology: Biomedicine, 2**,** B46-B53.
Reimers, N., Homann, A., Höschler, B., Langhans, K., Wilson, R. A., Pierrot, C.*, et al.* 2015. Drug-induced exposure of *Schistosoma mansoni* antigens SmCD59a and SmKK7. PLOS Neglected Tropical Diseases, 9**,** e0003593.
Rigter, I. M., Schipper, H. G., Koopmans, R. P., Kan, H. J. M. v., Frijlink, H. W., Kager, P. A.*, et al.* 2004. Relative bioavailability of three newly developed albendazole formulations: a randomized crossover study with healthy volunteers. Antimicrobial Agents and Chemotherapy, 48**,** 1051-1054.
Sabah, A. A., Fletcher, C., Webbe, G. and Doenhoff, M. J. 1986. *Schistosoma mansoni*: chemotherapy of infections of different ages. Experimental Parasitology, 61**,** 294-303.
Sacan, A., Ekins, S. and Kortagere, S. 2012. Applications and limitations of *in silico* models in drug discovery. *In:* Larson, R. S. (ed.) Bioinformatics and Drug Discovery. Totowa, NJ: Humana Press**,** p: 87-124.
SAP, S. a. p. The quality and validity of animal experiments *In:* J. Fitzi Ratghen, H. H., ed. 10th conference on animal testing, 2017 Olten. Altex Proceedings, 18.
Schwab, C. H. 2010. Conformations and 3D pharmacophore searching. Drug Discovery Today: Technologies, 7**,** e245-e253.
Secor, E. W. 2014. Water-based interventions for schistosomiasis control. Pathogens and Global Health, 108**,** 246-254.
Shoop, W. L., Mrozik, H. and Fisher, M. H. 1995. Structure and activity of avermectins and milbemycins in animal health. Veterinary Parasitology, 59**,** 139-56.
Singh, N., Chaput, L. and Villoutreix, B. O. 2020. Virtual screening web servers: designing chemical probes and drug candidates in the cyberspace. Briefings in Bioinformatics.
Steinmann, P., Zhou, X.-N., Du, Z.-W., Jiang, J.-Y., Xiao, S.-H., Wu, Z.-X.*, et al.* 2008. Tribendimidine and albendazole for treating soil-transmitted helminths, *Strongyloides stercoralis* and *Taenia spp.*: open-label randomized trial. PLOS Neglected Tropical Diseases, 2**,** e322-e322.
Stothard, J. R., Sousa-Figueiredo, J. C., Betson, M., Bustinduy, A. and Reinhard-Rupp, J. 2013. Schistosomiasis in african infants and preschool children: let them now be treated! Trends in Parasitology, 29**,** 197-205.
Tilney, L. G., Connelly, P. S., Guild, G. M., Vranich, K. A. and Artis, D. 2005. Adaptation of a nematode parasite to living within the mammalian epithelium. Journal of Experimental Zoology, 303A**,** 927-945.
trials.gov, N.-c. 2017. First in man clinical trial of emodepside (BAY 44-4400) [Online]. Available: https://clinicaltrials.gov/ct2/show/study/NCT02661178?cond=emodepside&draw=2&rank=1 [Accessed 07.10.2020 2020].
Tritten, L., Silbereisen, A. and Keiser, J. 2011. *In vitro* and *in vivo* efficacy of monepantel (AAD 1566) against laboratory models of human intestinal nematode infections. PLOS Neglected Tropical Diseases, 5**,** e1457-e1457.
Valentim, C. L. L., Cioli, D., Chevalier, F. D., Cao, X., Taylor, A. B., Holloway, S. P.*, et al.* 2013. Genetic and molecular basis of drug resistance and species-specific drug action in schistosome parasites. Science (New York, N.Y.), 342**,** 1385-1389.
White, N. J. 2013. Pharmacokinetic and pharmacodynamic considerations in antimalarial dose optimization. Antimicrobial Agents and Chemotherapy, 57**,** 5792.

WHO 2006. Preventive chemotherapy in human helminthiasis: coordinated use of anthelminthic drugs in control interventions - A manual for health professionals and programme managers. .
WHO 2015. Water sanitation and hygiene for accelerating and sustaining progress on neglected tropical diseases: a global strategy 2015-2020.
WHO 2017. Guideline: preventive chemotherapy to control soil-transmitted helminth infections in at-risk population groups

Guideline: preventive chemotherapy to control soil-transmitted helminth infections in at-risk population groups. Geneva: WHO.
WHO. 2020a. Schistosomiasis [Online]. Available: https://www.who.int/news-room/fact-sheets/detail/schistosomiasis [Accessed 04.11 2020].
WHO. 2020b. Soil-transmitted helminth infections [Online]. Available: https://www.who.int/news-room/fact-sheets/detail/soil-transmitted-helminth-infections [Accessed 04.11.2020].
WHO. 2020c. Strongyloidiasis [Online]. Available: https://www.who.int/intestinal_worms/epidemiology/strongyloidiasis/en/ [Accessed 04.11 2020].
Wimmersberger, D., Coulibaly, J. T., Schulz, J. D., Puchkow, M., Huwyler, J., N'Gbesso, Y.*, et al.* 2018. Efficacy and safety of ivermectin against *Trichuris trichiura* in preschool-aged and school-aged children: a randomized controlled dose-finding trial. Clinical Infectious Diseases, 67**,** 1247-1255.
Winiwarter, S., Bonham, N. M., Ax, F., Hallberg, A., Lennernäs, H. and Karlén, A. 1998. Correlation of human jejunal permeability (*in vivo*) of drugs with experimentally and theoretically derived parameters. A multivariate data analysis approach. Journal of Medicinal Chemistry, 41**,** 4939-49.
Xiao, S. H., Catto, B. A. and Webster, L. T., Jr. 1985. Effects of praziquantel on different developmental stages of *Schistosoma mansoni in vitro* and *in vivo*. The Journal of Infectious Diseases, 151**,** 1130-7.
Xie, T. and Zaidi, H. 2016. Development of computational small animal models and their applications in preclinical imaging and therapy research. American Association of Physicists in Medicine, 43**,** 111-131.
Zhang, J., Krugliak, M. and Ginsburg, H. 1999. The fate of ferriprotorphyrin IX in malaria infected erythrocytes in conjunction with the mode of action of antimalarial drugs. Molecular and Biochemical Parasitology, 99**,** 129-41.

Appendix

Curriculum *Vitae*

Valentin Buchter

Hegenheimerstrasse 240
CH-4055 Basel
valentin.buchter@gmail.com
linkedin.com/in/valentin-buchter-1582a6126
+41 79 483 82 20
Date of birth: 30. May 1990
Nationality: Swiss and Argentinian

SKILLS

Subject knowledge: MSc pharmacist with a PhD in microbiology specialized in drug development.

Research methods: HPLC-MS, PK studies on laboratory animals, qPCR, laboratory animal experimentation, *in vitro* drug activity assays, drug screening, scientific writing.

Soft skills (with certificate): project management, negotiation skills, scientific writing and writing productivity, literature search, logic and argumentation, team leadership.

Leadership experience: member of a team of 6 pharmacists, with 20 people in charge (2013 – 2015). Course: "successful team leadership" (2018) and "lead and build a successful work environment" (2020).

Communication and presentation skills: Oral presentation in Geneva health forum 2018. Participant in two courses on presentation skills. Several oral presentations during the course of the PhD. Delegate of the "Wissensbox Mikroskopie": present science projects and microscopy in public primary schools.

Organization and planning: Organizer of the first neglected tropical disease flash talks at Swiss TPH. PhD student representative at Swiss TPH. Theorical-practical Course in project management. Biology students block course guiding for three years.

Software: RStudio, FIJI – ImageJ, CFX maestro, Graph Pad Prism, PK Solver, Word, Excel, Power point.

WORK EXPERIENCE

Mar 2021 - **Scientific collaborator**. Federal Office of Public Health, Berne, Switzerland

Sept 2017- Dec 2020 **PhD candidate.** Helminths drug development unit. Thesis title: "Improved treatments for helminth infections, new formulations and drug candidates" Swiss TPH, University of Basel, Switzerland

- Multiple stages of drug development pipeline: *In vitro, in silico, in vivo*, drug formulation improve, drug screening
- Pharmacokinetic studies
- Drug sensitivity assays
- Fluorescence microscopy

06.2017 – 08.2017 **Internship in parasitology lab work**, Helminth Drug Development unit. Swiss TPH, Basel, Switzerland.

- SOP writing
- Drug screening

04.2015 - 06.2016 **Backpacker trip, over South America, Cuba, Mexico, Southeast Asia.**
Worked in various different jobs in tourism area.

07.2013 - 04.2015 **Pharmacist in Italian Hospital of Buenos Aires**, Buenos Aires, Argentina
- Member of team of pharmacists in different Hospital sectors:
- Vaccines: Sector responsible pharmacist • 5 people in charge
- High impact medication (HIV, Cancer, Autoimmune diseases)
- Hospital-pharmacy pharmacist.

02.2013 – 06.2013 **Pharmacy internship. Italian Hospital of Buenos Aires**, Buenos Aires
Final work for graduation
- Work in Clinic sector, medicines preparation, sterilization
- Vaccines, high impact medication and pharmacy.

07.2011– 11.2011 **Auxiliary teacher in physiology subject, University of Buenos Aires**

ACADEMIC FORMATION

Sept 2017- today **PhD candidate in microbiology.** University of Basel, Switzerland

04.2008 - 12.2013 **Pharmacy MSc**. University of Buenos Aires, Argentina

03.2011 – 11.2011 **Formation for auxiliary teacher in physiology.** University of Buenos Aires

04.2011 – 11.2011 **Research assistant in research team**, Prof. Dr. Ana Maria Balaszuck. University of Buenos Aires
- Basic science research using Western Blot & electrophorese techniques. • In vivo studies

AWARDS

Swiss government excellence scholarship. 3 years scholarship for performing the PhD in Switzerland. 84.600 CHF netto + Expenses (around 22.400 CHF)

FURTHER FORMATION

2017 – 2020 13 courses on diverse soft skills in the frame of the PhD.

Oct.2017 • **LTK module 1:** Introductory course in laboratory animal science. FELASA accredited course F027/08. University of Zürich, Switzerland.

04.2014 - 11.2014 • **Course "Update on immunizations"**, Ramon Gutierrez Hospital. April – November 2014, Buenos Aires, Argentina

04.2014 – 08.2014 • **Course "Project management for health sciences"**. Italian Hospital of Buenos Aires. April – Aug 2014. Buenos Aires, Argentina

CONGRESS AND NETWORK

03.2020 **German society for parasitology**. Poster accepted, event cancelled (SARS CoV-2)

11.2018 & 11.2019 **SSTMP**: Swiss society of tropical medicine and parasitology. PhDs retreat with oral presentations in parasitology and round-table discussions

04.2018 **Geneva health forum 2018**: Speaker and participant

STUDENTS SUPERVISION

2017, 2018, 2019	**Co-supervision of Bachelor block course in Biology** – University of Basel. Study and hypothesis design, helminths laboratory work, drug activity assays. Duration: 40 hours per course.
2011	**Assistant lecturer in subject Physiology**. University of Buenos Aires, Argentina. Duration: 24 hours + preparatory work

LANGUAGES

English	Excellent speaking and writing
German	Second native language
Spanish	Native speaker
French	Good speaking, good writing. DELF B1 & DELF B2
Italian	Basic knowledge

List of publications

Buchter V, Hess J, Gasser G, Keiser J. Assessment of tegumental damage to Schistosoma mansoni and S. haematobium after in vitro exposure to ferrocenyl, ruthenocenyl and benzyl derivatives of oxamniquine using scanning electron microscopy. Parasites & Vectors. 2018; 11(1):580.

Buchter V, Priotti J, Leonardi D, Lamas MC, Keiser J. Preparation, Physicochemical Characterization and *In Vitro* and *In Vivo* Activity Against *Heligmosomoides polygyrus* of Novel Oral Formulations of Albendazole and Mebendazole. Journal of Pharmaceutical Sciences. 2020; 109(5):1819-26.

Buchter, V., Ong, Y..C., Mouvet, F., Ladaycia, A., Lepeltier, E., Rothlisberger, U., Keiser, J. and Gasser, G. (2020), Multidisciplinary Preclinical Investigations on Three Oxamniquine Analogues as Novel Drug Candidates for Schistosomiasis. Chem. Eur. J. Accepted Author Manuscript. Doi:10.1002/chem.202002856

Buchter V, Hofmann D, Häberli C, Keiser, Jennifer. (2020), Characterization of moxidectin against *Strongyloides ratti: in vitro* and *in vivo* activity and pharmacokinetics in the rat model. ACS infectious diseases. DOI: 10.1021/acsinfecdis.0c00435

Buchter V, Schneeberger P and Keiser J. In Press 2020: Validation of a human-serum-based *in vitro* growth method for drug screening on juvenile development stages of Schistosoma mansoni.